DNA binding studies of fluorinated bioactive heterocyclic compounds

By

Mariam Mojally

A thesis submitted in the partial fulfillment of the requirements for the award of

Doctor of Philosophy in Medicinal Chemistry

At the University of Loughborough

Department of Chemistry

Research Supervisors

Dr. George Weaver
Dr. Paul Lucas

2014

CERTIFICATE OF ORIGINALITY

This is to certify that I am responsible for the work submitted in this thesis, that the original work is my own except as specified in acknowledgments or in footnotes, and that neither the thesis nor the original work contained therein has been submitted to this or any other institution for a degree.

…………………………………………………..(Signed)

…………………………………………………(Date)

Dedication

This research work is dedicated to my Father, Mother, and Husband Waleed, my children Wisal, Abdulah, Abdulrahman and Abdulrahim and to all my family.

Acknowledgment

I would like to express my special appreciation and thanks to my supervisors Dr. G.W.Weaver and Dr. P. Lucas for their guidance, encouragement, enthusiastic supervision, invaluable advice through the duration of the research project and allowing me to grow as research scientist.

I am thankful to Umm Al-Qura University for the scholarship and Loughborough University.

I extend my thanks to Dr. Weaver research group and all research students in laboratories F009 and F001 for their help and assistance and friendship.

I would like to thank my family for their support and patience throughout these studies.

I would like to record a special thanks to the technical staff for all their assistance. They include Dr. Simon Teat at the Advance Light Source and Dr. Mark Elsgood for X-ray crystallography, Dr. Mark Edgar for NMR spectroscopy, Mr. Alastair Daley and Mrs. Pauline King for elemental analysis and for GC mass spectrometry. We acknowledge the EPSRC National mass spectrometry facility, Swansea University, for mass spectrometry.

Abstract

Fluorinated heterocyclic compounds have drug like properties and possess a valuable biological activity due to their rigid chemical structures and the high solubility profile. Novel fluorinated heteroarenes have been synthesised by S_NAr reaction of a range of fluorinated arenes including pentafluoropyridine, hexafluorobenzene and pentafluorotoluene to introduce a range of groups specially nitriles, benzimidazole, carbazole and benzimidazole. A number of cyclization reactions have been investigated with the aim of forming polycyclic structures that could act as DNA intercalators.

The synthesised compounds have been characterized by elemental analysis, IR, ^{1}H and ^{19}F NMR spectroscopy and single crystal analysis. These compounds have been screened for their biological activities including DNA thermal denaturation assay, UV-Visible spectroscopy, fluorescence spectroscopy, X-ray co-crystallization and antimicrobial activity study. Some of the compounds showed potential DNA bonding activity in particular the carbazole derivatives.

Abbreviations

A	Adenine
ACTD	Actinomycin D
bs	Broad signal
C	Cytosine
DCM	Dichloromethane
DMF	Dimethylformamide
DMSO	Dimethylsulfoxide
DNA	Deoxyribonucleic acid
EB	Ethidium bromide
EDTA	Ethylenediaminetetraacetic acid
EtOH	ethanol
FDA	Food drug administration
FdUrd	5-fluoro-2'-deoxyuridine
5-FU	5-fluorouracil
G	Guanine
GC-MS	Gas chromatography mass spectrometry
HRMS	High resolution mass spectrometry
NaH	Sodium hydride
***n*-BuLi**	Normal butyllithium
NMR	Nuclear magnetic resonance
RNA	Ribonucleic acid
RT	Room temperature
SS-DNA	Salmon sperm DNA
T	Thymine

THF	Tetrahydrofuran
TLC	Thin layer chromatography
Tm	Melting temperature
TMEDA	N,N,N,N-tetramethylethylenediamine
tRNA	Transfer ribonucleic acid
TS	Thymidylate synthase
UV	Ultraviolet

Contents

Chapter 1: Introduction

Chapter 2: Results and discussion

Chapter 3: Experimental

List of figures

List of schemes

List of tables

Chapter 1

Introduction

1. Introduction

Heterocyclic chemistry is very important during lead optimization in drug discovery and development in the pharmaceutical industry, and the majority of the therapeutic agents contain at least one heterocyclic sub-unit within their chemical structure. Many functional heterocyclic compounds have drug like properties and possess valuable biological activity due to their rigid chemical structures and high solubility profile. Increasingly studies have focused on discovery and synthesis of a variety of heterocyclic derivatives via the chemistry of highly fluorinated heteroaromatic schemes.[1,2] The presence of fluorine in drug molecules has been found to have many beneficial effects.

Henri Moissan established the field of fluorine chemistry in the late 19th century with the first isolation of elemental fluorine in 1886. At that time the extreme reactivity of fluorine narrowed the spreading of fluorinated compounds. This situation changed in the 1960s and 1970s with the introduction of selective and safe fluorinated reagents that were compatible with regular laboratory procedures and instruments and therefore agreeable to elaboration of novel fluorinated lead substances.[3,4] The fluorinated heterocyclic compounds are critical in various technological developments and have become important intermediate products in the synthesis of various pharmaceuticals, agrochemicals, fluoropolymers and in material science in what can be named "the modern age of fluorine chemistry".[3,4,5] The development of synthetic organofluorine chemistry and the proper understanding of the role of fluorine in biological behavior of the compounds have been facilitated to synthesise more effective and leading fluorine containing pharmaceutical candidates.[6,7,8] Moreover, it has been estimated that around 20-25% of medicines consist of fluorinated substances[4,9,10,11] and among the various drugs in the world, more than 150 pharmaceutical candidates are fluorinated compounds which is comparatively a large number compared to other halogen containing drugs.[12] Gakh and Burnet (2011) indicated that the use of fluorinated biologically active substances in medicinal chemistry increased steadily between 1957-2006 from about 7% to about 15% according to the food drug administration (FDA).[13]

1.1. Fluorine physical characteristics

Fluorine is the most reactive electronegative element with very low polarizability [4,14,15] and a very low bond dissociation energy F-F (155 kJ/mol).[16] In contrast the bond dissociation energy for C-H and C-F are 411 kJ/mol and 485 kJ/mol respectively.[16] Fluorine atom has the second smallest van der Waals radius (1.47 Å), which is sited

between hydrogen (1.20 Å)[17] and oxygen (1.52 Å)[17] and allows fluorine to behave like a hydroxyl group and contribute in hydrogen bonding interactions.[3] The low polarizability affecting the fluorine and the three non bonding electron pairs are important physical characteristics of biological activity of fluorinated compounds.[3,10,14,15] In addition, the high reactivity of fluorine is referred to the strong bond between fluorine and other elements and a very weak F-F bond. Also the greater strength of the C-F bond over the C-H bond results in high chemical stability of fluorinated compounds.[3,18] The physical and chemical properties of the molecule can be changed significantly by introducing a fluorine atom to the molecule. As a consequence of these characteristics, a group containing fluorine could be used to substitute a non-fluorinated one in a biologically active molecule, which could change the activity of the compound, lipophilicity, bioavailability and metabolic stability dramatically. This ability to modify the pharmaceutical behavior of a compound by adding fluorine atoms clarifies why medicinal and bioorganic chemistry of fluorine has become an active area of research, and why a large number of pharmaceutical candidates contain fluorine atoms.[2,12,19]

1.2. Biological impact of fluorination

1.2.1. Absorption
The xenobiotic molecule has to be absorbed and penetrate several barriers without being changed or eliminated before reaching the macromolecule target. The absorption properties of the molecule can be modified by fluorination, as it is known ionisable drug absorption depends on the lipophilicity of charged and neutral species. Fluorine substitution can modify the ionisation of the substance at pH 7.4, consequently the lowering of the pKa of nitrogen containing heterocyclic compounds or amines by fluorination enhance the absorption particularly for the oral administrated drugs.[12]

1.2.2. Lipophilicity
The blood brain barrier permeability of a lead molecule can be increased by introducing a fluorine atom in a specific position resulting in enhanced affinity of the compound to the target molecule. In addition, lipophilicity is usually increased when a fluorine atom is introduced to an aromatic ring or if a fluorine atom is located in the vicinity of a basic nitrogen atom.[9] Some fluorinated groups are isosteric with several functional groups and they can mimic them in the interaction with the target biological macromolecules such as

3

receptors, nucleic acids and enzymes and this is a very critical strategy in the design and synthesis of receptor ligands, enzyme inhibitors and mechanism-based inhibitors.[12]

1.2.3. Metabolism

The stability of molecules against metabolic oxidation can be increased by exchanging a proton with fluorine atom due to the higher dissociation energy of C-F bond versus C-H bond (the dissociation energy of a C-F and C-H bonds are 485 kJ/mol and 411 kcal/mol respectively).[9,16] Furthermore, because the fluorine atom is rare in nature, it is less likely to be degraded by naturally occurring enzymes, thus it can help to enhance the drug metabolic stability.[7] The fluorinated analogue of a biologically active compound is normally recognized by the same enzyme, receptor or nucleic acid target. The specific physicochemical properties of fluorine modify the interactions between the compound and the constituents of the biological medium. Because of the size difference between the hydrogen atom and the fluorine atom, the replacement of hydrogen with one or more fluorine atoms can adjust the conformation of the molecule, consequently altering enzyme or receptor binding affinity, or changing the main metabolic process of the therapeutic agents.[3,10,14,20]

1.3. S_NAr reactions of perfluoroarenes

There is now a substantial body of literature on organofluorine chemistry.[21,22] A vast range of nucleophiles have been shown to react with perfluoroarenes in S_NAr reactions with nucleophiles based on C, O, N, S and P. Examples of reactions involving hexafluorobenzene **1** are shown in scheme 1. The anion of diethyl phosphonate reacts with hexafluorobenzene **1** through the phosphorus atom to give phosphonate **2**.[23] Hexafluorobenzene **1** also reacts readily with alkyllithiums such as methyllithium and forms pentafluorotoluene **3**.[24] The sodium salt of benzyl alcohol reacts with hexafluorobenzene **1** to give ether **4**.[24] Hexafluorobenzene **1** reacts with amines such as morpholine to give tertiary amine **5**.[25] Sulfur nucleophiles are particular effective and hexafluorobenzene **1** reacts with sodium hydrogensulfide to give pentafluorobenzenethiol **6**.[26]

Scheme 1. Various S$_N$Ar reactions of hexafluorobenzene
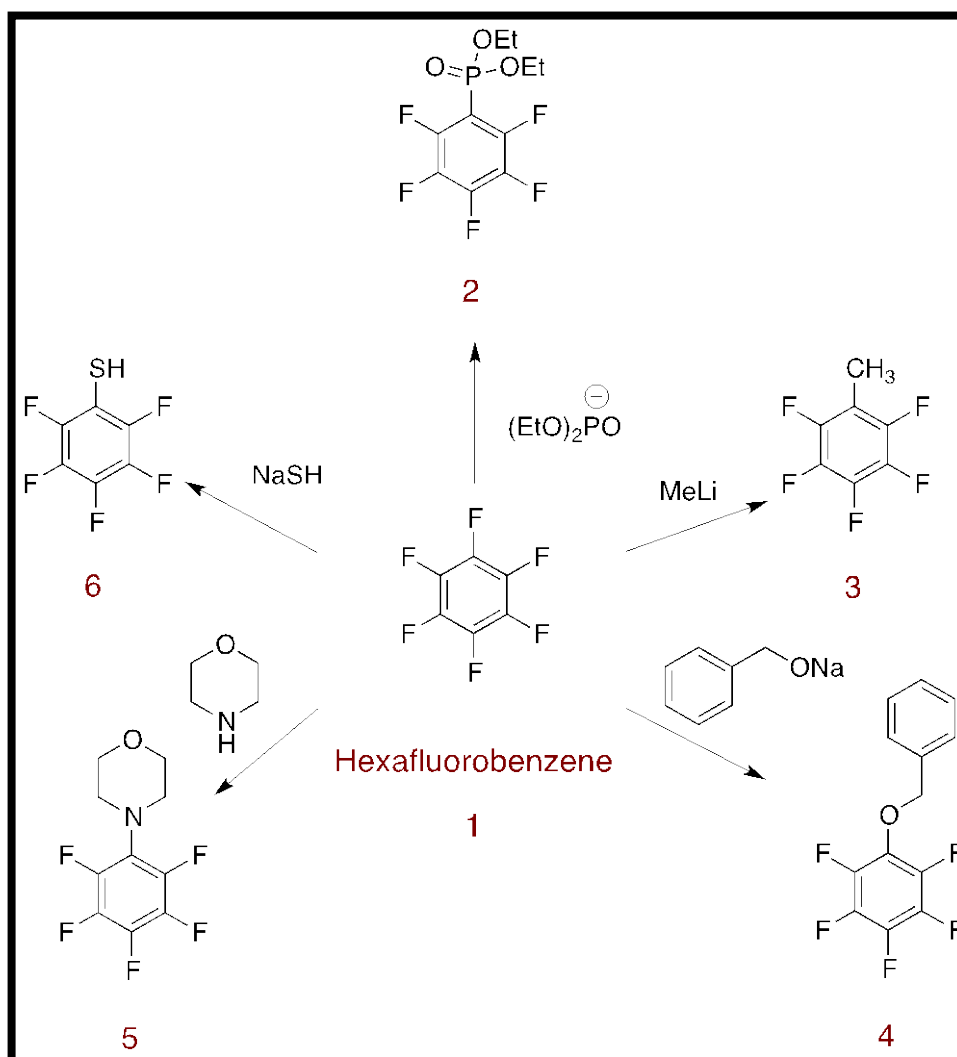
In each case the nucleophile adds to the electron deficient fluorinated ring to form an anionic tetrahedral intermediate **7**, with the charge delocalized across the five remaining sp^2 hybridised carbons, and stabilized by the inductive effect of the fluorine atoms as shown in Scheme 2. Only the most important resonance structure **7**, with the charge on the central carbon with the maximum orbital coefficient, is shown. Rearomatisation then occurs with loss of a fluoride ion to form the product.[22]

Scheme 2. Mechanism of S_NAr reaction
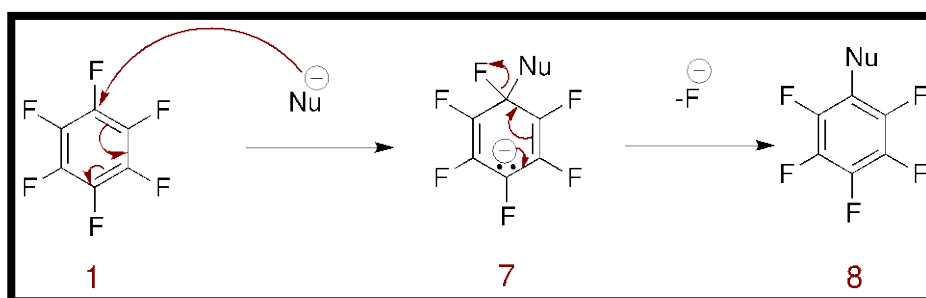
Addition of a further nucleophile is possible and the same, or a different, nucleophile can add to mono-substituted perfluorobenzene derivatives (Scheme 3).

Scheme 3. 1,4-Disubstitution of hexafluorobenzene
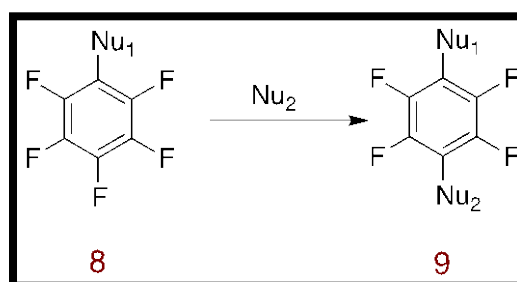
For example normal butyllithium (*n*-BuLi) reacts twice with hexafluorobenzene **1** forming initially **10**, and then addition of a second molecule affords 1,4-dibutyl tetrafluorobenzene **11** (Scheme 4).[27]

Scheme 4. Reaction of hexafluorobenzene with butyllithium[27]
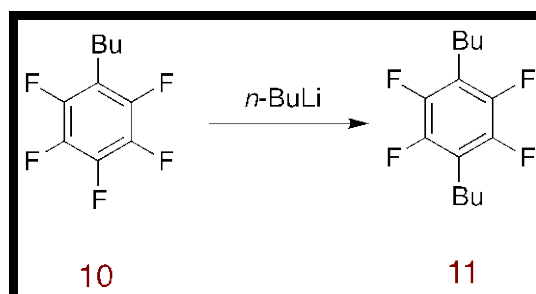
When two molecules of the same nucleophile attack, predominantly the 1,4-disubstituted product is obtained, due to the destabilizing effect of *para*-fluorine if the nucleophile attacks at any other position, as shown in Scheme 5.

Scheme 5. Mechanistic basis of orientation in di-substitution of hexafluorobenzene
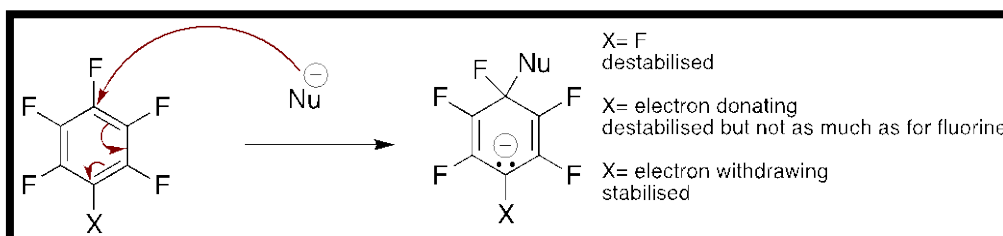
Attack at the 4-position is promoted by the strongly inductive effect of one ipso, and two *ortho*, fluorines. A *para*-fluorine however destabilizes the intermediate due to repulsion by the small lone pairs on the fluorine atom of the electrons accumulating in the p-orbital on C-1 (largest orbital coefficient in the delocalized π-system). The *meta* fluorines have a slight activating effect which has been ascribed to a dipole effect.[28, 29] Similarly if a different nucleophile adds to a mono-substituted perfluorobenzene derivative, 1,4-addition is also preferred, although minor amounts of the *ortho* substituted compound is sometimes observed. Reaction of ethyl pentafluorobenzoate **12**, for example, with sodium ethoxide gives the 1,4-disubstituted product **13** in 96 % with only a trace amount of the 1,2-disubstituted compound **14** (Scheme 6).[30]

Scheme 6. Reaction of ethyl pentafluorobenzoate with sodium ethoxide[30]
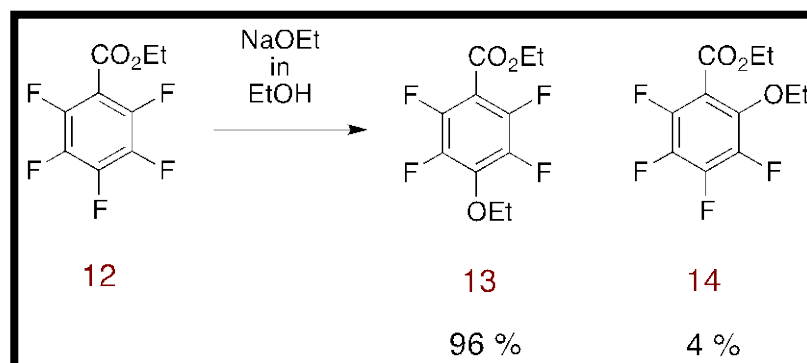
Even when the first group added is an electron donating group, 1,4 addition is still observed to avoid the repulsive effect of a *para*-fluorine atom. For example addition of a phenol such as 2-bromophenol **15** to hexafluorobenzene **1** gives the 1,4-bis ether **17** via the mono-substituted complex **16**.[31] In fact it is often found that the 1,4-disubstitution product is formed predominantly during attempts to effect mono-substitution. The second nucleophile often reacts more readily with the first-formed product e.g. **16** than with the starting material due to the presence of a destabilising *para*-fluorine. Any other atom in the *para*-position generally makes that compound more reactive. From a synthetic point of view a large excess of the starting perfluoroarene is often required in order to obtain useful yields of mono-substituted compounds (Scheme 7).

Scheme 7. Reaction of hexafluorobenzene with 2-bromophenol[31]
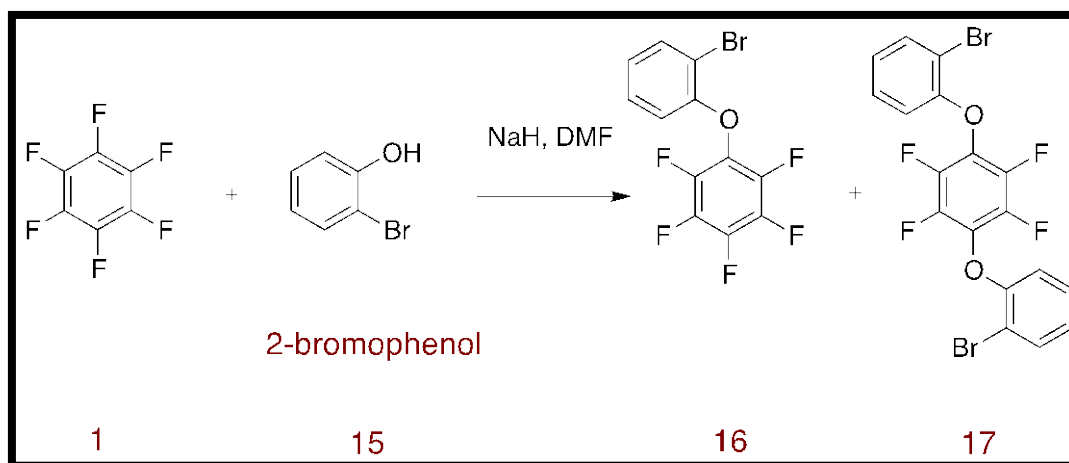
The vast majority of disubstitution reactions lead to the 1,4-disubstituted product, but there are a few exceptions where 1,2-disubstitution can occur. This usually arises where the first substituent can coordinate to the incoming nucleophile. For example reaction of the sulfone **18** with ethylmagnesium bromide forms the product **20** where the ethyl group has added *ortho* to the sulfone group (Scheme 8).[32]

Scheme 8. 1,2-Disubstitution occurs in the case of a coordinating sulfone
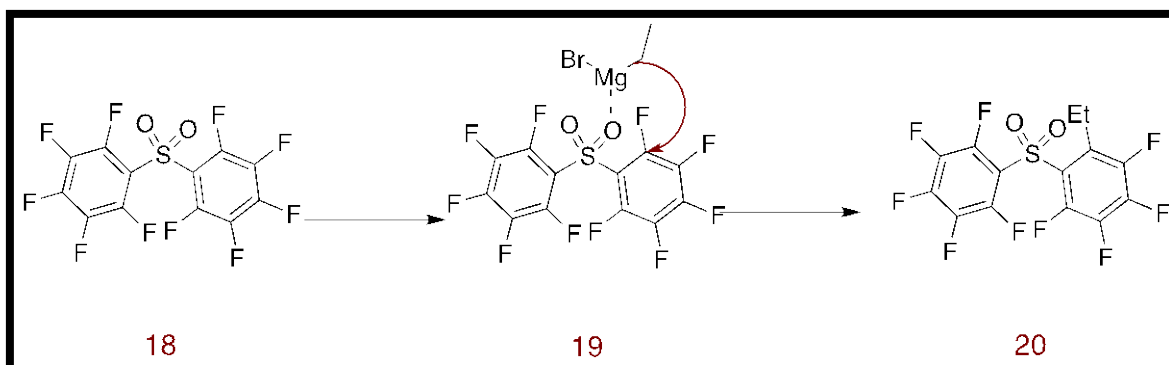
1.3.1. Perfluorinated pyridine

Sandford et al., in 2010 have established that perfluoroheteroaromatic systems such as pentafluoropyridine are excellent core scaffolds for the synthesis of various highly functionalized heteroaromatic and ring fused polycyclic compounds.[1] Pentafluoropyridine is highly reactive toward nucleophilic attack due to the presence of five highly electronegative fluorine atoms attached to the heterocycle and the ring nitrogen, and all five fluorines atoms can be replaced by nucleophiles in S_NAr reactions.[33] Scheme 9 outlines the possible principle of the order of the nucleophilic substitution in pentafluoropyridine **21** and this order of the nucleophilic attack can depend on the effect of each substituent once attached to the heterocyclic ring as well as to the nature of the attacking nucleophile.[1,33,34,6]

Scheme 9. General approach to the synthesis of pentasubstituted pyridine systems
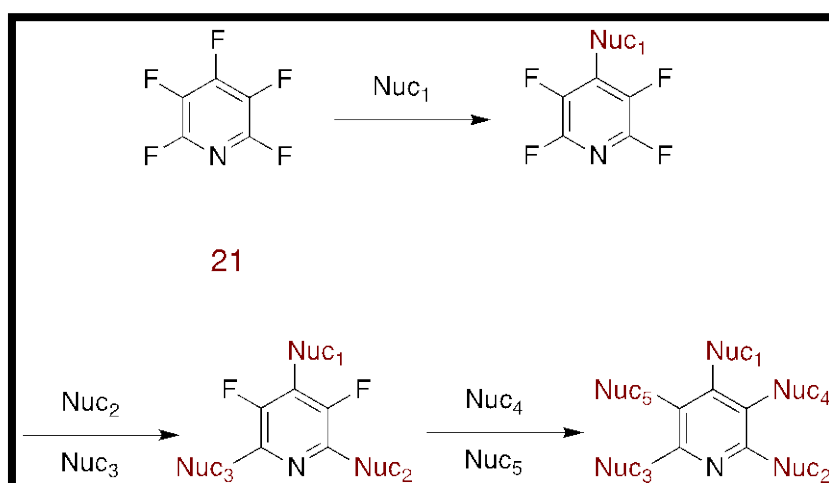
The first nucleophile again adds at the 4-position, *para* to the stabilizing nitrogen, and avoiding the repulsion of a *para*-fluorine atom. Subsequent nucleophiles then attack at C-2 and C-6 which are adjacent to the ring nitrogen. The final nucleophiles tend to add to C-3 and C-5. Scheme 10 shows some examples of the general strategy of the nucleophilic substitution of pentafluoropyridine **21**. Reaction of ethyl acetoacetate with pentafluoropyridine **21** in the presence of sodium hydride (NaH) under reflux in tetrahydrofuran (THF) for 70 h provided enol ester **22** that arose from the replacement of fluorine by the anion of ethyl acetoacetate.[1] Phenyllithium reacted with pentafluoropyridine **21** and formed biaryl **23**.[35] Reaction of the highly nucleophilic hydrazine with pentafluoropyridine **21** afforded compound **24**.[36] In all three examples the addition of the nucleophile occurs at C-4 (Scheme 10).

Scheme 10. S$_N$Ar reactions of pentafluoropyridine
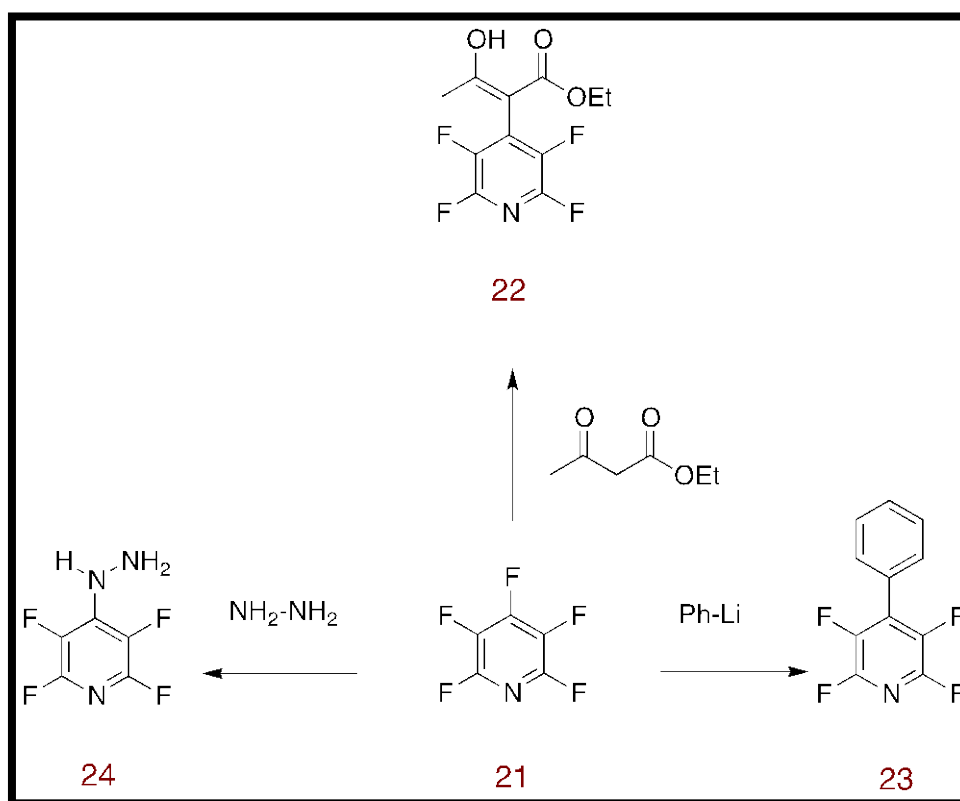
Di- and tri-substitution is possible as shown by the examples in Scheme 11.[33,37] The sodium salt of benzenesulfinic acid reacted with pentafluoropyridine **21** to form sulfone **25** in high yield. Treatment of this compound with diethylamine led to formation of **26** in moderate yield, and the amine group was shown by ^{19}F NMR spectroscopy to have added

at the 2-position. On the other hand reaction of **25** with ethylenediamine led to the tri-substitution product **27** in 92 % yield. In this case addition is most likely to have occurred firstly at the more reactive C-2 position, with the other amino group then attacking C-3 to form the piperazine ring. This reaction shows the possibility of forming an additional fused ring and this approach is a key theme of the Weaver group research.

Scheme 11. Di-and tri-substitution reactions of pentafluoropyridine[37]
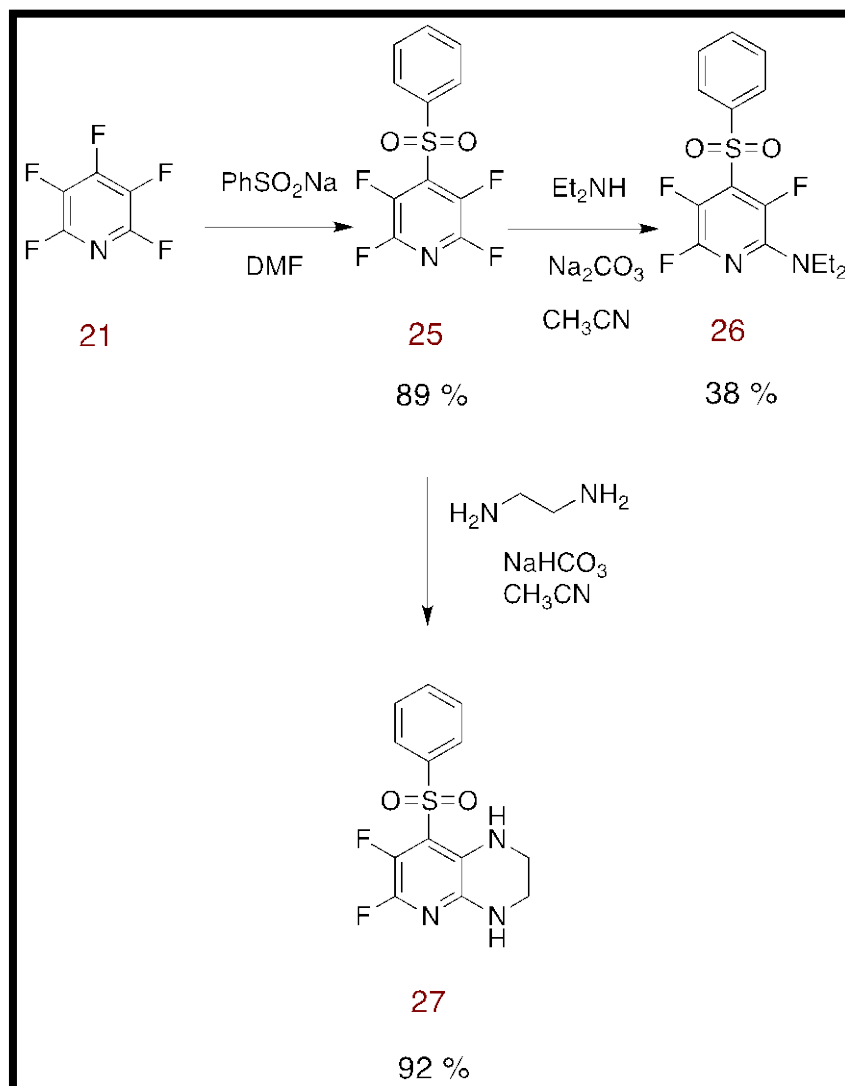
A further example of ring formation is shown in Scheme 12 and involved the reaction of pentafluoropyridine **21** with 2-iminopiperidine **28** which provided the tricyclic compound **29** after heating with NaHCO$_3$ at 180 °C for 30 minutes under microwave irradiation. Initial attack at C-4 is most likely to have occurred, followed by a second S$_N$Ar reaction at C-3 to close the imidazole ring.[37]

Scheme 12. Reaction of pentafluoropyridine with 2-iminopiperidine[37]
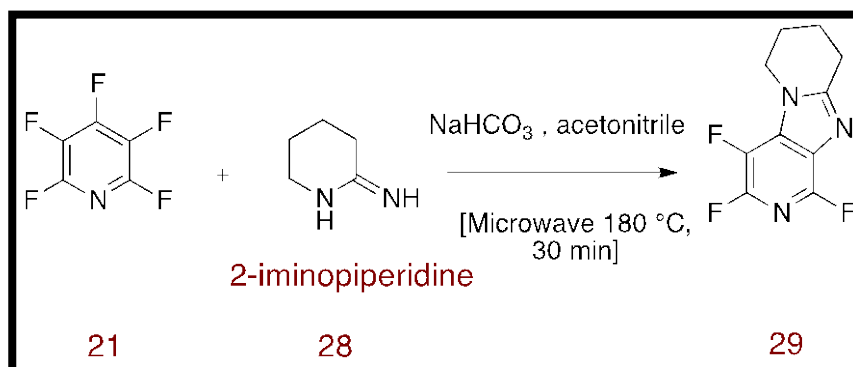
In contrast, the reaction of pentafluoropyridine **21** with acetamidine **30** in the presence of NaHCO$_3$ under reflux in acetonitrile for 17 h gave the uncyclized amidine derivative **31** (Scheme 13).[37] It is not clear why compound **31** failed to cyclize under these conditions, although the temperature employed was lower than in the case of **29**.

Scheme 13. Reaction of pentafluoropyridine with acetamidine[37]
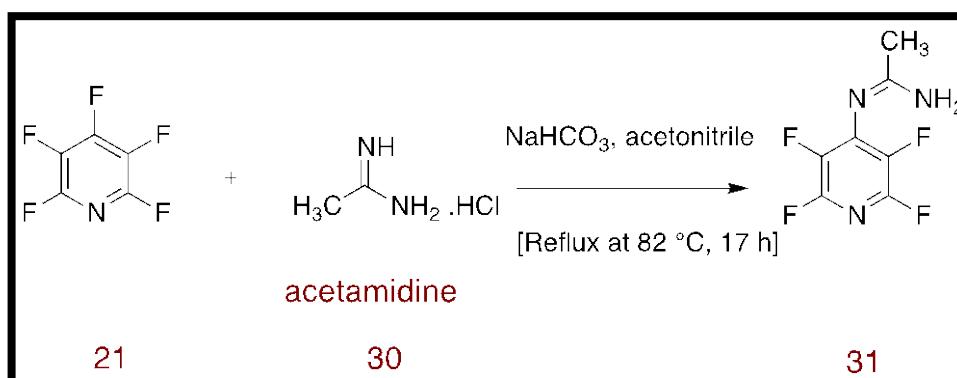
One aim of the research in the group is to effect ring formation of fluorinated aryl ethers such as **32** (Scheme 14). Lithiation of compound **32** was investigated by treatment with two equivalents of *n*-BuLi in THF at −78 °C followed by warming to room temperature (RT) and provided the benzo-bis-benzofuran **33** (Scheme 14).[31]

Bromine-lithium exchange in **32** was believed to have generated a highly nucleophilic aryllithium which then effected on S$_N$Ar reaction on the *ortho*-position of the central perfluorobenzene ring forming the fused benzofuran structure; the reaction occurring at both ends of the molecule. The regioisomer formed can be accounted for by consideration of the site of attack by the second to react aryllithium group. This would attack *para* to the carbon of the first-formed benzofuran ring rather than *para* to fluorine.[31]

Scheme 14. Cyclization of bis-ether (32) to benzo[1,2-b:4,5-b']bis[b]benzofuran (33)[31]
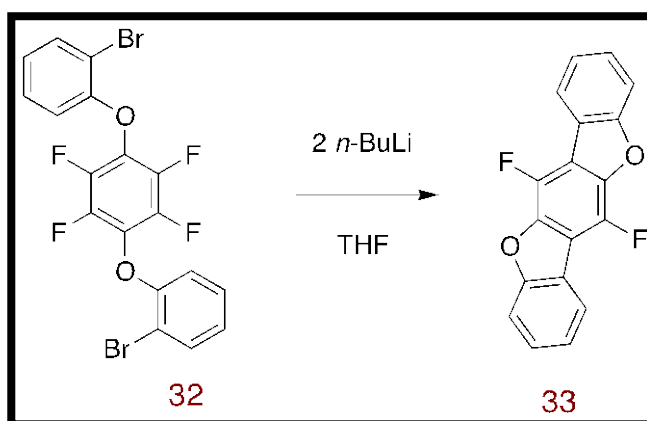
Lithium-bromine exchange in ether **34** was expected to generate an aryllithium which would lead to intramolecular substitution of the fluorine at C-3 of the pyridine ring to close the furan ring forming **35**. However treatment of the tetrafluoropyridyl ether **34** with *n*-BuLi in THF at low temperature afforded a compound which was not the expected tricyclic furan **35**. Spectroscopic analysis indicated that the tetrafluoropyridine ring was intact. The product was shown to be the 2-(tetrafluoropyrid-4-yl)phenol **36** indicating that the reaction had proceeded by a Smiles type rearrangement. It appears that the aryllithium formed prefers to attack at C-4 rather than at C-3 to avoid the destabilizing effect of a *para*-fluorine, even though this means the reaction has to proceed via a strained four-membered ring intermediate. Treatment of the phenol **36** with sodium hydride in DMF did then give the fused benzofuran **37** quantitatively with the phenoxide oxygen effecting nucleophilic substitution of the fluorine atom at 3-position of the pyridine ring (Scheme 15).[31]

**Scheme 15. Smiles reaction was observed in lithiation of
4-(2-bromophenoxy)tetrafluoropyridine[31]**
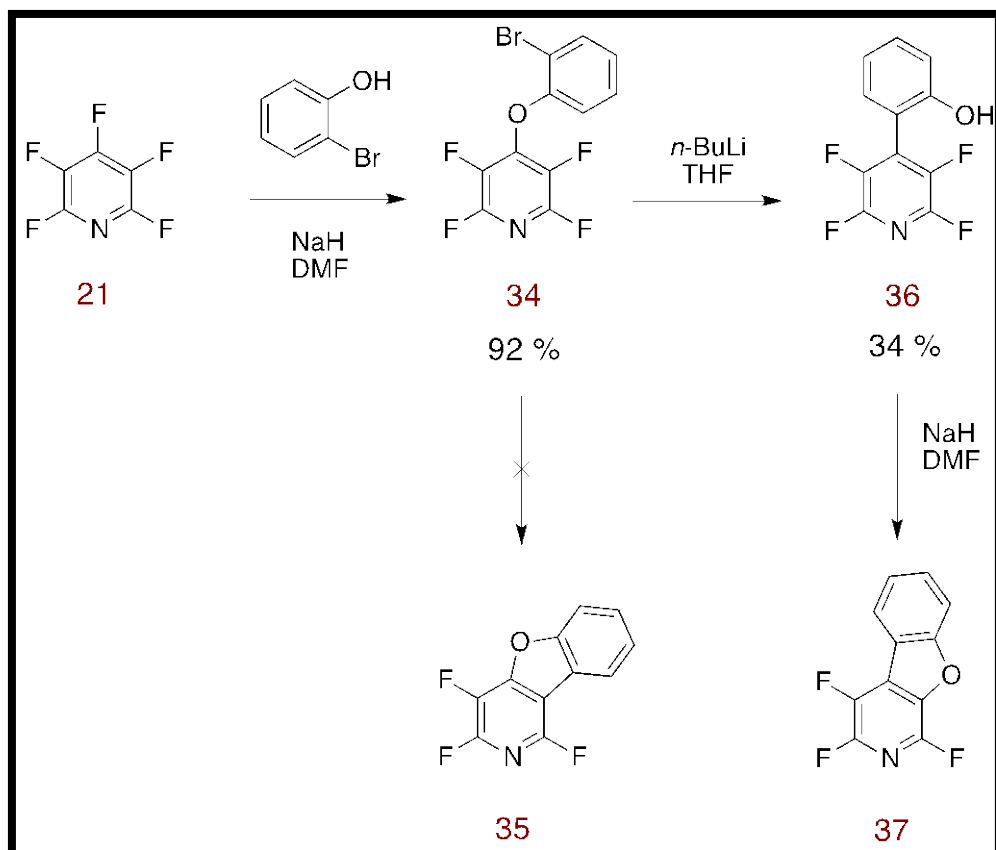
When the corresponding thioether **38** was treated with *n*-BuLi, direct cyclization occurred by S_NAr reaction at C-3 and no rearrangement was observed. The anion stabilizing effect of the sulfur is believed to lower the activation energy for attack at C-3 overriding the repulsive effect of the *para*-fluorine (Scheme 16).[31]

**Scheme 16. Normal cyclization occurred in the case of
4-(2-bromophenylsulfanyl) tetrafluoropyridine[31]**
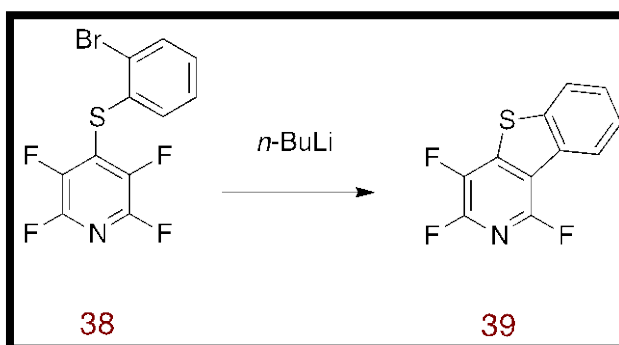
It was planned to focus on the chemistry of fluorinated arenes relevant to heterocyclic drug synthesis.

1.4. Fluorinated pharmaceutical agents

1.4.1. Thymidylate synthase inhibitors

Wide ranges of fluorinated cancer treatment drugs are now available for curing tumors. The most common drugs broadly used are 5-fluoropyrimidines, for example 5-fluorouracil (5-FU) and 5-fluoro-2'-deoxyuridine (FdUrd) (Figure 1). The key strategy of 5-FU is inhibition of cell division in cancerous tissue, while 5-FU and its derivatives play a critical role in mechanism-based inhibition of the enzyme thymidylate synthase (TS), since the TS enzyme is responsible for the synthesis of the compounds that act as the building block for DNA repair and synthesis in particular thymine.[11]
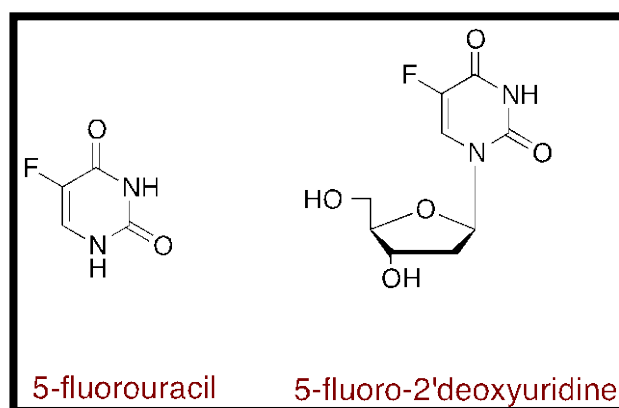
Figure 1. Examples of TS inhibitors

1.5. DNA binding studies of organic fluorinated compounds

1.5.1. DNA-drug interactions

Deoxyribonucleic acid (DNA) is a nucleic acid that holds the genetic information which is required to identify the biological progress of cell life.[38,39] A highly dynamic natural molecule, it consists of two tightly intertwined strands forming a double helix.[40,41] The double strand is held together by hydrogen bond interactions between complementary base pairs units (Figure 2).[41,42] Each strand is made of subunits called nucleotides. Each nucleotide is made of a sugar (deoxyribose), a phosphate group, and a nitrogenous base, which is Adenine (A), Guanine (G), Cytosine (C), or Thymine (T). The bases form complementary A–T and G–C pairs across the helix.

The integrity of DNA is a vital feature of cell life, since the molecule carries hereditary information and instructs important biological processes of living cells such as transcription (gene expression and protein synthesis) and replication (a key step in cell division and growth).[43,44,45] It is important to understand the mechanism of genetic processes of differentiation and cell growth; moreover it is one of the most promising biological targets for developing anti cancer agents that aim to limit tumor cell growth. [38,40,45,46,47,48] Targeting DNA to control cell functions by interfering with replication or by modulating transcription appears logical.[47] When a small molecule binds to DNA and affects, alters or inhibits DNA functions, these compounds act as drugs when alteration or inhibition of DNA functions is necessary to treat or control certain diseases.[47] This theory is significant in biology and medicinal chemistry to design and synthesis novel DNA targeted compounds for treating genetic origin diseases such as cancer.[49]
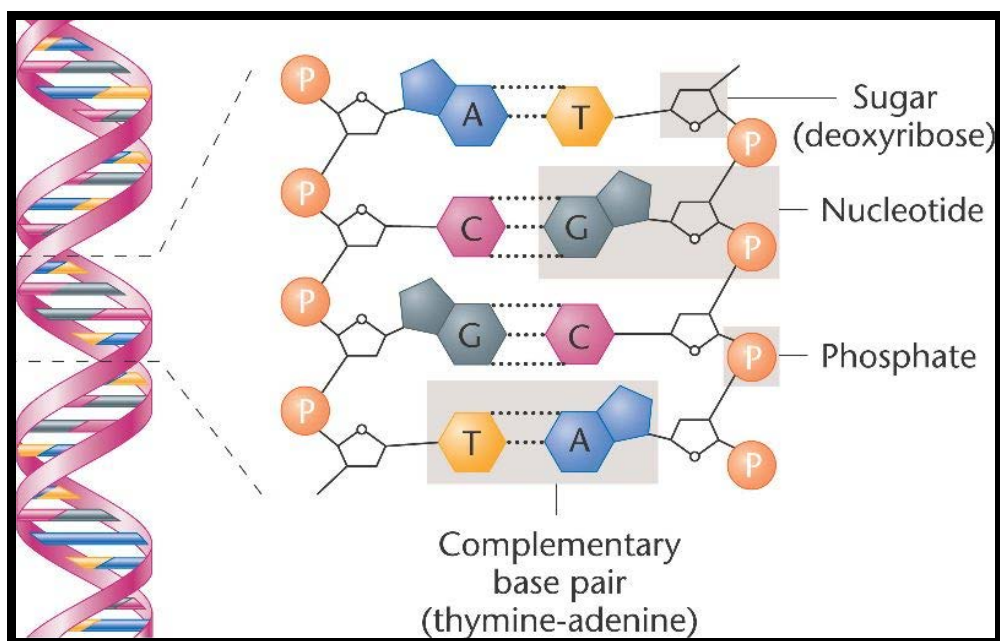
Figure 2. DNA double helix

1.5.2. Types of DNA-drug interaction

The pharmaceutical compounds interact with DNA in different ways:

(i) Through control of transcription factors and polymerases. In this interaction the drugs interact with proteins that bind to DNA.

(ii) Through binding of small ligand molecules to DNA double helix.[47]

16

The small organic molecules that interact with DNA can be classified into three different groups, alkylating agents, groove binding agents and intercalating agents.

1.5.2.1. Alkylating agents

Alkylating agents can cause DNA damage by formation of cross-links, bonds between atoms in the DNA. In this process, the alkylating agent that has two DNA binding sites will bind covalently with two bases of DNA. This cross-linking of the two strands of DNA prevents the use of that DNA as a template for further Ribonucleic acid (RNA) and DNA synthesis. Consequently, the replication and transcription of DNA will be inhibited and will lead to cell death. An example of cross linking agent is cisplatin that makes intra- and inter-strand cross-links through replacement of chloride ligands by the nitrogen atoms on the purine bases (Figure 3).[44,47,50,51] An example of an alkylating agent is chlorambucil which forms cross links by alkylation of the N-7 position of guanine or adenine (Figure 4).[52]
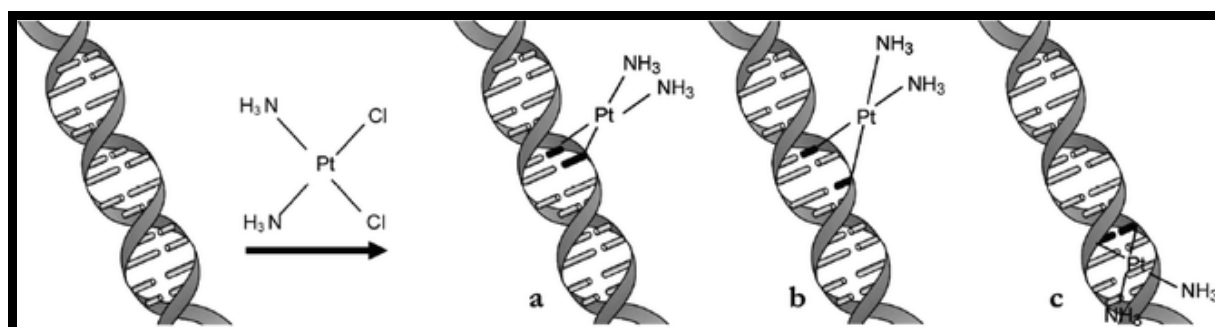
Figure 3. Cisplatin covalently bound to DNA interastrand [structure a and b], interstrand [structure c]
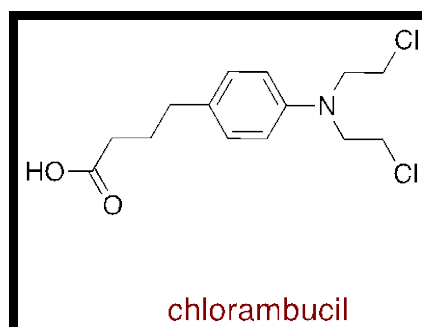
Figure 4. The structure of chlorambucil

1.5.2.2. Groove binding agents

Groove binding compounds are crescent-shape or narrow curved shaped molecules, which are isohelical to the curves of the DNA. These compounds are able to bind with the major or minor grooves of DNA without causing large changes to the DNA. The major groove is wide and relatively small and shallow, and approximately 22 Å in width. The minor groove is deeper and narrower, and only about 12 Å in width (Figure 5).[53] Some small compounds such as netropsin bind to the minor groove of DNA by hydrogen bonding, electrostatic and van der Waals interactions.[47,54] Netropsin is a naturally occurring basic oligopeptide that display good antibiotic activities against viruses, fungi and bacteria (Figure 6).[55,56]
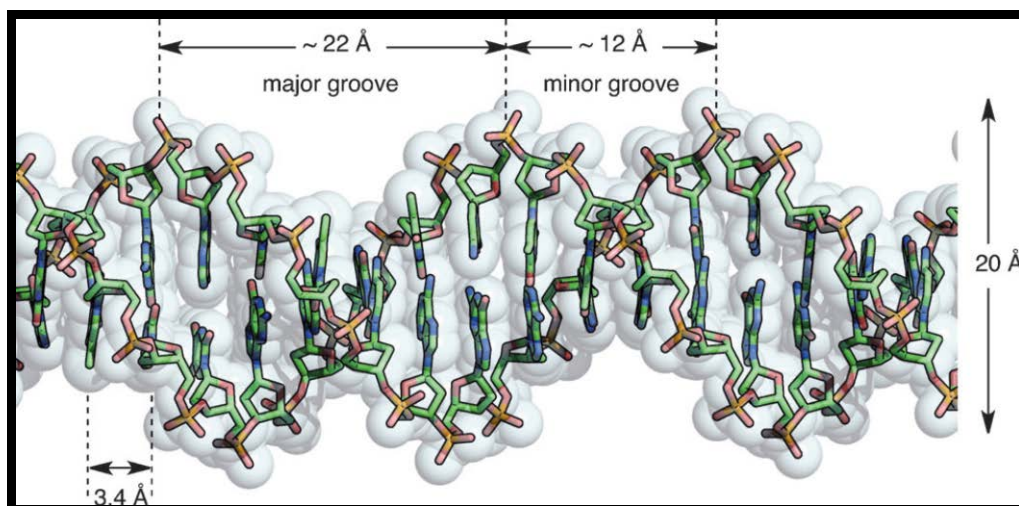
Figure 5. Representation of minor and major grooves of B-DNA structure
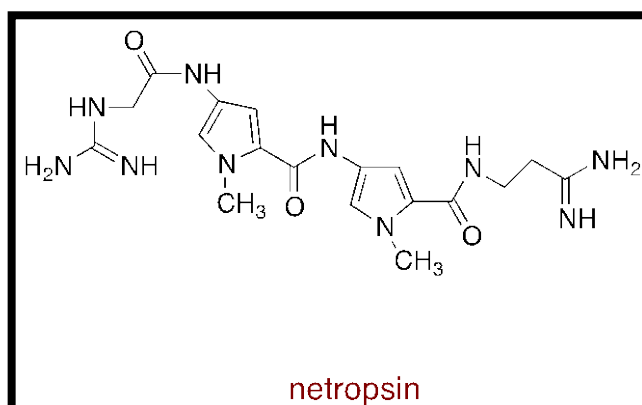
Figure 6. Groove binding agent netropsin

1.5.2.3. Intercalating agents

Intercalating agents are flat aromatic or hetero-aromatic molecules, which slide and stack at proper sites between adjacent DNA base pairs leading to significant π-electron overlap and double helix distortion.[40,46,47,54,57,58,49] These compounds stack perpendicular to DNA backbone and bind to DNA non-covalently in a reversible manner without breaking up the hydrogen bonds between the DNA base pairs. The stability of the DNA-intercalator complex is sustained with van der Waals, hydrophobic, hydrogen bonding and charge transfer forces. When an intercalating agent is inserted between DNA base pairs, a decrease in the DNA helical twist and lengthening of the DNA occurs, consequently delaying or preventing cell replication and growth. Therefore, DNA intercalating compounds are widely used in chemotherapeutic treatment to inhibit DNA replication in rapidly growing cancer cells.[47,48]

DNA- intercalating agents which impair the stability of DNA double helix can be either mono or bis-intercalators.

Monointercalating agents

Monointercalating compounds are able to intercalate between double stranded DNA but can also bind single-stranded DNA with high affinity. An example of well known monointercalating agent is acridine orange (Figure 7).[44]

Bis-Intercalating agents

Bis-intercalating agents have two potential intercalating rings systems connected by linkers, which can differ in rigidity and length.[48] An example of cyclo-bis-intercalator that exhibited DNA unwinding properties is bis-acridine A (Figure 7).[44]
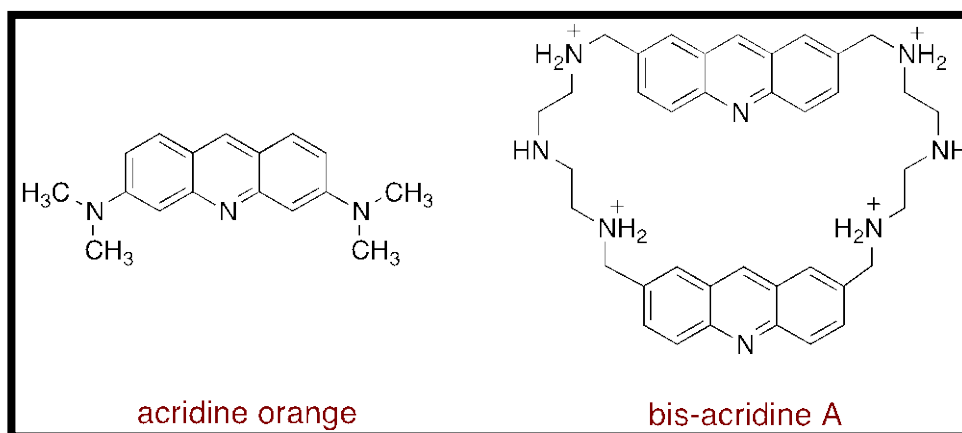
Figure 7. Mono and bis intercalating compounds

1.5.3. Techniques used to study drug–DNA interactions

Experimentally there are a variety of techniques, which can be performed to study drug-DNA interaction; in the present study five different techniques were used, which are DNA thermal denaturation studies, DNA-drug complex co-crystallization, UV-Visible spectroscopy, fluorescence spectroscopy and antimicrobial activity also investigated against a gram positive strain (*Escherichia coli*) and a gram negative strain (*Staphylococcus aureus*).

1.5.3.1. DNA thermal denaturation assay

The term DNA denaturation means the melting of a DNA double strand to generate two single strands by breaking the hydrogen bonds between the base pairs in the double helix. DNA thermal denaturation refers to the heat treatment over a critical temperature leading to denaturation of DNA double helix into single strand components in the presence or absence of a drug.[54,59,60] The most common method to study the DNA melting transition is investigating the alteration in ultraviolet (UV) absorbance of a dilute DNA solution with gradual increase in the temperature.[41,61] DNA absorbs the UV light strongly at 260 nm and by increasing the temperature the melting of DNA increases as well as the absorbance until the complete denaturation of the DNA happens and the absorbance remains constant in any further heating after DNA melting.[59] The temperature at which half of the DNA is denatured is called the melting temperature (*Tm*). Also it means the half of DNA bases of a single strand do not interact with their complementary bases on the other strand and *Tm* values normally fall between 50 °C and 100 °C.[22,46] When the DNA is monitored by UV spectroscopy and the temperature elevated gradually, a sigmoidal curve is obtained from

absorption data, which determines the *Tm* value and represents DNA denaturation. When the same DNA is complexed with an intercalator or other DNA binding molecule and monitored by UV spectroscopy under the same thermal conditions, another sigmoidal curve is obtained but this time the curve is shifted to higher temperature compared to the curve that obtained from DNA without any intercalator. The *Tm* value of DNA-intercalator complex is always higher than the *Tm* value of the DNA alone due to the high stability of the DNA-drug complex (Figure 8).[46]
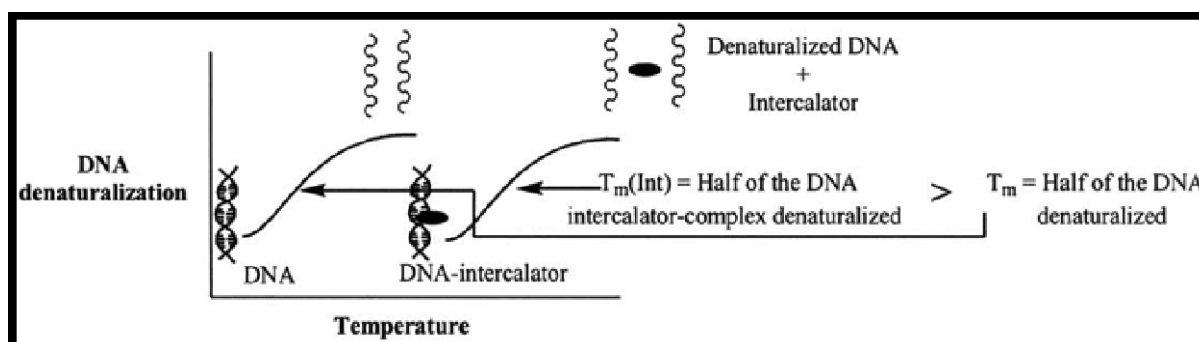
Figure 8. Curve of temperature vs. DNA denaturation in the presence or absence of DNA-intercalating agent

1.5.3.2. DNA crystallization method

Macromolecular X-ray crystallography is an important method for determining the three-dimensional structure of DNA-drug complexes. DNA crystallography has the same experimental and basic theoretical foundations as protein crystallography. The main steps in DNA and protein crystallography are crystal growth and X-ray diffraction data collection. However, there are some variations in the methods of crystal growth and, data collection between DNA and protein crystallography. In DNA crystallography the quality and the quantity of the required materials is critical and the complications in crystal growth can be affected by the source or nature of the biological material.

There are several procedures to crystallize biological macromolecules and all of which aim to bring the biological macromolecules solution to a supersaturation state and many parameters affect the crystallization of macromolecules. While stabilization, purification, storage and handling of macromolecules are also critical steps prior crystallization process.[37] In addition, intrinsic physico-chemical parameters such as, supersaturation (concentration of macromolecules and precipitants), temperature, pH, purity and ionic strength of the buffer, pressure, magnetic and electric field, viscosity effects and the

difference in concentration between DNA/drug solution and the crystallizing (dehydrating) solution are important factors. The biochemical and biophysical parameters including binding of ligands (cofactors, substrates), purity of the macromolecules and possible bacterial contamination are very significant in crystallization of the DNA. Moreover, nucleation and crystal growth can be affected by the method used. Thus it advisable to try a range of crystallization methods to achieve the best crystallization.[62]

Crystallization by vapour diffusion methods

The most common method in macromolecules crystallization is the vapour diffusion technique, first used for tRNA (transfer ribonucleic acid) crystallization. It is suitable for very small volumes less than 2 µL. The principle of this technique is based on crystallization of a biological macromolecule in a droplet with buffer, crystallizing agent and additives, which is equilibrated against a reservoir containing a solution of crystallizing agent more concentrated than the droplet. Equilibration occurs by diffusion of the volatile substances such as organic solvent or water molecules, until the vapour pressure of the reservoir and the vapour pressure in the droplet become the same. The droplet volume changes when the equilibration happens by water exchange from the droplet to the reservoir leading to changes in the concentrations of all droplet components. This principle relates for three crystallization methods, hanging drop, sitting drop and sandwich drop (Figure 9).[62] If crystallization is successful the drop containing the crystals can be taken up in a capillary for transfer to the X-ray diffractometer.
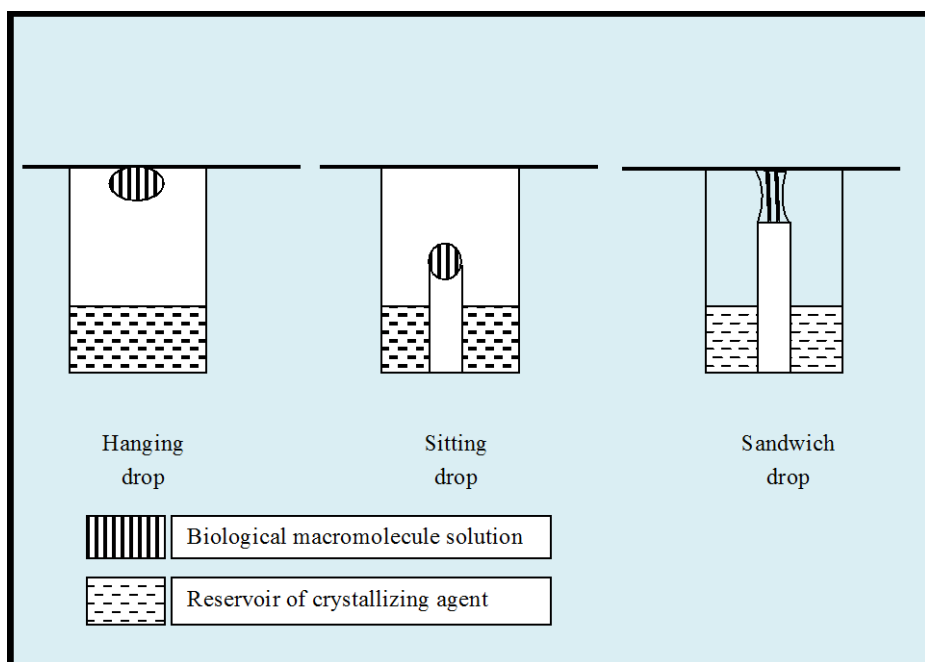
Figure 9. Schematic representation of crystallization by vapour diffusion methods

1.5.3.3. UV-visible absorption spectroscopy

UV-visible absorption spectroscopy is one of the most common and the simplest technique that is used to study both the stability of DNA and their interactions with small molecules. UV-visible absorption spectroscopy can be used to study and investigate the DNA-Drug interactions by monitoring the alterations in the absorption properties of the DNA molecule or drug molecule. Normally, the molecules used as ligands display an absorption band, which can be easily distinguished in the visible region. To identify whether there is any interaction between the DNA and the molecule the simplest way is study the shifting of the position of the maximum of this band from when the drug is free in solution to when the drug is bound to DNA. It has been assumed that the strength of the interaction between the DNA and the ligand could be indicated with the magnitude of this shift.[47,63] DNA UV-visible absorption spectra show a broad band (200-350 nm) in the UV region with a maximum absorption at 260 nm and the absorbance ratios (A_{260} / A_{280} and A_{260} / A_{230}) can indicte the purity of DNA. This ratio should be in the range of 1.8-1.9 to ensure that DNA is sufficiently free of protein.[47]

1.5.3.4. Fluorescence spectroscopy

Fluorescence spectroscopy is another important technique that used to investigate the interactions between DNA and small ligands molecules. The high sensitivity and the selectivity are the main advantages of molecular fluorescence over other techniques. The

data of the fluorescence spectra are normally obtainable as emission spectra, which is a plot of the fluorescence intensity versus wavelength (nm) or wavenumber (cm^{-1}). Emission spectra differ significantly and are related to the chemical structure of the compounds and the solvent that used to dissolve it. Compounds containing aromatic functional groups with low-energy π-π transition levels have a large number of transitions and more intense and useful fluorescence compared to compounds containing aliphatic and alicyclic carbonyl structures or highly conjugated double-bond structures.[47,64] In this technique and in the various analytical tools based on fluorescence emission the mode of DNA-drug binding can be determined. The fluorescence intensity normally increases with the effective interaction between the molecule and DNA. Hence, in case of intercalating compounds, the molecules are inserted between DNA base pairs of the double helix. The rotation of the unbound molecules favors the radiationless deactivation of the excited state, but a significant increase in the fluorescence emission is observed if the molecules are bound rigidly in the DNA. The opposite is the case for groove binding compounds and a decrease in the fluorescence intensity will observed in the presence of DNA because the molecules are exposed on the outer surface of the helix where they can interact with external fluorescence quenchers in the surrounding solution.[47,65,66]

1.5.3.5. Antimicrobial activity

In medicinal chemistry a considerable and critical part of the preclinical evaluation of any novel compound involves characterisation and judging its influence on bacteria in *vitro*. The antibacterial activity of the compound is determined by its ability to selectively interfere with bacterial growth and survival. In drug development these important stages are sometimes difficult as they are between the highly challenging antibacterial discovery process and difficult task of demonstrating safety and efficacy in *vivo*.[67] Disk diffusion method is one of the oldest methodologies for antimicrobial susceptibility assay, and still one of the most widely used antimicrobial susceptibility investigation methods in routine clinical laboratories.[68] The protocol of disk diffusion method is based on saturated small disks 6 mm in diameter with different concentrations of test compound, which are stacked in solidified inoculated agar with the examined bacterial strain in petri dishes. The plate is allowed to incubate at 37 °C for 24 h or 48 h. If the compound has antimicrobial activity it will show a clear zone around the disk and the zone edge should be judged with the naked eye with the plate held about 30 cm from the eye.[69] Criteria for activity is based on inhibition zones (mm); an inhibition zone of more than 20 mm indicates significant

activity, for 18-20 mm inhibition is good, 15-17 mm is low, and below 11-14 mm is non-significant activity.[70]

Chapter 2
Results and Discussion

2. Results and discussion

2.1. Aim of the project

The aim of this study was to synthesise novel heteroarene and fluorinated heteroarene compounds with potential bioactivity. In particular for the synthesis of new heterocycles, it was planned to exploit the easy S_NAr reaction of fluorinated arenes such as hexafluorobenzene and pentafluoropyridine to introduce a range of groups, specifically nitriles, benzimidazoles, carbazoles and benzamides which will allow subsequent ring fusion processes to be carried to generate polycyclic structures, which could act as DNA intercalators or allow biaryl type links to be set up to generate conformationally flexible polyaryl systems with potential activity for DNA groove binding (Scheme 17).

Scheme 17. General approach to ring forming reactions
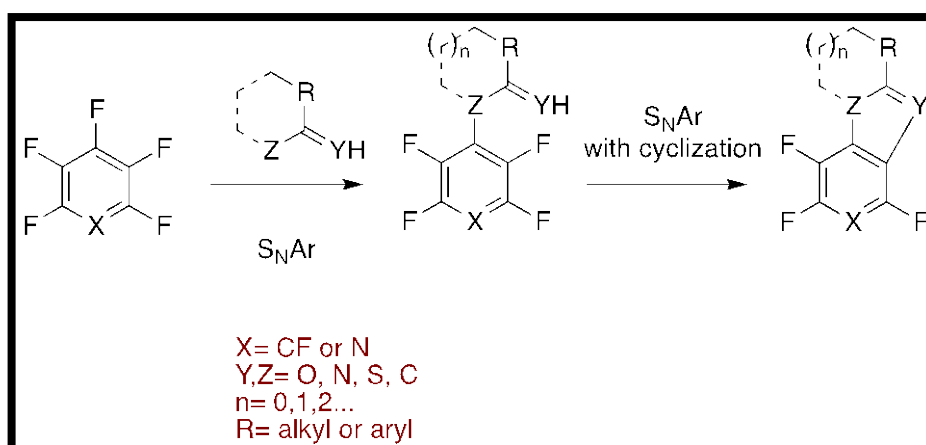
In addition consideration and investigation of the biological activity of the synthesised compounds as DNA binding molecules or antimicrobial agents was to be carried out using DNA thermal denaturation assay, UV absorption, ethidium bromide fluorescence displacement experiments, DNA-compound co-crystallization and antimicrobial activity assays.

The main key to this work was to study possible interactions between the synthesised compounds as possible groove binding, or intercalating agents, with DNA base pairs by different binding mechanisms including hydrogen bonding and electrostatic forces.

2.2. Organic synthesis

In medicinal chemistry N-heterocycles are very important compounds because of their biological and technological significance. Nitrogen plays an important role in the interaction of small molecules and drug targets, and the large percentage of presently used drugs contain N-heterocyclic moieties.[71] These compounds have a remarkable synthetic importance and their utilization in organic synthesis is useful. Moreover, organic scientists have studied the preparation of N-heterocycles from useful starting materials intensively. For example N-heterocycles can be synthesise from nitro compounds, nitrile compounds or amino compounds or their derivatives containing a nitrogen atom.[72]

Research in the group involves using perfluoroarenes, many of which are now commercially available, as convenient starting materials for heterocyclic synthesis where new rings can be readily formed by S_NAr reaction using appropriate bis-nucleophilic precursors.

2.2.1. Synthesis of fluorinated benzonaphthyridine derivatives

Naphthyridine and their benzonaphthyridine derivatives are compounds of current interest in medicinal chemistry due to their wide spectrum of biological activities such as antibacterial, antiviral and anticancer activity.[73,74] This class of compounds have been studied intensively and it has been reported by Ferraris and co-workers[75] that compound 5H-5,6-dihydrobenzo[c][1,8]naphthyridine (Figure 10) is an active benzonaphthyridine derivative which used in treatment the ischemic injuries.[75]

5H-5,6-dihydrobenzo[c][1,8]naphthyridine
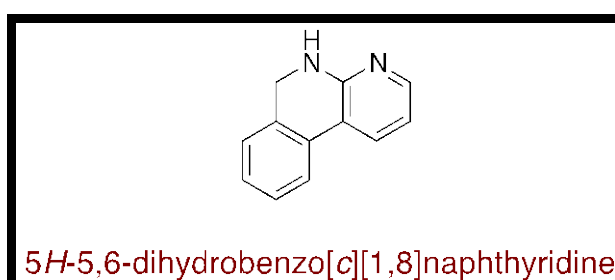
Figure 10. Example of an active benzonaphthyridine derivative

As mentioned before the fluorine atom can change the biological properties of organic compounds by influencing its metabolism. That because of the specific physicochemical characteristics of fluorine atom which increase the lipophilicity of the compound, its small van der Waals radius and high electronegativity, which make it very similar to hydroxyl group and allow the fluorine atom to be a valuable resource for enhancing the therapeutic

efficacy of biologically active compounds.[76] Based on the above interest it was decided to design and synthesise fluorinated benzonaphthyridine derivatives using pentafluoropyridine as readily available starting material. Reaction of pentafluoropyridine **21** with ethyl 2-nitrophenylacetate **41** was expected to give tetrafluoropyridine derivative **42** (Scheme 19), the precursor to a benzonaphthyridine **43a** or **43b** (Scheme 20).

The first step of the reaction was the esterification of 2-nitrophenylacetic acid **40** using ethanol and H_2SO_4 (Scheme 18). The target product 2-nitro-phenyl-acetic acid ethyl ester **41** was afforded after recrystallization as pale yellow crystals with 37 % yield. ^{1}H NMR spectroscopy proved the successful synthesis of the target product by showing the expected signals of the aromatic and the aliphatic protons, δ_H (400 MHz, $CDCl_3$) 8.13 (1H, dd, J 8.4 and 1.2 Hz), 7.60 (1H, td, J 7.2 and 1.2 Hz), 7.48 (1H, td, J 8.4 and 1.6 Hz), 7.36 (1H, dd, J 7.6 and 0.8 Hz), 4.18 (2H, q, J 6.8 Hz), 4.02 (2H, s), 1.26 (3H, t, J 6.8 Hz). Moreover mass spectrometry showed the correct mass of compound **41**, HRMS (ESI) m/z found 232.0576, $C_{10}H_{11}NO_4Na^+$ requires 232.0580.

Scheme 18. Esterification of 2-nitrophenyl acetic acid
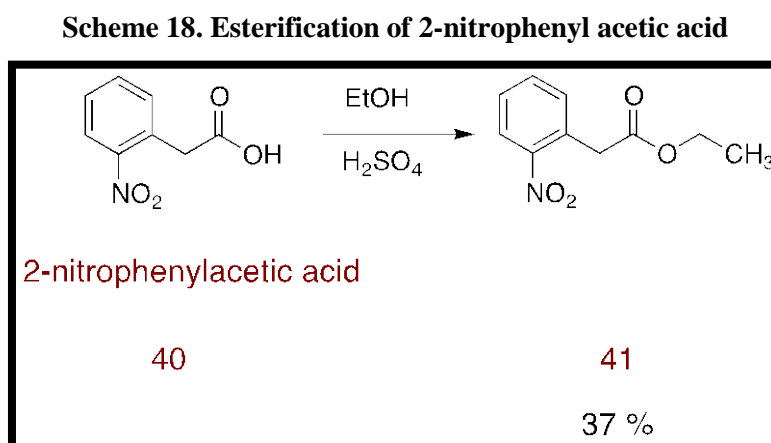
The second step for the synthesis of the fluorinated benzonaphthyridine derivative was the reaction of ethyl ester **41** with one equivalent of pentafluoropyridine in the presence of NaH as base and dimethylformamide (DMF) as a solvent to form tetrafluoropyridine derivative **42** (Scheme 19). By adding ethyl ester **41** to a stirred suspension of NaH in DMF fizzing was observed in the mixture indicating that ethyl ester **41** deprotonated and then reacted with pentafluoropyridine by S_NAr reaction. The reaction was successful but due to the low yield (13 %) of product **42** and detection of the starting material and some impurities with ^{1}H NMR spectroscopy, the number of moles of pentafluoropyridine increased to enhance the chance of the combination between pentafluoropyridine and

ethyl ester **41** to give larger yield of fluorinated ethyl ester **42**. Moreover the reaction condition was modified by using THF instead of DMF as this was easier to remove. Stirring under a N_2 atmosphere at RT for 24 h then improved the yield to 93 %. ^{19}F NMR spectroscopy proved the successful synthesis of the target product **42** and showed two multiplet signals for two pairs of fluorine atoms in the range 72.91-72.73 (2F, m) and 21.17-20.99 (2F, m). Mass spectrometry found the expected mass for the tetrafluoropyridine derivative **42**, HRMS (ESI) *m/z* found 357.0512 (M−H)$^{-}$ $C_{15}H_9F_4N_2O_4$ requires 357.0504. IR spectroscopy showed the expected signals for the main functional groups in the compound **42** with the following signals v_{max}/cm^{-1} (film) 1737 (C=O), 1531 (NO$_2$), 1348 (NO$_2$).

Scheme 19. Reaction of pentafluoropyridine with 2-nitrophenyl acetic acid ethyl ester (41)
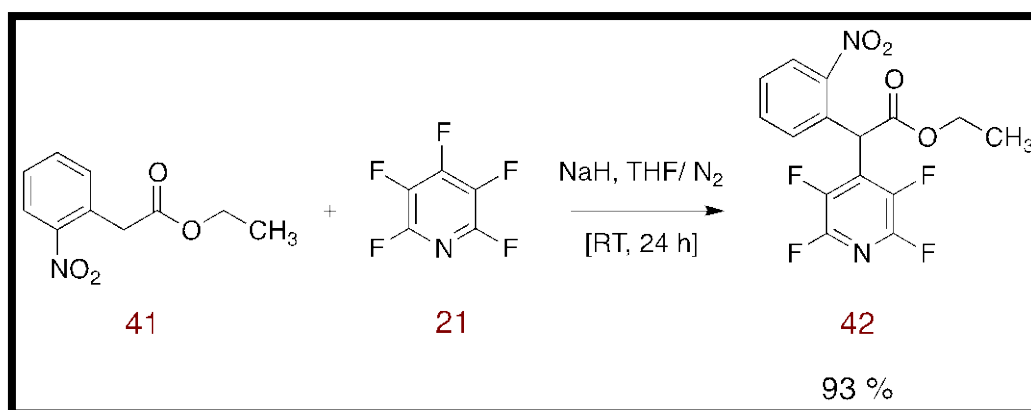
It has been reported that nitro compounds could be successfully cyclized to nitrogen heteroaromatic structures by heating them with reducing agents such as metallic iron.[77] It was hoped that heating compound **42** in the presence of metallic iron and HCl (aq) would allow the reduction of nitro group to an amino group which consequently could substitute one fluorine atom and form tricyclic structure by S$_N$Ar reaction (Scheme 20). The data analysis suggested that the fluorinated ethyl ester **42** had reacted and orange crystals were afforded. Mass spectrometry found the expected mass ion for the cyclized compound **43a**, HRMS (ESI) *m/z* found 307.0705 (M−H)$^{-}$, $C_{15}H_{10}F_3N_2O_2$ requires 307.0700. Unfortunately ^{19}F NMR spectrum was quite complicated and displayed a number of signals, which could not be fully interpreted. Some signals could have been due to nitroso or hydroxylamine intermediates which had not cyclized to the fluorinated dihydro benzonaphthyridine **43a** or **43b**. The spectroscopic data suggests some of the product **43a**

had formed but the material could not be obtained completely pure.

Scheme 20. Cyclization of fluorinated ethyl ester (42)
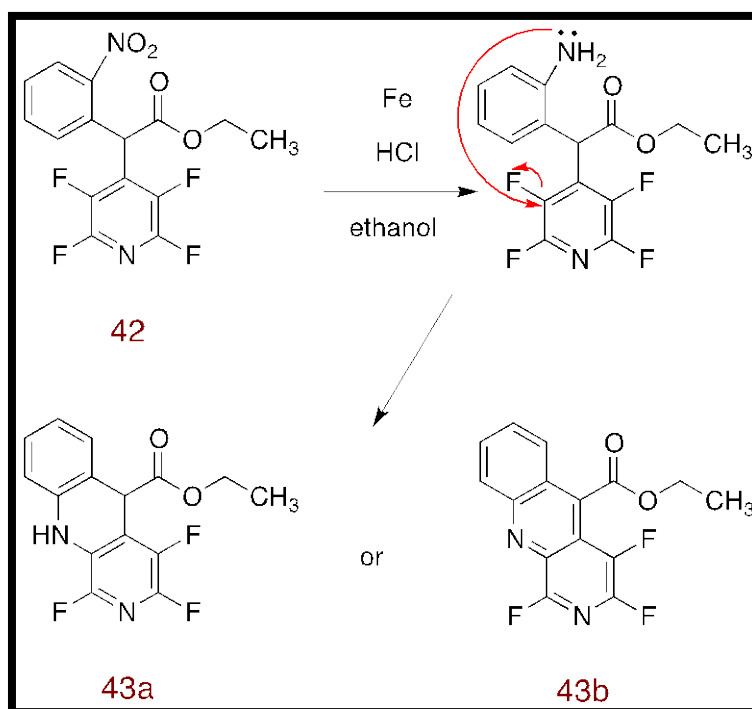
2.2.2. Synthesis of fluorinated indole heterocycles using pentafluorotoluene

In drug discovery the indole scaffold is one of the most important subunits for developing and synthesizing new drug candidates. Extensive research on indole chemistry has increased the number of biologically active synthetic compounds and natural products. A variety of indole containing compounds demonstrate a good therapeutic effect as anti-inflammatories.[78] Synthesis of fluorinated indole organic compounds will affect significantly the biological activity of the compounds and should lead to an improvement in the pharmacodynamic and pharmacokinetic characteristics of the compound.[76] Although several approaches have been developed in the field of indole synthesis, fluorinated analogues indole based biologically active compounds are not well known.[76] Because of that we designed some fluorinated indole based compounds using pentafluorotoluene as a core scaffold and as a source of fluorine atoms and reacted it with a range of different nitrile compounds. The reaction was based on deprotonation of the methyl group in pentafluorotoluene with NaH, and addition of the anion to a nitrile group, followed by nucleophilic substitution of the neighboring fluorine atom by the resulting imine anion, to generate novel fluorinated indole derivatives (Scheme 21). The proposed

compounds could then be further elaborated into intercalators or groove binders, or tested directly for anti-microbial activity.

Scheme 21. Proposed mechanism of the reaction of pentafluorotoluene with nitrile groups
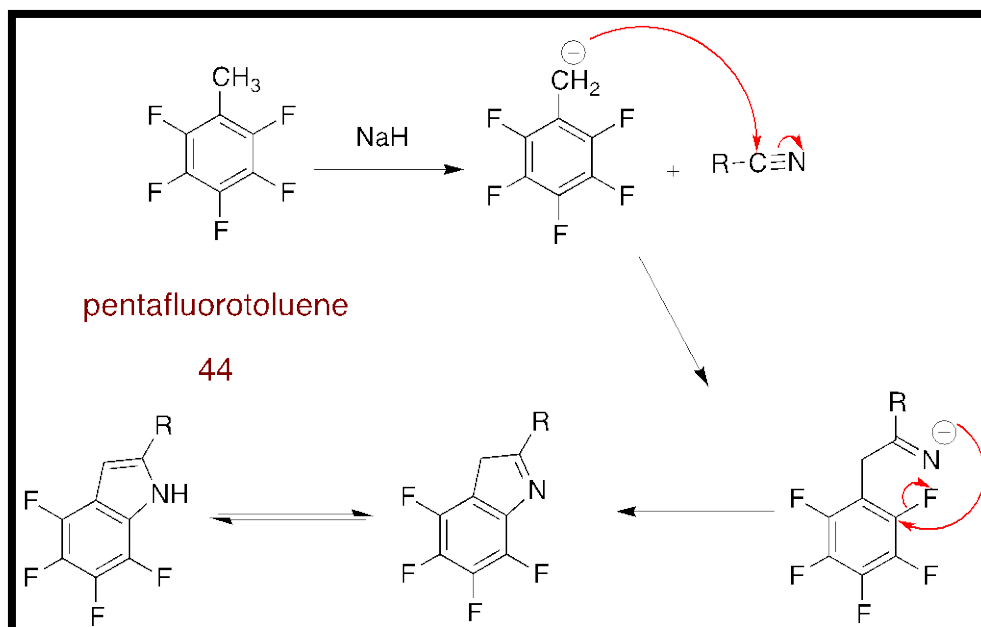
2.2.2.1. Reaction of pentafluorotoluene with benzonitrile

Reaction of pentafluorotoluene **44** with benzonitrile **45** in the presence of NaH as base and THF as solvent worked well at RT and compound **46** was formed successfully (Scheme 22). ^{19}F NMR spectroscopy showed four different signals corresponding to four fluorine atoms, δ_F (376 MHz, CDCl$_3$) 17.21-17.18 (1F, m), 17.15-17.11 (1F, m), 2.99-2.96 (1F, m), 2.93-2.90 (1F, m). The ^{1}H NMR spectrum showed a singlet at 7.28 for the indole H-3 proton and signals for the phenyl group. The NH signal could not be observed. In addition, mass spectrometry found the expected mass of the target compound **46**, HRMS (ESI) m/z found 264.0446 (M–H)$^-$, C$_{14}$H$_6$F$_4$N requires 264.0442, and IR analysis detected a broad signal at 3066 v_{max}/cm^{-1} for the N-H group. Different nitrile groups have been studied to synthesise a series of fluorinated indole novel compounds using pentafluorotoluene as core scaffold (Table 1).

Scheme 22. Reaction of pentafluorotoluene with benzonitrile

benzonitrile

44   45   46
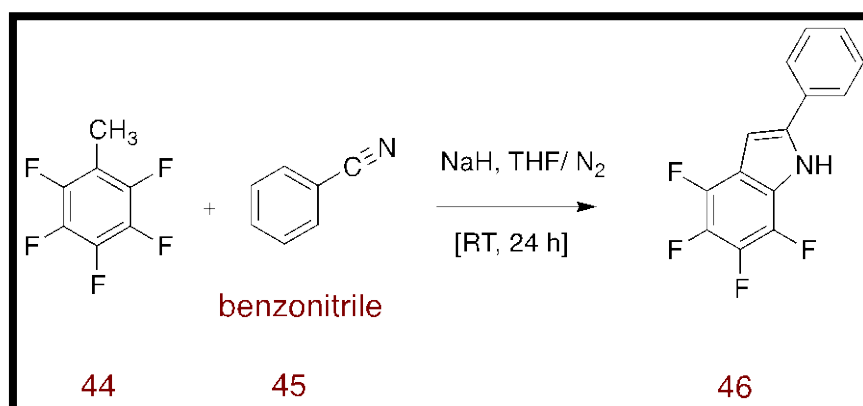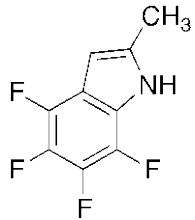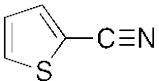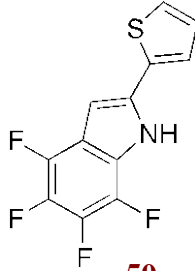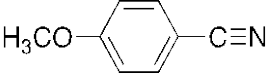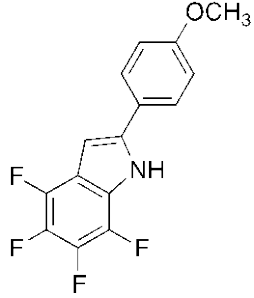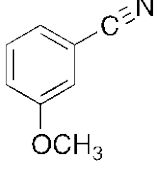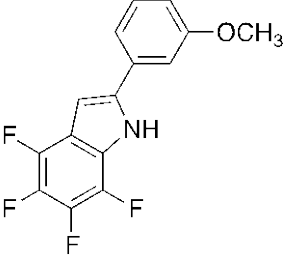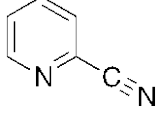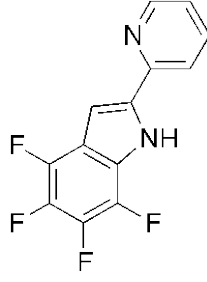
Table 1. Reaction of different nitriles with pentafluorotoluene

R	Results	Conditions	Expected product	Yield %
H$_3$C−C≡N acetonitrile **47**	Indole formed	Acetonitrile used as a solvent, RT (24 h), NaH	**48**	52 %
2-thiophenecarbonitrile **49**	Two un identified products formed	1) DMF, NaH, RT (24 h). 2) THF, NaH, 66 °C (24 h).	**50**	-
4-methoxybenzonitrile **51**	No indole	1) DMF, NaH, RT (24 h). 2) THF, NaH, RT (24 h). 3) DMF, NaH, at 80 °C. 4) THF, NaH, reflux at 66 °C.	**52**	-
3-methoxybenzonitrile **53**	No indole	1) DMF, NaH, RT (24 h). 2) THF, NaH, RT (24 h).	**54**	-
2-pyridinecarbonitrile **55**	Un expected triazine **57** (Scheme 23)	THF, NaH, RT (24 h).	**56**	-

Reaction of acetonitrile **47** with pentafluorotoluene **44** was studied under different conditions. In the presence of a mixture of DMF and THF as solvents at RT, or heated at 60 °C, unfortunately the reaction did not work well, and the ^{1}H and ^{19}F NMR spectra were complicated. Moreover IR analysis detected a signal at 2222 v_{max}/cm^{-1}, which suggested the presence of the starting nitrile group in the sample. Because of that it was then decided to do the reaction in concentrated solution using acetonitrile as solvent. Interestingly the reaction worked well and the target fluorinated indole derivative **48** was afforded in 52 % yield (Table 1). ^{19}F NMR spectroscopy proved the presence of four fluorine atoms in the product by detecting four multiplet signals, δ_F (376 MHz, CDCl$_3$) 20.63-20.59 (1F, m), 20.08-19.99 (1F, m), 17.23-17.14 (1F, m), 2.99-2.91 (1F, m). Mass spectrometry found the expected mass for the target product **48**, HRMS (ESI) m/z found 202.0289 (M–H)$^-$, C$_9$H$_4$F$_4$N, requires 202.0285. Unfortunately all attempts to crystallize the oily product failed.

2-Thiophenecarbonitrile **49** was reacted with pentafluorotoluene **44** under different conditions and the results were quite different. In the presence of DMF as solvent IR spectrum showed a signal for the starting nitrile, v_{max}/cm^{-1} (film) 2226 but ^{19}F NMR spectroscopy suggested the formation of the target compound **50** (Table 1) as a major product by detecting four different fluorine signals. Mass spectrometry found the exact mass for the target product **50**, HRMS (ESI) m/z found 270.0011 (M–H)$^-$, C$_{12}$H$_4$F$_4$NS requires 270.0006. ^{1}H NMR spectroscopy showed the expected signals for the thiophene ring protons of the target product but the proton in the indole ring was not observed, as it is expected to be around 7.1-7.3 ppm but it could be masked with chloroform signal. Unfortunately, the product was afforded as yellow oil and TLC showed tailing because of that it was not possible to purify the product and it was decided to change the reaction conditions to get better results. Using boiling THF as solvent rather than DMF the results also changed, interestingly the starting nitrile signal was not detected in the IR spectrum and mass spectrometry found the expected mass for the target product **50**, However, ^{19}F NMR spectroscopy was unexpected and showed two different patterns of multiplet signals in the range 17.20-17.10 (m) and 3.00-2.90 (m). Moreover, the ^{1}H NMR spectrum also could not show the indole ring proton expected at 7.1-7.3 ppm. The product was crystallized but sadly the crystals were powder like and not suitable for X-ray crystallography because of that it was not possible to identify the product that formed.

Reaction of 4-methoxybenzonitrile **51** with pentafluorotoluene **44** was studied in various conditions to synthesise compound **52** (Table 1). Different solvents were used at RT such as DMF and THF and NaH as base, unfortunately the reactions did not work well and ^{1}H NMR spectroscopy detected the expected signals of the starting material and IR spectroscopy showed a sharp signal for starting nitrile group at 2218 v_{max}/cm^{-1}. Because of that the reaction was heated for 24 h at 80 °C in DMF as solvent, or at 66 °C in THF as solvent. Unfortunately the reactions did not work and the starting material was identified with spectroscopic analysis. The failure of the 4-methoxybenzonitrile **51** to react may have been due to the lower electrophilicity of the nitrile group, which is conjugated to the electron donating methoxy group. Because of that it was decided to try 3-methoxybenzonitrile **53** which could be more electrophilic as methoxy group not in the *para* position and that might prevent the easy donation of electrons from methoxy group. Again the reaction did not work by using THF or DMF as solvents at RT and the target compound **54** was not afforded and starting material was detected with ^{1}H NMR spectroscopy. Also mass spectrometry could not find the target product as well as the TLC, which showed only one spot corresponding to the starting material.

In the reaction of 2-pyridinecarbonitrile **55** with pentafluorotoluene **44** interestingly an unexpected complex compound formed rather than the target compound **56** (Table 1), in the presence of NaH as base and THF as solvent at RT. Pentafluorotoluene **44** did not react with 2-pyridinecarbonitrile **55** but the latter reacted with two further 2-pyridinecarbonitrile **55** molecules forming the triazine compound **57** (Scheme 23). In addition the triazine then co-crystallized with a molecule of pyridine-2-carboxamide, which must have formed by reaction of the nitrile **55** with traces of water present in the reaction mixture. ^{1}H NMR spectroscopy confirmed the product had been formed by detecting several doublet and triplet signals for aromatic rings between 7-9 ppm. Moreover, ^{19}F NMR spectroscopy suggested the absence of fluorine atoms in the sample and the final evidence of the synthesis of the unexpected product was obtained with X-ray crystallography (Figure 11). The X-ray structure showing how the amide group forms hydrogen bonds to two of the pyridine substituents of the triazine.

Scheme 23. Attempted reaction of pentafluorotoluene with 2-pyridinecarbonitrile
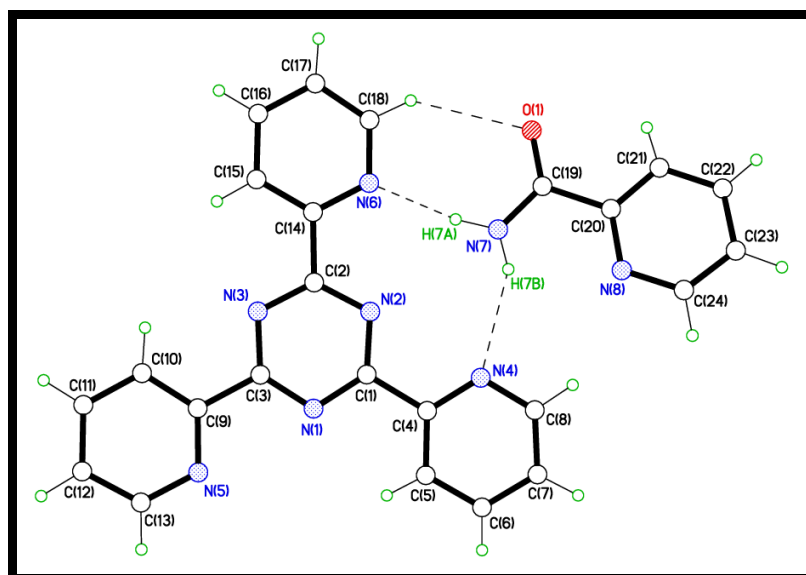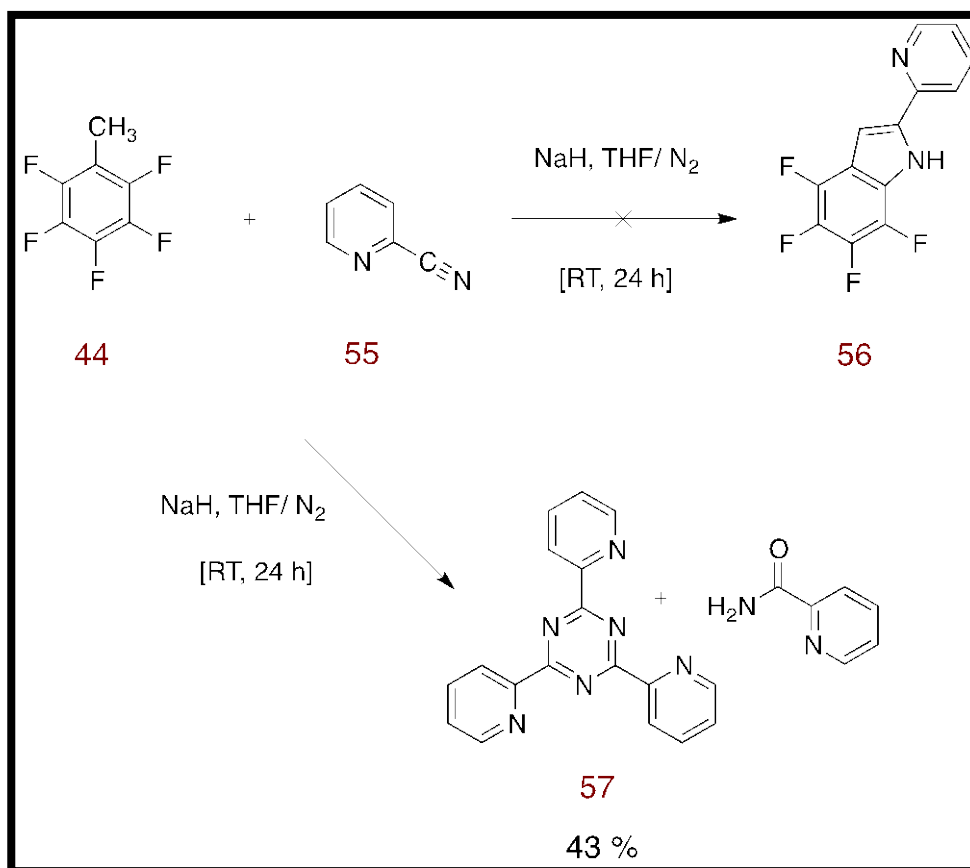
Figure 11. X-ray crystal structure of complex (57)

2.2.3. Synthesis of thiazole and pyrazole heterocycles

Thiazole derivatives are becoming increasingly important in the pharmaceutical industry and they have a variety of applications in the field of medicinal chemistry. Dawood *et al*., 2013 reported that thiazole derivatives showed strong anticancer activity on a human lung cancer cell line. Moreover, thiazole derivatives act as anti-inflammatory agents and showed their anti-cancer activity by reporting their inhibitory profile against human hepatocellular carcinoma cell line.[79] It is considered several thiazole scaffolds have an excellent anti-cancer activity by inhibiting the epidermal growth factor receptor-tyrosine kinase enzyme such as the pyrazolyl thiazole derivative (Figure 12) which plays a critical role in cell growth regulation.[79]
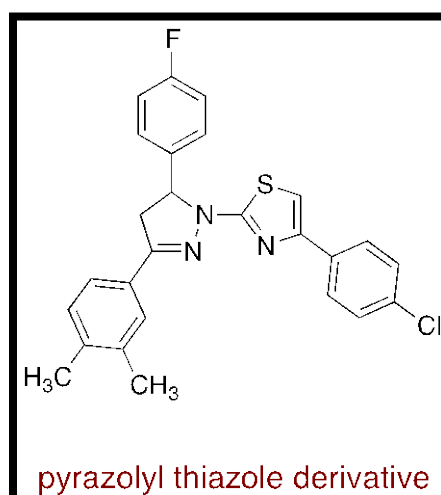
Figure 12. Pyrazolyl thiazole derivative

Pyrazole and N-substituted pyrazoles derivatives have several chemical and pharmaceutical applications due to their versatile biological activities. It has been reported that pyrazoles involved in several active compounds, can act as antimicrobial, antitumor, antileukemia, antidepressant and antifungal agents. Interestingly a typical model of pyrazole containing a diaryl-heterocyclic template celecoxib (Figure 13) proved its activity as safe gastrointestinal anti-inflammatory agent by selective inhibition of cyclooxygenase enzyme.[80]
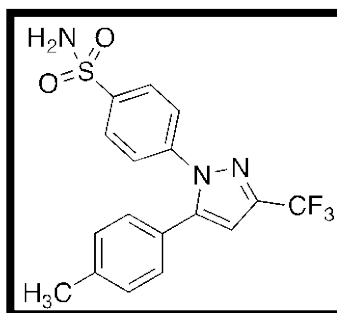
Figure 13. The structure of celecoxib

As a result of a remarkable pharmacological efficiency of thiazole and pyrazole derivatives, and in continuation of the authors' efforts to synthesise new anticancer agents, it was planned to design a series of novel fluorinated thiazole and pyrazole compounds using pentafluoropyridine, hexafluorobenzene and pentafluorobenzaldehyde as starting materials in order to evaluate their biological activity, while also studying the synthetic and mechanistic aspects of the reactions.

2.2.3.1. *Synthesis of fluorinated thiazole derivatives using pentafluoropyridine and thiobenzamide*

Pentafluoropyridine **21** was reacted with thiobenzamide **58** with the hope of forming thiazole **60** (Scheme 24). However in practice, reaction of pentafluoropyridine **21** and thiobenzamide **58** did not work well in the presence of NaH as base and DMF as solvent and the target product **60** was not afforded. The data analysis suggested the unstable compound **59** was formed but it broke down to benzonitrile **61** and tetrafluoropyridine-4-thiol **62** which is reversibly converted to tetrafluoro1*H*-pyridine-4-thione **63** and that was proved with IR spectrum which detected the nitrile group of benzonitrile, v_{max} / cm^{-1} (film) 2222. ^{19}F NMR spectroscopy detected two multiplet peaks in the range 74.16-73.94 (2F, m) and 26.88-26.72 (2F, m) which could correspond to either the tetrafluopyridine-4-thiol **62** or tetrafluoro-1*H*-pyridine-4-thione **63**. In addition mass spectrometry found the expected mass for tetrafluoro-pyridine-4-thiol **62** or tetrafluoro-1*H*-pyridine-4-thione **63**, HRMS (ESI) *m/z* found 181.9692 (M–H)$^{-}$, C$_5$F$_4$NS, requires 181.9693 and IR spectrum detected N-H signal, v_{max} / cm^{-1} (film) 3460 (N-H). Interestingly by changing the solvent from DMF to THF this was not the case, and the compound **59** was afforded after column chromatography purification as a yellow oil (0.914 g, 80 %). ^{1}H NMR spectroscopy showed the expected signals for the aromatic protons of the benzene ring, δ_H (400 MHz

CDCl$_3$) 7.68-7.48 (5H, m), 7.29 (1H, bs, NH) and mass spectrometry displayed the exact mass for the compound **59**, HRMS (ESI) *m/z* found 286.0273, C$_{12}$H$_6$F$_4$N$_2$S requires 286.0182. Nitrile signal did not appear in the IR spectrum and that proved the compound **59** did not break down to benzonitrile **61** and tetrafluoropyridinethiol **62**, moreover ^{19}F NMR spectroscopy exhibited two multiplet peaks for two pairs of fluorine atoms in the range 74.27-74.03 (2F, m) and 27.01-26.83 (2F, m).

To avoid the breakdown of compound **59** which may be catalyzed by base it was attempted to cyclize the compound **59** by heating in THF at 66 °C without any base, but unfortunately the cyclization reaction did not work, and the starting compound was detected by ^{19}F NMR spectroscopy, which showed the same two multiplet signals of the starting compound.

Scheme 24. Reaction of pentafluoropyridine with thiobenzamide

21 + thiobenzamide 58 → NaH, THF / N₂ [RT, 24 h] → 59 80 %

[RT, 24 h] NaH, DMF / N₂

59

THF [Reflux 66 °C, 24 h]

60

2,3,5,6-tetrafluoro-pyridine-4-thiol 62 + benzonitrile 61

2,3,5,6-tetrafluoro-1*H*-pyridine-4-thione 63
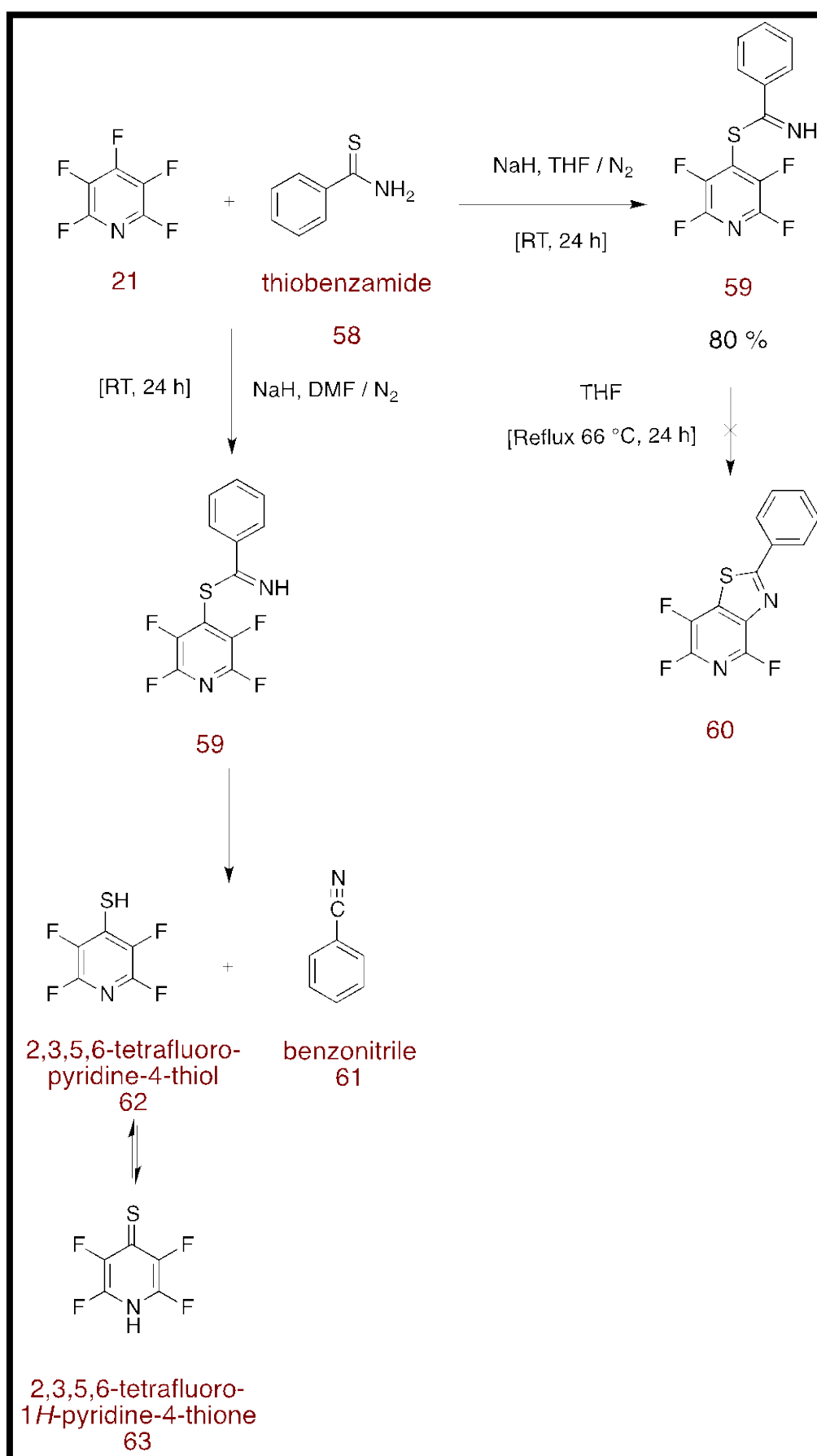
2.2.3.2. Synthesis of fluorinated thiazole derivatives using pentafluoropyridine and naphthalene-1-thiocarboxamide

Reaction of pentafluoropyridine **21** with naphthalene-1-thiocarboxamide **64** aimed to synthesise the heterocyclic compound **66** (Scheme 25) which could show potential DNA binding activity. Compound **65** was formed and it was again shown to be unstable with break down to naphthalene-1-carbonitrile **67** and tetrafluoropyridine-4-thiol **62** which is reversibly converted to tetrafluoro-1*H*-pyridinethione **63** as was observed previously. The occurrence of naphthalene-1-carbonitrile **67** was proved with mass spectrometry and the expected mass was displayed, HRMS (ESI) *m/z* found 153.0584, $C_{11}H_7N$ requires 153.0584, and IR detected the nitrile group signal, v_{max} / cm^{-1} (film) 2224 (C≡N). In addition ^{1}H NMR spectrum showed the aromatic rings signals between 7-8 ppm for naphthaline-1-carbonitrile **67**, δ_H (400 MHz, DMSO-d$_6$) 8.33 (1H, d, *J* 8.4 Hz), 8.18 (1H, dd, *J* 7.2 and 0.8 Hz), 8.13 (2H, t, *J* 8.0 Hz), 7.82(1H, td, *J* 7.2 and 1.2 Hz), 7.74 (1H, td, *J* 7.2 and 1.2 Hz), 7.69 (1H, dd, *J* 8.4 and 7.2 Hz). The ^{19}F NMR spectroscopy showed multiplet signals for two pairs of fluorine atoms in the range 74.16-73.94 (2F, m) and 26.88-26.72 (2F, m), which suggested the presence of compound **62** or compound **63**. In addition mass spectrometry found the exact mass for compound **62** or compound **63**, HRMS (ESI) *m/z* found 181.9692 (M–H)$^-$, C_5F_4NS, requires 181.9693.

Scheme 25. Reaction of pentafluoropyridine with naphthalene-1-thiocarboxamide

21   naphthalene-1-thiocarboxamide 64   65   66

62   naphthalene-1-carbonitrile 67

63
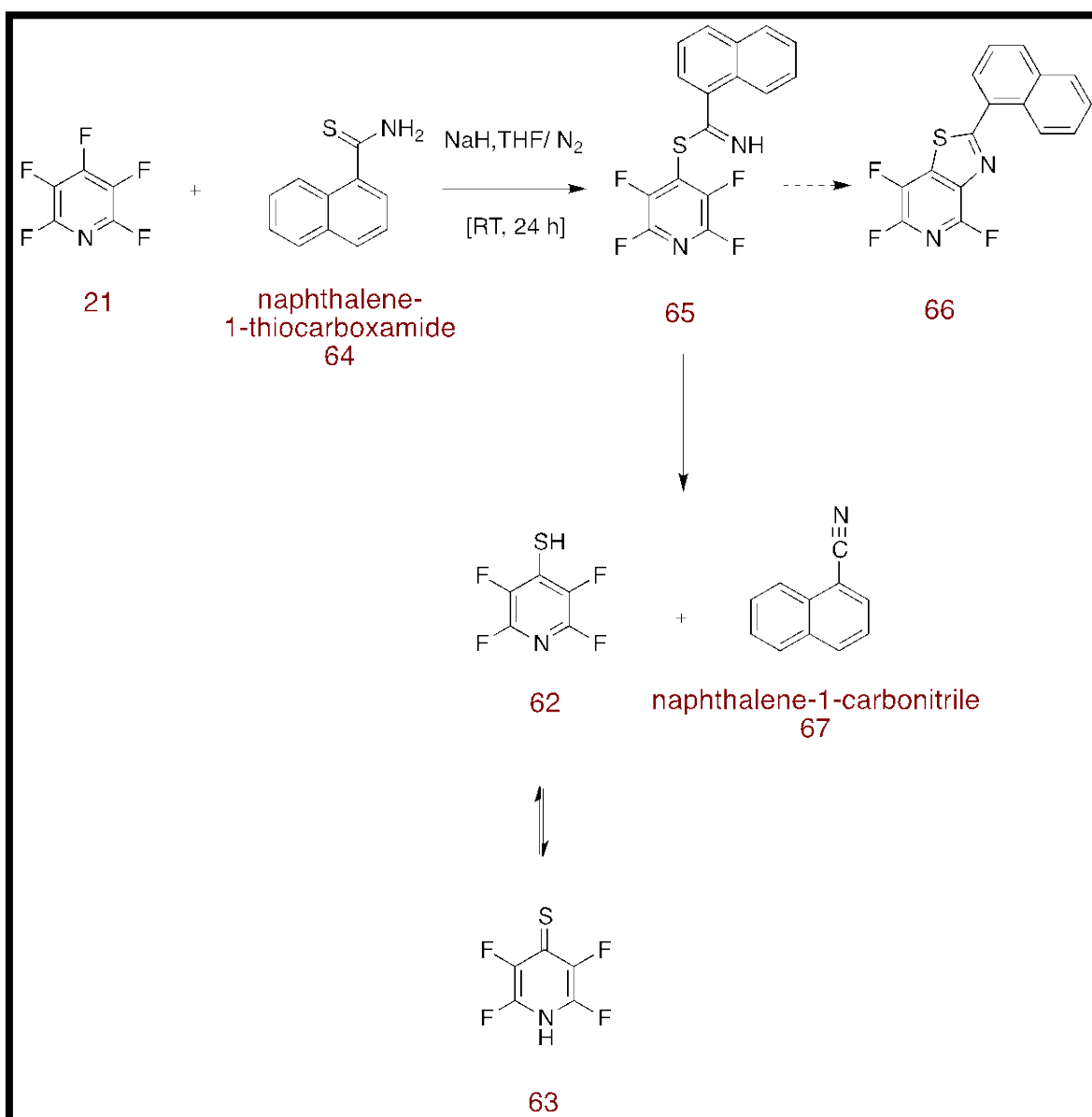
2.2.3.3. Synthesis of fluorinated thiazole derivatives using hexafluorobenzene and naphthalene-1-thiocarboxamide

Hexafluorobenzene **1** was reacted with naphthalene-1-thiocarboxamide **64** and the reaction aimed to synthesise fluorinated heterocyclic thiazole derivative **68**, which could possess a good DNA binding activity (Scheme 26). In contrast to the previous reactions involving pentafluoropyridine, the reaction worked well at RT in the presence of NaH as base and THF as solvent and the product was formed a semi-crystalline solid. Recrystallization from ethanol and chloroform gave shiny creamy crystals but unfortunately only in 16 % yield with m.p 165-168 °C. ^{19}F NMR spectroscopy indicated the presence of the target compound **68** by demonstrating four fluorine signals, δ_F (376 MHz, CDCl$_3$) 23.80 (1F, dd, *J* 20 and 15 Hz), 14.79 (1F, dd, *J* 19 and 14 Hz), 3.96 (1F, t, *J* 19 Hz), 3.24 (1F, t, *J* 20 Hz). The expected mass of the target molecule was displayed by GC-MS with *m/z* at 333. However it was unable to obtain an accurate mass measurement by electrospray ionisation due to the non-polar nature of the fluorinated molecule. This problem has been observed a number of times in the group with polyfluorinated compounds failing to ionize by ESI, but the nominal low resolution molecular ion signal was detected by GC-MS which employs electron impact ionization. The difference in reactivity between the pentafluoropyridine and hexafluorobenzene is not clear, and it cannot account for the failure of the pyridine derivatives to cyclize when closure of the thiazole occurred in the case of the hexafluorobenzene.

Scheme 26. Reaction of hexafluorobenzene and naphthalene-1-thiocarboxamide
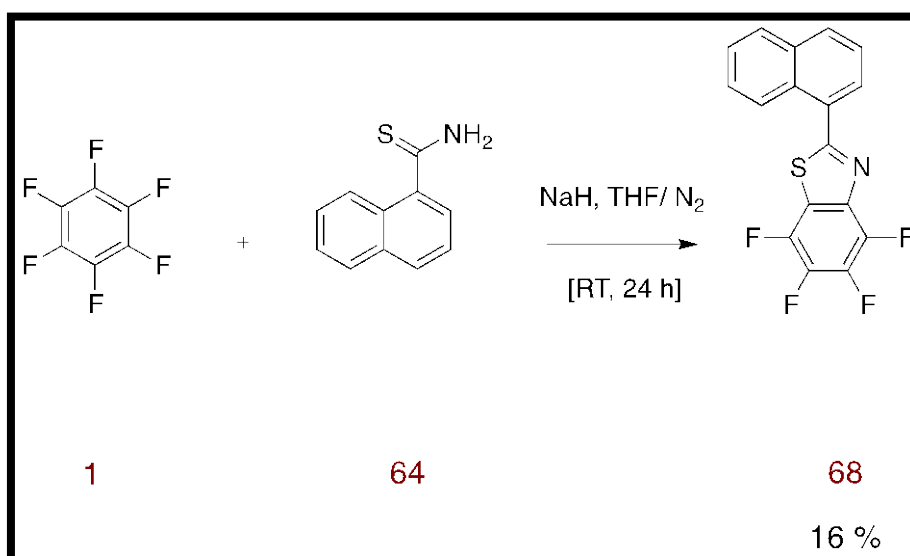
2.2.3.4. Synthesis of fluorinated fused thiazole derivatives using pentafluoropyridine and 2-mercaptobenzimidazole

Reaction of pentafluoropyridine **21** with 2-mercaptobenzimidazole **69** was investigated with the aim of synthesising polycyclic compound **72** by sequential S_NAr reaction (Scheme 27). The reaction was studied in different solvents and conditions but a product only was formed in the presence of NaH as base and a mixture of THF and DMF as solvents. The properties of the solid product isolated were not consistent with the tetracyclic structure **72**, and it was first believed the product to be the mono-adduct **70**, since a signal at 298 was observed in the mass spectrum, HRMS (ESI) *m/z* found 298.0071 (M−H)⁻, $C_{12}H_4F_4N_3S$ requires 298.0068. The ^{19}F NMR spectrum showed four signals that were also not consistent with structure **70**, although it was thought the four signals observed, rather than the expected two, could have explained by hindered rotation. It was then decided to see if further treatment of this compound would lead to formation of the tetracycle **72**. However the material was recovered unchanged after treatment with sodium hydride in boiling dioxane. Then a good crystal of the new compound was obtained and the structure was shown by X-ray crystallography (Figure 14). Surprisingly the structure was shown to be compound **71** in which a tetrafluoropyridine ring had added both to the sulfur atom and one of the nitrogens of the benzimidazole ring. The identification of this structure then explained the ^{19}F NMR spectrum and the four signals observed matched correctly with the two pairs of fluorine atoms on two pyridine rings. Further analysis of the mass spectrum showed a signal at 446, HRMS (ESI) *m/z* found 446.9962 (M−H)⁻, $C_{17}H_3F_8N_4S$ requires 446.9956 agreeing with the new structure. The signal first observed at 298 must have due to a trace amount of product **70**. Elemental analysis fitted with the expected composition for a molecular formula of $C_{17}H_4F_8N_4S$ (448) calculated C, 45.55; H, 0.90; N, 12.50. Found C, 45.41; H, 0.92; N, 12.00.

Scheme 27. Reaction of pentafluoropyridine with 2-mercaptobenzimidazole

2-mercaptobenzimidazole

21   69   70

71

27 %

72
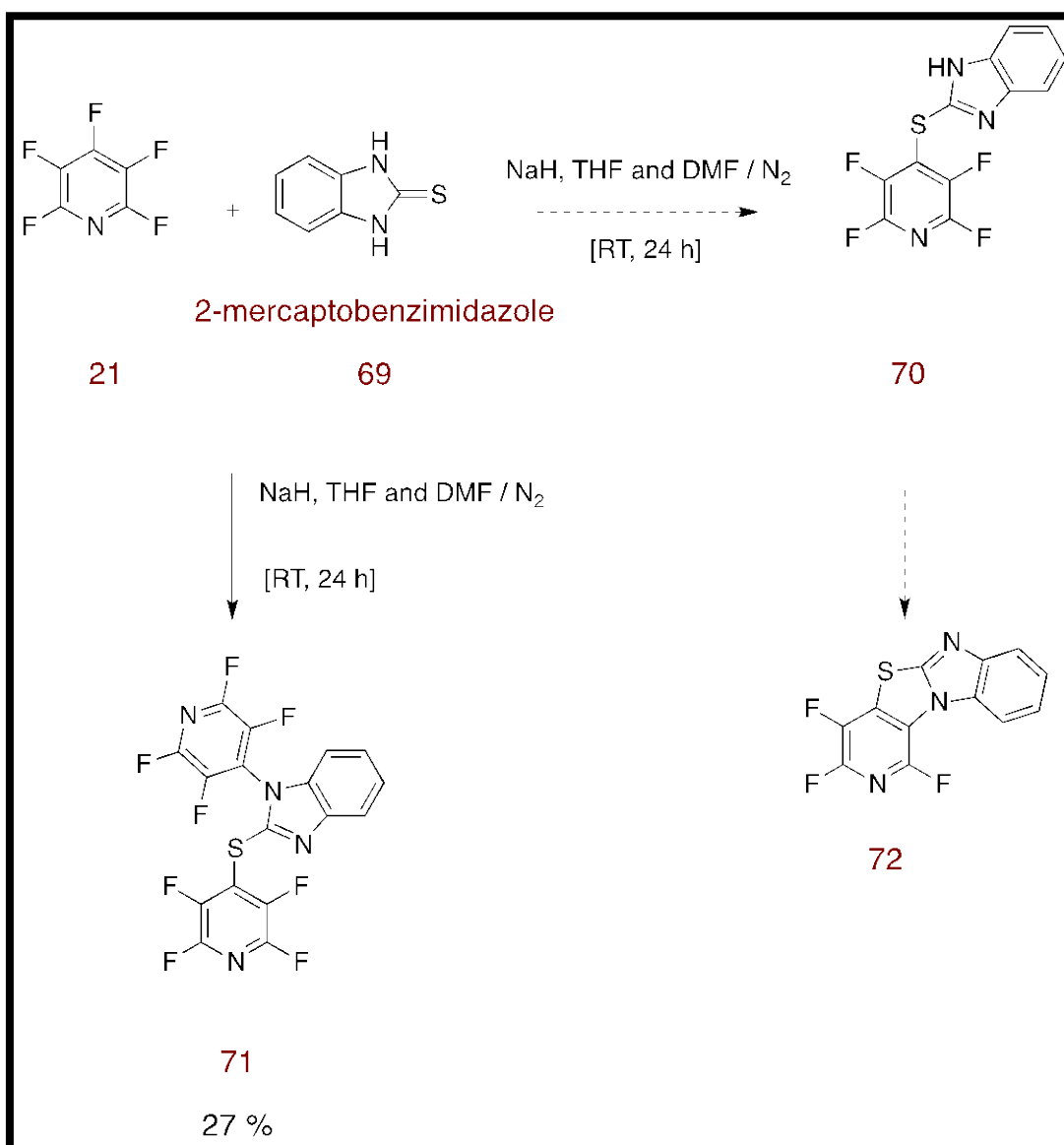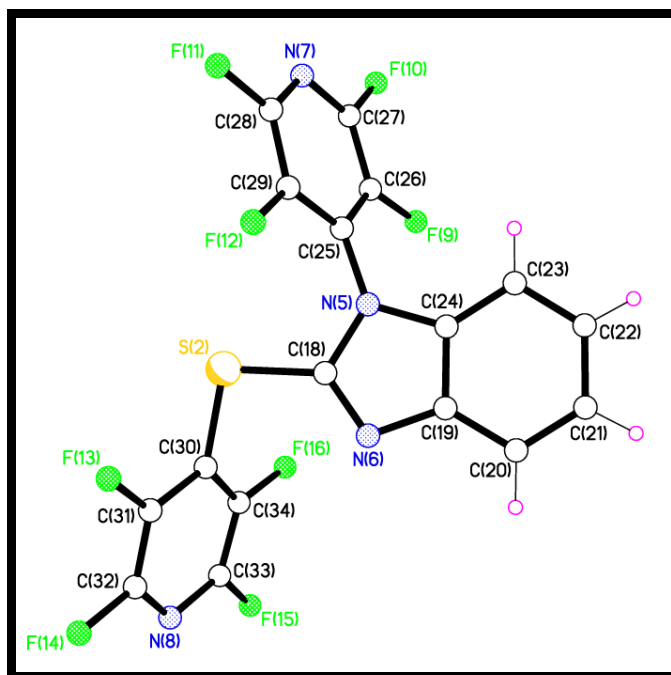
Figure 14. X-ray crystal structure of compound (71)

2.2.3.5. Synthesis of fluorinated fused thiazole derivatives using pentafluoropyridine and 2-mercapto-4(3H)-quinazolinone

Reaction of pentafluoropyridine **21** with 2-mercapto-4(3H)-quinazolinone **73** was aimed at synthesising tetracyclic fluorinated thiazole derivative **74** and **75** which could possess good DNA binding activity. In the presence of a mixture of solvents THF and DMF at RT the reaction worked and the data suggested the presence of the cyclized thiazole derivative **74** or **75** (Scheme 28). ^{19}F NMR spectroscopy showed three signals for three different fluorine atoms, δ_F (376 MHz, CDCl$_3$) 106.50 (1F, dd, *J* 30 and 10 Hz), 74.44 (1F, dd, *J* 22 and 10 Hz), 16.26 (1F, dd, *J* 29 and 22 Hz), as well as the GC mass spectrometry which showed the expected mass of the cyclized compound **74** or **75**, GC-MS (EI) *m/z* 307 but unfortunately the yield was very low (4 %). Due to the small quantity of **74** or **75** obtained it was not possible to determine which of the two possible regioisomers **74** or **75** had been formed.

Unfortunately, by repeating the reaction on larger scales to get a higher yield, under the same conditions, the uncyclized compound **76** was obtained and that was suggested by ^{19}F NMR spectroscopy which demonstrated two signals, δ_F (376 MHz, DMSO-d$_6$) 70.60-70.43 (2F, m) and 28.73-28.54 (2F, m).

The possible cyclization of compound **76** to **74** or **75** (Scheme 29) was studied under different conditions. Firstly NaH was used as base in the presence of dioxane as solvent

under reflux at 101 °C for 24 h to deprotonate the N-H group and allow the cyclization of the compound by nucleophilic aromatic substitution S_NAr reaction. According to spectroscopic data the cyclization reaction did not work and the uncyclized starting compound was recovered. Because of that a stronger base was used to allow cyclization of the compound **76**, which was potassium bis(trimethylsilyl)amide solution in the presence of THF as solvent at −78 °C, but still the cyclization reaction did not work and only the uncyclized compound **76** was detected by spectroscopic analysis.

Scheme 28. Reaction of pentafluoropyridine with 2-mercapto-4(3H)-quinazolinone
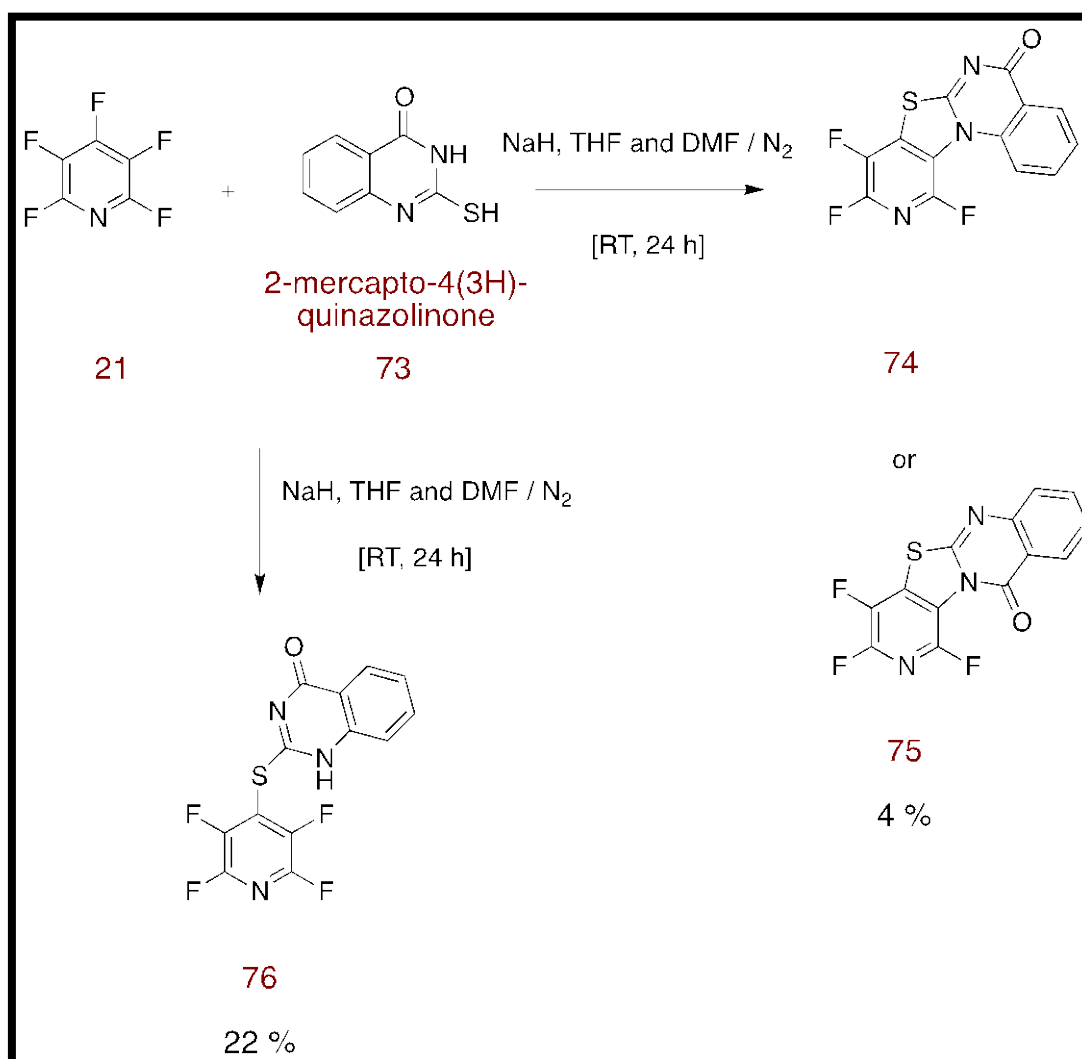
Scheme 29. Attempted cyclization of tetrafluoro-pyridine quinazoline derivative (76)
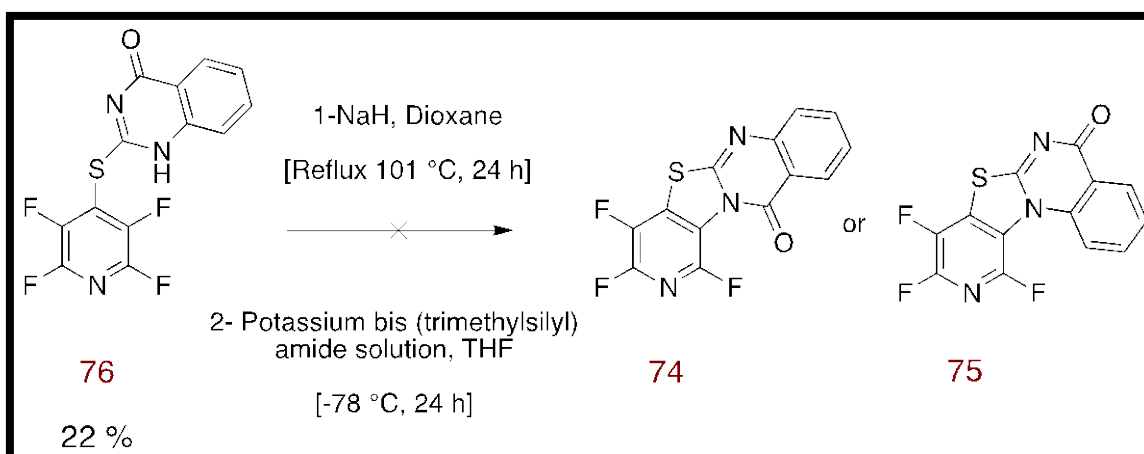
2.2.3.6. Synthesis of fluorinated thiazole derivatives using pentafluorobenzaldehyde and 2-mercapto-4(3H)-quinazolinone

Due to the successful addition of the mercaptoquinazolinone to pentafluoropyridine it was decided to investigate the behavior of this compound towards other fluorinated arenes. Reaction of pentafluorobenzaldehyde **77** with 2-mercapto-4(3H)-quinazolinone **73** worked well in the presence of a mixture of THF and DMF as solvents and NaH as base at RT and compound **78** was afforded (Scheme 30). ^{19}F NMR spectroscopy proved the presence of the uncyclized compound **78** with two multiplet signals for two pair of fluorine atoms, δ_F (376 MHz, DMSO-d$_6$) 30.19-30.10 (2F, m) 16.27-16.17 (2F, m). In addition the mass spectrometry showed the expected mass of the uncyclized compound, HRMS (ESI) m/z found 353.0018 (M–H)$^-$, C$_{15}$H$_5$F$_4$N$_2$O$_2$S requires 353.0013.

In order to try and cyclize compound **78** and get either of the possible tetracyclic fluorinated thiazole derivatives **79** or **80** (Scheme 30) NaH base was used in the presence of dioxane as solvent under reflux at 101 °C for 24 h. The reaction aimed to deprotonate (N-H) group and allow cyclization of the compound by nucleophilic aromatic substitution S$_N$Ar reaction, but the cyclization did not work and according to the spectroscopic data, the starting material, uncyclized compound **78** was afforded.

Scheme 30. Reaction of pentafluorobenzaldehyde with 2-mercapto-4(3H)-quinazolinone
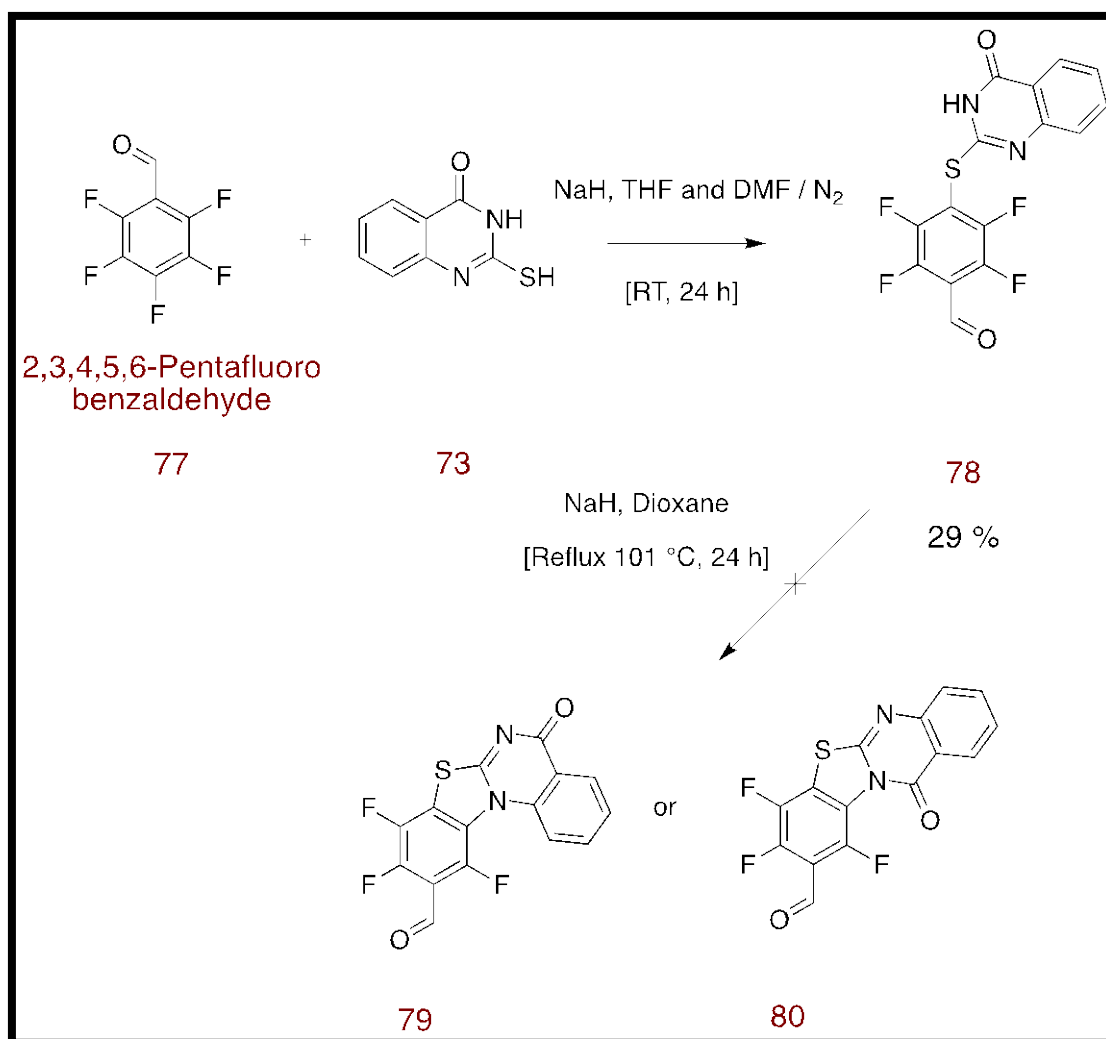
2.2.4. Synthesis of fluorinated benzothieno derivatives

Thienopyridines derivatives have attracted much attention in medicinal chemistry due to their isosterism with indolopyridine and showed potential biological activity. They have been reported in the literature as antifungal, antibacterial and anticancer agents.[81,82] Benzothienopyridines possess a π-electron rich thiophene ring and π-electron deficient pyridine ring. These annelated aromatic heterocycles are attracting the attention of organic chemists.[82] It has been reported by Weaver *et al.*, 2011 that ring closing reactions of substituted polyfluoroarenes is a quick way to generate polycyclic compounds. Using lithium-bromine exchange 2-bromophenyl perfluoroaryl sulfides or ethers formed fluorinated benzofurans or benzothiophenes by S_NAr substitution reaction of the adjacent fluorine atom in the perfluoroaryl subunit.[31] As part of our investigations in this area it was planned to study ring closure by lithiation of bromoaryl ethers and sulfides containing

a perfluoroarene ring and it was wished now to further explore the chemistry of these ring systems both from a mechanistic point of view and synthetically to make potentially biologically active compounds.

2.2.4.1. Synthesis of fluorinated benzothiophene using 2-bromothiophenol and pentafluoropyridine[31]

Fused thiophenes had been prepared previously in the group and it was hoped to explore further the chemistry of these new fluorinated compounds. For example it was planned to study displacement of the fluorines in **83** and **85** to build up potential intercalator compounds, which will be discussed later.

The same fluorinated precursor that was investigated by Weaver *et al.*, 2011 was resynthesised and cyclized with the same procedure in order to obtain the fluorinated benzothiophene subunit. The plan was to displace the remaining fluorine atoms that may, in principle, be displaced by nucleophiles to create biologically active molecules. Thus reaction of pentafluoropyridine **21** with 2-bromothiophenol **81** worked well at RT in the presence of NaH as base and DMF as solvent and the target compound **82** (Scheme 31) was successfully synthesised with 21 % yield. The target compound was fully characterized with ^{1}H NMR spectroscopy which detected the benzene ring protons, δ_H (400 MHz, CDCl$_3$) 7.47 (1H, dd, *J* 7.6 and 1.2 Hz) 7.38 (1H, d, *J* 7.6 Hz) 7.17 (1H, td, *J* 7.6 and 1.6 Hz) 7.11 (1H, td, *J* 7.6 and 2.0 Hz). Moreover, the ^{19}F NMR spectrum showed two multiplet signals for two pair of fluorine atoms, δ_F (376 MHz, CDCl$_3$) 70.81-70.76 (2F, m), 25.38-25.28 (2F, m)

Lithiation of 4-(2-bromo-phenylsulfanyl)-2,3,5,6-tetrafluoro-pyridine **82** was expected to result in lithium-bromine exchange and then intramolecular substitution of the fluorine at C-3 of the pyridine ring to close the thiophene ring. The reaction worked well and the cyclized compound 1,3,4-trifluoro-benzo[4,5]thieno[3,2-c]pyridine **83** (Scheme 31) was afforded in 66 % yield. The data was in good agreement with that reported previously by Weaver *et al.*, 2011.[31]

Scheme 31. Reaction of pentafluoropyridine with 2-bromothiophenol[31]
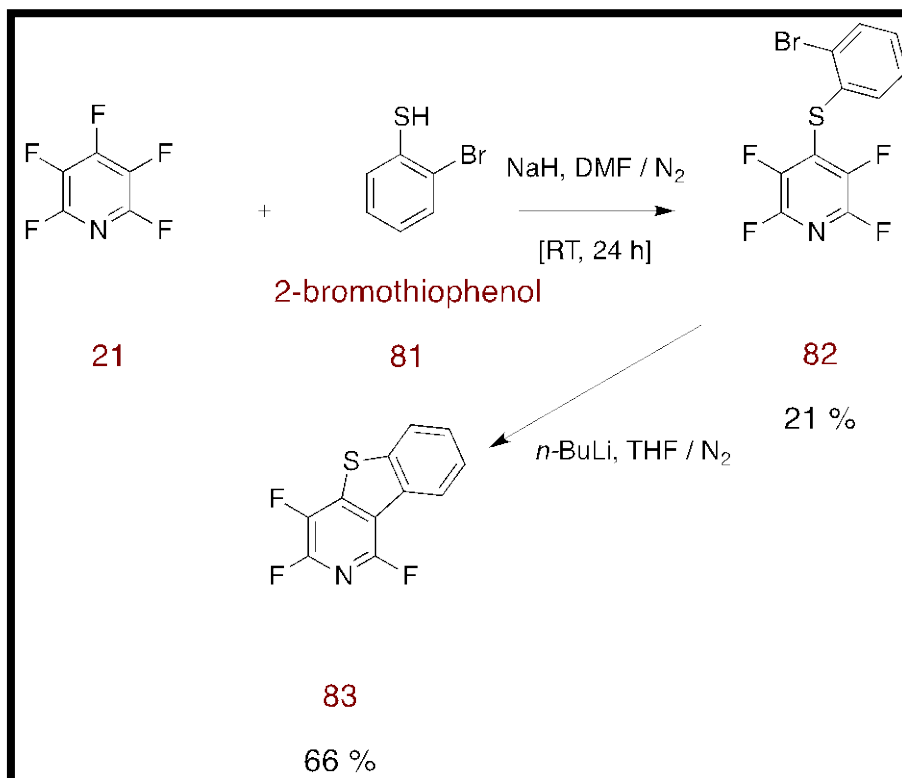
2.2.4.2. Synthesis of fluorinated benzothiophene using 2-bromothiophenol and hexafluorobenzene[31]

Hexafluorobenzene **1** was reacted with 2-bromothiophenol **81** in 1:2 equivalents in order to synthesise bis-bromophenylsulfanyl tetrafluorobenzene derivative **84** (Scheme 32). The reaction worked well in DMF and the 1,4-disubstitution product **84** was afforded after crystallization. ^{19}F NMR spectroscopy displayed one single peak for four identical fluorine atoms, δ_F (376 MHz, DMSO-d$_6$) 31.18 (4F, s). When the bis-sulfide **84** was treated with two equivalents of *n*-BuLi in THF (Scheme 32) cyclization occurred between both bromophenyl groups and the central fluorinated benzene ring and the known pentacyclic compound **85** was afforded in 85 % yield.[31] Investigations into the displacement of the fluorines in this compound are discussed in section 2.2.8.10.

Scheme 32. Reaction of hexafluorobenzene with 2-bromothiophenol[31]
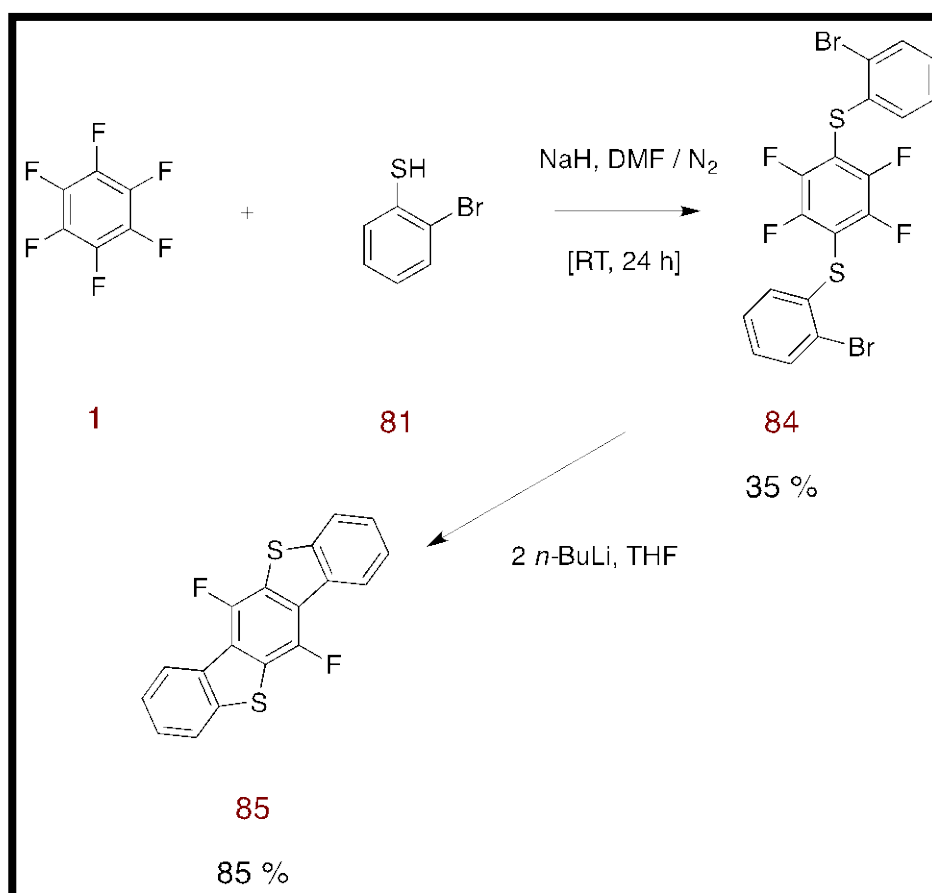
2.2.5. Synthesis of fluorinated benzofuran derivatives

One of the most important sources of antiproliferative products is benzofuran derivatives. It has been reported that benzofuran derivatives showed a selective and potent cytotoxic activity and antiproliferative effect against cancer cell line.[83] Thus as a part of our project in synthesis of bioactive DNA binding compounds, it was thought that benzofuran-based fluorinated analogs could display DNA binding activity. It was also of interest to extend the lithiation studies developed by Weaver *et al*., 2011. Lithiation of 2-bromophenyl perfluoroaryl ethers had led to either cyclization to benzofurans or Smiles-type rearrangement to phenols. The plan was to study this reaction further with 1-bromo-2-naphthol to see if compound **88** or **90** would form on lithiation (Scheme 34).

2.2.5.1. Synthesis of 4-(3-bromonaphthalen-2-yloxy)-2,3,5,6-tetrafluoro-pyridine (87)

Reaction of pentafluoropyridine **21** with 1-bromo-2-naphthol **86** worked well in the presence of DMF at RT and the target compound **87** (Scheme 33) was afforded in 100 % yield. ^{19}F NMR spectroscopy showed two multiplet peaks for two pairs of fluorine atoms,

δ_F (376 MHz, CDCl$_3$) 73.29-73.12 (2F, m), 6.10-5.94 (2F, m). In addition, the mass spectrometry showed the expected mass of compound **87**, HRMS (ESI) *m/z* found 369.9528 (M–H)$^-$, C$_{15}$H$_5$^{79}BrF$_4$NO requires 369.9496 and the elemental analysis proved the purity of the product, analysis (%) calculated for C$_{15}$H$_6$BrF$_4$NO (370): C, 48.64; H, 1.62; N, 3.80. Found C, 48.52; H, 1.56; N, 3.80. X-ray crystallography proved the synthesis of the target compound **87** (Figure 15) again confirming addition had occurred at C-4.

Scheme 33. Reaction of pentafluoropyridine with 1-bromo-2-naphthol
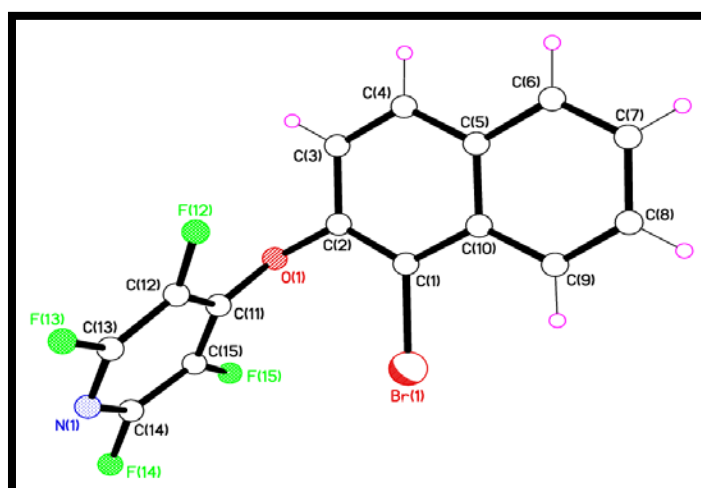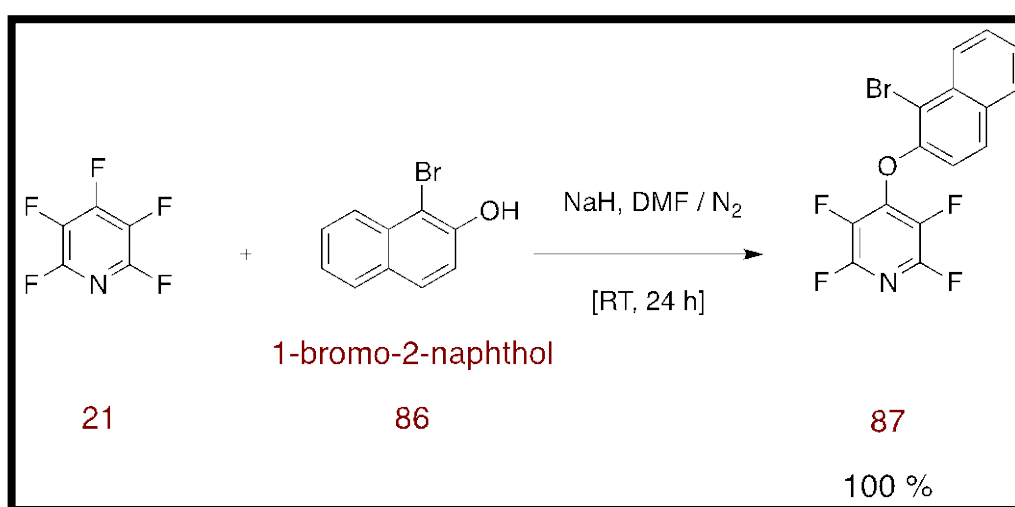
Figure 15. X-ray crystal structure of compound (87)

2.2.5.2. Ring closing of 4-(3-bromonaphthalen-2-yloxy)-2,3,5,6-tetrafluoropyridine (87)

Lithiation of the easily prepared 4-(3-bromonaphthalen-2-yloxy)tetrafluoropyridine **87** was expected to form the trifluoro-aza-benzo-furan derivative **90** by lithium-bromine exchange, and then intramolecular substitution of the fluorine at C-3 of the pyridine ring to close the furan ring (Scheme 34). However treatment of the tetrafluoropyridine derivative **87** with *n*-BuLi in THF at low temperature afforded a product, which was not the expected tetracyclic furan **90**, but it was a mixture of compounds consisting mainly of **88** and with a trace amount of **89**. IR and ^{1}H NMR spectroscopy indicated the presence of an alcohol group, v_{max} / cm^{-1} (film) 3411 (O-H), δ_H 7.77-7.69 (1H, bs, OH). Mass spectrometry also suggested the presence of a mixture of two compounds **88** and **89**, GC-MS (EI) *m/z* 293 major and 273 minor. Thus, the reaction had proceeded by Smiles type rearrangement [84] rather than S$_N$Ar reaction at the 3-position of the pyridine ring as had been observed by Weaver *et al.*, 2011 in the case of 2-bromophenyl tetrafluoropyrid-4-yl ether.[31] The two compounds **88** and **89** unfortunately could not be separated by column chromatography. This minor by-product was proposed to be the tetracyclic structure **89**, likely to have formed by cyclization of the first-formed Smiles rearrangement product **88** under the basic conditions of the reaction. However it could not be ruled out that the minor compound might be structure **90,** if cyclization had occurred without rearrangement. The low amount of material formed did not allow further analysis in the time available. Interestingly, a different outcome was observed when the lithiation was conducted in the presence of N,N,N,N-tetramethylethylenediamine (TMEDA) in THF at -78 °C. In this experiment a trifluoro cyclized compound, **90**, was afforded in 16 % yield after column chromatography. ^{19}F NMR spectroscopy proved the presence of a cyclized compound by exhibiting three signals for three fluorine atoms, δ_F (376 MHz, CDCl$_3$) 8.03 (1F, d, *J* 26 Hz), 1.76 (1F, d, *J* 21 Hz), 72.81 (1F, dd, *J* 26 and 21 Hz), and the mass spectrum gave the expected mass of the cyclized compound **90**, GC-MS (EI) m/z 273. The ^{19}F NMR spectrum showed the presence of a clean (in terms of fluorine) single compound containing three fluorine atoms. The ^{1}H NMR spectrum however showed a complex series of multiplets in the aromatic region consistent, but not fully in accord (in terms of integration), with the proposed structure **90**. Some aromatic impurities may still have been present. The product formed in this reaction could potentially be the alternative ring fused product **89**, but in the absence of any sign of Smiles rearrangement product, this seems unlikely, and it is believed that direct cyclization occurred in the presence of

TMEDA as an additive. Further work would be required to verify the structures of the two fused tetracyclic products. The proposed mechanism is shown in the following scheme (Scheme 34).

Scheme 34. Cyclization of 4-(3-bromo-naphthalen-2-yloxy)-2,3,5,6-tetrafluoro-pyridine (87)
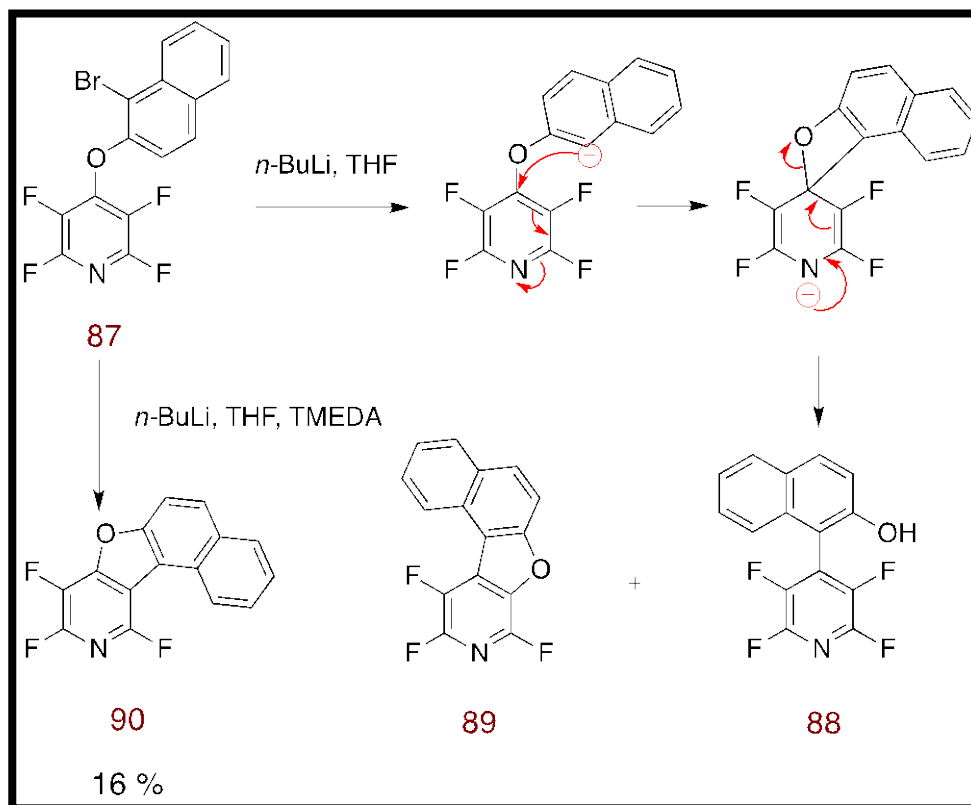
2.2.5.3. Synthesis of 2-bromo-3-pentafluorophenyloxynaphthalene (91)

 In order to extend this chemistry it was planned to turn to the corresponding reaction with hexafluorobenzene. Reaction of hexafluorobenzene **1** with 1-bromo-2-naphthol **86** at RT in DMF worked well and the target compound **91** (Scheme 35) was afforded after column chromatography as white crystals in 11 % yield with m.p. 112-114 °C. ^{19}F NMR spectrum showed the expected signals for the target compound **91**, δ_F (376 MHz, CDCl$_3$) 7.86 (2F, d, J 17 Hz), 2.41 (1F, t, J 23 Hz), 0.21-0.13 (2F, m).

Scheme 35. Reaction of hexafluorobenzene with 1-bromo-2-naphthol
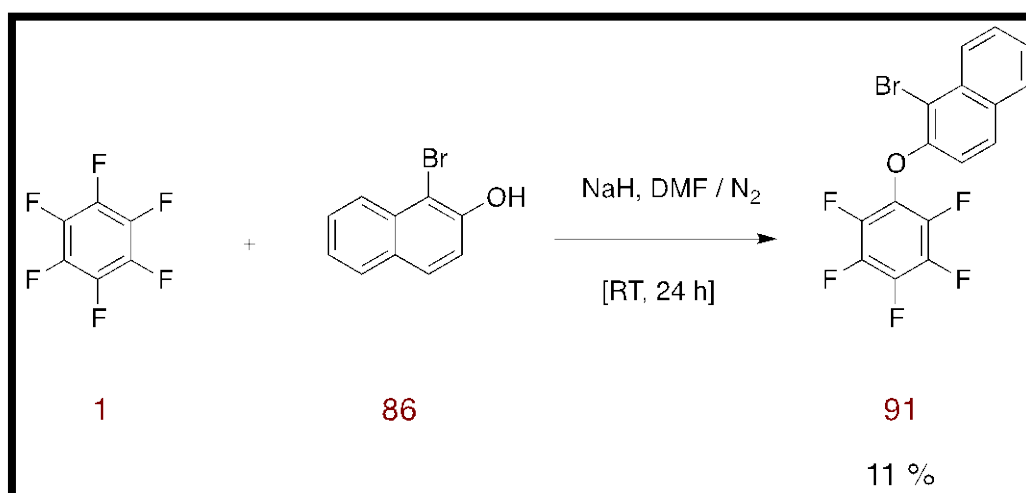
2.2.5.4. Synthesis of bromo 3-[2,3,5,6-tetrafluoro-4-(naphthalene-2-yloxy)-phenoxy]-naphthalene (92)

Reaction of hexafluorobenzene **1** with two equivalents of 1-bromo-2-naphthol **86** was studied in DMF but it did not go to completion and only substitution by one 1-bromo-2-naphthol occurred. However in the presence of THF and using the syringe pump to add hexafluorobenzene **1** very slowly the reaction worked and di-substitution of hexafluorobenzene occurred and the target compound **92** (Scheme 36) was formed although in a low 11 % yield. ^{19}F NMR spectroscopy proved the formation of the target compound **92** by showing one singlet peak for four identical fluorines due to the symmetry of the compound, δ_F (376 MHz, CDCl$_3$) 61.81 (4F, s). Due to the low amount of compound **92** it was not possible to study the lithiation reactions.

Scheme 36. Reaction of hexafluorobenzene with 2 equivalents of 1-bromo-2-naphthol
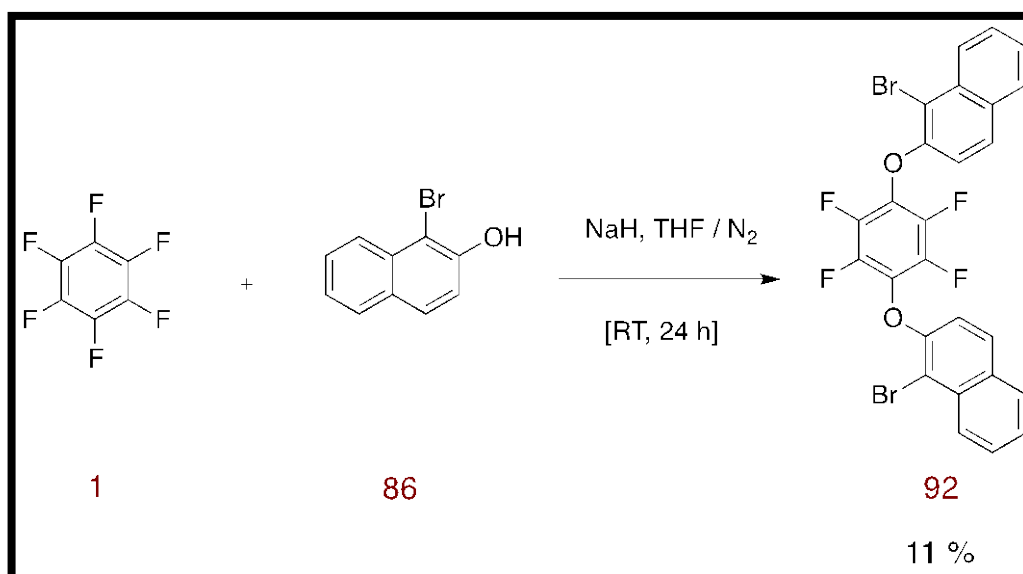
2.2.6. Synthesis of fluorinated 4-methylbenzenesulfonamide derivatives

To further extend the lithiation cyclization strategy to nitrogen containing compounds it was planned to investigate the synthesis of N-(2-bromophenyl)-4-methylbenzenesulfonamide. It has been reported that benzenesulfonamide derivatives have important applications in medicinal, analytical, catalytic and pharmaceutical chemistry.[85,86] These compounds are widely used in treatment of *Streptococci* infections and some benzenesulfonamide derivatives are used as an effective inhibitors in cancer treatment and other diseases treatment such as heart failure and cystic fibrosis.[86] In the interest of these applications the present study investigated the synthesis of fluorinated benzenesulfonamide derivatives using pentafluoropyridine and hexafluorobenzene to achieve novel, more effective, pharmaceutical fluorinated benzenesulfonamide derivatives, which might show a potential DNA binding activity. It was hoped that the toluenesulfonyl group would increase the acidity of the N-H allowing easy deprotonation, and readily reaction of the anion with perfluoroarenes. Once added, for example in compound **96** (Scheme 38), the bromobenzene ring could be lithiated to see if the resulting aryllithium would cyclize onto the fluorinated ring by S_NAr reaction, or induce Smiles-type rearrangement as had been observed in the case of tetrafluoropyridyl ethers. This would extend this approach and allow nitrogen containing heterocycles to be formed.

2.2.6.1. Synthesis of N-(2-bromophenyl)-4-methylbenzenesulfonamide (95)

The title compound was synthesised by reaction of 2-bromoaniline **93** with p-toluenesulfonyl chloride **94** in pyridine (Scheme 37). When the reaction was heated over night at 80 °C the target compound did not form and a complex dark coloured mixture was afforded with a complicated NMR spectrum. However by leaving the reaction to stir at RT for 72 h the target product N-(2-bromophenyl)-4-methylbenzenesulfonamide **95** was afforded in 87 % yield. ^{1}H NMR spectroscopy displayed the expected signals of the target compound and X-ray crystallography showed the structure of the target product (Figure 16). Mass spectrometry found the exact mass of compound **95**, HRMS (ESI) *m/z* found 323.9702 (M–H)$^-$, $C_{13}H_{11}{}^{79}BrNO_2S$ requires 323.9699 In addition elemental analysis demonstrated the presence of pure product, analysis (%) calculated for $C_{13}H_{12}BrNO_2S$ (324): C, 47.86; H, 3.71; N, 4.29. Found C, 47.83; H, 3.71; N, 4.29.

Scheme 37. Reaction of 2-bromoaniline with p-toluenesulfonylchloride
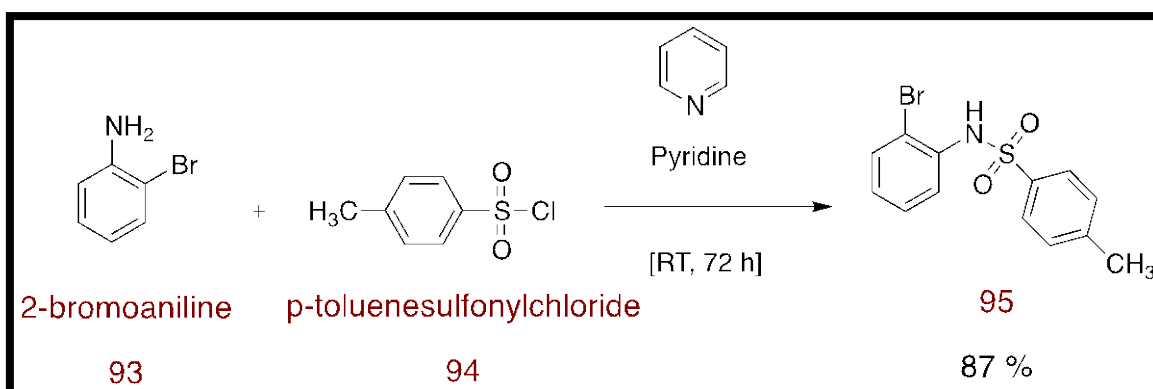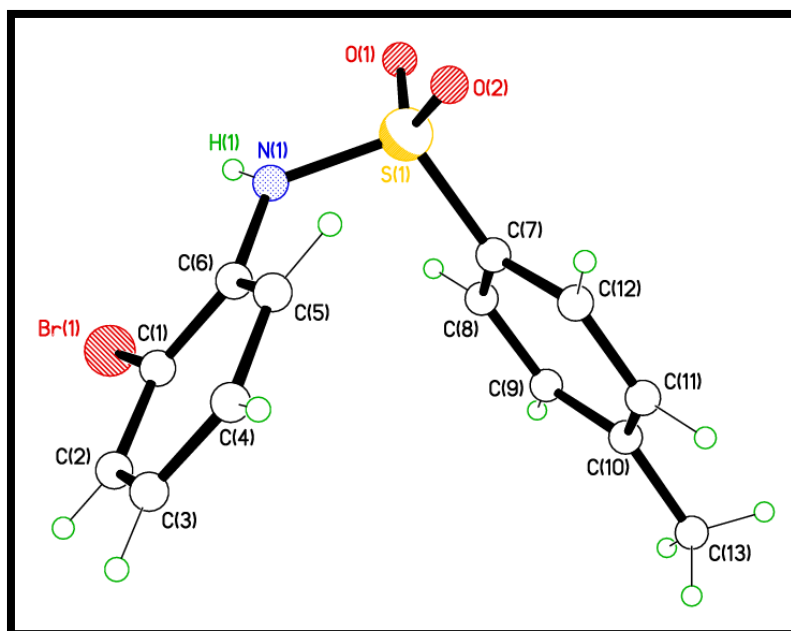
Figure 16. X-ray crystal structure of N-(2-bromophenyl)-4-methylbenzenesulfonamide (95)

2.2.6.2. Synthesis of N-(2-bromophenyl)-4-methyl-N-(2,3,5,6-tetrafluoropyridine-4-yl)-benzenesulfonamide (96)

Reaction of pentafluoropyridine **21** with compound **95** was one of the most difficult reactions in the project and the target compound **96** (Scheme 38) was not afforded directly and several conditions had to be investigated to successfully synthesise the target fluorinated compound **96**. In the presence of NaH as base to deprotonate the N-H group of compound **95** in THF at RT, the target compound **96** was not formed and only the starting material was detected with GC-MS. By increasing the equivalents of pentafluoropyridine **21** in THF at RT again only the starting material was detected in the GC-MS and the target compound **96** was still not formed. By changing the reaction conditions, and leaving the reaction mixture to stir in boiling THF for 24 h, a complicated material was afforded according to TLC and ^{1}H NMR spectrum. By using a mixture of THF and DMF as solvents under reflux at 66 °C for 2 h and then allowing the reaction mixture to stir at RT for 24 h, interestingly the target compound **96** was afforded after column chromatography purification as white crystals in 23 % yield. ^{19}F NMR spectroscopy proved the presence of the target fluorinated compound **96** by displaying two multiplet signals for two pairs of fluorine atoms, as well as mass spectrometry found the exact mass of the target compound, δ_F (376 MHz, CDCl$_3$) 72.82-72.65 (2F, m), 8.53-8.37 (2F, m); HRMS (ESI) *m/z* found 472.9588 (M–H)$^-$, C$_{18}$H$_{10}$^{79}BrF$_4$N$_2$O$_2$S requires 472.9588.

Scheme 38. Reaction of pentafluoropyridine with compound (95)

21   **95**   **96**

23 %
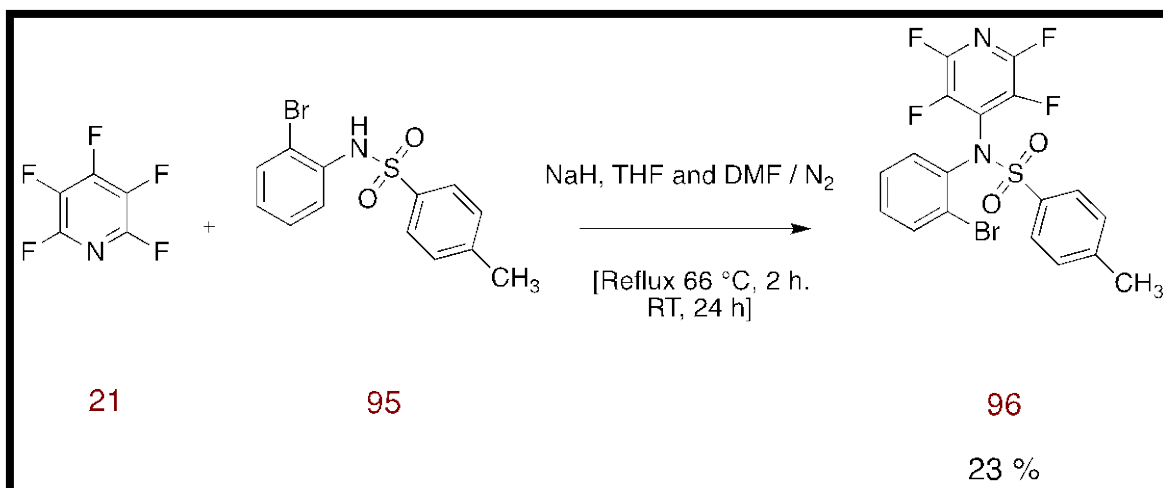
2.2.6.3. Synthesis of N-(2-bromophenyl)-4-methyl-N-(2,3,4,5,6-pentafluorophenyl)-benzenesulfonamide (97)

After the successful synthesis of compound **96** in the previous reaction it was hoped to extend the reaction using hexafluorobenzene.

The reaction of hexafluorobenzene **1** with benzenesulfonamide derivative **95** (Scheme 39) in a mixture of THF and DMF as solvents did not work even in the same reaction conditions of the case of pentafluoropyridine reaction. The mass spectrometry and TLC analysis detected the starting compound **95**.

Scheme 39. Attempted reaction of hexafluorobenzene with compound (95)

1   **95**   **97**
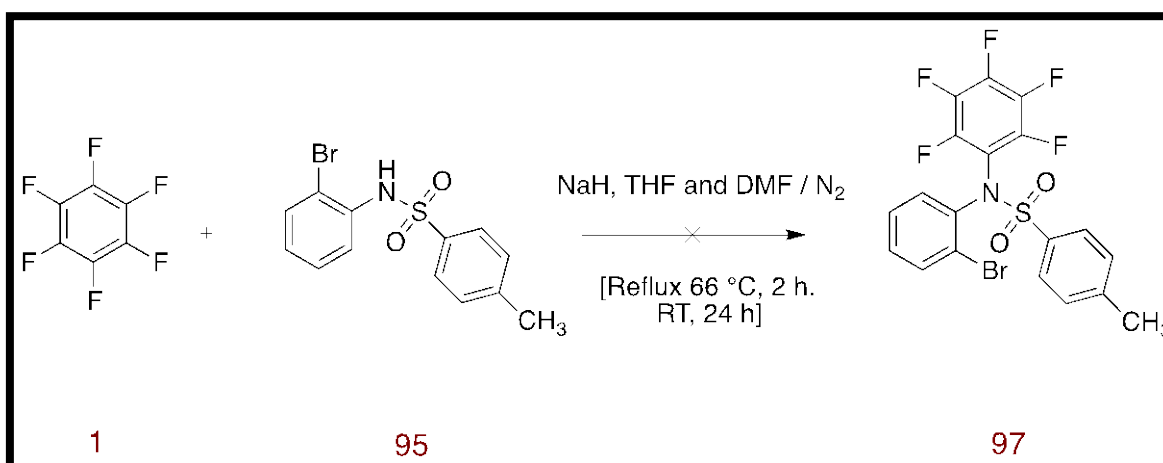
2.2.6.4. Cyclization of N-(2-bromophenyl)-4-methyl-N-(2,3,5,6-tetrafluoropyridine-4-yl)-benzenesulfonamide (96)

Reductive debromination reaction was investigated for compound **96** in order to cyclize the compound by an intramolecular S_NAr process (Scheme 40). The first cyclization reaction was studied with *n*-BuLi in THF; unfortunately the reaction did not work well. The second cyclization reaction was investigated with iron powder in ethanol and under reflux at 78 °C for 24 h, again still the reaction did not work and the starting material was detected with spectroscopic analysis. Due to the low yields of the starting uncyclized compound **96**, the difficulty of preparing it in larger yield, and the lack of time we stopped this investigation.

Scheme 40. Attempted cyclization of N-(2-bromophenyl)-4-methyl-N-(2,3,5,6,-tetrafluoropyridine-4-yl)-benzenesulfonamide (96)
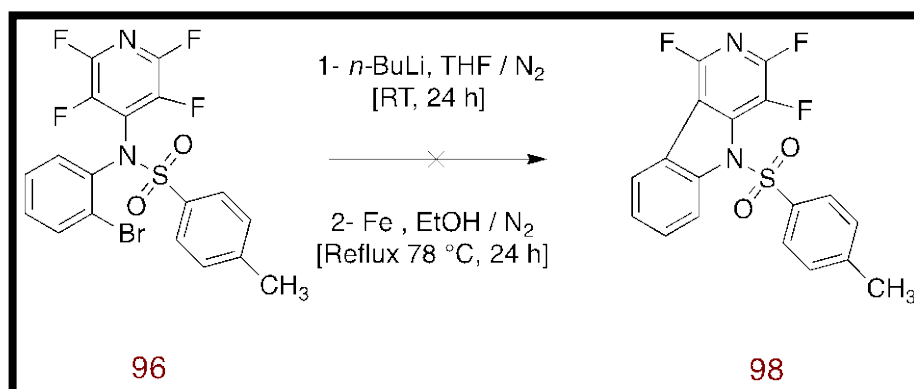
2.2.7. Synthesis of fluorinated aryl carbazole derivatives

Nitrogen containing heterocyclic aromatic compounds such as carbazole and its derivatives are important substances in drug design and synthesis, and have a significant attention of medicinal chemists because of their biological activity. The tricyclic carbazole nucleus exists in many natural alkaloids and synthetic derivatives, and possesses desirable electronic and charge transport characteristics, as well as a large π-conjugated system for organoelectronic applications. Moreover, several functional groups are easily introduced into the structurally rigid carbazole ring to alter the biological activities of the compound.[87,88,89] These characteristics result in the extensive potential applications of carbazole based derivatives in the field of medicinal chemistry as antitumor agents, anti-inflammatory agents, antimicrobial and antioxidative substances.[87,90] For example, the carbazomycins are an extraordinary class of carbazole

scaffold antibiotics.[91] Carbazomycin A and carbazomycins B (Figure 17) showed a high activity growth inhibition of phytopathogenic fungi and have antibacterial and anti-yeast activities.[89]
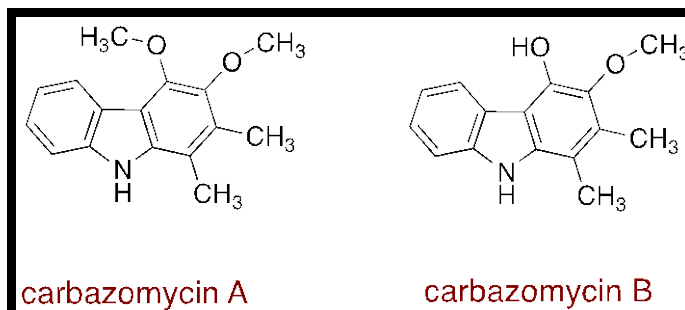
Figure 17. The structure of carbazomycins

In the interest of the above suggestions, it was planned to design and synthesise systems that combined more than one bio labile component, namely carbazole and a fluorinated aromatic substrate to provide a potentially biologically active DNA binding structure. It was hoped the large π surface of the carbazole ring would be desirable for intercalation into duplex DNA and allow effective π−π stacking. The N-H group in carbazole derivatives can be easily deprotonated, for example with sodium hydride, and it was expected that such anions would add readily to perfluoroarenes by S_NAr reaction to allow rapid assembly of polycyclic aromatic structures with potential for elaboration into DNA binding molecules.

2.2.7.1. Synthesis of 9-[1-(9H-fluorene-9-yl)-2,3,5,6-tetrafluoro-pyridine-4-yl]-9H-carbazole (100)

Reaction of hexafluorobenzene **1** with carbazole **99** in ratio 1:2 equivalents afforded the target compound **100** (Scheme 41), after recrystallization from hot toluene, as yellow crystals with m.p. 344-350 °C. ^{1}H and ^{19}F NMR spectroscopy demonstrated the presence of the target compound **100**, δ_H (400 MHz, CDCl$_3$) 8.22 (4H, d, J 7.6 Hz), 7.56 (4H, t, J 7.2 Hz), 7.43 (4H, t, J 7.2 Hz), 7.35 (4H, d, J 8.0 Hz); δ_F (376 MHz, CDCl$_3$) 21.00 (4F, s); as well as the mass spectrum which showed the expected mass of the target molecule, GC-MS (EI) with a peak at m/z 480. The final evidence for the presence of the target compound **100** was the X-ray crystal diffraction analysis, which confirmed the structure of the title compound (Figure 18). Interestingly X-ray analysis also detected the presence of unexpected product **101** (Figure 19) since four carbazole rings were attached to one

hexafluorobenzene ring. Unfortunately TLC analysis showed only one spot and mass spectroscopy could not observe the expected mass for the unexpected compound **101** as well as ^{19}F NMR spectrum detected only one signal, which means compound **101** must be present as a very minor component and the major compound is the expected dicarbazole compound **100**.

Scheme 41. Reaction of hexafluorobenzene with carbazole
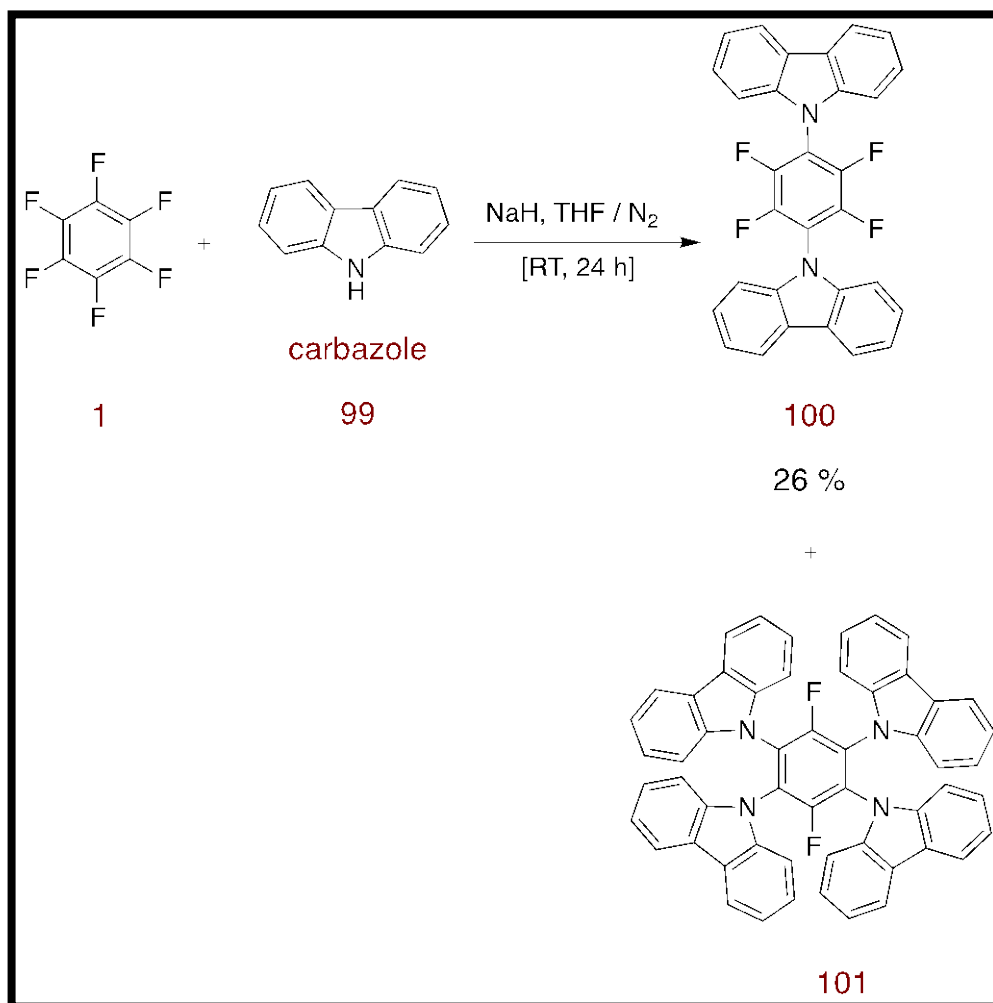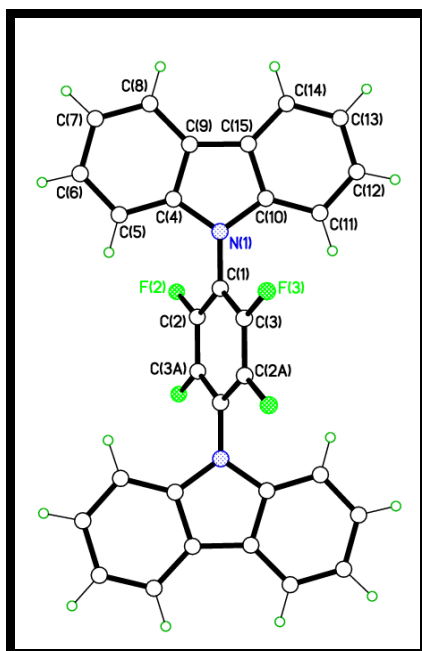
Figure 18. X-ray crystal structure of compound (100)
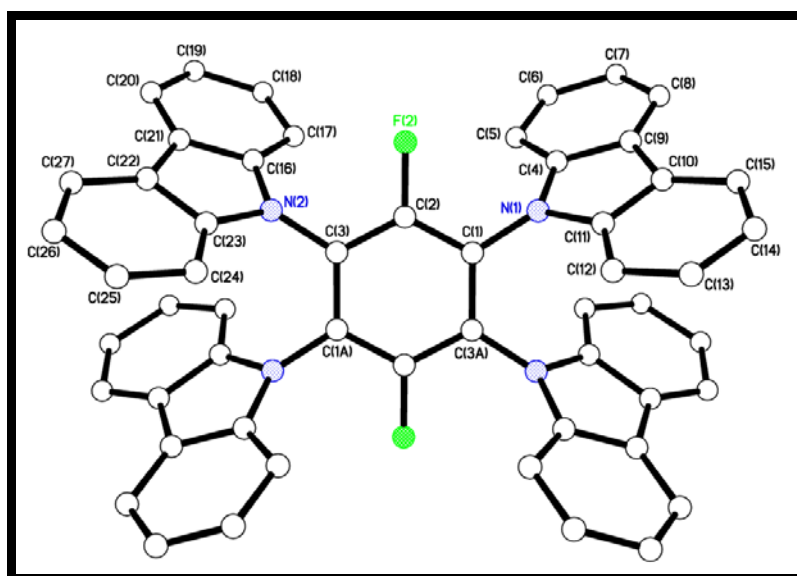
Figure 19. X-ray crystal structure of unexpected minor compound (101)

2.2.7.2. Synthesis of 9-pentafluorophenyl-9H-carbazole (102)

This reaction aimed to synthesise monocarbazole derivative **102** (Scheme 42), using a ratio 1:1 of carbazole:hexafluorobenzene. In this case only dicarbazole derivative **100** was afforded. Because of that it was decided to increase the ratio of hexafluorobenzene in the reaction mixture. Carbazole:hexafluorobenzene 1:10 equivalents was used and carbazole was added very slowly to the reaction mixture using a syringe pump to increase the chance of monocarbazole **102** formation. Spectroscopic data and TLC suggested the

presence of a mixture of mono and dicarbazole derivatives, and column chromatography allowed us to separate the mixture. The monocarbazole derivative **102** was afforded as white crystals in 11 % yield and the dicarbazole derivative **100** was afforded as yellow crystals in 22 % yield. The first formed product **102** appears to be more reactive than the starting hexafluorobenzene **1**, and addition of a second molecule of the nucleophile occurs readily. This phenomenon has been observed previously in the group and may be due to the repulsive effect of a *para*-fluorine atom in the starting hexafluorobenzene **1**.

Scheme 42. Reaction of hexafluorobenzene with carbazole
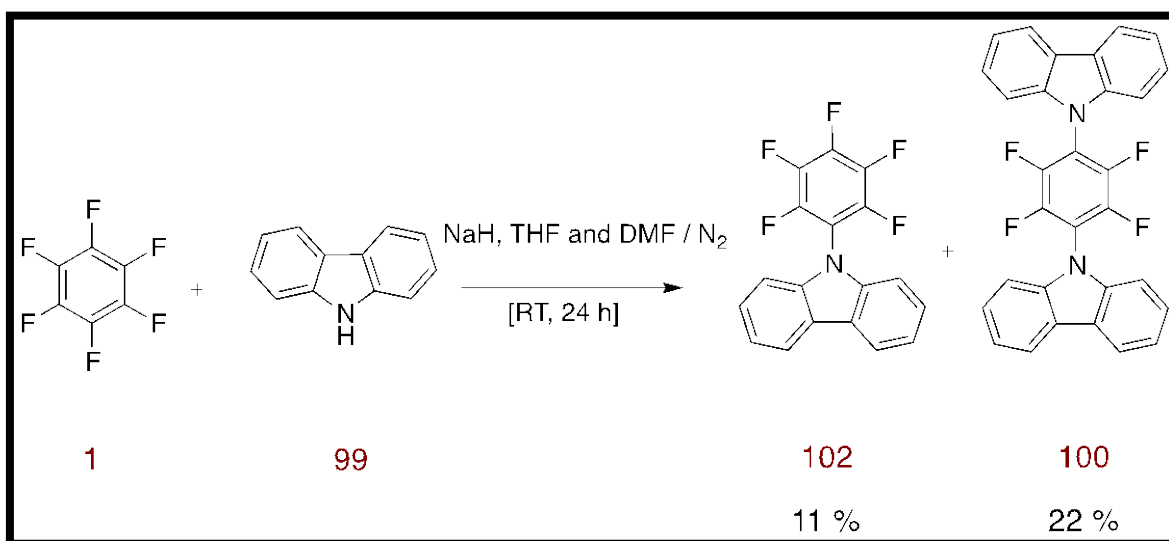
2.2.7.3. Synthesis of 9-(2,3,5,6-tetrafluoropyridine-4-yl)-9H-carbazole (103)

The synthesis of 9-(2,3,5,6-tetrafluoropyridine-4-yl)-9H-carbazole **103** was investigated by reaction of pentafluoropyridine **21** with carbazole **99** at RT in the presence of NaH as base and a mixture of THF and DMF as solvents (Scheme 43). TLC analysis showed the presence of the starting carbazole **99**, and column chromatography purification allowed us to get the target product **103** as yellow crystals in 51 % yield. ^{1}H NMR and ^{19}F NMR spectroscopy proved the presence of the compound **103** and mass spectrometry found the expected mass of the compound, GC-MS (EI) *m/z* 316.
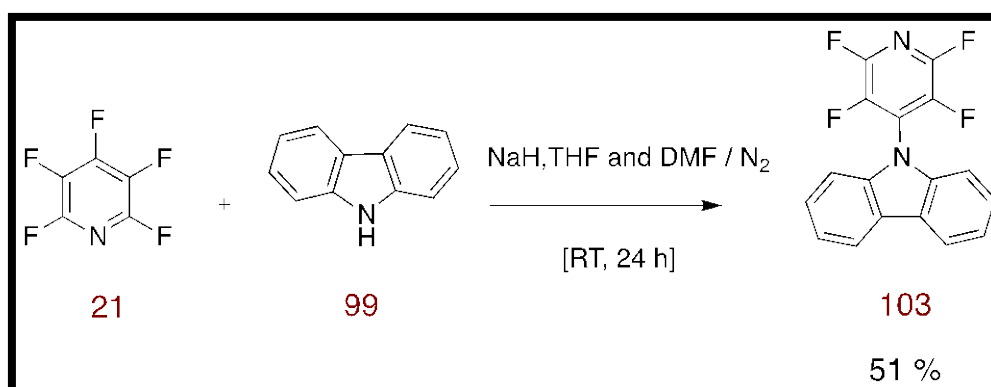
Interestingly by repeating the experiment in the same conditions to collect more material of the target product **103** to do further reactions, the spectroscopic data suggested the presence of unexpected tricarbazole derivative **104** (Scheme 44) with m.p. 217-221 °C.^{19}F NMR spectroscopy displayed one signal for two fluorine atoms due to the symmetry of the compound, δ_F (376 MHz, CDCl$_3$) 39.65 (2F, s). ^{1}H NMR spectroscopy showed multiplet peaks for carbazole rings suggesting the formation of tricarbazole derivative **104**, δ_H (400 MHz, CDCl$_3$) 8.19-8.09 (m), 7.63-7.56 (m), 7.48-7.38 (m), 7.36-7.30 (m). Unfortunately neither orbitrap nor GC-MS found the exact mass of the target tricarbazole derivative **104**. Even addition of silver ions to try to form a charged complex failed to allow characterisation by mass spectrometry.

Scheme 44. Tricarbazole compound (104) afforded by reaction of hexafluorobenzene with carbazole
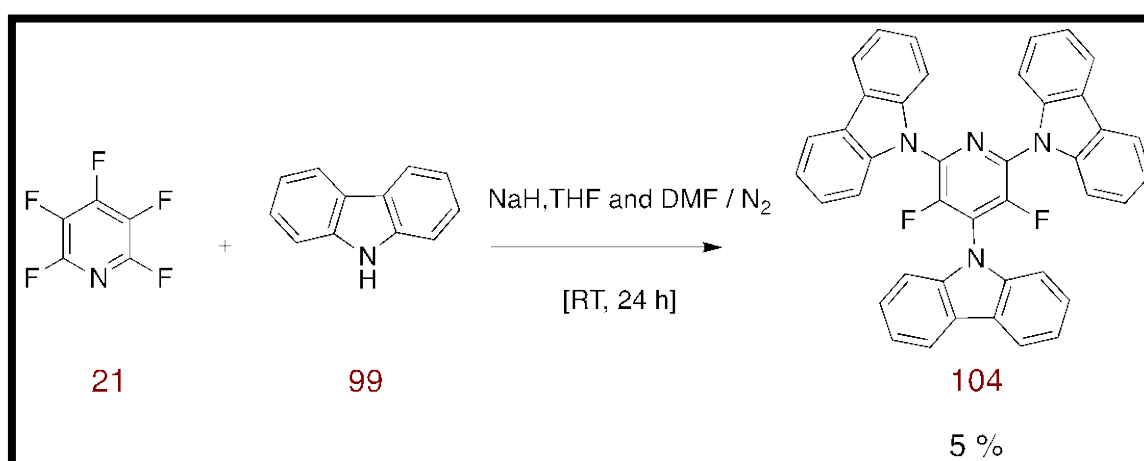
2.2.7.4. Synthesis of 9-(2,3,5,6-tetrafluoro-4-methylphenyl)-9H-carbazole (105)

The compound 9-(2,3,5,6-tetrafluoro-4-methylphenyl)-9H-carbazole **105** (Scheme 45) was successfully synthesised by reaction of carbazole **99** with pentafluorotoluene **44** in the presence of NaH as base and a mixture of THF and DMF as solvents under reflux at 66 °C for 48 h. The product was afforded as white crystals in 37 % yield and m.p. 153-155 °C. Mass spectrometry found the expected mass of the target compound **105**, GC-MS (EI) *m/z* 329 and ^{19}F NMR spectroscopy showed two signals for two pairs of fluorine atoms, δ_F (376 MHz, CDCl$_3$) 19.80-19.72 (2F, m), 17.14-17.05 (2F, m). The final evidence was the X-ray crystal diffraction analysis, which confirmed the structure of the title compound **105** (Figure 20).

Scheme 45. Reaction of pentafluorotoluene with carbazole
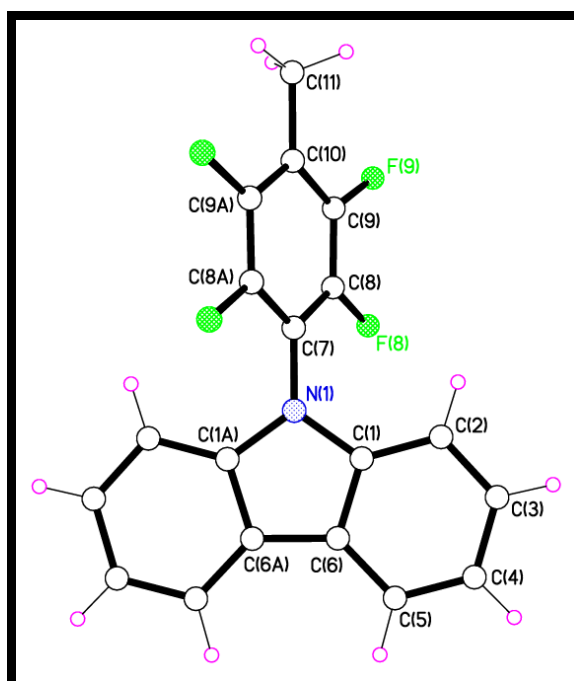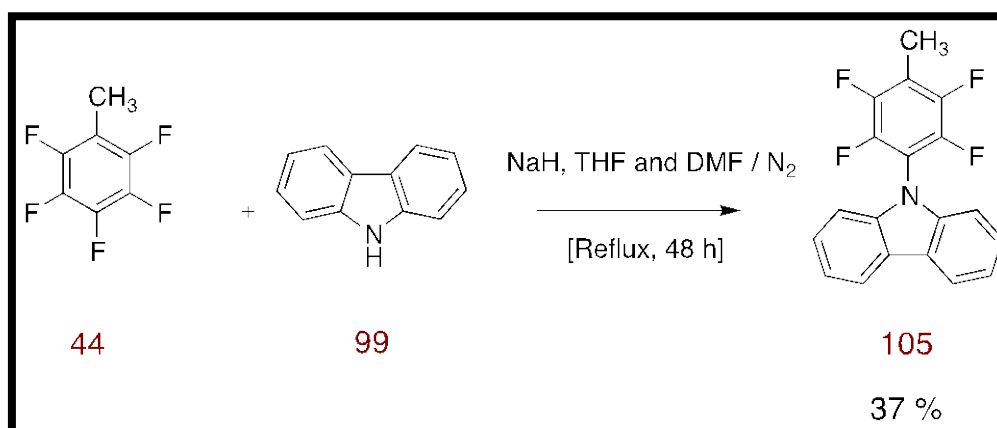
Figure 20. X-ray crystal structure of compound (105)

2.2.7.5. Synthesis of 4-carbazol-9-yl-2,3,5,6-tetrafluorobenzaldehyde (107)

With the success of the reaction of carbazole and pentafluorotoluene it was hoped to study if the process could be extended to pentafluorobenzaldehyde **106**. Different conditions were investigated to synthesise the target compound **107** (Scheme 46), but unfortunately it was not possible to synthesise the desired aldehyde. The product material in all conditions showed complicated TLC analysis and ^{1}H NMR and ^{19}F NMR spectroscopy. After carrying out column chromatography on the sample, ^{19}F NMR spectroscopy showed two multiplet signals with minor impurities which suggested the formation of the target compound **107**, but GC mass spectrometry detected only the starting carbazole and did not find the target compound **107**. ^{1}H NMR spectroscopy showed the expected signals for the starting carbazole but did not reveal the carbonyl group proton, which expected to be around 10-11 ppm.

Scheme 46. Attempted reaction of pentafluorobenzaldehyde with carbazole
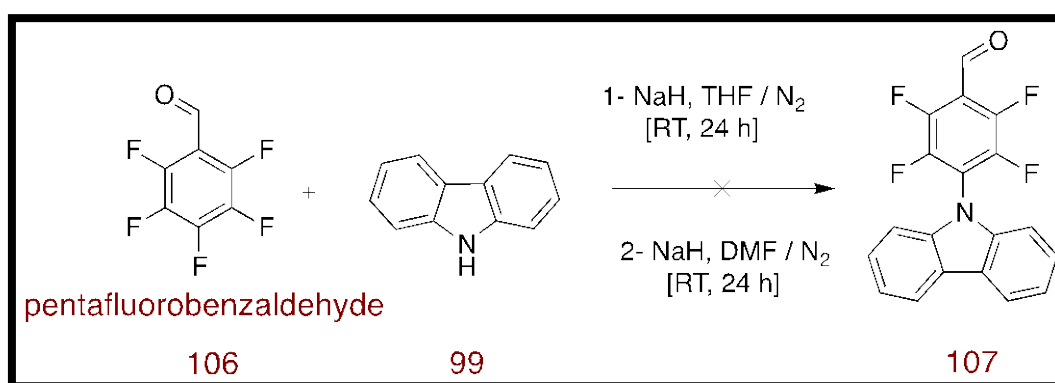
2.2.7.6. Synthesis of tetrafluoro di-carbazole derivative (109)

Because the reaction of carbazole **99** with pentafluorobenzaldehyde **106** did not work (section 2.2.7.5) it was decided to use more reactive perfluorinated compound pentafluorobenzoyl chloride **108** (Scheme 47). Interestingly in the ratio 1:1 equivalents of pentafluorobenzoyl chloride:carbazole in a mixture of THF and DMF at RT addition of carbazole **99** had occurred at both the acid chloride and at the 4-position of the perfluorophenyl ring. The acid chloride **108** had acylated the nitrogen of one carbazole and then undergone S_NAr reaction at the 4-position with a second carbazole anion. ^{19}F NMR spectroscopy showed two signals for compound **109**, δ_F (376 MHz, CDCl$_3$) 22.95-22.86 (2F, m), 22.54-22.43 (2F, m). Two smaller signals at 43.89 and 42.40 indicated the presence of a minor fluorine-containing by-product, but this could not be identified. Mass

spectrometry found the exact mass of di-carbazole compound **109**, HRMS (ESI) *m/z* found 509.1269 (M+H)$^+$, $C_{31}H_{17}F_4N_2O$ requires 509.1272.

Scheme 47. Reaction of pentafluorobenzoyl chloride with carbazole
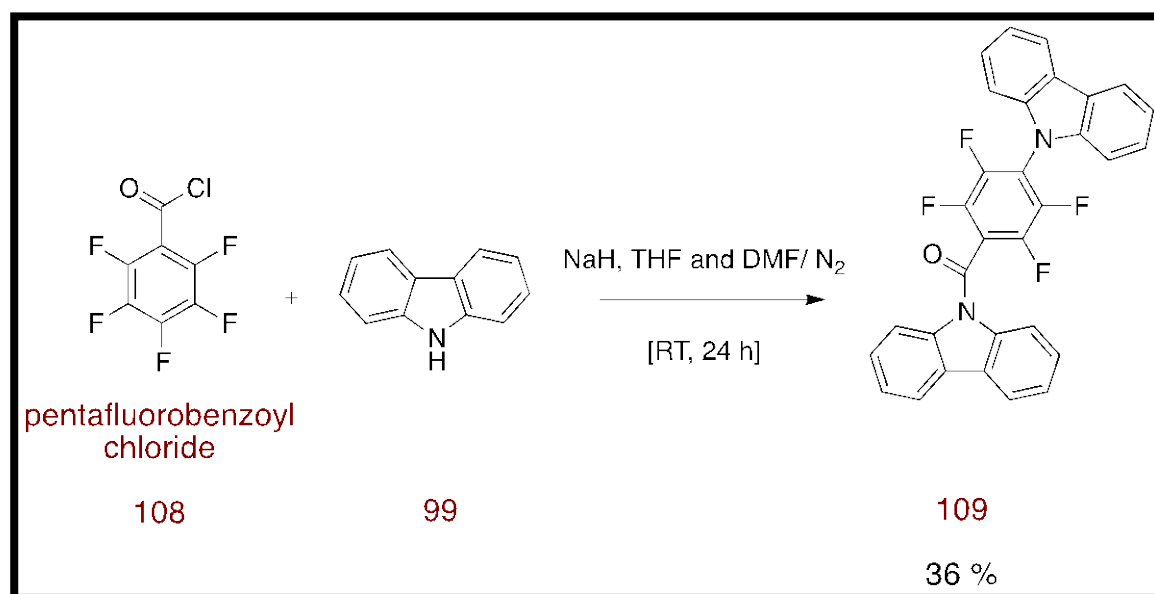
2.2.7.7. Synthesis of 4-carbazol-9-yl-2,3,5,6-tetrafluorobenzamide (111)

Then it was planned to investigate addition of carbazole to a more stable carboxylic acid derivative, namely pentafluorobenzamide **110** to see if clear addition to the 4-position would occur. Reaction of carbazole **99** with pentafluorobenzamide **110** worked well at RT in the presence of a mixture of THF and DMF as solvents and NaH as base and the target compound **111** was successfully synthesised, (Scheme 48). 4-Carbazol-9-yl-2,3,5,6-tetrafluorobenzamide **111** was afforded as yellow crystals with m.p. 203-206 °C, as pure product as proved with elemental analysis, analysis (%) calculated for $C_{19}H_{10}F_4N_2O$ (358): C, 63.68; H, 2.79; N, 7.82. Found C, 63.22; H, 2.72; N, 7.87. Mass spectrometry exhibited the expected mass of the title compound, GC-MS (EI) *m/z* 358, and the ^{19}F NMR spectrum revealed two signals for two pairs of fluorine atoms, δ_F (376 MHz, CDCl$_3$) 23.18-23.09 (2F, m), 21.64-21.55 (2F, m). In addition X-ray crystallography proved the structure of the target carbazole derivative **111** (Figure 21). The X-ray structure showed the carbazole ring to be twisted out of the plane of the tetrafluorobenzamide ring.

Scheme 48. Reaction of pentafluorobenzamide with carbazole

pentafluorobenzamide

110   99   111

48 %
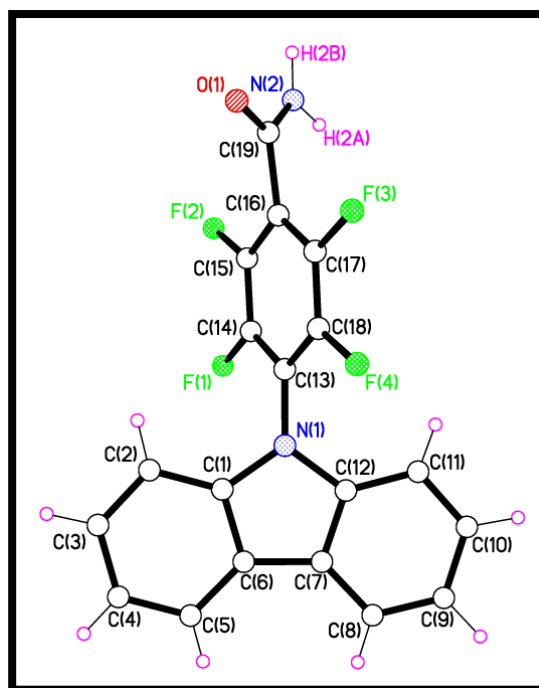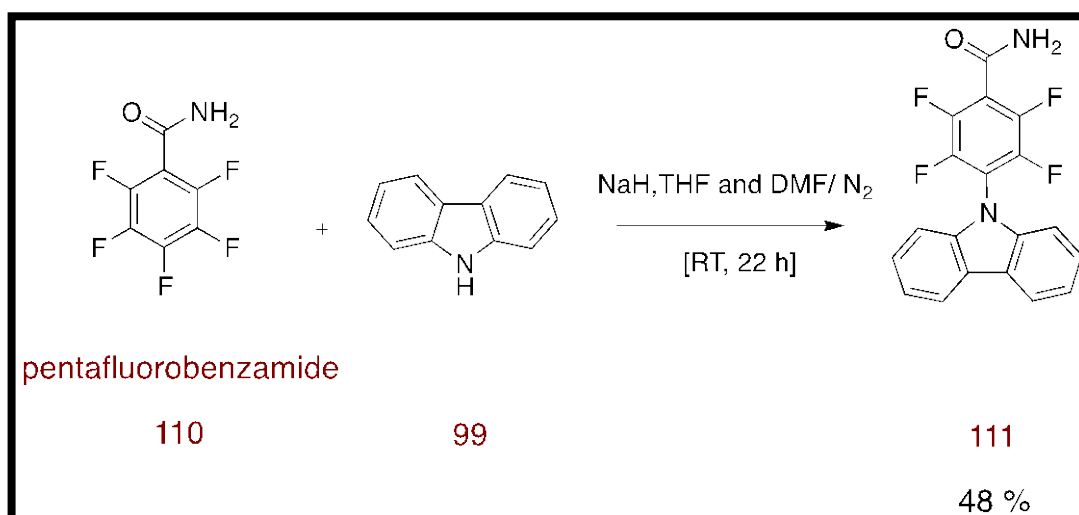
Figure 21. X-ray crystal structure of compound (111)

2.2.7.8. Synthesis of 3,4-dihydro-7-carbazol-9-yl-5,6,8-trifluoro-1H-quinolin-2-one (114)

In order to improve water solubility of the new derivatives to allow study of their interaction with DNA it was decided to investigate addition to the 3-(pentafluorophenyl) propionamide **112** which has a flexible polar side chain. The target carbazole derivative **113** (Scheme 49) was not formed but the cyclized compound **114** was produced and showed carbazole had successfully added to C-4 of 3-(pentafluorophenyl)-propionamide

112 as well the amide side chain cyclizing to form a dihydroquinolin-2-one. The base NaH was used in slightly excess to deprotonate NH group of starting carbazole, but also affected deprotonation of the NH_2 group in amide and consequently the tricyclic carbazole derivative was formed by nucleophilic substitution reaction of a further fluorine atom. The spectroscopic data suggested the presence of the carbazole derivative **114** in 63 % yield. Mass spectrometry found the exact mass of the compound **114**, HRMS (ESI) *m/z* found 365.0912 (M–H)$^-$, $C_{21}H_{12}F_3N_2O$ requires 365.0907. ^{19}F NMR spectroscopy showed three fluorine signals rather than the two expected for uncyclized **113**.

Scheme 49. Attempted reaction of 3-(pentafluorophenyl)propionamide with carbazole
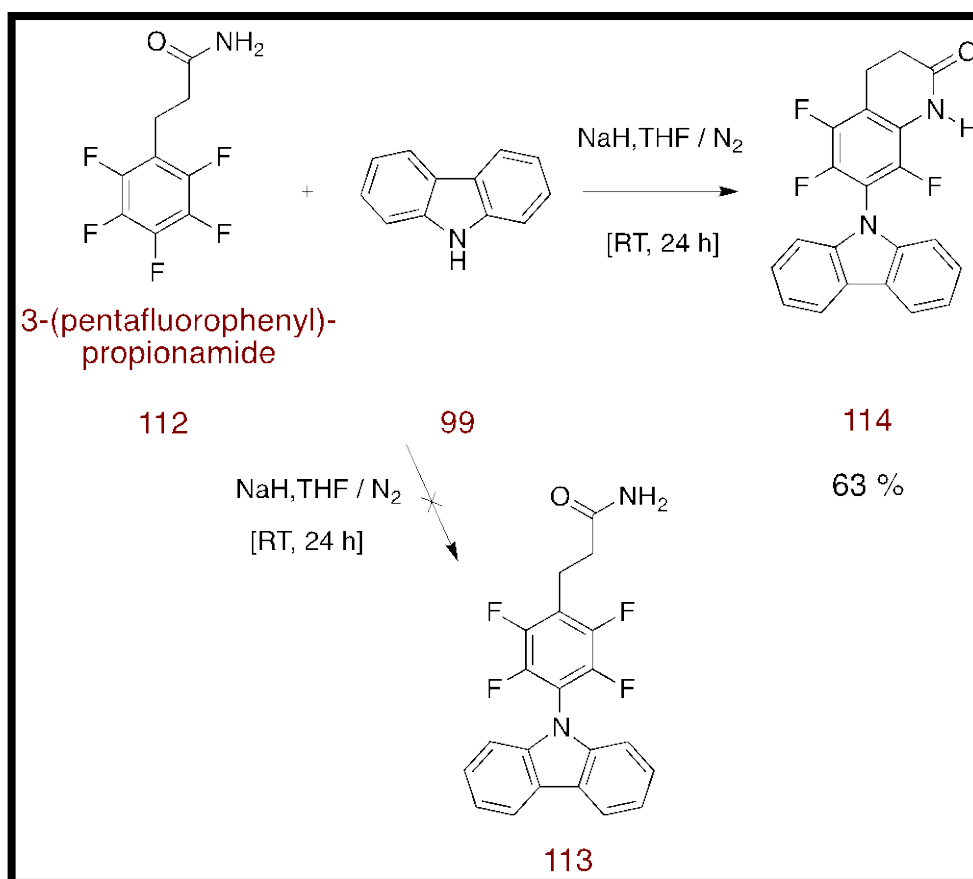
2.2.7.9. Study the reaction of carbazole with methyl pentafluorobenzoate (115)

A useful substituent for further functionalization of potential drug molecules would be an ester group. Therefore it was decided to investigate whether the carbazole anion would also add to the 4-position of methyl pentafluorobenzoate **115** (Scheme 50). The mono carbazole compound **116** was formed in 16 % yield at RT in the presence of NaH as base and THF as solvent and the product was isolated as white crystals with m.p. 148-152 °C.

^{19}F NMR spectroscopy showed two signals for two pairs of fluorine atoms, δ_F (376 MHz, CDCl$_3$) 24.46-24.37 (2F, m), 21.17-21.08 (2F, m). The expected mass of the target molecule was displayed by GC-MS (EI) with a peak at *m/z* 373, as well as the IR analysis which displayed the expected signals for the functional groups in the structure, v_{max} /cm^{-1}(film) 1736 (C=O), 1296 (C-O). The successful synthesis of mono carbazole compound **116** was confirmed by X-ray crystallography (Figure 22).

In a further experiment to try to improve the yield the reaction of methyl pentafluorobenzoate **115** and carbazole **99** was repeated but the reaction condition was changed and in this case the mixture was refluxed at 66 °C in THF (Scheme 50). The work-up procedure afforded yellow oil but after recrystallization processes with hot ethanol the white crystals isolated had a higher m.p. 179-181 °C. The desired compound **116** was not formed, and the bis-substituted product **117** was formed instead in low yield 15 % only. ^{19}F NMR spectroscopy showed three signals which suggest the bis-carbazole compound formed, δ_F (376 MHz, CDCl$_3$) 40.64 (1F, d, *J* 13 Hz), 29.01 (1F, d, *J* 22 Hz), 24.57 (1F, dd, *J* 22 and 13 Hz). Moreover mass spectrometry found the exact mass of the compound **117**, HRMS (ESI) *m/z* found 520.1387, C$_{32}$H$_{19}$F$_3$N$_2$O$_2$ requires 520.1393. The higher reaction temperature may have encouraged formation of the di-substitution product **117**, although its production is surprising since two equivalents of the pentafluorobenzoate were employed. Possibly the mono-substitution product **116** was formed but it could not be isolated.

Scheme 50. Reaction of methyl pentafluorobenzoate with carbazole

methyl pentafluorobenzoate

115

99

NaH, THF / N$_2$

[RT, 24 h]

116

16 %

NaH, THF / N$_2$

[Reflux 66 °C, 24 h]

117

15 %
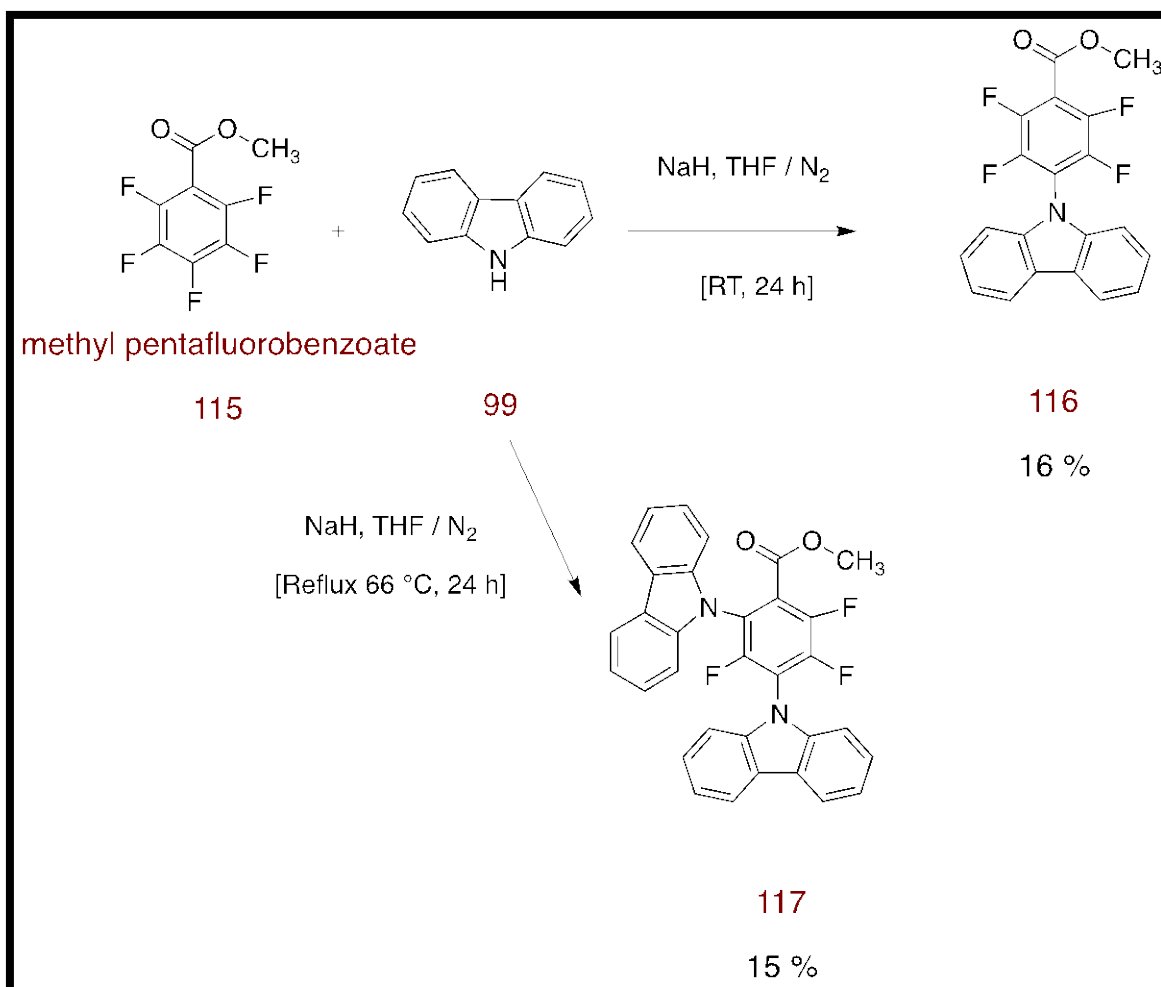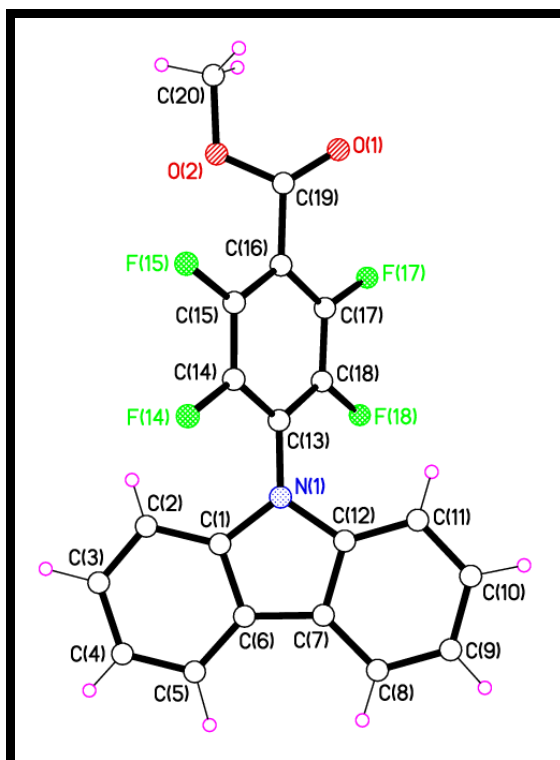
Figure 22. X-ray crystal structure of compound (116)

2.2.7.10. Synthesis of di-carbazole derivatives from decafluorobiphenyl

To extend the range of fluorinated heterocycles it was hoped to explore S_NAr reaction of the commercially available decafluorobiphenyl **118**. It was planned to study carbazole as a nucleophile due to its success in reacting with other fluoroarenes.

Carbazole derivative **119** was successfully synthesised at RT in ratio of starting materials carbazole:decafluorobiphenyl in 2:1 equivalents in the presence of a mixture of THF and DMF as solvents (Scheme 51). Recrystallization with hot ethanol afforded the title compound as white crystals with m.p. 296-298 °C in 76 % yield.^{19}F NMR spectroscopy demonstrated the expected signals for the target compound **119**, δ_F (376 MHz, CDCl$_3$) 25.69 (4F, s), 20.90 (4F, s). Unfortunately as discussed earlier, the exact mass could not be observed with orbitrap mass spectrometry or with GC mass spectrometry, but elemental analysis suggested the presence of the target compound as pure product, analysis (%) calculated for C$_{36}$H$_{16}$F$_8$N$_2$ (628): C, 68.78; H, 2.54; N, 4.45. Found C, 68.06; H, 2.43; N, 4.33.

Scheme 51. Synthesis of di-carbazole derivative (119) from decafluorobiphenyl
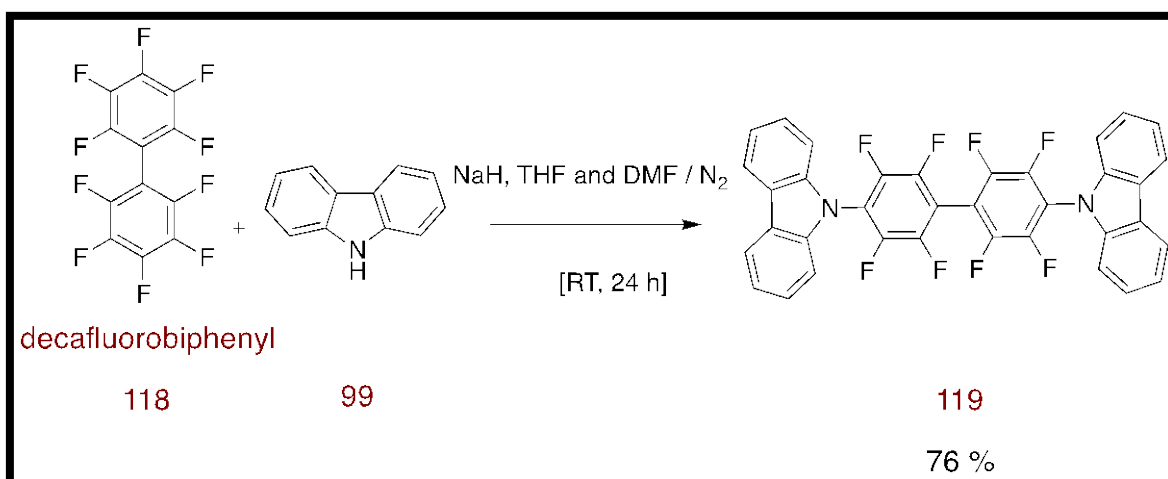
2.2.7.11. Synthesis of mono-carbazole derivatives from decafluorobiphenyl

Then it was planned to prepare the mono-carbazole adduct **120** (Scheme 52) which would allow addition of other nucleophiles at the 4`-position of the unsubstituted pentafluorophenyl ring. The reaction of carbazole:decafluorobiphenyl in a 1:1 ratio at RT was therefore studied, using a mixture of THF and DMF as solvents. Decafluorobiphenyl was added to a stirred suspension of NaH and carbazole was added very slowly using a syringe pump to increase the chance of formation of mono-carbazole derivative **120** than di-carbazole derivative **119**. Interestingly the final product was a mixture of three compounds, which were separated by column chromatography. The major compound was dicarbazole derivative **119** with 22 % yield, monocarbazole derivative **120** was afforded in 29 % yield and the minor compound was alcohol **121**, which was obtained in 7 % yield. The spectroscopic analysis showed the evidence of formation of these compounds and highlighted in the experimental section in more details. The formation of the phenol derivative **121** may have been due to traces of sodium hydroxide in the reaction mixture generated from sodium hydride and moisture.

Scheme 52. Study the reaction of carbazole with decafluorobiphenyl
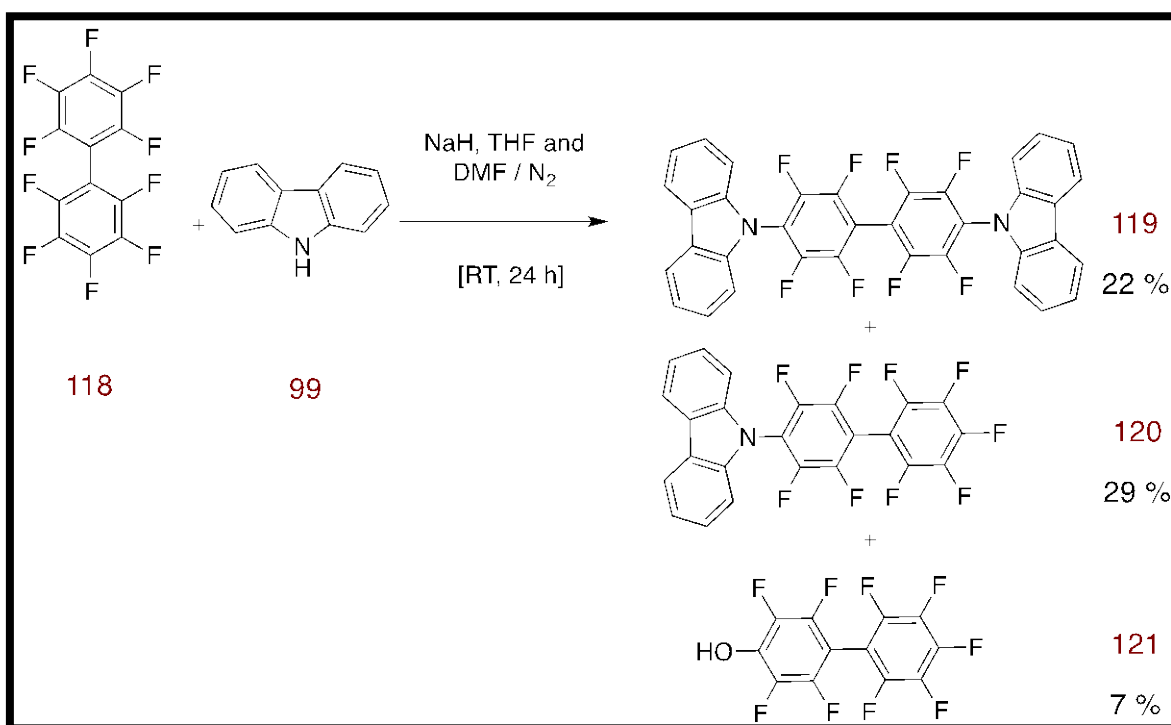
2.2.7.12. Study the reaction of 9-(2,3,5,6-tetrafluoro-4-methylphenyl)-9H-carbazole (105) with nitriles

Because of the limited success of the previous investigation of indole heterocyclic derivatives using pentafluorotoluene **44** and nitriles (Section 2.2.2), it was hoped to study the reaction of carbazole derivative **105** with nitriles (Scheme 53) with the aim of deprotonating the methyl group and adding resulting anion to the nitrile with the expectation that the imine anion formed might cyclize onto the tetrafluorobenzene ring as discussed previously (Section 2.2.2). It was hoped that the bulky carbazole ring would block the lower half of the molecule preventing side reactions at the 3,4 or 5 positions that might have hampered the reaction in the previous examples. It was also expected the carbazole derivative would be crystalline allowing easier isolation and characterization. Three different nitriles were studied 4-methoxybenzonitrile, benzonitrile and acetonitrile. Again treating compound **105** with NaH and any of the three nitriles unfortunately failed to give the desired indoles (**122** - **123** – **124**) and the starting compound **105** was detected by the spectroscopic analysis. The continued lack of success in forming indoles then prompted us to investigate other areas and the study of reaction with nitriles was discontinued.

Scheme 53. Investigation the reaction of compound (105) with nitriles
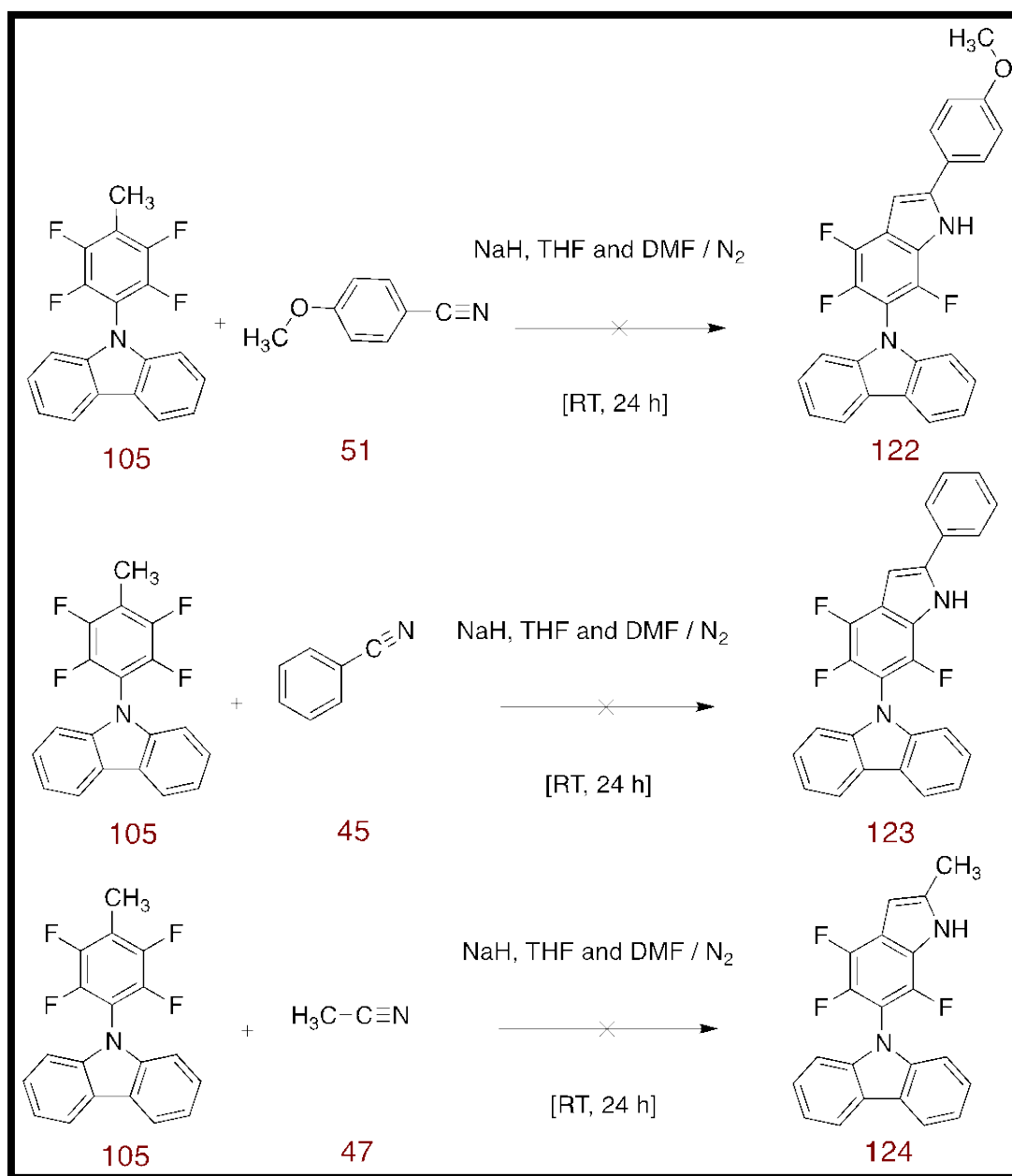
2.2.8. Synthesis of bis-intercalating agents

Organic intercalating agents are the compounds that interact with the DNA double strand reversibly. Bis intercalating organic compounds involve two potential intercalating ring systems connected together by a linker, which can be of different length and different rigidity. Due to more than one intercalating unit bis-intercalating agents possess higher DNA binding constants and sequence selectivity and exhibit slower dissociation than mono intercalating compounds.[48]

In the interest of the above suggestion it was hoped to design and synthesise a series of potentially bis-intercalating compounds using the novel fluorinated compounds that had been synthesised in this study. In addition it was planned to exploit the reactivity of the aldehyde group in derivatives of perfluorobenzaldehyde towards imine formation, or of the remaining ring fluorines on the aromatic nucleus to S_NAr reaction. It was hoped diamine compounds would act as bis-nucleophiles and allow two potential intercalating compounds to be linked together to increase their DNA binding potency. It was planned to study if improved binding would occur through thermal melting and UV and fluorescence assays.

2.2.8.1. Study the reductive amination of pentafluorobenzaldehyde and 2,2-(ethylenedioxy)bis(ethylamine)

In order to synthesise bis-intercalating compounds it was hoped to investigate the reaction of pentafluorobenzaldehyde **106** and aliphatic amine 2,2-(ethylenedioxy)bis(ethylamine) **125** (Scheme 54) in 2:1 ratio to synthesise compound **127** as a core scaffold for fluorinated-bis intercalators which will be involved in further studies later. The reaction worked well at RT in DCM as solvent, $NaBH_4$ was used to reduce the intermediate imine **126** and the target compound **127** was afforded in 77 % yield. ^{19}F NMR spectroscopy detected the expected fluorine signals for the target compound, δ_F (376 MHz, CDCl$_3$) 17.68-17.52 (4F, m), 5.80 (2F, t, *J* 20 Hz), -0.52 to -0.73 (4F, m) and mass spectrometry displayed the expected mass of the title compound, HRMS (ESI) *m/z* found 509.1272 (M+H)$^+$, $C_{20}H_{19}F_{10}N_2O_2$ requires 509.1281.

Pentafluorobenzaldehyde **106** and aliphatic amine 2,2-(ethylenedioxy)bis(ethylamine) **125** also studied in the ratio of 1:1 equivalents to synthesise the target compound **129** (Scheme 55) to be involved in further studies in the project to synthesise water soluble mono-intercalating compounds. Mass spectrometry suggested the presence of the target compound **129** and found the expected molecular formula of the compound, HRMS (ESI) *m/z* found 329.1277 (M+H)$^+$, $C_{13}H_{18}F_5N_2O_2$ requires 329.1283. Unfortunately ^{19}F NMR and ^{1}H NMR spectroscopy and elemental analysis showed some impurities and TLC analysis showed tailing, because of that the sample could not be purified and it was not studied further.

Scheme 54. Synthesis of a potential bis-intercalating scaffold (127)

2,2-(ethylenedioxy)bis(ethylamine)

106

125

1- DCM / MgSO$_4$ / N$_2$
[RT, 5 h]

126

2- EtOH / NaBH$_4$
[RT, 1 h]

127

77 %
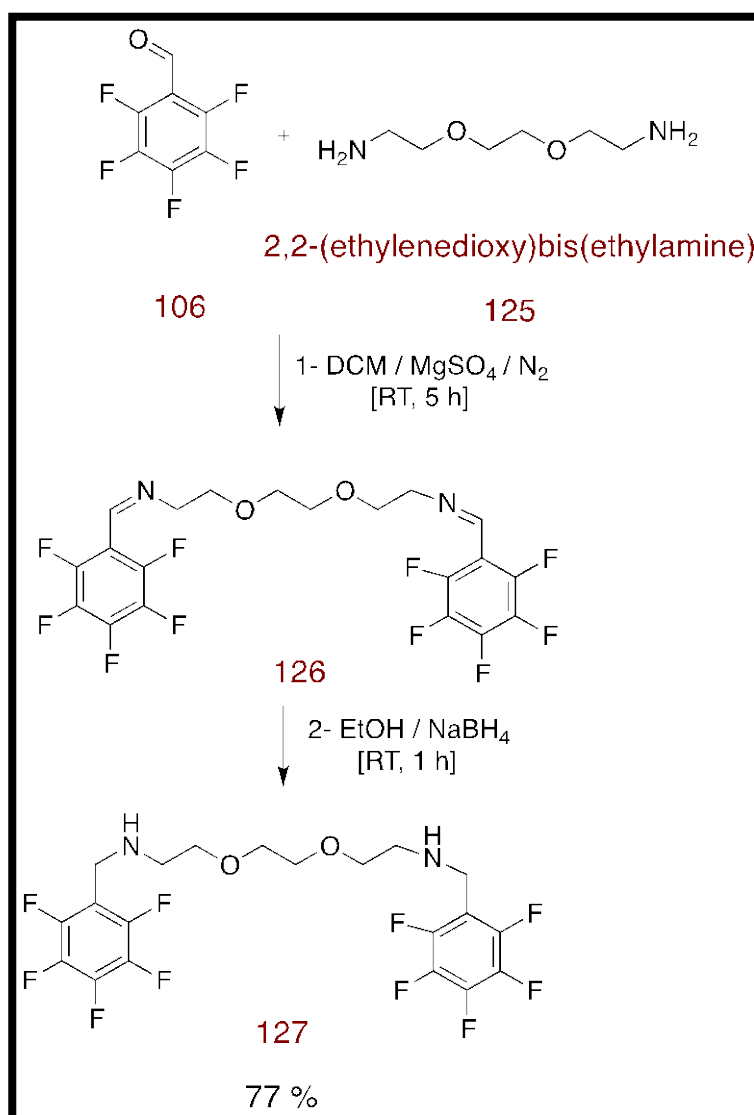
Scheme 55. Synthesis of a potential bis-interlacing scaffold (129)
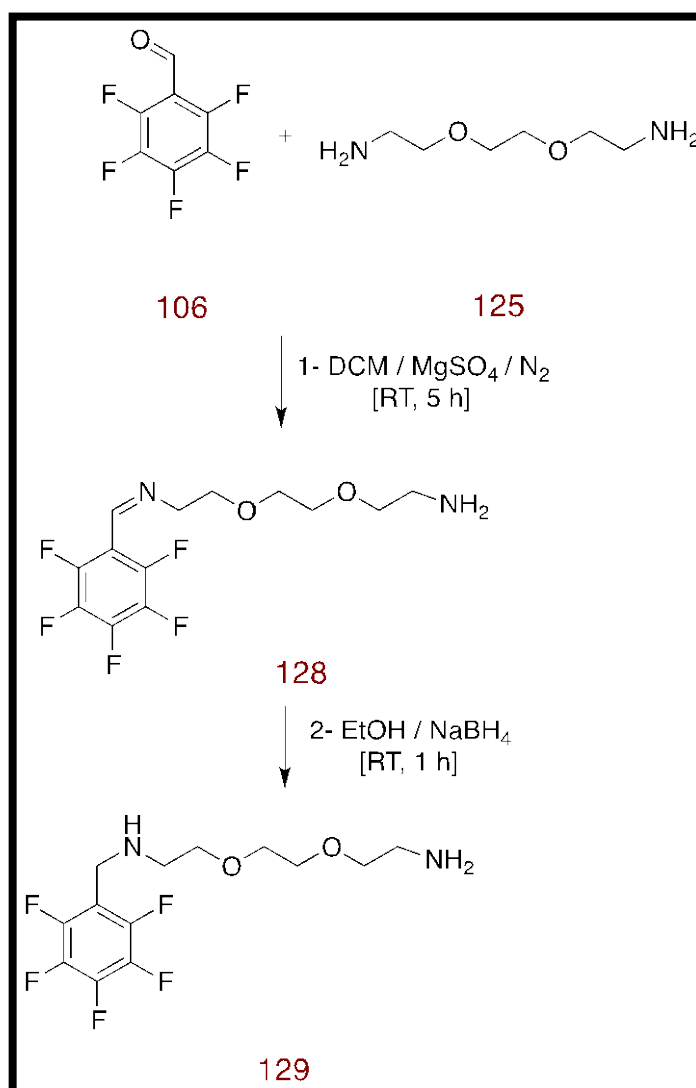
2.2.8.2. Investigation of the reaction of carbazole with bis-intercalator scaffold (127)

After successful formation of compound **127** it was planned to investigate the possibility of interacting it with carbazole to synthesise bis-intercalating compound **130** (Scheme 56). Carbazole **99** was reacted with compound **127** in the ratio 2:1 equivalents at RT in the presence of NaH as base and THF as solvent. The work-up procedure afforded sticky yellow material and column chromatography purification yielded yellow crystals with m.p. 238-241 °C. Mass spectrometry gave the exact molecular formula of the target compound **130**, HRMS (ESI) *m/z* found 803.2627 (M+H)$^{+}$, $C_{44}H_{35}F_8N_4O_2$ requires 803.2627. ^{1}H NMR spectrum showed some signals consistent with the predicted structure although they were weak, and signals possibly due to starting carbazole were also observed. The ^{19}F NMR spectrum also did not show the expected two signals of two pairs

of fluorine atoms but exhibited three signals, different from the signals of the starting compound **127**, which might suggest the formation of some of the target compound. The elemental analysis was far from the calculated values, which could also suggest fluorinated impurities in the sample that could not be removed with column chromatography. Unfortunately, the crystals were not suitable for X-ray crystallography and further investigations are still required to fully characterize the compound.

Scheme 56. Study reaction of carbazole with compound (127)
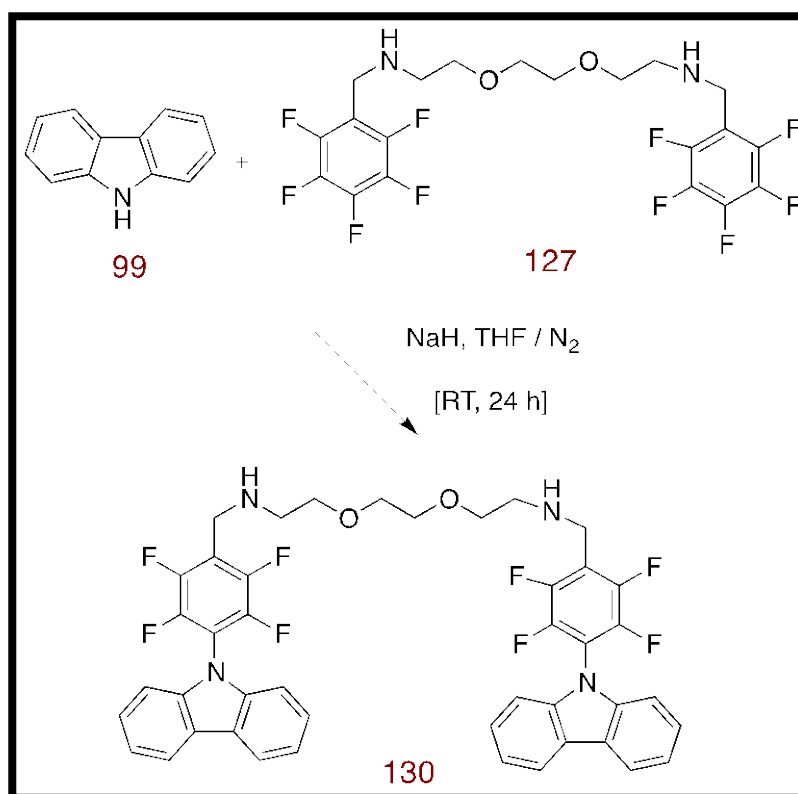
2.2.8.3. Study the reaction of 1-bromo-2-naphthol with bis-intercalator scaffold (127)

The reaction of 1-bromo-2-naphthol **86** with compound **127** was carried out in THF at RT in the presence of NaH as base to deprotonate bromonaphthol **86** hoping to displace the 4-position fluorine atom in compound **127** by nucleophilic substitution reaction (Scheme 57). If formed compound **131** would represent a useful substrate for cyclization using the lithiation strategy already developed. Work-up procedure gave a yellow oil and column chromatography purification yielded yellow oil as well. Again ^{19}F NMR spectroscopy showed three signals very close to signals of the starting compound **127**. Mass spectrometry could not find the expected mass of the target compound **131**. It appears the

reaction was unsuccessful and the target compound **131** was not formed despite the success of related reactions with phenolic nucleophiles.

Scheme 57. Attempted reaction of 1-bromo-2-naphthol with compound (127)
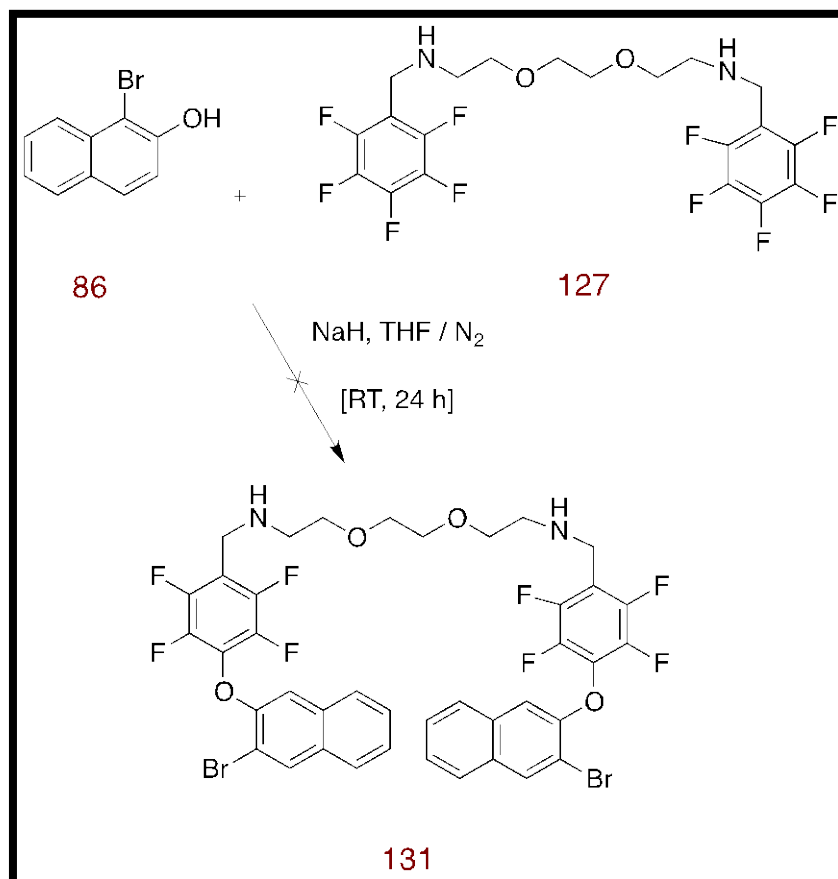
2.2.8.4. Study the reaction of di-carbazole (100) with 2,2-(ethylenedioxy)bis(ethylamine) (125) to form a potential bis-intercalator

Two equivalents of di-carbazole derivative **100** were reacted with one equivalent of aliphatic amine **125** in order to form compound **132** that might possess potential DNA intercalating activity (Scheme 58). The reaction was carried out at RT in a mixture of THF and DMF as solvents in the presence of two equivalents of Et$_3$N to neutralise the HF by-product. Unfortunately the reaction did not work and only the starting material was recovered according to ^{19}F NMR spectroscopy, which showed a singlet peak at 20.72 ppm. Mass spectrometry could not find the expected mass of the target compound. Further studies on this reaction to incorporate one or two amine chains onto carbazole derivative **100** are discussed in section 2.2.9.2.

Scheme 58. Attempted synthesis of a potential bis-intercalator from bis-carbazole derivative (100)
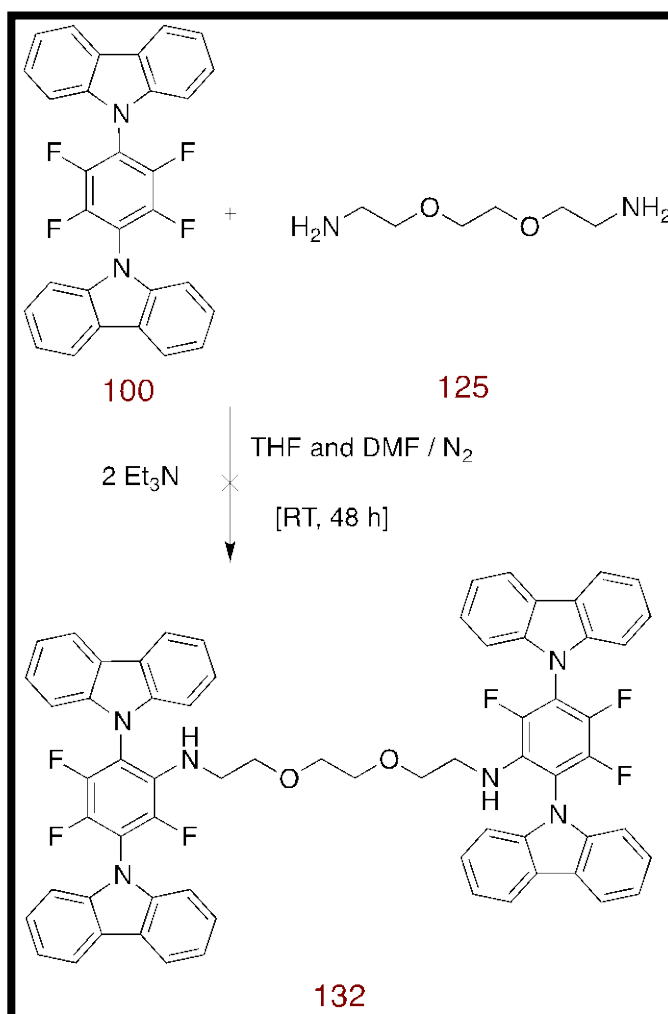
2.2.8.5. Investigation of the synthesis of a potential bis-intercalator from mono carbazole derivative (103)

After the failed attempt to synthesise a potential bis intercalator using di-carbazole derivative **100** it was planned to use the mono carbazole derivative **103** hoping it to be more reactive than the di-carbazole one. It was expected that the amine linker be add at the 2-position of the pyridine ring. The starting amine chain and mono carbazole derivative were used in the ratio 1:2 equivalents to allow addition of two mono carbazole derivatives to one amine chain. Interestingly the reaction worked well in boiling THF for 24 h and the target compound **133** was successfully synthesised (Scheme 59). Work up procedure gave creamy crystals and TLC analysis suggested the presence of the starting mono carbazole. Column chromatography purification yielded **133** as white crystals (0.332 g, 64 %) with m.p. 66-73 °C. ^{19}F NMR spectroscopy showed three multiplet

signals in the range, 70.95-70.78 (m), 15.36-15.24 (m), 1.71-1.63 (m), confirming addition at C-2. Mass spectrometry found the expected mass of the target compound **133**, HRMS (ESI) *m/z* found 741.2407 (M+H)$^+$, $C_{40}H_{31}F_6N_6O_2$ requires 741.2407. Elemental analysis was close to the calculated values although the value for the percentage of carbon was high, analysis (%) calculated for $C_{40}H_{30}F_6N_6O_2$ (740): C, 64.86; H, 4.08; N, 11.35. Found C, 67.52; H, 3.73; N, 11.97.

Scheme 59. Synthesis of a potential bis-intercalator from mono carbazole derivative (103)
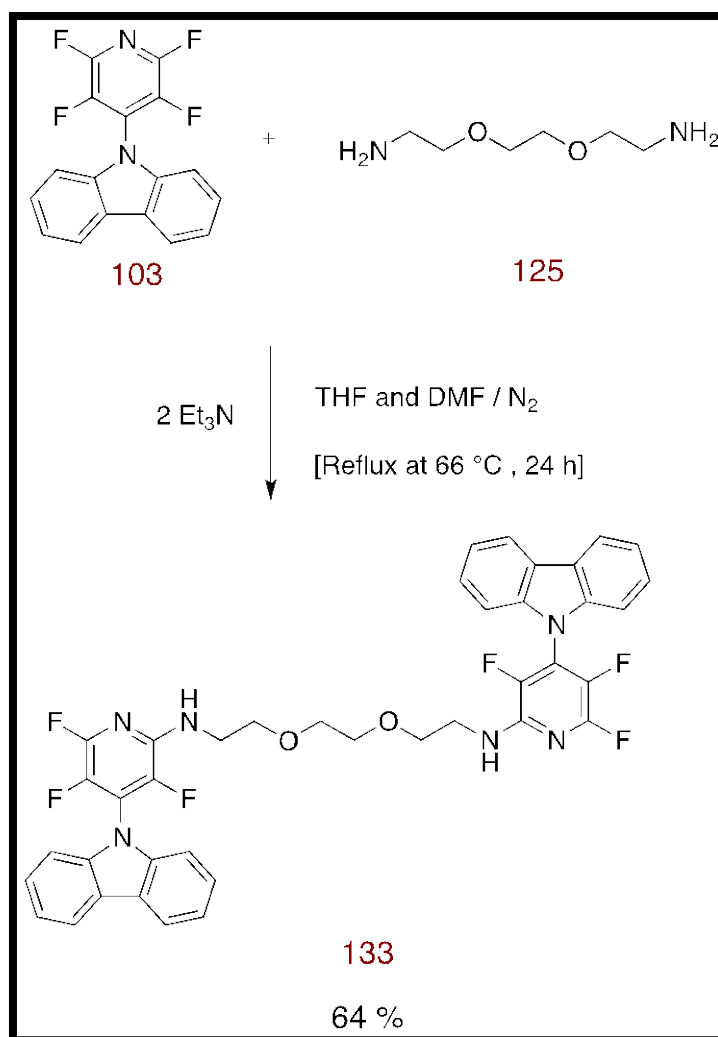
2.2.8.6. Investigation of the synthesis of a potential bis-intercalator from biphenyl carbazole derivative (119)

After an unsuccessful attempt to synthesise a potential bis-intercalator compound **132** from di-carbazole derivative **100** in the previous reaction (Section 2.2.8.4) it was decided to use di-carbazole derivative **119**, hoping in this case the reaction could work well with the aim of synthesising a potential bis-intercalating compound **134** (Scheme 60). The reaction mixture was heated at 101 °C in dioxane for 24 h in the presence of two equivalents of Et_3N to neutralize HF by-product in the reaction mixture. The starting material di-carbazole derivative **119** and the amine chain was in ratio 2:1 equivalents to allow di-nucleophilic substitution of the amine chain with two fluorine atoms to form compound **134**. ^{1}H NMR spectroscopy did not show the expected signals of the target compound **134** and displayed only carbazole ring signals, which suggest just the starting compound **119** was present and no signals for the amine chain. ^{19}F NMR spectroscopy also showed two signals characteristic of the starting material.

Then it was planned to study the possibility of formation a potential DNA bis-intercalator using mono carbazole adduct to decafluorobiphenyl compound **120** (Scheme 61). The starting mono carbazole derivative **120** and the amine chain **125** was in ratio 2:1 equivalents and fortunately the reaction worked well in boiling dioxane for 24 h and the target compound **135** was successfully isolated in 93 % yield. ^{1}H NMR spectroscopy showed the expected signals for the target compound **135**, δ_H (400 MHz, CDCl$_3$) 8.18 (4H, d, J 7.6 Hz), 7.49 (4H, td, J 7.2 and 1.2 Hz), 7.38 (4H, td, J 8.0 and 0.8 Hz), 7.26 (4H, d, J 8.0 Hz), 4.73- 4.65 (2H, bs, NH), 3.80-3.72 (8H, m), 3.76 (4H, s). The ^{19}F NMR spectrum showed four signals in accord with the four pairs of fluorine atoms in the differentially di-substituted biphenyl system. Mass spectrometry also found the expected mass of the target compound, HRMS (ESI) m/z found 1069.2052 (M–H)$^-$, $C_{54}H_{29}F_{16}N_4O_2$ requires 1069.2041. The successful formation of both **133** and **135**, and the lack of reaction of **100** and **119** towards the amine, indicate both electronic and steric effects are controlling the nucleophilic substitution. The bulky carbazole rings, and the presence of a repulsive *para*-fluorine atom disfavor addition of a nucleophile in both **100** and **119**.

Scheme 60. Attempted synthesis of a potential bis-intercalator from carbazole derivative (119)

119

125

2 Et₃N   Dioxane / N₂

[Reflux at 101 °C , 24 h]

134
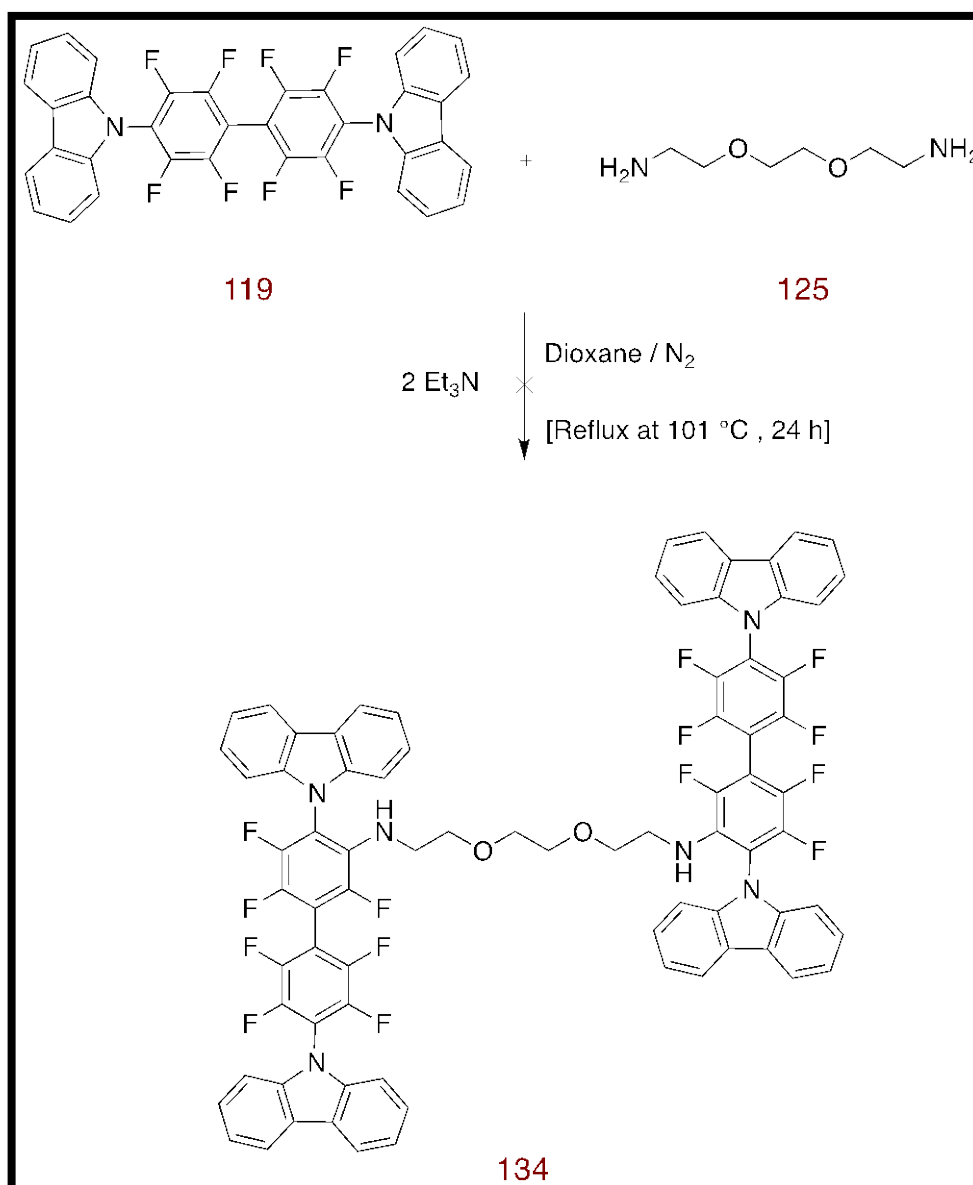
Scheme 61. Synthesis of a potential bis-intercalator from carbazole derivative (120)

120   125

Dioxane / N$_2$

2 Et$_3$N

[Reflux at 101 °C , 24 h]

135

93 %
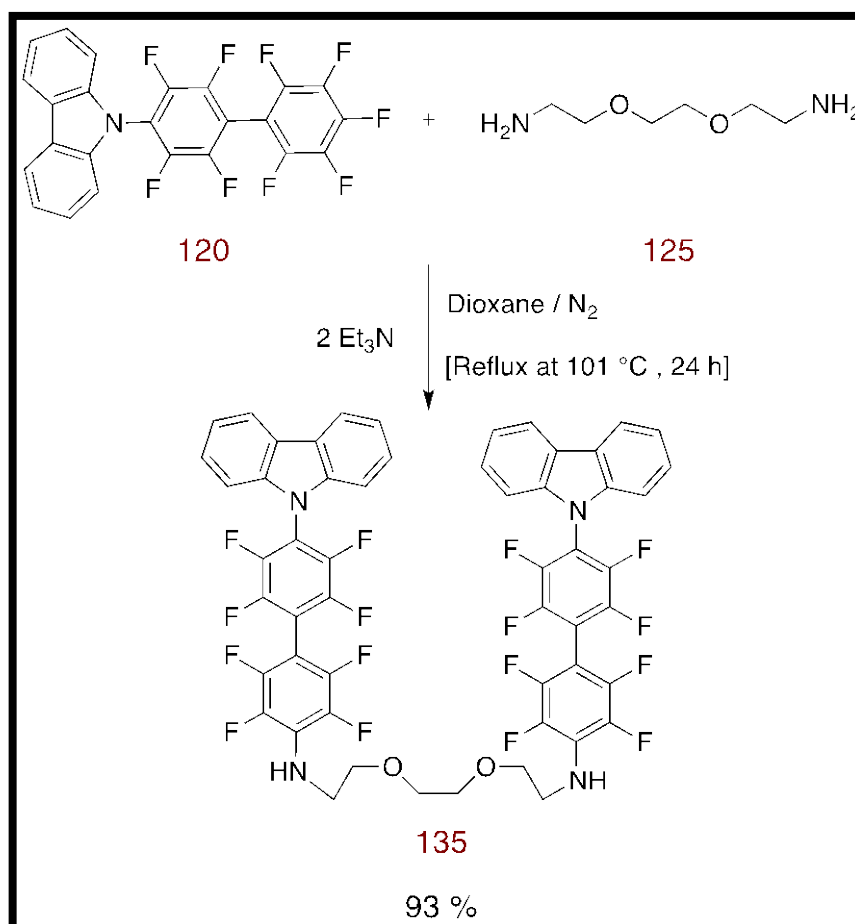
2.2.8.7. Study the synthesis of a potential bis intercalator from carbazole derivative (105)

In order to study the possibility of synthesise a potential bis-intercalator from carbazole derivative **105** it was planned to investigate the reaction under different conditions (Scheme 62). The reaction was carried out in boiling dioxane for 24 h and the starting carbazole derivative **105** and the amine chain **125** was in ratio 2:1 equivalents. And also the reaction was studied in a mixture of THF and DMF under reflux at 66 °C for 24 h and again the starting carbazole derivative **105** and the amine chain **125** was in ratio 2:1 equivalents. Unfortunately the reaction did not work well in either condition and the starting carbazole derivative **105** was recovered each time. ^{19}F NMR spectrum showed the two signals which consistent with the starting carbazole derivative **105**. As well as ^{1}H NMR spectroscopy was consistent with the starting **105** but did not show the expected signals of the target compound **136**. GC-MS found the mass of the starting carbazole

derivative **105** at 329 and all these information suggested the failure of the reaction. The similar de-activating effects present in **100** and **119** may also operating in compound **105**.

Scheme 62. Attempted synthesis of a potential bis intercalator from carbazole derivative (105)
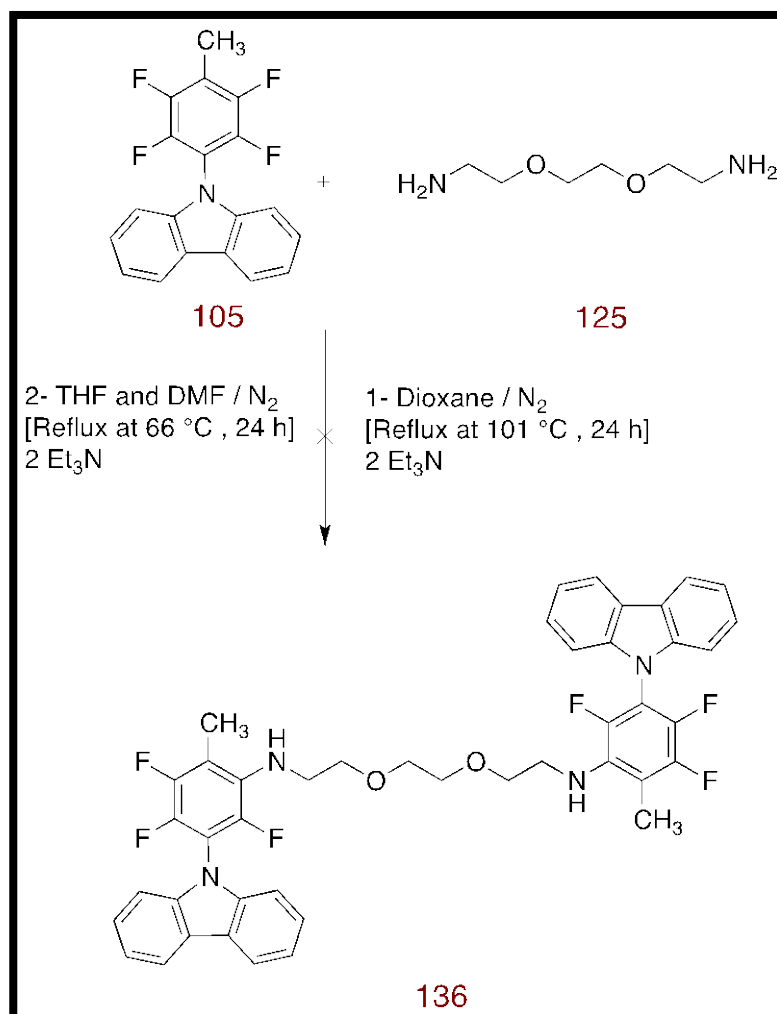
2.2.8.8. Study the reaction of trifluoro tetracyclic compound (90) with amine chain (125)

Moving to new type of a potential intercalator it was hoped to study the possibility to form bis adduct to amine chain **125** using trifluoro tetracyclic compound **90** prepared as discussed earlier (Section 2.2.5.2). According to the spectroscopic analysis the reaction of tetracyclic **90** and amine chain **125** in boiling dioxane failed to form the potential bis-intercalator **137** (Scheme 63). It was expected the amine would attack the more exposed *ortho* position of the fluorinated pyridine ring, which would also be the electronically preferred site of attack *para* to carbon. The ^{1}H NMR and ^{19}F NMR spectra of the reaction

product however were very complicated and TLC showed tailing, because of that the compound could not be purified. Due to the low yield and the difficulty of forming the starting **90**, as well the lack of time, it was not possible to modify the conditions and no further studies on this idea were pursued.

Scheme 63. Attempted synthesis of a potential bis intercalator from trifluoro tetracyclic compound (90)
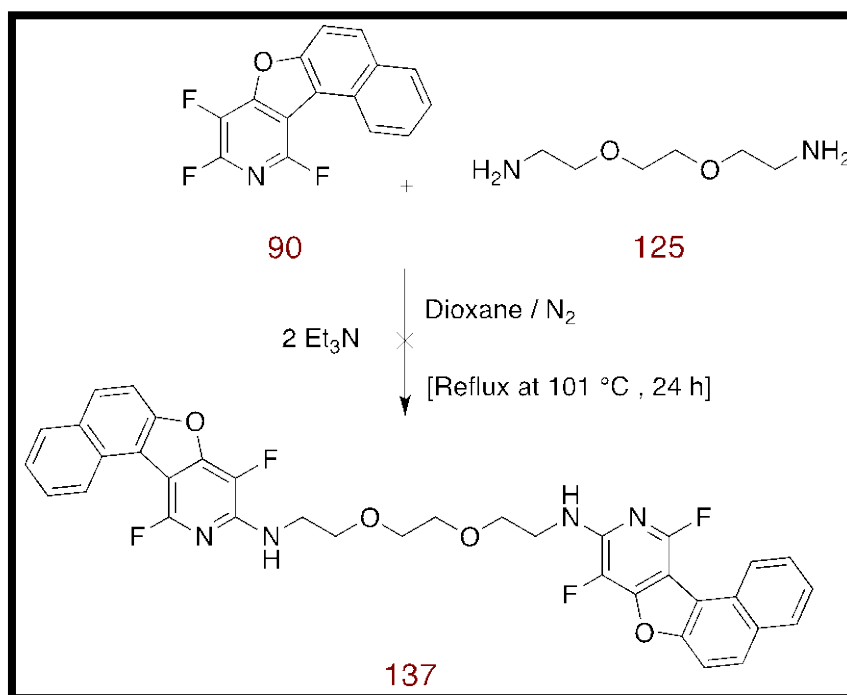
2.2.8.9. Investigation of the reaction of compound (68) with amine chain (125)

To develop further examples of possible intercalators the reaction of compound **68** with amine chain **125** was carried out in boiling dioxane for 24 h and the starting compound **68** and the amine chain **125** was in ratio 2:1 equivalents (Scheme 64). Unfortunately the reaction did not work and the starting **68** was recovered as shown by the ^{19}F NMR spectrum with the same four fluorine signals for the starting **68**. Mass spectrometry could not find the expected mass of the target compound **138**. It is not clear at which of the four fluorinated carbons attack would have occurred although attack *para* to sulfur may be the most likely.

Scheme 64. Attempted synthesis of a potential bis intercalator from compound (68)
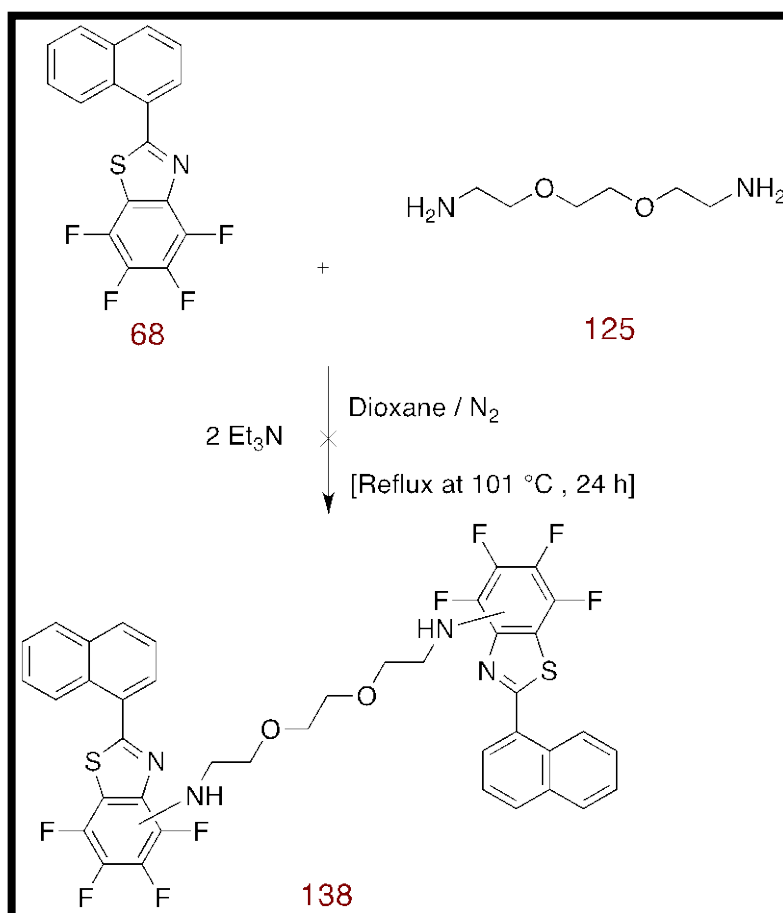
2.2.8.10. Study the reaction of compound (85) with amine chain (125)

After successful synthesis of compound **85** it was planned to study the possibility to synthesise a potential bis intercalator **139** (Scheme 65). Compound **85** was reacted with amine chain **125** in the ratio of 2:1 equivalents in the presence of a mixture of THF and DMF under reflux at 66 °C for 24 h. The reaction did not work and only the starting **85** was detected with the spectroscopic analysis. Unfortunately the reaction could not be studied further due to the low yield and the difficulty of forming the starting **85**, as well as the lack of time, it was not possible to modify the conditions, and no further studies on this idea were pursued.

Scheme 65. Attempted synthesis of a potential bis intercalator from compound (85)
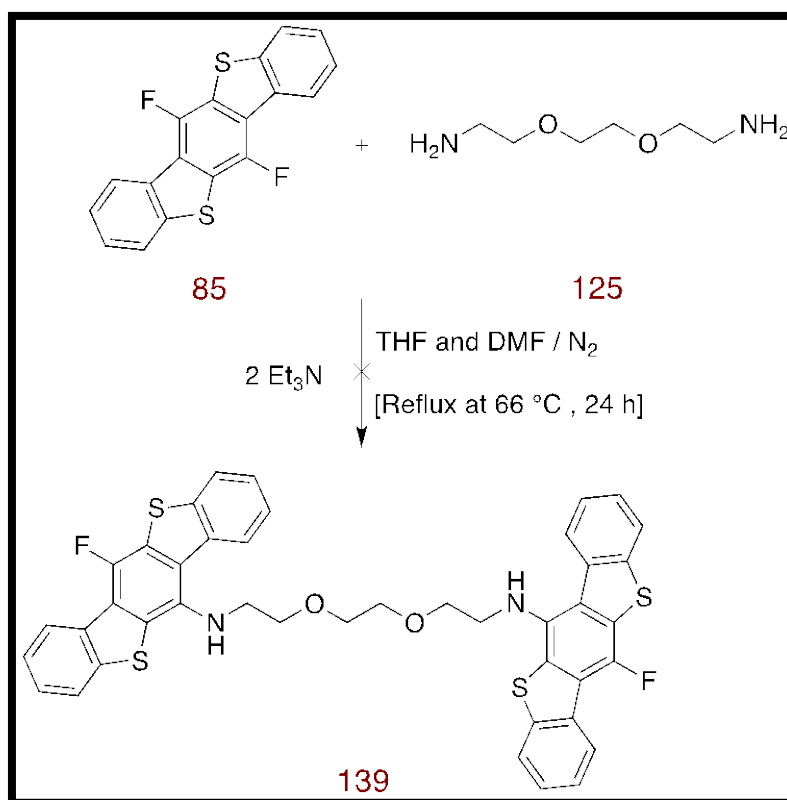
2.2.9. Investigation of the addition of amine side chains to the synthesised compounds in the study

During the biological assays it had been found that some of the compounds had poor solubility in the buffers employed. For the purpose of enhancing the water solubility of the novel synthesised compounds in the project it was planned to study the possibility to introduce one or more hydrophilic side chains to the compounds. Addition of such solubilizing groups could again be achieved by S_NAr reaction of one of the remaining fluorine atoms in the molecule.

2.2.9.1. Control reaction of adding side chain to carbazole derivative (100)

The lack of reaction of the bis-carbazole derivatives **100** and **119** prompted further investigation to see if other nucleophiles could be introduced at the less reactive positions (2-, 3-, 5-, 6-) in the 1,4-disubstituted derivatives. To study the possibility of introducing a more reactive nucleophile to carbazole derivative **100** as a third substituent, ethoxide was used as a control reaction for a start to the idea. The reaction worked in THF at RT in ratio 1:1 equivalents of ethanol and compound **100** in the presence of NaH as base to generate ethoxide ion (Scheme 66). The final product was a mixture of carbazole

derivative **140** and the starting compound **100** as shown by GC-MS with *m/z* values at 480 and 506 for both starting compound **100** and the target compound **140** respectively. TLC showed tailing and compound **140** not isolated by column chromatography.

In order to add two side chains to carbazole derivative **100** ethoxide and carbazole derivative **100** was used in ratio 2:1 equivalents in a mixture of THF and DMF under reflux at 66 °C. ^{19}F NMR spectroscopy suggested that the product was a mixture of carbazole derivative **140** and **141** and **142** in which two ethoxide ions had added, δ_F (376 MHz, CDCl$_3$) (for **140**) 26.59 (1F, d, *J* 10 Hz), 19.34 (1F, dd, *J* 23 and 10 Hz), 18.64 (1F, d, *J* 23 Hz), (for **141** and **142**) 25.24 (2F, s), 25.08 (2F, s). GC-MS found the expected mass for compound **140** with *m/z* values at 506 and the expected mass for compound **141** and **142** at 532. Again the compounds was not isolated by column chromatography, and also attempted recrystallization failed to separate the three compounds. Reaction with ethoxide demonstrated it was possible to effect substitution of the remaining fluorines in bis-carbazole **100**.

Scheme 66. Control reaction of adding ethoxide to carbazole derivative (100)

93
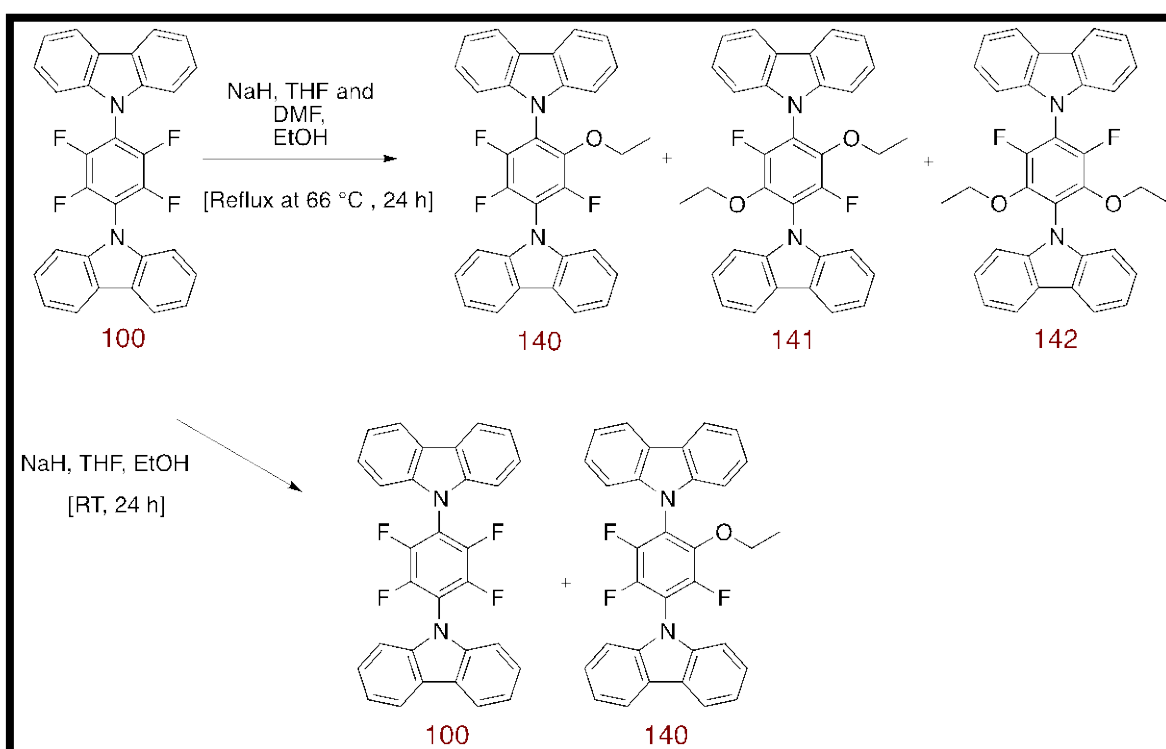
2.2.9.2. Study the reaction of carbazole derivative (100) with amine chain (125)

After the success of adding one and two side chains to carbazole derivative **100** it was planned to study further the reaction of carbazole derivative **100** with amine chain **125** (Scheme 67). Carbazole derivative **100** was therefore treated with amine chain **125** in the presence of NaH as base in a mixture of THF and DMF as solvents. ^{19}F NMR spectroscopy showed three signals, which could be consistent with the target product, compound **143**, however ^{1}H NMR spectroscopy was not consistent with the expected compound. In addition mass spectrometry could not find the exact mass of the desired compound and no conclusive prove of the formation of **143** could be obtained.

Scheme 67. Attempted reaction of carbazole derivative (100) with the amine chain (125)
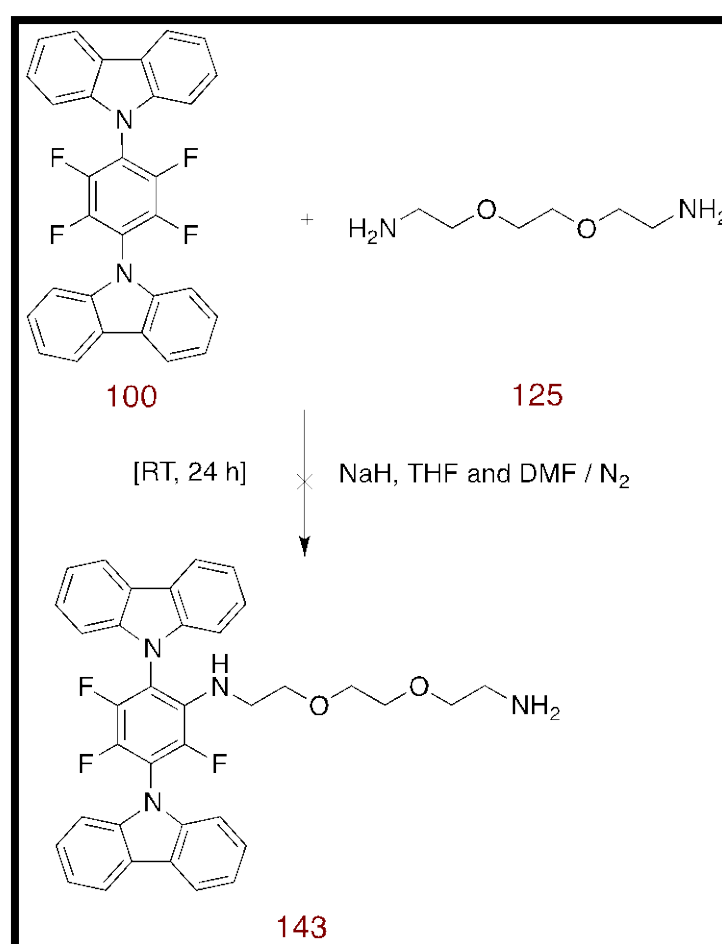
2.2.9.3. Investigation of the reaction of carbazole derivative (119) with amine chain (125)

In order to extend the reaction of amine chain **125** with previously synthesised carbazole derivatives, compound **119** was used. To study the possibility of adding two amine side chains to carbazole derivative **119**, two equivalents of amine chain **125** were reacted with one equivalent of carbazole derivative **119** in boiling THF for 24 h (Scheme 68). ^{19}F NMR spectroscopy suggested the presence of the starting carbazole derivative **119** by observing two signals identical to the starting compound. The ^{1}H NMR spectrum was also consistent with the starting compound and mass spectrometry could not find the expected mass of the target product, suggesting no reaction even with an excess of the amine.

Scheme 68. Attempted reaction of carbazole derivative (119) with amine chain (125)
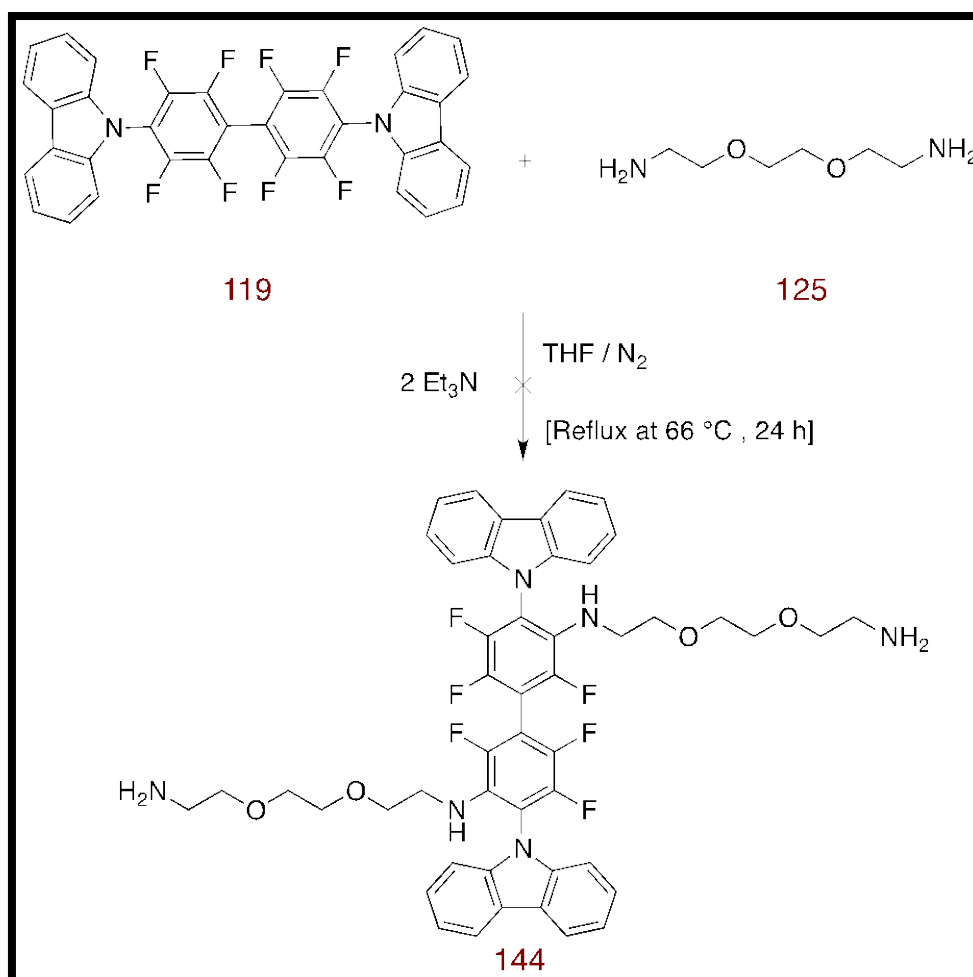
2.2.9.4. Study the reaction of carbazole derivative (105) with amine chain (125)

Then it was hoped to investigate the ability to adding one amine chain **125** to carbazole derivative **105** in ratio 1:1 equivalents in boiling THF for 24 h (Scheme 69). ^{19}F NMR spectroscopy showed two signals identical to the starting carbazole **105** and GC-MS found the expected mass of the starting carbazole at 329. It appears the fluorines in **105** are resistant to nucleophilic substitution due to similar steric and electronic reasons as described for **100** and **119**.

Scheme 69. Attempted reaction of carbazole derivative (105) with amine chain (125)
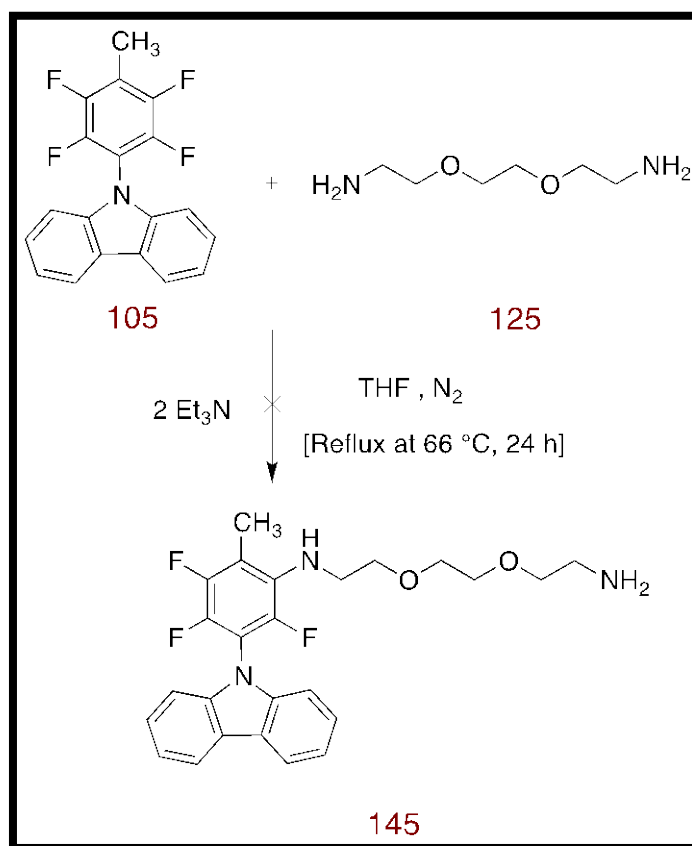
2.2.9.5. Study the reaction of carbazole derivative (103) with amine chain (125)

Then it was planned to study the possibility of adding two amine chains **125** to the pyridyl carbazole derivative **103** by treating it with two equivalents of amine chain **125** in boiling THF for 24 h (Scheme 70). ^{19}F NMR spectroscopy showed one singlet peak at 40.07 (s) for two equivalent fluorine atoms, which suggested the formation of compound **147**, where it was expected to see two different signals for each fluorine atom if carbazole derivative **146** was formed as may be expected if addition occurred to avoid the presence

of a *para*-fluorine atom. Mass spectrometry could not find the expected molecular formula for neither **147** nor **146**. ^{1}H NMR spectroscopy showed the expected signals of carbazole ring at the range 7-8 ppm and abroad signal for NH at 5.25 ppm, and there are signals at the range 3-4 ppm, but still not completely consistent with compound **147**. Further investigation is still required to fully characterize the product.

Scheme 70. Reaction of carbazole derivative (103) with amine chain (125)
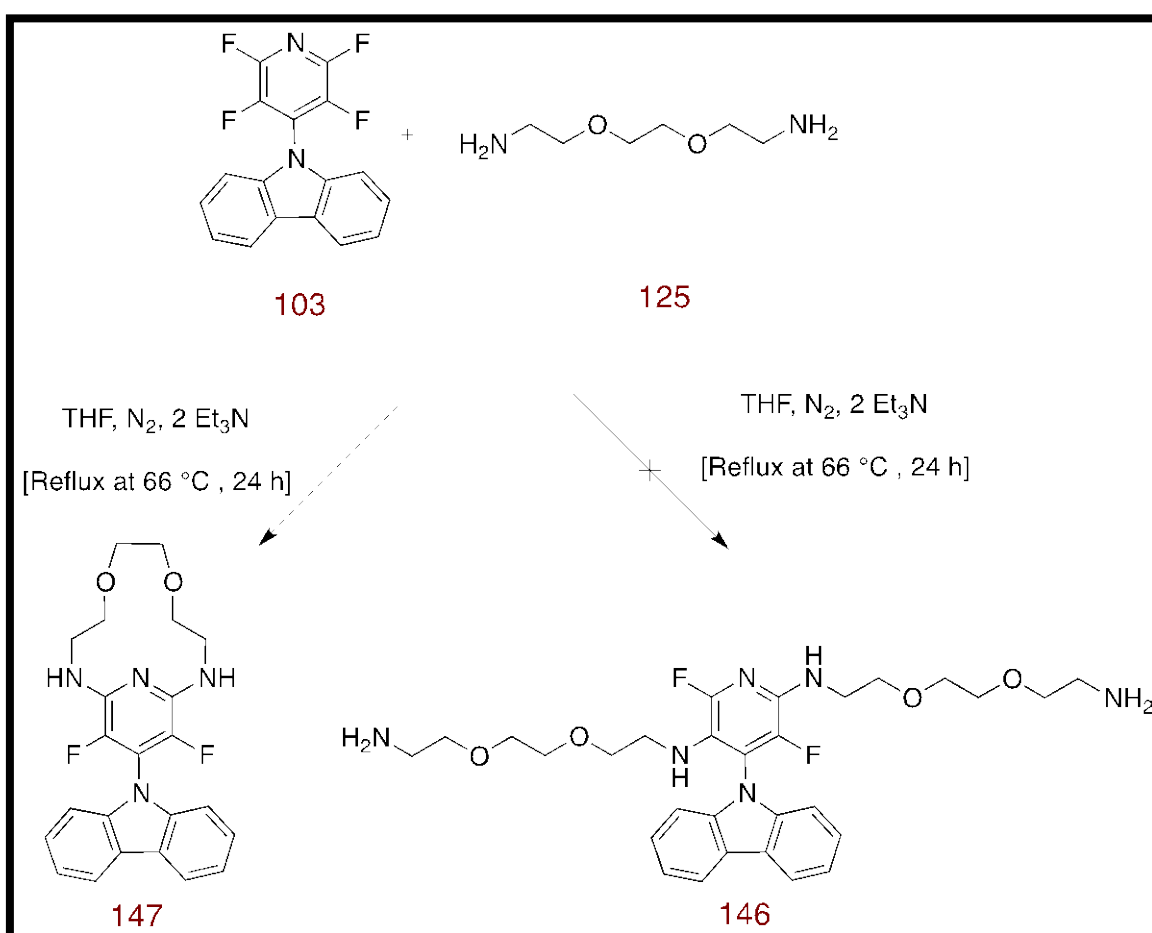
2.2.10. Synthesis of positively charged compounds

In medicinal chemistry most of the effective DNA intercalating agents are positively charged compounds, which improves binding to the DNA, which has a negatively charged phosphate backbone. Ethidium bromide (EB) a well known DNA intercalating agent includes a positive charge in its structure (Figure 23).[45] Another example of positively charged DNA binding compound is daunomycin (Figure 24) a drug of the

anthracycline antibiotics family which have a good effect in treating a variety of cancers.[92, 93]

In order synthesise biologically active positively charged compound it was planned to design a positively charged scaffold and then investigate the possibility to introduce the charged scaffold to the previously synthesised compounds in the project by S_NAr reaction. Such charged compounds would also exhibit improved water solubility.
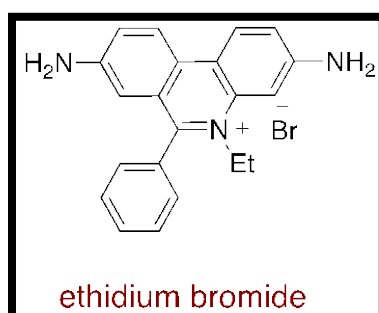
Figure 23. The structure of ethidium bromide
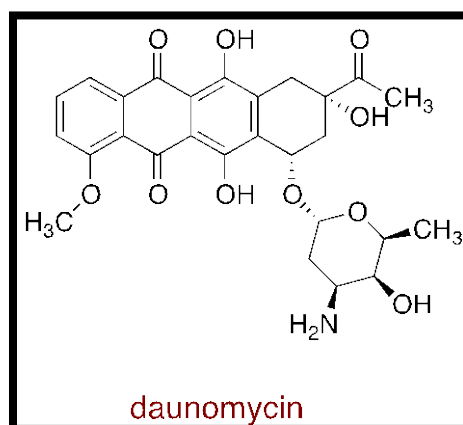
Figure 24. The structure of daunomycin

2.2.10.1. Synthesis of the positively charged scaffold (150)

In order to prepare a suitable positively charged unit which could be introduced into the perfluoroarene derivatives synthesised by S_NAr reaction it was decided to alkylate a nitrogen heterocycle, such as isoquinoline, to form an isoquinolinium salt in which the N-alkyl substituent could be easily deprotonated to form a positive nitrogen which could act as a nucleophile in the proposed S_NAr reactions.

98

The positively charged scaffold has been synthesised according to Krohnke and Angew[94] by reacting isoquinoline **148** with ethyl bromoacetate **149** in boiling ethyl acetate (Scheme 71). The reaction worked well and the known target compound **150** was afforded in 73 % yield. Mass spectrometry found the expected molecular formula of the target compound cation only, HRMS (ESI) *m/z* found 216.1015, $C_{13}H_{14}NO_2$ requires 216.1019 and IR found carbonyl group signal, v_{max}/cm^{-1} (film) 1740 (C=O) in accordance with literature data.

Scheme 71. Reaction of isoquinoline with ethyl bromoacetate
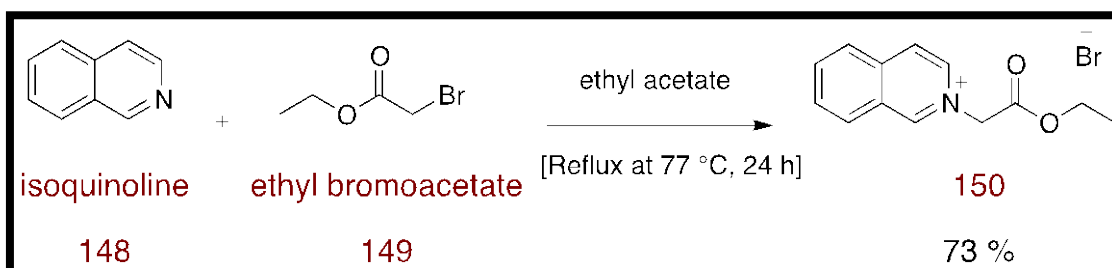
2.2.10.2. Reaction of the positively charged scaffold (150) with carbazole derivative (103)

In order to improve the biological activity of the previously synthesised carbazole derivative **103** it was planned to study the possibility of replacing one fluorine atom with the positive scaffold **150** (Scheme 72). The positive scaffold **150** was treated with one equivalent of NaH in the presence of DMF at RT to deprotonate the methylene group of compound **150**, one equivalent of carbazole derivative **103** was added to the reaction with the aim of nucleophilic substitution of one fluorine atom of compound **103** with the positively charged scaffold **150**. Unfortunately ^{1}H NMR spectroscopy was not consistent with the target product **151** and only carbazole ring signals were shown. ^{19}F NMR spectroscopy showed several new signals, which were not consistent with **151** and suggested a mixture of products had formed. Unfortunately it was not possible to separate these chromatographically.

Scheme 72. Attempted reaction of the positive scaffold (150) with carbazole derivative (103)
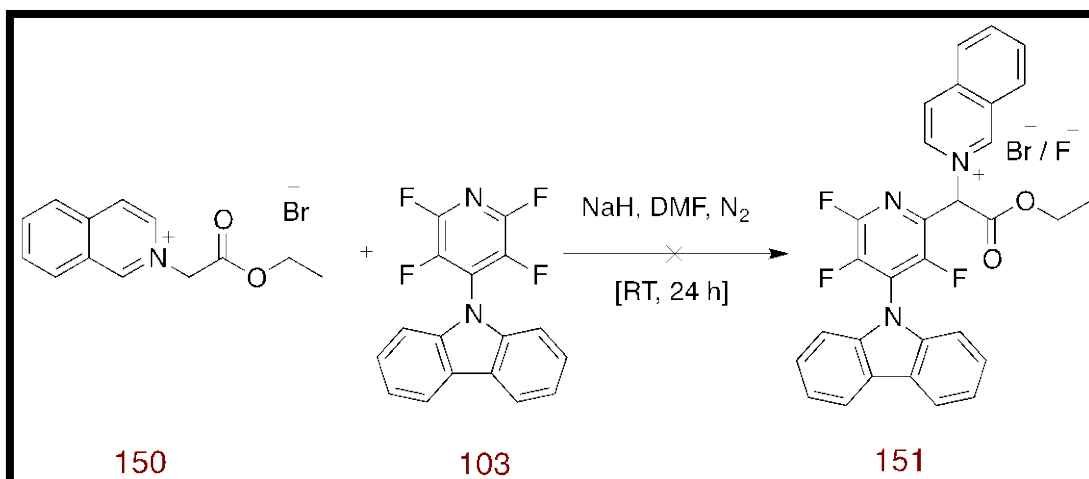
2.2.10.3. Investigation of the reaction of the positive scaffold (150) with carbazole derivative (102)

For further investigation of the possibility of adding the positively charged scaffold compound **150** to previously synthesised carbazole derivative **102** again compound **150** was treated with one equivalent of NaH in the presence of DMF at RT to deprotonate the methylene group of compound **150** (Scheme 73). One equivalent of carbazole derivative **102** was added to the reaction with the aim of nucleophilic substitution of one fluorine atom of carbazole derivative **102** with the positively charged scaffold **150**. ^{1}H and ^{19}F NMR spectrum were consistent with the starting carbazole derivative **102** and no evidence for the formation of **152** was obtained.

Scheme 73. Attempted reaction of the positive scaffold (150) with carbazole derivative (102)
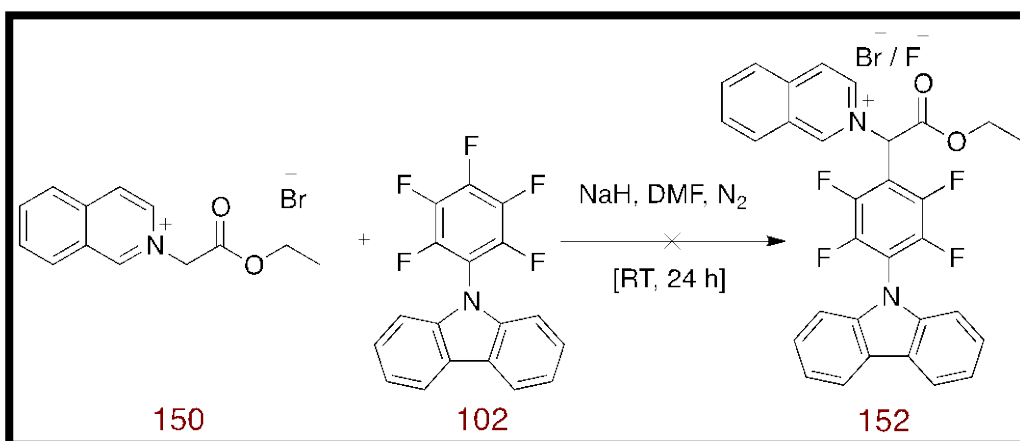
2.3. DNA binding studies

2.3.1. DNA thermal denaturation assay

In the present study it was planned to investigate DNA binding activity of the novel synthesised fluorinated compounds with a number of different assays. One of the most common assays that determine the DNA binding activity of organic compounds is the study of the melting temperature of the DNA in the presence or absence of the organic molecule.

Actinomycin D (ACTD) was used as a standard DNA intercalating agent in DNA binding studies. ACTD (Figure 25) is a well-known antibiotic and anticancer drug which has a high affinity for interacting with double strand DNA and dissociates slowly, leading to termination of DNA transcription and replication.[95,96,97] As a result, ACTD can be used as a lead compound to synthesise and develop more effective double stranded DNA intercalating agents[96].

The *Tm* values for a selection of the synthesised fluorinated heterocycles were measured in triplicate using calf thymus DNA in trisma base buffer. The mean values were calculated and the results are displayed in Figure 26. In addition Δ*Tm* values were investigated (Δ*Tm* = *Tm* DNA-compound complex − *Tm* DNA) (See appendix 5.2 for the full data). The main source of errors that might interfere the results the apparatus and experimental errors were considered.
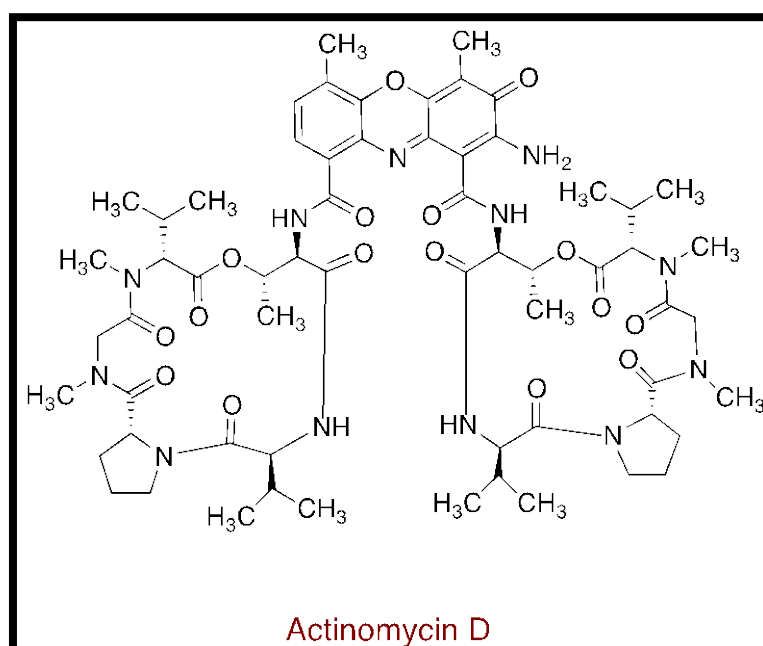
Figure 25. The structure of actinomycin D
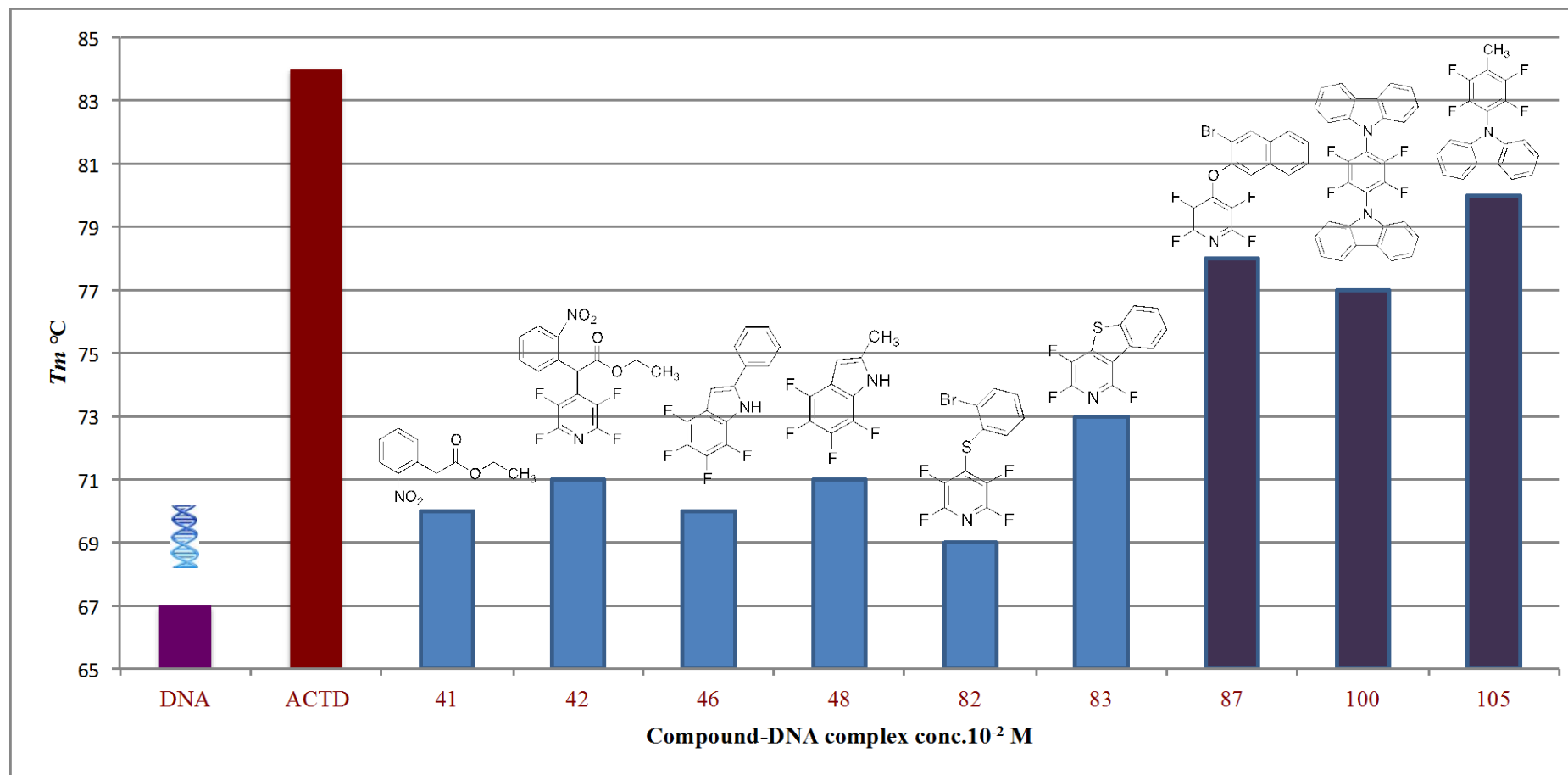
Figure 26. Comparison of *Tm* values of novel fluorinated compounds-DNA complex

According to figure 26, the *Tm* values for DNA and DNA-ACTD complex was 67 °C and 84 °C respectively and Δ*Tm* of DNA-ACTD was 17 °C. The tested compounds showed an increase in *Tm* values relative to the value for the DNA. Interestingly compounds **87** and **105** recorded the highest reading of 78 °C with Δ*Tm* 11 °C for naphthalene compound **87**, and of 80 °C with Δ*Tm* 13 °C for carbazole derivative **105** (close to the ACTD value). These compounds contain larger aromatic groups, the bromonaphthalene and carbazole rings, which would be expected to function better as intercalators. It was expected compound **100** containing two carbazole rings to bind most strongly. However the *Tm* value was slightly lower (77 °C with Δ*Tm* 10 °C) than for monocarbazole derivative **105**. This could be due to the non-planar nature of the molecule as was shown by X-ray crystallography (Section 2.2.7.1). The X-ray structure showed the carbazole ring to be twisted out of the plane of the tetrafluorobenzene ring. The rest of tested compounds recorded higher *Tm* values than the value of the DNA, but the low Δ*Tm* in the range 3-6 °C suggested only weak binding. As a result the tested compounds all showed potential DNA binding activity.

2.3.2. UV-visible absorption spectroscopy assay

The interaction of the fluorinated synthesised compounds with DNA was determined by UV absorption spectroscopy assay. The changes in the absorbance of the tested compound in the presence or absence of DNA gives an idea about the interaction of the organic molecule with DNA. Based upon the variation in absorbance, the intrinsic binding constant/association constant (K) of the drug with DNA can be determined according to Benesi-Hildebrand equation: [98]

$$\frac{A_o}{A - A_o} = \frac{\in G}{\in H - G - \in G} + \frac{\in G}{\in H - G - \in G} \times \frac{1}{K[DNA]}$$

Where K is the association / binding constant, A_o and A are the absorbances of the drug and its complex with DNA, respectively, and ε_G and ε_{H-G} are the absorption coefficients of the drug and the DNA-drug complex, respectively. The K value was determined from the intercept -to- slope ratio of A_o / A-A_o vs. 1/ [DNA] plot.

In addition the Gibbs free energy (ΔG) was calculated for each complex by the following equation:[98]

$$\Delta G = -RT \ln K$$

Where R is the general gas constant (8.314 JK^{-1}mol^{-1}) and T is the room temperature (298 K).

2.3.2.1. UV-visible spectra of netropsin

According to figure 27, netropsin as a known DNA binding agent showed a strong absorption at 300 nm. A decrease in the absorption was observed on increasing the DNA concentration starting with 9.6 µM, 18 µM, 27 µM, 35 µM, 43 µM, and 50 µM DNA. The K value was found to be (1×10^5 M^{-1}) and ΔG was -28.5 kJ.mol^{-1}.
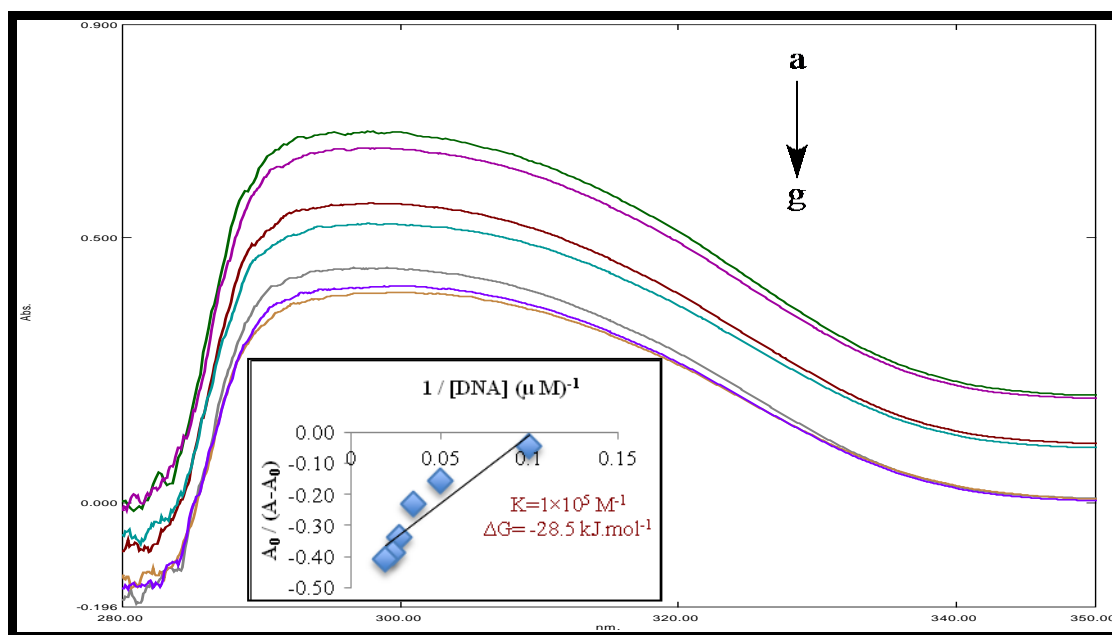
Figure 27. UV-visible spectra of netropsin in presence and absence of DNA

Absorption spectra of 1×10^{-5} M of netropsin in absence (a), and in the presence of 9.6 µM (b), 18 µM (c), 27 µM (d), 35 µM (e), 43 µM (f), and 50 µM (g) DNA. The arrow shows increasing DNA concentration. Inside graph is the plot of $A_0 / (A-A_0)$ vs. 1/ [DNA] for determination of K and ΔG values. (R^2=0.8614 for six points).

The comparison of the binding constant value of netropsin with the binding constant values of the synthesised compounds are shown in figure 28. All the synthesised compounds showed affinity to bind with DNA in UV-visible spectroscopy assay. Interestingly carbazole derivative **120** showed high binding affinity, and it is possible that this compound acts as an intercalator. The tetrafluorotolyl carbazole **105** showed a high ΔTm value in the DNA thermal denaturation experiments supporting the idea that a carbazole group was beneficial to binding. The ΔTm value unfortunately could not be obtained for **120** due to technical problems with the instrument at this stage in the project.

The potential bis-intercalators **133** and **135** were expected to show significantly increased binding if the two aromatic moities in each compound could both act as intercalators. Disappointingly both compounds showed weaker binding than **120**, suggesting alternative interaction with the DNA.

133   **135**
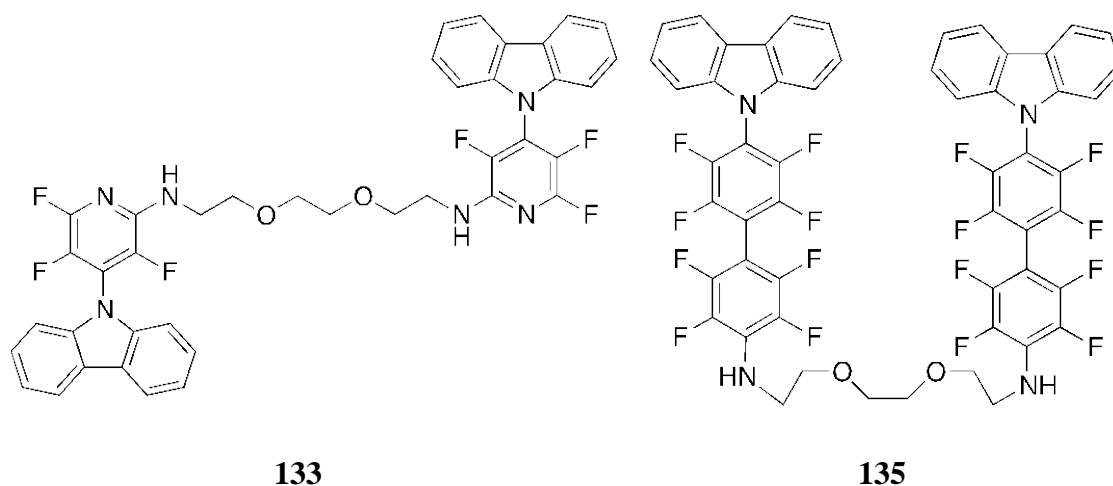
Other compounds **46**, **68**, **71**, **76**, **102**, **111**, and **117** showed very weak DNA binding affinity. Compounds **42**, **48**, **59**, **83**, **84**, **87**, **90**, **96**, **100**, **103**, **105**, **109**, **114** and **116** showed a good DNA binding affinity but not high as the reference compound netropsin. Further work however is required to gain a detailed understanding of the nature of the binding. (UV spectra for tested compounds are presented in appendix 5.3).
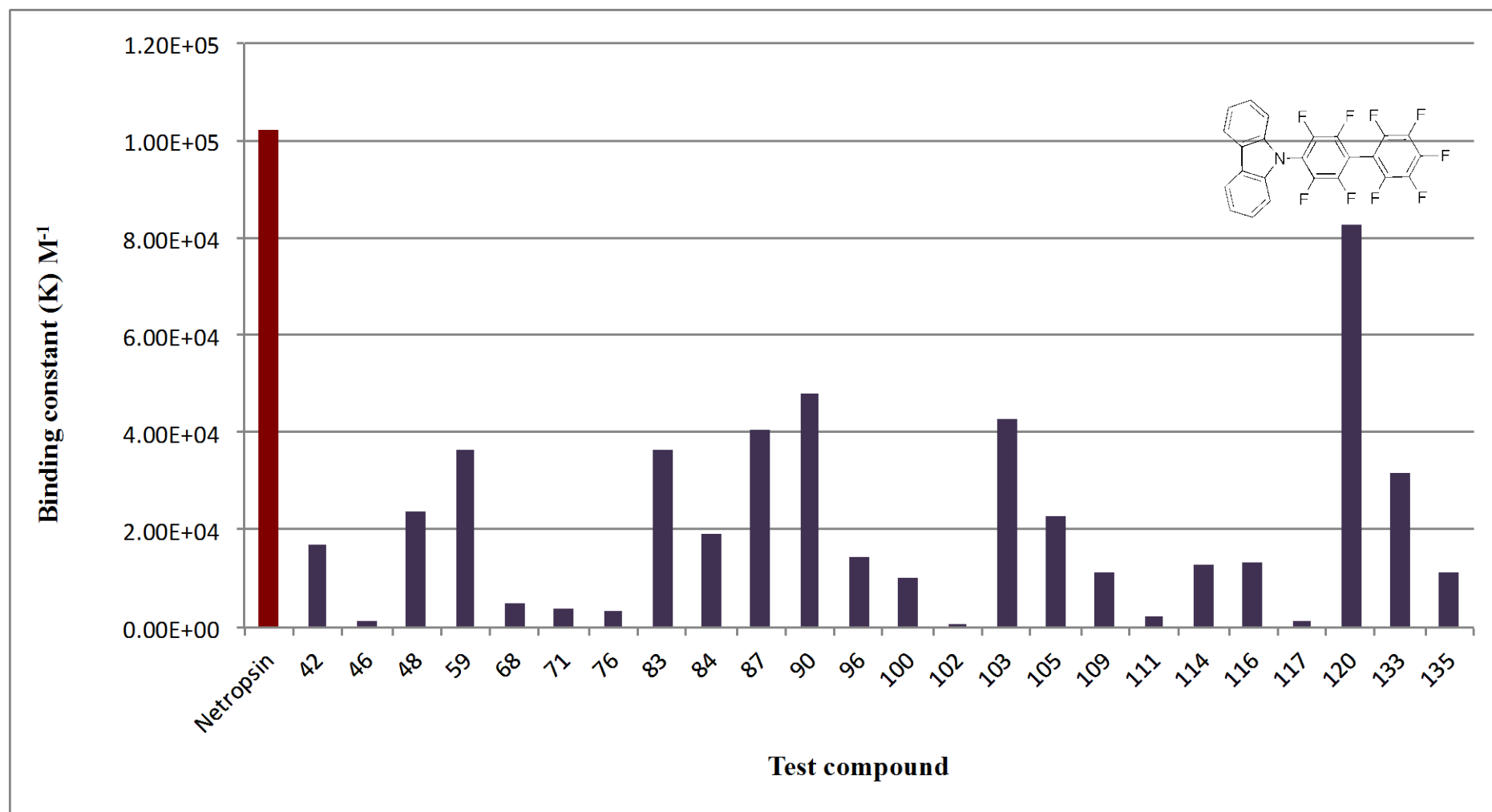
Figure 28. Binding constant values from UV-visible spectroscopy assays of the synthesised compounds compared with netropsin, and showing the structure of carbazole derivative (120) displaying the highest binding

2.3.3. EB fluorescence displacement assay

The quenching fluorescence assay is one method which provides further information about the binding mode of drugs with DNA. In this study ethidium bromide (EB) is one of the common fluoroprobes and was selected as a probe to investigate the interactions of the synthesised compounds with DNA by a spectral method. It can insert into the DNA base pairs and bind to DNA strongly as an intercalator, which causes an increase in the fluorescence intensity (emission wavelength 605). The improved fluorescence in presence of EB can be quenched by the addition of a second molecule. Therefore by intercalating a second molecule into DNA, the fluorescence intensity of the EB-DNA will decrease, because the drug will compete with EB in binding with DNA. In addition the extent of interaction between the drug and DNA can be determined by the extent of fluorescence quenching of EB bound to DNA.[70,47] When EB is intercalatively bound to DNA, the EB fluorescence increases in intensity from 20-100 times that of the free nonintercalatively bound dye (Figure 29). The extent of interaction between the drug and DNA can be determined by the extent of fluorescence quenching of EB bound to DNA.[45]
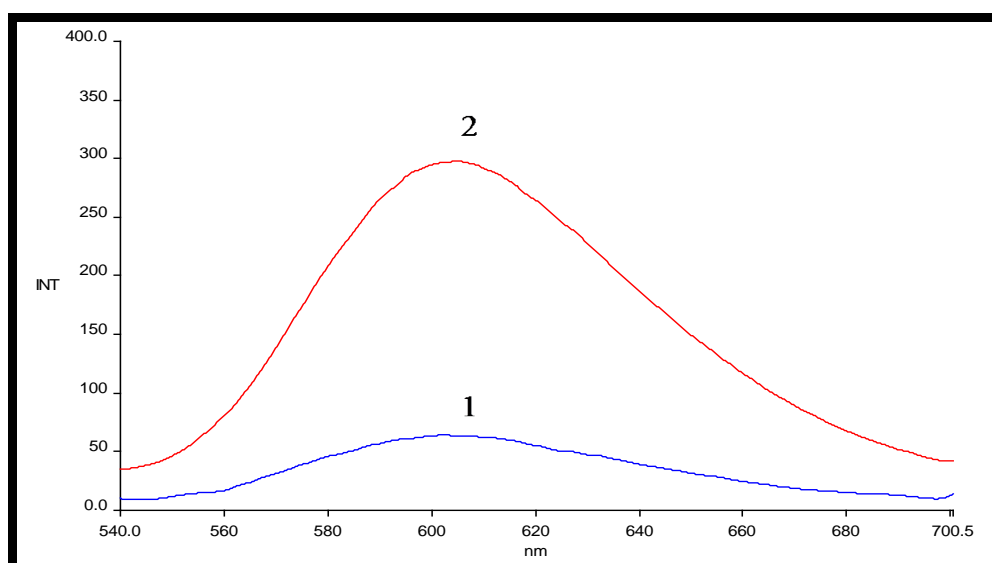
Figure 29. Emission spectra of EB 1×10^{-6} M in the absence of DNA (1) and in the presence of DNA 1.5×10^{-4} M (2)

2.3.3.1. EB fluorescence displacement assay of netropsin

In the present study netropsin was used as reference DNA binding agent to displace the ethidium bromide. According to figure 30, by increasing the netropsin concentration the fluorescence intensity decreased which indicated netropsin interacts with DNA as a groove binder and releases EB from EB-DNA system. Another possibility is netropsin binds to DNA in different binding sites and changes the conformation of DNA, which causes a decrease in the fluorescence intensity. The K value for netropsin-DNA complex was found to be 7.1×10^4 M^{-1} and the Gibbs free energy was -27.6 $kJ.mol^{-1}$, the negative value of ΔG showing a spontaneous process.
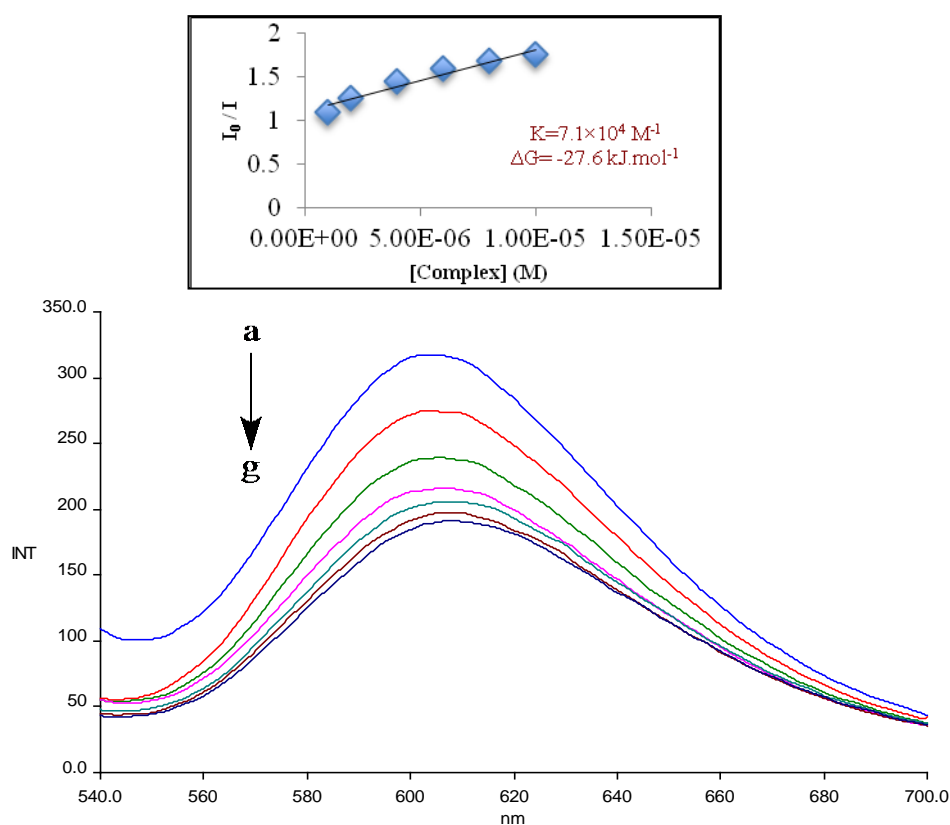
Figure 30. Emission spectra of DNA-EB in trisma base buffer on titration of netropsin.

K_{ex} = 480 nm; [EB] = 1×10^{-6} M; [DNA] 1.5×10^{-4} M. The arrow shows the increase of the complex concentration, [netropsin] (a) 0.0, (b) 1×10^{-6}, (c) 2×10^{-6}, (d) 4×10^{-6}, (e) 6×10^{-6}, (f) 8×10^{-6}, (g) 1×10^{-5} M. Inside graph is the plot of I_0 / I vs. complex concentration for determination of the K and ΔG values. (R^2 = 0.94173 for six points).
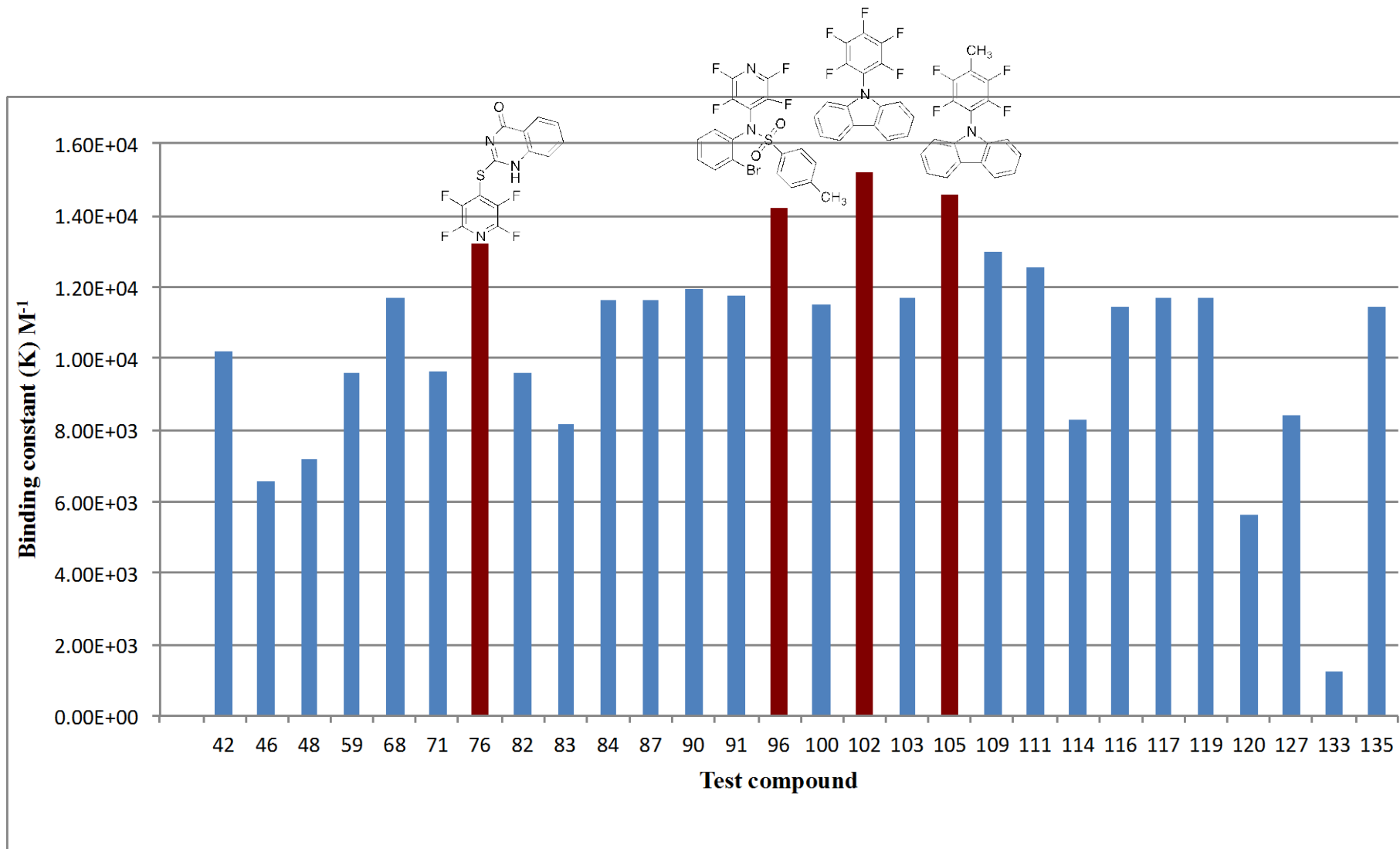
Figure 31. Binding constant values from EB displacement assay of the synthesised compounds

According to figure 31, all the synthesised compounds showed some affinity to bind with DNA in the EB displacement assay, although in comparison to the reference compound netropsin binding were very weak (netropsin $K = 7.1 \times 10^4 \, M^{-1}$). Compounds **76**, **96**, **102** and **105** indicated the highest K values compared to other compounds. Therefore these compounds showed the stronger affinity to bind with DNA than the other synthesised compounds. The decrease in fluorescence suggests these compounds could be binding to the DNA as grove binders, although the exact nature of the interaction is not yet known. The higher values for **102** and **105**, which contain a carbazole ring, suggest this group is beneficial for binding as was observed in the thermal melting and UV studies.

2.3.4. Vapour diffusion DNA-compound complex crystallization

For a deep investigation of the DNA binding activity of the novel fluorinated compounds that were synthesised in the project, it was hopped to co-crystallize the compound with the well known synthetic short DNA sequence CGCGAATTCGCG.[99] The X-ray structure of CGCGAATTCGCG oligo is well known in the literature[39] and the stereo structure of the Netropsin-CGCGAATTCGCG complex is well known as well.[56]

The hanging drop crystallization method was studied in cacodylate buffer in the presence of magnesium chloride, with the purpose of obtaining crystals suitable for X-ray crystallography. Multiwell plates were used as well as capillary tubes under different conditions at RT and at 3 °C in the refrigerator. Compounds **41**, **42**, **46**, **48**, **59**, **68**, **71**, **76**, **82**, **83**, **84**, **87**, **90**, **91**, **96**, **100**, **102**, **103**, **105**, **111**, **114**, **116**, **117**, **119**, **120**, **127**, **133**, **135** were all investigated.
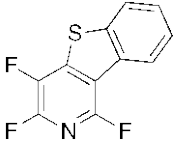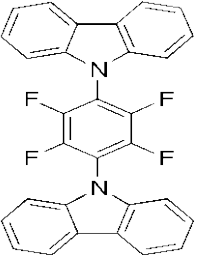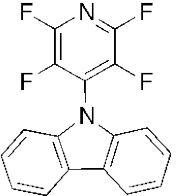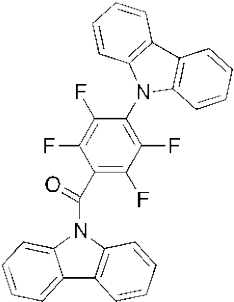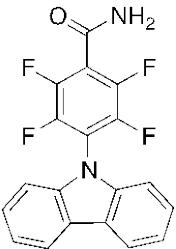
Unfortunately all attempts failed to yield suitable crystals for X-ray crystallography, although the samples were left to crystallize for a long time, up to 6-8 months. In some cases clustered crystals formed, but were not suitable for X-ray crystallography to obtain the X-ray crystal structure. Disappointingly no crystals obtained to give information about the detailed binding interactions of any of the compounds studied.

2.4. Antimicrobial activity

In vitro biological screening tests of the synthesised fluorinated compounds were carried out for antibacterial cytotoxicity. The antibacterial activity was tested against two bacterial strains Gram-positive strain (*Escherichia coli*) and Gram-negative strain (*Staphylococcus aureus*). The disk diffusion method was used in these assays and each experiment was performed in triplicate. Criteria for activity is based on the diameter of

the inhibition zone (mm); an inhibition zone more than 20 mm indicates significant activity, for 18-20 mm inhibition is good, 15-17 mm is low, and below 11-14 mm is non-significant activity.[70,100] The following compounds in 10^{-2} M were tested, **42**, **46**, **48**, **59**, **68**, **71**, **76**, **82**, **84**, **87**, **90**, **91**, **96**, **102**, **105**, **114**, **116**, **117**, **119**, **120**, **127**, **133**, **135** but showed no zone inhibition at all. Compounds **83**, **100**, **103**, **109** and **111** showed inhibition zone and reading of the zone inhibition represents the mean value of these readings, which are shown in table 2. Disappointingly the antibacterial activity assay demonstrated that the tested compounds showed non-significant activity against the bacteria because the inhibition zones were below 11-14 mm. Because the high concentration 10^{-2} M did not show a significant inhibition, the lower concentrations of the compounds did not studied. Consequently the fluorinated synthesised compounds in the present study did not show a good antibacterial activity against (*Escherichia coli*) or (*Staphylococcus aureus*) strains, despite the evidence for DNA binding. Further studies would be required to understand the exact interaction of the compounds with bacterial cells.

Table 2. Antimicrobial activity of some fluorinated synthesised compounds

Compound	Average zone of inhibition (mm)	
	Escherichia coli	*Staphylococcus aureus*
Compound **83**	0	7
Compound **100**	7	0
Compound **103**	0	7
Compound **109**	0	7
Compound **111**	0	8

2.5. Conclusions

The research in this project has resulted in the successful synthesis and characterisation of 31 new fluorinated organic compounds by nucleophilic aromatic substitution of fluorine in commercially available perfluoroarenes including hexafluorobenzene, pentafluoropyridine, pentafluorotoluene, pentafluorobenzaldehyde, ethyl pentafluorobenzoate and decafluorobiphenyl. A number of novel substituted, and ring fused, fluorinated heterocycles have been prepared including indole, carbazole and benzofuran derivatives. A Smiles rearrangement has been identified during attempts to cyclize a bromonaphthyloxytetrafluoro pyridine. Carbazole was successfully introduced into number of perfluoroaromatics and pentafluoropyridine by nucleophilic aromatic substitution reaction with its N-anion. Carbazole was introduced into perfluoroaromatics and pentafluoropyridine in one, two or three positions by nucleophilic aromatic substitution reaction. The novel fluorinated compounds that had been synthesised in the study were used to synthesise potential bis-intercalating agents using 2,2-(ethylenedioxy)bis(ethylamine). The new structures of the new compounds have been determined by a combination of ^{1}H and ^{19}F NMR spectroscopy, mass spectrometry, IR spectroscopy and in some cases elemental analysis. The X-ray crystal structures of 9 compounds have been determined.

A number of compounds synthesised have been shown to bind to DNA by a combination of thermal melting, UV absorption and fluorescence measurements, although the exact nature of the binding has not been determined. Attempts to co-crystallize the compounds with a synthetic oligonucleotide were unsuccessful. Studies on the antimicrobial activity of a range of the new compounds showed they had little activity against Gram-positive strain (*Escherichia coli*) and Gram-negative strain (*Staphylococcus aureus*).

2.6. Future work

The synthetic work has generated several areas where further investigation would be desirable. Reductive cyclization of 2-bromoaryl perfluoroaryl ethers, sulfides and amines using reactive methods such as Rieke magnesium, iron or copper could be explored as an alternative to the bromine-lithium exchange promoted by *n*-BuLi in which side reactions and addition of butyl groups to the substrate can occur. Study of the effect of such methods on cyclization versus Smiles rearrangement would be of interest. Further development of methods to predict and control the stepwise addition of nucleophiles to perfluoroarenes should be undertaken to study the orientation effects of the added groups,

and to improve reactivity as the number of available fluorines atoms falls with progressive substitution.

In terms of the biological properties of the compounds further work should be undertaken to improve water solubility of the molecules by adding hydrophilic amino or hydroxyl containing groups. Further synthesis of positively charged derivatives or those containing basic groups capable of protonation should be undertaken.

Further attempts to co-crystallize the products synthesised with DNA strands of known composition should be carried out, to allow a more detailed understanding of the molecular interactions involved in binding activity. A number of the compounds described in this thesis are being taken forward in a further project to test for in *vitro* anti-cancer activity.

Chapter 3
Experimental

3. Experimental

3.1. General

Anhydrous conditions were obtained by using oven/flame-dried glassware being purged with nitrogen prior to the addition of chemical reagents. A nitrogen atmosphere was maintained throughout reactions where necessary through the use of a nitrogen balloon.

Commercially available solvents were used and not subjected to further purification, except THF, which was distilled as needed from benzophenone and sodium. DMSO was purchased dry from a commercial supplier. Light petroleum refers to the fractions with a boiling point between 40-60 °C.

NMR spectra were recorded (^{1}H, ^{19}F and ^{13}C) using a Bruker 400 MHz NMR instrument or a Jeol ECS-400 instrument with internal standard tetramethylsilane or hexafluorobenzene for ^{19}F NMR spectra. Chemical shifts are reported in ppm for both forms of spectra and coupling constant are recorded in hertz. ^{1}H NMR spectra were recorded at 400 MHz, ^{19}F NMR spectra at 376 MHz and ^{13}C NMR spectra were recorded at 100 MHz. DEPT was used to assign environment (CH, CH_2, CH_3) to each carbon atom in the ^{13}C NMR spectra. The solvent system used for NMR measurements is specified in brackets.

A Thermofisher Exactive (orbitrap) mass spectrometer was used to obtain high-resolution mass spectra, with ESI as the ionization mode. The solvent used for all samples was methanol.

GC-MS was performed on a Fisons 8060 with a DB5MS column of 30 m length and split less injection.

A Perkin-Elmer spectrum 65FT-IR spectrophotometer was used to obtain infrared spectra. Liquid sample were acquired using a thin film on a sodium chloride disc. Solid samples were acquired using a KBr disc.

Melting points were recorded using as Electro thermal-IA 9100 melting point instrument.

TLC analysis was carried out on Merck TLC silica gel 60 F_{254} aluminum backed plates and were visualized by vanillin stain or under UV light at 254 nm using a U.V.P chromate-vue cabinet model CC-60.

Column chromatography was carried out on Merck Kiesel 60 silica gel. The eluent and concentration used is specified in brackets.

For biological activity assays calf thymus DNA and salmon sperm DNA and short synthetic CGCGAATTCGCG DNA were purchased from Sigma. Spectra UV at 250 was

used for UV absorption assays and Perkin Elmer Luminescence Spectrometer S50B was used for fluorescence assay and a UV- visible spectrophotometer Varian Cary 300 Bio was used for melting temperature assay. *Muller Hinton* agar, petri dish 90 × 14 mm (diameter and height respectively) and Townson + Mercer incubator was used to incubate the bacteria in anti microbial activity study.

3.2. Organic synthesis

3.2.1. Reaction of (2-nitrophenyl)-acetic acid ethyl ester with pentafluoropyridine

41
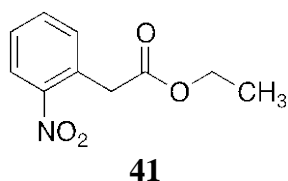
2-Nitrophenylacetic acid (4.13 g, 20 mmol) was dissolved in ethanol (50 mL) and conc. H_2SO_4 (3 drops) was added to the mixture. The mixture was heated under reflux at 78 °C for 24 h. The reaction mixture was allowed to cool to RT and $NaHCO_3$ (2 spatulas) was added and filtered. The solvent was evaporated to dryness to reveal **41** as a pale yellow crystals (1.56 g, 37 %); m.p. 66-69 °C; δ_H (400 MHz, $CDCl_3$) 8.13 (1H, dd, *J* 8.4 and 1.2 Hz), 7.60 (1H, td, *J* 7.2 and 1.2 Hz), 7.48 (1H, td, *J* 8.4 and 1.6 Hz), 7.36 (1H, dd, *J* 7.6 and 0.8 Hz), 4.18 (2H, q, *J* 6.8 Hz), 4.02 (2H, s), 1.26 (3H, t, *J* 6.8 Hz); HRMS (ESI) *m/z* found 232.0576, $C_{10}H_{11}NO_4Na^+$ requires 232.0580; v_{max}/cm^{-1} (film) 1734 (C=O), 1540 (NO_2), 1345 (NO_2), 1215, 1179; Analysis (%) calculated for $C_{10}H_{11}NO_4$ (209): C, 57.4; H, 5.30; N, 6.70. Found C, 56.82; H, 4.90; N, 6.70.

42
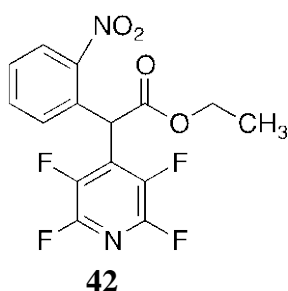
A solution of (2-nitrophenyl)-acetic acid ethyl ester **41** (0.62 g, 3 mmol) in THF (5 mL) was added dropwise to a stirred suspension of NaH (60 % dispersion in mineral oil) (0.18 g, 8 mmol) in THF (5 mL) under N_2 and left to stir at RT for 1 h. A solution of pentafluoropyridine (0.98 g, 6 mmol) in THF (5 mL) was added dropwise to the reaction mixture and left to stir at RT for 24 h. The solvent was evaporated and then water (10 mL)

was added dropwise to the residue. The reaction mixture was extracted with dichloromethane (DCM) (25 mL × 3) and the combined organic layers dried over MgSO$_4$, filtered and evaporated to give **42** as a brown oil (1.00 g, 93 %); δ$_H$ (400 MHz, CDCl$_3$) 8.09 (1H, dd, *J* 8.0 and 1.6 Hz), 7.56 (1H, td, *J* 7.6 and 1.2 Hz), 7.49 (1H, td, *J* 8.0 and 1.2 Hz), 7.12 (1H, d, *J* 7.6 Hz), 6.19 (1H, s), 4.21 (2H, q, *J* 6.8 Hz), 1.19 (3H, t, *J* 6.8 Hz); δ$_F$ (376 MHz, CDCl$_3$) 72.91-72.73 (2F, m), 21.17-20.99 (2F, m); HRMS (ESI) *m/z* found 357.0512 (M–H)$^-$, C$_{15}$H$_9$F$_4$N$_2$O$_4$ requires 357.0504.; v_{max}/cm^{-1} (film) 1737 (C=O), 1654, 1531 (NO$_2$), 1348 (NO$_2$), 1469, 1202, 1106, 1094.

43a   **43b**
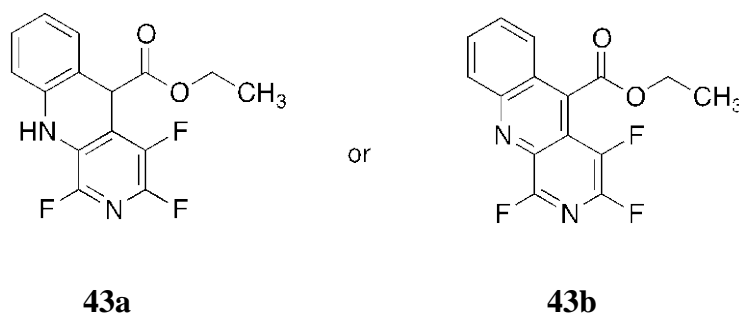
The cyclization of fluorinated ethyl ester **42** was done in the presence of iron powder as electron donor and aqueous HCl as a source of hydrogen (Scheme 20). Ethanol (7.5 mL) was added to the mixture of compound **42** (0.35 g, 1 mmol), iron powder (0.16 g, 3 mmol) and HCl (1 M, 7.5 mL) and the mixture refluxed at 78 °C for 2 h. Some solid particles appeared in the mixture and then the mixture allowed cooling at room temperature, filtered and washed with DCM. The filtrate extracted with DCM (25 mL × 3) and the combined organic layers dried over MgSO$_4$, filtered and evaporated to afford a yellow oil. Column chromatography purification using 10:1 light petrol:diethyl ether as eluting solvent afforded orange crystals (0.048 g). m.p. 159-162 °C. Neither ^{1}H nor the ^{19}F NMR spectra were fully consistent with proposed structure **43a**. The mass spectrum did show a signal consistent with the required molecular formula **43a**, HRMS (ESI) *m/z* found 307.0705 (M–H)$^-$, C$_{15}$H$_{10}$F$_3$N$_2$O$_2$ requires 307.0700. The IR spectrum suggested the presence of a carbonyl group, v_{max}/cm^{-1} (film) 1735 (C=O). The spectroscopic data suggested some of the product **43a** had formed but the material could not be obtained completely pure.

3.2.2. Reaction of pentafluorotoluene with benzonitrile
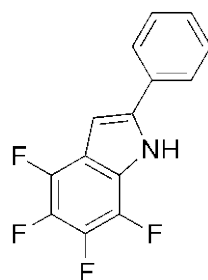
46

A solution of pentafluorotoluene (0.36 g, 2 mmol) in THF (2 mL) was added dropwise to a stirred suspension of NaH (60 % dispersion in mineral oil) (0.20 g, 5 mmol) in THF (2 mL) under N_2 and left to stir at RT for 1 h. A solution of benzonitrile (0.41 g, 4 mmol) in THF (2 mL) was added dropwise to the reaction mixture and left to stir at RT for 24 h. The solvent was evaporated and then water (10 mL) was added to the residue. The reaction mixture was extracted with diethyl ether (25 mL × 3) and the combined organic layers dried over $MgSO_4$, filtered and evaporated to give **46** as a colorless oil (0.64 g, essentially quantitative). δ_H (400 MHz, $CDCl_3$) 7.69-7.66 (2H, m), 7.62 (1H, tt, *J* 7.6 and 1.2 Hz), 7.49 (2H, t, *J* 7.6 Hz), 7.28 (1H, s), (NH signal not observed); δ_F (376 MHz, $CDCl_3$) 17.21-17.18 (1F, m), 17.15-17.11 (1F, m), 2.99-2.96 (1F, m), 2.93-2.90 (1F, m); HRMS (ESI) *m/z* found 264.0446 (M–H)$^-$, $C_{14}H_6F_4N$ requires 264.0442; v_{max}/cm^{-1} (film) 3066 (N-H), 1491, 1448, 1070.

3.2.3. Reaction of pentafluorotoluene with acetonitrile
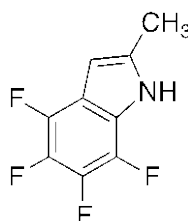
48

A solution of pentafluorotoluene (0.73 g, 4 mmol) in acetonitrile (2 mL) was added dropwise to a stirred suspension of NaH (60 % dispersion in mineral oil) (0.40 g, 10 mmol) in acetonitrile (2 mL) under N_2 and left to stir at RT for 24 h. The solvent was evaporated and then water (10 mL) was added to the residue. The reaction mixture was

extracted with diethyl ether (25 mL × 3) and the combined organic layers dried over MgSO$_4$, filtered and evaporated to give **48** as a reddish-brown oil (0.42 g, 52 %). δ$_H$ (400 MHz, CDCl$_3$) 7.28 (1H, s), 2.20 (3H, s), (NH signal not observed); δ$_F$ (376 MHz, CDCl$_3$) 20.63-20.59 (1F, m), 20.08-19.99 (1F, m), 17.23-17.14 (1F, m), 2.99-2.91 (1F, m); HRMS (ESI) *m/z* found 202.0289 (M–H)$^-$, C$_9$H$_4$F$_4$N, requires 202.0285; *v$_{max}$/cm^{-1}* (film) 3400 (NH), 2924 (CH), 2854 (CH), 1496, 1463, 1377.

3.2.4. Reaction of pentafluorotoluene with 2-pyridinecarbonitrile
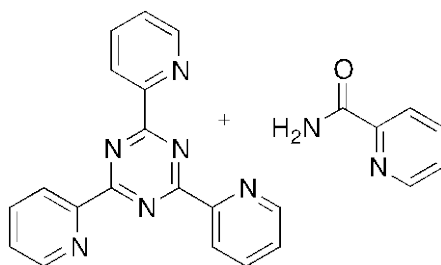
57

A solution of pentafluorotoluene (0.72 g, 4 mmol) in THF (2 mL) was added dropwise to a stirred suspension of NaH (60 % dispersion in mineral oil) (0.40 g, 10 mmol) in THF (2 mL) under N$_2$ and left to stir at RT for 1 h. A solution of 2-pyridinecarbonitrile (2.12 g, 8 mmol) in THF (2 mL) was added dropwise to the reaction mixture and left to stir at RT for 24 h. The solvent was evaporated and then water (10 mL) was added to the residue. The reaction mixture was extracted with DCM (25 mL × 3) and the combined organic layers dried over MgSO$_4$, filtered and evaporated to give creamy crystals of trimer product **57** (0.37 g, 43 %). m.p. 243-248 °C; δ$_H$ (400 MHz, CDCl$_3$) 8.91 (3H, dd, *J* 4.8 and 0.8 Hz), 8.81 (3H, dd, *J* 8.0 and 0.8 Hz), 8.51 (1H, d, *J* 4.0 Hz), 8.15 (1H, dt, *J* 8.8 and 1.2 Hz), 7.92 (3H, td, *J* 7.6 and 1.6 Hz), 7.79 (1H, td, *J* 7.6 and 1.6 Hz), 7.50 (3H, dd, *J* 7.6 and 4.8 Hz), 7.39 (1H, ddd, *J* 7.6, 4.8 and 1.2 Hz) (NH$_2$ signal not observed); ^{19}F (376 MHz, CDCl$_3$) No signals observed; HRMS and GC-MS could not find the expected mass of either component of either of the formed compound; *v$_{max}$/cm^{-1}* (film) 3369 (N-H), 1693 (C-O).

3.2.5. Reaction of pentafluoropyridine with thiobenzamide
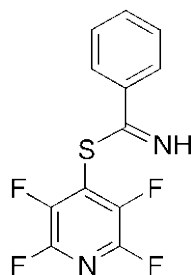
59

A solution of thiobenzamide (0.50 g, 4 mmol) in THF (3 mL) was added dropwise to a stirred suspension of NaH (60 % dispersion in mineral oil) (0.48 g, 12 mmol) in THF (3 mL) under N_2 and left to stir at RT for 1 h. A solution of pentafluoropyridine (2.01 g, 12 mmol) in THF (1 mL) was added dropwise to the reaction mixture and left to stir at RT for 24 h. The solvent was evaporated and then water (10 mL) was added to the residue. The reaction mixture was extracted with diethyl ether (25 mL × 3) and the combined organic layers dried over $MgSO_4$, filtered and evaporated to give a brown oil. Column chromatography purification with light petrol as eluting solvent afforded **59** as a yellow oil (0.914 g, 80 %). δ_H (400 MHz, CDCl$_3$) 7.68-7.48 (5H, m), 7.29 (1H, bs, NH); δ_F (376 MHz, CDCl$_3$) 74.27-74.03 (2F, m), 27.01-26.83 (2F, m); HRMS (ESI) *m/z* found 286.0273, $C_{12}H_6F_4N_2S$ requires 286.0182, v_{max}/cm^{-1} (film) 1624 (C=N), 1377, 1234.

3.2.6. Reaction of pentafluoropyridine with naphthalene-1-thiocarboxamide
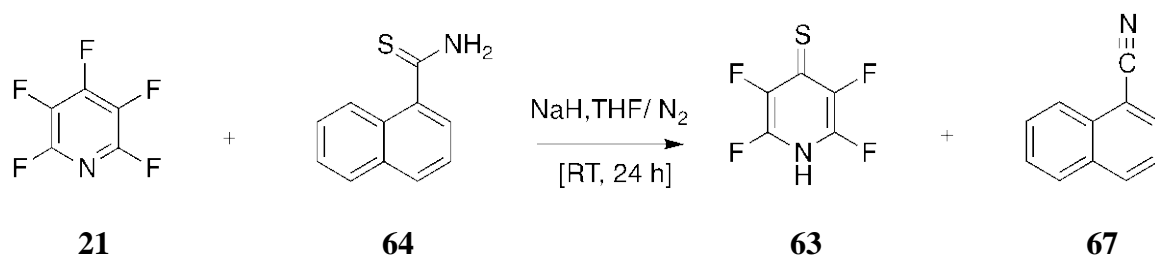
21 **64** **63** **67**

A solution of naphthalene-1-thiocarboxamide (0.37 g, 2 mmol) in THF (2 mL) was added to a stirred suspension of NaH (60 % dispersion in mineral oil) (0.24 g, 6 mmol) in THF (2 mL) under N_2 and left to stir at RT for 1 h. A solution of pentafluoropyridine (1.01 g, 6 mmol) in THF (2 mL) was added to the reaction mixture and left to stir at RT for 24 h. The solvent was evaporated and then water (20 mL) was added to the residue. Solid

particles precipitated, and were filtered to give 1.04 g of white crystals which was a mixture of **63** and **67**, m.p. 59-61 °C.

Compound **63**, δ_F (376 MHz, DMSO-d$_6$) 74.16-73.94 (2F, m), 26.88-26.72 (2F, m); HRMS (ESI) *m/z* found 181.9692 (M–H)$^-$, C$_5$F$_4$NS, requires 181.9693; ν_{max} / cm^{-1} (film) 3460 (N-H) and 1627 (C=S).

Compound **67**, δ_H (400 MHz, DMSO-d$_6$) 8.33 (1H, d, *J* 8.4 Hz), 8.18 (1H, dd, *J* 7.2 and 0.8 Hz), 8.13 (2H, t, *J* 8.0 Hz), 7.82(1H, td, *J* 7.2 and 1.2 Hz), 7.74 (1H, td, *J* 7.2 and 1.2 Hz), 7.69 (1H, dd, *J* 8.4 and 7.2 Hz); HRMS (ESI) *m/z* found 153.0584, C$_{11}$H$_7$N requires 153.0584, and; ν_{max} / cm^{-1} (film) 2224 (C≡N).

3.2.7. *Reaction of hexafluorobenzene with naphthalene-1-thiocarboxamide*
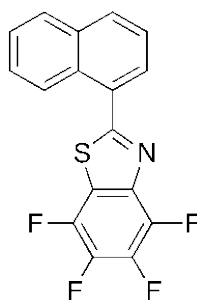
68

A solution of hexafluorobenzene (1.116 g, 6 mmol) in THF (2 mL) was added dropwise to a stirred suspension of NaH (60 % dispersion in mineral oil) (0.24 g, 6 mmol) in THF (2 mL) under N$_2$. A solution of naphthalene-1-thiocarboxamide (0.374 g, 2 mmol) in THF (3 mL) was added dropwise to the reaction mixture and left to stir at RT for 48 h. The solvent was evaporated and then water (10 mL) was added to the residue. The reaction mixture was extracted with DCM (25 mL × 3) and the combined organic layers dried over MgSO$_4$, filtered and evaporated to give **68** as yellow crystals (0.108 g, 16 %). m.p. 165-168 °C; δ_H (400 MHz, CDCl$_3$) 8.28 (1H, dd, *J* 8.0 and 0.8 Hz), 8.12 (1H, d, *J* 8.0 Hz), 7.97-7.94 (2H, m), 7.73 (1H, td, *J* 6.8 and 1.2 Hz), 7.66 (1H, td, *J* 6.8 and 1.2 Hz), 7.57 (1H, dd, *J* 8.4 and 7.2 Hz); δ_F (376 MHz, CDCl$_3$) 23.80 (1F, dd, *J* 20 and 15 Hz), 14.79 (1F, dd, *J* 19 and 14 Hz), 3.96 (1F, t, *J* 19 Hz), 3.24 (1F, t, *J* 20 Hz); GC-MS (EI) *m/z* 333; ν_{max} / cm^{-1}(film) 2923, 1514, 1466, 1340.

3.2.8. Reaction of pentafluoropyridine with 2-mercaptobenzimidazole
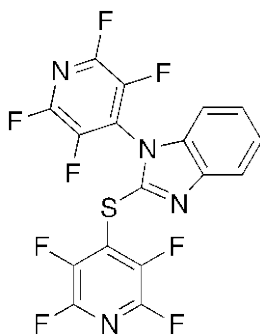
71

A solution of pentafluoropyridine (16.90 g, 100 mmol) in THF (2 mL) and a solution of 2-mercaptobenzimidazole (3 g, 20 mmol) in DMF (3 mL) and THF (10 mL) were added dropwise to a stirred suspension of NaH (60 % dispersion in mineral oil) (1.6 g, 50 mmol) in THF (4 mL) under N_2 and left to stir at RT for 24 h. The solvent was evaporated and then water (20 mL) was added to the residue. The reaction mixture was extracted with DCM (25 mL × 3) and the combined organic layers dried over $MgSO_4$, filtered and evaporated to give **71** as creamy crystals (2.44 g, 27 %). m.p. 112-115 °C; δ_H (400 MHz, CDCl$_3$) 7.85-7.80 (1H, m), 7.49-7.45 (2H, m), 7.23-7.19 (1H, m); δ_C (100 MHz, CDCl$_3$) 145-134 (a cluster of weak signals was observed due to the pyridine ring carbons exhibiting multiplet coupling to fluorine), 143.38 (Cq), 134.94 (Cq), 126.07 (CH), 124.99 (CH), 120.80 (CH), 110.05 (CH); δ_F (376 MHz, CDCl$_3$) 77.42-77.05 (2F, m), 74.37-73.97 (2F, m), 27.03-26.87 (2F, m), 19.26-19.12 (2F, m); HRMS (ESI) *m/z* found 446.9962 (M–H)$^-$, $C_{17}H_3F_8N_4S$ requires 446.9956; v_{max} /cm^{-1} (film) 1630, 1474, 1246, 975, 952; Analysis (%) calculated for $C_{17}H_4F_8N_4S$ (448): C, 45.55; H, 0.90; N, 12.50. Found C, 45.41; H, 0.92; N, 12.00.

3.2.9. Reaction of pentafluoropyridine with 2-mercapto-4(3H)-quinazolinone
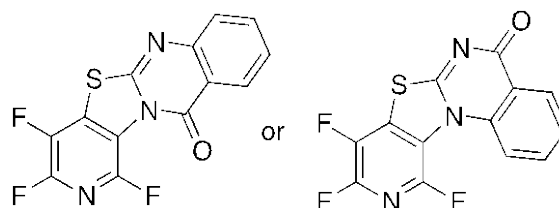
74　　　　　　　**75**

A solution of 2-mercapto-4(3H)-quinazolinone (0.712 g, 4 mmol) in THF (8 mL) and DMF (1 mL) was added dropwise to a stirred suspension of NaH (60 % dispersion in mineral oil) (0.40 g, 10 mmol) in THF (4 mL) under N_2 and left to stir at RT for 1 h. A solution of pentafluoropyridine (1.014 g, 6 mmol) in THF (3 mL) was added dropwise to the reaction mixture and left to stir at RT for 24 h. The solvent was evaporated and then water (10 mL) was added to the residue. The reaction mixture was extracted with diethyl ether (25 mL × 3) and the combined organic layers dried over $MgSO_4$, filtered and evaporated to give yellow oil. Recrystallization with diethyl ether afforded **74** or **75** as creamy crystals (0.045 g, 4%). m.p. 242-246 °C; δ_H (400 MHz, $CDCl_3$) 8.34 (1H, ddd, J 8.0, 1.6 and 0.4 Hz), 7.79 (1H, td, J 7.2 and 1.6 Hz), 7.61 (1H, dd, J 7.6 and 0.4 Hz), 7.50 (1H, td, J 7.6 and 1.2 Hz); δ_F (376 MHz, $CDCl_3$) 106.50 (1F, dd, J 30 and 10 Hz), 74.44 (1F, dd, J 22 and 10 Hz), 16.26 (1F, dd, J 29 and 22 Hz); GC-MS (EI) m/z 307; v_{max} / cm^{-1}(film) 1712 (C=O), 1147, 1124, 1022.
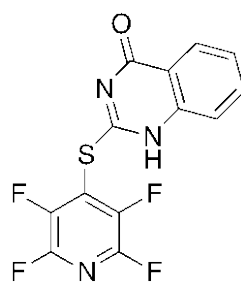
76

A solution of 2-mercapto-4(3H)-quinazolinone (1.424 g, 8 mmol) in THF (16 mL) and DMF (2 mL) was added dropwise to a stirred suspension of NaH (60 % dispersion in mineral oil) (0.40 g, 10 mmol) in THF (4 mL) under N_2 and left to stir at RT for 1 h. A solution of pentafluoropyridine (2.704 g, 16 mmol) in THF (3 mL) was added dropwise to the reaction mixture and left to stir at RT for 24 h. The solvent was evaporated and then water (10 mL) was added to the residue, creamy crystals was formed, and were filtered to give **76** (0.57 g, 22 %). m.p. 206-210 °C; δ_H (400 MHz, DMSO-d_6) 8.06 (1H, dd, J 8.0 and 1.2 Hz), 7.74 (1H, td, J 7.2 and 1.6 Hz), 7.48 (1H, td, J 7.2 and 1.2 Hz), 7.38 (1H, dd, J 8.0 and 0.4 Hz), (NH signal not observed); δ_F (376 MHz, DMSO-d_6) 70.60-70.43 (2F, m), 28.73-28.54 (2F, m); HRMS (ESI) m/z found 326.0023 (M–H)$^-$, $C_{13}H_4F_4N_3OS$ requires 326.0017; v_{max} / cm^{-1} (film) 3583 (N-H), 1688 (C=O), 1466, 1264, 1161.

3.2.10. Reaction of pentafluorobenzaldehyde with 2-mercapto-4(3H)-quinazolinone

78

A solution of 2-mercapto-4(3H)-quinazolinone (2.67 g, 30 mmol) in THF (50 mL) and DMF (5 mL) was added dropwise to a stirred suspension of NaH (60 % dispersion in mineral oil) (0.80 g, 20 mmol) in THF (3 mL) under N_2 and left to stir at RT for 1 h. A solution of pentafluorobenzaldehyde (5.88 g, 30 mmol) in THF (3 mL) was added dropwise to the reaction mixture and left to stir at RT for 24 h. The solvent was evaporated and then water (10 mL) was added to the residue, solid particles formed, and were filtered and recrystallized from hot ethanol to give **78** as white crystals (3.07 g, 29 %). m.p. 250-252 °C; δ_H (400 MHz, DMSO-d_6) 13.5-12.7 (1H, bs, NH), 10.23 (1H, s), 8.05 (1H, dd, *J* 8.0 and 1.2 Hz), 7.71 (1H, td, *J* 7.2 and 1.6 Hz), 7.45 (1H, td, *J* 8.0 and 0.8 Hz), 7.31 (1H, d, *J* 7.6 Hz); δ_F (376 MHz, DMSO-d_6) 30.19-30.10 (2F, m), 16.27-16.17 (2F, m); HRMS (ESI) m/z found 353.0018 (M–H)$^-$, $C_{15}H_5F_4N_2O_2S$ requires 353.0013; v_{max} / cm^{-1}(film) 3583 (N-H), 1682 (C=O), 1592, 1384, 1246.

3.2.11. Reaction of pentafluoropyridine with 2-bromothiophenol[31]
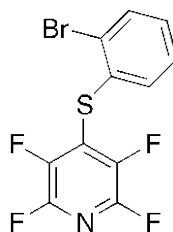
82

A solution of 2-bromothiophenol (3.78 g, 20 mmol) in DMF (1 mL) was added dropwise to a stirred suspension of NaH (60 % dispersion in mineral oil) (1.6 g, 40 mmol) in DMF (4 mL) under N_2 and left to stir at RT for 1 h. A solution of pentafluoropyridine (10.14 g,

60 mmol) in DMF (1 mL) was added dropwise to the reaction mixture and left to stir at RT for 24 h. The solvent was evaporated and then water (10 mL) was added to the residue. The reaction mixture was extracted with DCM (25 mL × 3) and the combined organic layers dried over MgSO$_4$, filtered and evaporated to give **82** as reddish brown oil (1.405 g, 21 %). δ_H (400 MHz, CDCl$_3$) 7.47 (1H, dd, *J* 7.6 and 1.2 Hz), 7.38 (1H, d, *J* 7.6 Hz), 7.17 (1H, td, *J* 7.6 and 1.6 Hz), 7.11 (1H, td, *J* 7.6 and 2.0 Hz); δ_F (376 MHz, CDCl$_3$) 70.81-70.76 (2F, m), 25.38-25.28 (2F, m); GC-MS (EI) *m/z* 337 and 339; v_{max} / cm^{-1} (film) 1507, 1447, 1234, 1103, 1020, data in agreement with literature values.

3.2.12. Cyclization of 4-(2-bromophenylsulfanyl)-2,3,5,6-tetrafluoropyridine (82)[31]
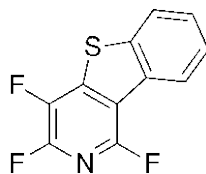
83

A solution of 4-(2-bromophenylsulfanyl)-2,3,5,6-tetrafluoropyridine **82** (0.68 g, 2 mmol) in THF (10 mL) was stirred at -78 °C under N$_2$ and treated dropwise with a solution of *n*-BuLi in hexane (2.5 M, 0.9 mL, 2 mmol). The mixture was stirred and allowed to warm to RT for 24 h. The solvent was evaporated and then water (10 mL) was added to the residue. The reaction mixture was extracted with diethyl ether (25 mL × 3) and the combined organic layers dried over MgSO$_4$, filtered and evaporated to give **83** as a brown oil (0.315 g, 66 %). δ_H (400 MHz, CDCl$_3$) 8.38-8.35 (1H, m), 7.95-7.92 (1H, m), 7.63-7.16 (2H, m); HRMS (ESI) *m/z* found 240.0088 (M+H)$^+$, C$_{11}$H$_5$F$_3$NS requires 240.0045; v_{max} / cm^{-1} (film) 1618, 1480, 1438, 1253, 1025, consistent with the literature values.

3.2.13. Reaction of hexafluorobenzene with 2-bromothiophenol[31]
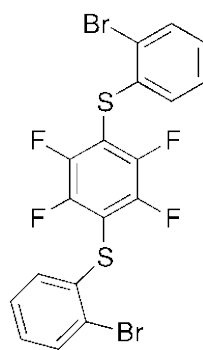
84

A solution of 2-bromothiophenol (0.78 g, 4 mmol) in DMF (1 mL) was added dropwise to a stirred suspension of NaH (60 % dispersion in mineral oil) (0.20 g, 5 mmol) in DMF (8 mL) under N_2. Hexafluorobenzene (0.38 g, 2 mmol) was added dropwise to the reaction mixture and stirred at RT for 24 h. The solvent was evaporated and then water (25 mL) was added to the residue. The reaction mixture was extracted with diethyl ether (25 mL × 3) and the combined organic layers dried over $MgSO_4$, filtered and evaporated to give **84** as a yellow solid (0.85 g). Recrystallization from dichloromethane-light petroleum afforded pale yellow crystals (0.74 g 35 %). m.p. 138-139 °C (lit., 138 °C); δ_H (400 MHz, DMSO-d_6) 7.62 (2H, d, J 8.0 Hz), 7.49 (2H, dd, J 7.6 and 1.2 Hz), 7.17-7.11 (2H, m), 7.05-6.97 (2H, m); δ_F (376 MHz, DMSO-d_6) 31.18 (4F, s); HRMS (ESI) m/z found 521.8364, $C_{18}H_8{}^{79}Br_2F_4S_2$ requires 521.8376; v_{max} / cm^{-1}(film) 1445, 1388, 1237, 1014, 748. Data consistent with literature values.

3.2.14. Cyclization of 1,4-bis-(2-bromophenylsulfanyl)-2,3,5,6-tetrafluorobenzene (84)[31]
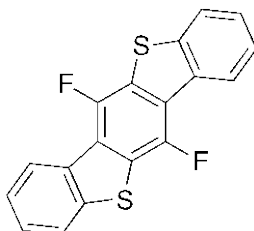
85

A solution of 1,4-bis-(2-bromophenylsulfanyl)tetrafluorobenzene **84** (0.957 g, 0.0018 mmol) in THF (2 mL) was stirred at -78 °C under N_2 and treated dropwise with a solution of n-BuLi in hexane (2.5 M, 1.6 mL). The mixture was stirred and allowed to warm to RT

for 24 h. The solvent was evaporated and then water (20 mL) was added to the residue. The reaction mixture was extracted with DCM (25 mL × 3) and the combined organic layers dried over MgSO$_4$, filtered and evaporated to give orange brown solid. Recrystallization from dichloromethane-light petroleum afforded **85** as fine pale yellow crystals (0.50 g, 85 %). m.p. 287-289 °C (lit., 287 °C) ; δ_H (400 MHz, CDCl$_3$) 8.49-8.47 (2H, m), 7.90-7.87 (2H, m), 7.56-7.54 (4H, m); δ_F (376 MHz, CDCl$_3$) 37.9 (2F, s); HRMS (ESI) *m/z* found 326.0036, C$_{18}$H$_8$F$_2$S$_2$ requires 326.0036; Data in agreement with literature values.

3.2.15. Reaction of pentafluoropyridine with 1-bromo-2-naphthol
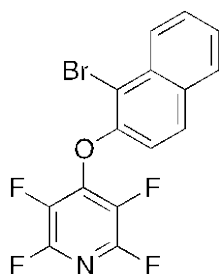
87

A solution of pentafluoropyridine (8.112 g, 48 mmol) in DMF (1 mL) and a solution of 1-bromo-2-naphthol (3.568 g, 16 mmol) in DMF (3 mL) were added dropwise to a stirred suspension of NaH (60 % dispersion in mineral oil) (0.80 g, 20 mmol) in DMF (3 mL) under N$_2$ and left to stir at RT for 24 h. The solvent was evaporated and then water (10 mL) was added to the residue, creamy crystals formed, and were filtered and recrystallized from light petrol to give **87** (5.971 g, 100 %). m.p. 77-80 °C; δ_H (400 MHz, CDCl$_3$) 8.28 (1H, d, *J* 8.4 Hz), 7.85 (2H, t, *J* 8.0 Hz), 7.67 (1H, t, *J* 7.2 Hz), 7.56 (1H, t, *J* 7.2 Hz), 7.24 (1H, d, *J* 8.4 Hz); δ_F (376 MHz, CDCl$_3$) 73.29-73.12 (2F, m), 6.10-5.94 (2F, m); HRMS (ESI) *m/z* found 369.9528 (M–H)$^-$, C$_{15}$H$_5$^{79}BrF$_4$NO requires 369.9496; v_{max} / cm^{-1}(film) 1480, 1429, 1218, 1078; Analysis (%) calculated for C$_{15}$H$_6$BrF$_4$NO (370): C,48.64; H, 1.62; N, 3.78. Found C, 48.52; H, 1.56; N, 3.80.

88   and   **89**

A solution of 4-(3-bromonaphthalen-2-yloxy)tetrafluoropyridine **87** (0.370 g, 1 mmol) in THF (2 mL) was stirred at -78 °C and treated dropwise with a solution of *n*-BuLi in hexane (2.5 M, 0.539 mL, 1 mmol). The solution turned orange and then faded to yellow over 50 min. The mixture was stirred and allowed to warm to room temperature for 24 h. The solvent was evaporated and then water (20 mL) was added to the residue. The reaction mixture was extracted with DCM (25 mL × 3) and the combined organic layers dried over MgSO$_4$, filtered and evaporated to give orange oil (0.182 g, approx. 60 % based on **88**). Column chromatography purification using 9:1 light petrol:diethyl ether as eluting solvent yielded yellow oil (0.146 g) of a mixture of two compounds mainly **88** and a trace of **89**.

Compound **88**, δ_H (400 MHz, CDCl$_3$) 7.91 (1H, d, *J* 8.8 Hz), 7.87 (1H, d, *J* 7.6 Hz), 7.77-7.69 (1H, bs, OH), 7.50 (1H, td, *J* 6.8 and 1.6 Hz), 7.43 (1H, td, *J* 7.2 and 1.6 Hz), 7.34 (1H, d, *J* 7.6 Hz), 7.23 (1H, d, *J* 8.8 Hz); δ_F (376 MHz, CDCl$_3$) 70.57-70.39 (2F, m), 22.78-22.61 (2F, m); GC-MS (EI) m/z 293; v_{max} / cm^{-1} (film) 3411 (O-H).

Compound **89**, ^{1}H NMR signals not visible in the mixture; ^{19}F NMR signals were observed in the range 67-72 ppm and 23-36 consistent with the proposed structure, but signals from other minor compounds prevented full assignment; GC-MS (EI) m/z 273.

3.2.17. Lithiation reaction of 4-(3-bromonaphthalene-2-yloxy)-2,3,5,6-tetrafluorpyridine (87) in the presence of TMEDA
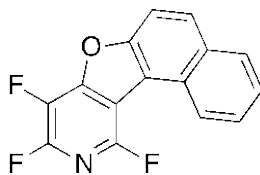
90

A solution of 4-(3-bromonaphthalen-2-yloxy)tetrafluoropyridine **87** (3.70 g, 10 mmol) in THF (8 mL) and TMEDA (2 mL) was stirred at -78 °C and treated dropwise with a solution of *n*-BuLi in hexane (2.04 M, 4 mL, 10 mmol). The solution turned to orange and then faded to yellow over 1 h. The mixture was stirred and allowed to warm to room temperature for 24 h. The solvent was evaporated and then water (20 mL) was added to the residue. The reaction mixture was extracted with DCM (25 mL × 3) and the combined organic layers dried over MgSO$_4$, filtered and evaporated to give yellow orange oil (2.319 g). Column chromatography purification using light petrol as eluting solvent afforded **90** as a white crystals (0.443 g, 16 %). m.p. 119-121 °C; δ_H (400 MHz, CDCl$_3$) 8.34 (d, *J* 8.4 Hz), 7.93-7.83 (m), 7.70 (td, *J* 7.2 and 1.6 Hz), 7.62-7.48 (m), 7.34-7.29 (m) (integral values not accurate); δ_F (376 MHz, CDCl$_3$) 8.03 (1F, d, *J* 26 Hz), 1.76 (1F, d, *J* 21 Hz), 72.81 (1F, dd, *J* 26 and 21 Hz); GC-MS (EI) m/z 273; v_{max} / cm^{-1} (film) 1624, 1594, 1496, 1470, 1456, 1405, 1217.

3.2.18. Reaction of hexafluorobenzene with 1-bromo-2-naphthol
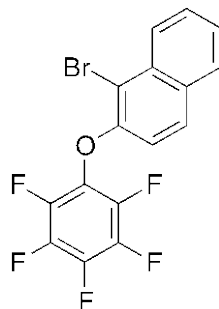
91

A solution of 1-bromo-2-naphthol (1.784 g, 8 mmol) in DMF (4 mL) was added dropwise to a stirred suspension of NaH (60 % dispersion in mineral oil) (0.4 g, 10 mmol) in DMF (2 mL) under N$_2$ and left to stir at RT for 1 h. A solution of hexafluorobenzene (14.88 g,

80 mmol) in DMF (1 mL) was added dropwise to the reaction mixture and it was left to stir at RT for 24 h. The solvent was evaporated and then water (20 mL) was added to the residue. The reaction mixture was extracted with DCM (25 mL × 3) and the combined organic layers dried over MgSO$_4$, filtered and evaporated to give reddish brown oil (1.598 g) column chromatography purification using light petrol as eluting solvent afforded **91** as white crystals (0.348 g, 11 %). m.p. 112-114 °C; δ_H (400 MHz, CDCl$_3$) 8.34 (1H, d, *J* 8.4 Hz), 7.85 (1H, d, *J* 8.0 Hz), 7.80 (1H, d, *J* 9.2 Hz), 7.68 (1H, td, *J* 7.2 and 2.0 Hz), 7.54 (1H, td, *J* 8.0 and 1.2 Hz), 7.01 (1H, d, *J* 8.8 Hz); δ_F (376 MHz, CDCl$_3$) 7.86 (2F, d, *J* 17 Hz), 2.41 (1F, t, *J* 23 Hz), 0.21-0.13 (2F, m); GC-MS (EI) *m/z* 388 and 390; v_{max} / cm^{-1} (film) 1596, 1514, 1355, 1254, 989; Analysis (%) calculated for C$_{16}$H$_6$BrF$_5$O (388): C, 49.61; H, 1.55. Found C, 49.05; H, 1.50.

3.2.19. Reaction of hexafluorobenzene with 2 equivalents of 1-bromo-2-naphthol

92

A solution of 1-bromo-2-naphthol (1.784 g, 8 mmol) in THF (3 mL) was added dropwise to a stirred suspension of NaH (60 % dispersion in mineral oil) (0.8 g, 20 mmol) in THF (2 mL) under N$_2$ and left to stir at RT for 1 h. A solution of hexafluorobenzene (0.744 g, 4 mmol) in THF (1 mL) was added dropwise by syringe pump to the reaction mixture and left to stir at RT for 24 h. The solvent was evaporated and then water (20 mL) was added to the residue. The reaction mixture was extracted with DCM (25 mL × 3) and the combined organic layers dried over MgSO$_4$, filtered and evaporated to give **92** as gray crystals after column chromatography purification using light petrol as eluting solvent (0.26 g, 11 %). m.p. 132-134 °C; δ_H (400 MHz, CDCl$_3$) 8.07 (2H, d, *J* 8.4 Hz), 7.81 (2H, d, *J* 7.6 Hz), 7.77 (2H, d, *J* 8.8 Hz), 7.60 (2H, td, *J* 6.8 and 1.2 Hz), 7.42 (2H, td, *J* 8.0 and

1.2 Hz), 7.31 (2H, d, J 9.2 Hz); δ_F (376 MHz, CDCl$_3$) 61.81 (4F, s); HRMS (ESI) could not observe the expected mass of the target compound; ν_{max} / cm^{-1}(film) 1502, 1255, 1237, 1041, 1021.

3.2.20. Reaction of 2-bromoaniline with p-toluenesulfonylchloride

95
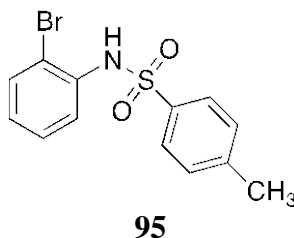
A solution of 2-bromoaniline (2.61 g, 15 mmol) in pyridine (2 mL) was added dropwise to a solution of p-toluenesulfonylchloride (2.85 g, 15 mmol) in pyridine (2 mL) under N$_2$ and left to stir at RT for 72 h. The solvent was evaporated and diethyl ether (50 mL) was added to the residue, white solids precipitated, and were filtered and dried to give **95** as white crystals (4.21 g, 87 %). m.p. 93-96 °C; δ_H (400 MHz, CDCl$_3$) 7.69 (1H, dd, J 8.4 and 1.6 Hz), 7.67 (2H, d, J 8.4 Hz), 7.43 (1H, dd, J 8.0 and 1.6 Hz), 7.29 (1H, td, J 8.0 and 1.2 Hz), 7.24 (2H, d, J 8.0 Hz), 6.99 (1H, td, J 7.2 and 1.6 Hz) + (1H, bs, NH), 2.40 (3H, s); δ_C (100 MHz, CDCl$_3$) 144.25 (Cq), 134.72 (Cq), 132.58 (CH), 129.67 (CH), 128.59 (CH), 127.34 (CH), 126.27 (CH), 122.54 (CH), 21.60 (CH$_3$), four Cq could not be observed. HRMS (ESI) m/z found 323.9702 (M–H)$^-$, C$_{13}$H$_{11}$^{79}BrNO$_2$S requires 323.9699; ν_{max} /cm^{-1} (film) 3297 (N-H), 1594, 1479, 1332 (SO$_2$), 1166, 1089, 1026; Analysis (%) calculated for C$_{13}$H$_{11}$BrNO$_2$S (324): C, 47.86; H, 3.71; N, 4.29. Found C, 47.83; H, 3.71; N, 4.29.

3.2.21. Reaction of pentafluoropyridine with N-(2-bromophenyl)-4-methylbenzenesulfonamide (95)

96
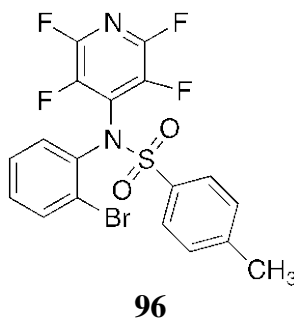
A solution of pentafluoropyridine (3.38 g, 20 mmol) in THF (2 mL) and a solution of N-(2-bromophenyl)-4-methylbenzenesulfonamide **95** (0.792 g, 2 mmol) in THF (6 mL) and DMF (2 mL) were added dropwise to a stirred suspension of NaH (60 % dispersion in mineral oil) (0.16 g, 4 mmol) in THF (2 mL) and heated under reflux at 66 °C for 2 h under N_2. After 2 h the reaction mixture allowed to stir at RT for 24 h. The solvent was evaporated and then water (20 mL) was added to the residue. The reaction mixture was extracted with DCM (25 mL × 3) and the combined organic layers dried over $MgSO_4$, filtered and evaporated to give a dark green oil (1.13 g). Column chromatography purification using 9:1 light petrol:diethyl ether as eluting solvent afforded **96** as white crystals (0.22 g, 23 %). m.p. 95-97 °C; δ_H (400 MHz, $CDCl_3$) 8.06 (1H, dq, *J* 8.0 and 1.6 Hz), 7.59 (2H, d, *J* 8.0 Hz), 7.52 (1H, dd, *J* 8.0 and 1.2 Hz), 7.48 (1H, td, *J* 7.6 and 1.6 Hz), 7.33 (1H, td, *J* 8.0 and 1.6 Hz), 7.29 (2H, d, *J* 8.0 Hz), 2.46 (3H, s); δ_C (100 MHz, $CDCl_3$) 144.28 (Cq), 135.80 (Cq), 134.70 (Cq), 132.59 (CH), 129.69 (CH), 128.60 (CH), 127.34 (CH), 126.29 (CH), 122.56 (CH), 115.72 (Cq), 21.62 (CH_3), the signals expected for the tetrafluoropyridine ring could not be detected; δ_F (376 MHz, $CDCl_3$) 72.82-72.65 (2F, m), 8.53-8.37 (2F, m); HRMS (ESI) *m/z* found 472.9588 (M–H)$^-$, $C_{18}H_{10}{}^{79}BrF_4N_2O_2S$ requires 472.9588; v_{max} / cm^{-1}(film) 1596, 1589, 1478, 1397, 1337, 1164, 1091.

3.2.22. Reaction of hexafluorobenzene with carbazole to synthesise dicarbazole derivative

100
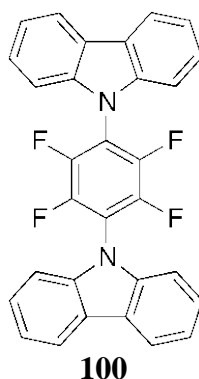
A solution of carbazole (1.336 g, 8 mmol) in THF (10 mL) was added dropwise to a stirred suspension of NaH (60 % dispersion in mineral oil) (0.40 g, 9 mmol) in THF (5 mL) under N_2 and left to stir at RT for 1 h. A solution of hexafluorobenzene (0.70 g, 4 mmol) in THF (1 mL) was added dropwise to the reaction mixture and stirred at RT for

24 h. The solvent was evaporated and then water (20 mL) was added to the residue. Yellow crystals precipitated, and were filtered to give **100** (0.502 g, 26 %). m.p. 344-350 °C; δ_H (400 MHz, CDCl$_3$) 8.22 (4H, d, *J* 7.6 Hz), 7.56 (4H, t, *J* 7.2 Hz), 7.43 (4H, t, *J* 7.2 Hz), 7.35 (4H, d, *J* 8.0 Hz); δ_F (376 MHz, CDCl$_3$) 21.00 (4F, s); GC-MS (EI) *m/z* 480; v_{max} /cm^{-1}(film) 1499, 1333, 1229, 1149, 1029.

3.2.23. Reaction of hexafluorobenzene with carbazole to synthesise monocarbazole derivative

102
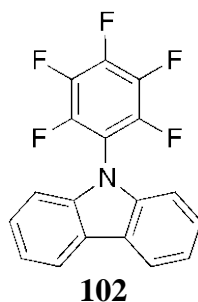
A solution of carbazole (0.33 g, 2 mmol) in THF (3 mL) and DMF (1 mL) was added dropwise to a stirred suspension of NaH (60 % dispersion in mineral oil) (0.2 g, 4 mmol) in THF (2 mL) under N$_2$ and left to stir at RT for 1 h. A solution of hexafluorobenzene (3.72 g, 20 mmol) in THF (1 mL) was added dropwise to the reaction mixture and stirred at RT for 24 h. The solvent was evaporated and then water (20 mL) was added to the residue, creamy solid particles precipitated, and were filtered (0.49 g) and column chromatography using light petrol eluting solvent gave **102** as white crystals (0.075 g, 11 %). m.p. 188-191 °C; δ_H (400 MHz, CDCl$_3$) 8.19 (2H, d, *J* 7.2 Hz), 7.51 (2H, t, *J* 8.0 Hz), 7.41 (2H, t, *J* 7.6 Hz), 7.17 (2H, d, *J* 8.0 Hz); δ_F (376 MHz, CDCl$_3$) 19.80-19.49 (2F, m), 8.82 (1F, t, *J* 22 Hz), 1.66-1.54 (2F, m); GC-MS (EI) *m/z* 333; v_{max} /cm^{-1} (film) 1523, 1511, 1444, 1332, 1284, 1027.

3.2.24. Reaction of pentafluoropyridine with carbazole

103
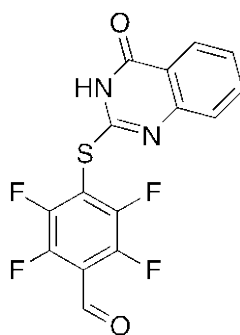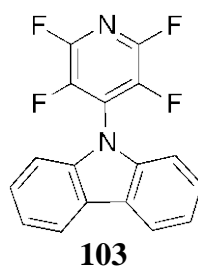
A solution of carbazole (1.67 g, 10 mmol) in THF (10 mL) and DMF (1 mL) was added dropwise to a stirred suspension of NaH (60 % dispersion in mineral oil) (0.8 g, 20 mmol) in THF (2 mL) under N_2 and left to stir at RT for 1 h. A solution of pentafluoropyridine (8.45 g, 50 mmol) in THF (1 mL) was added dropwise to the reaction mixture and stirred at RT for 24 h. The solvent was evaporated and then water (20 mL) was added to the residue. Creamy solid particles precipitated, and were filtered (3.978 g) and purified by column chromatography using 8:2 light petrol:diethyl ether as eluting solvent to give **103** as creamy crystals (1.62 g, 51 %). m.p. 190-194 °C; δ_H (400 MHz, CDCl$_3$) 8.14 (2H, d, J 7.6 Hz), 7.49 (2H, t, J 7.6 Hz), 7.40 (2H, t, J 7.6 Hz), 7.20 (2H, d, J 8.0 Hz); δ_F (376 MHz, CDCl$_3$) 74.44-74.27 (2F, m), 20.16-19.96 (2F, m) with very minor impurities; GC-MS (EI) m/z 316; v_{max} / cm^{-1}(film) 1638, 1618, 1514, 1466, 1255, 1159, 1061.

104
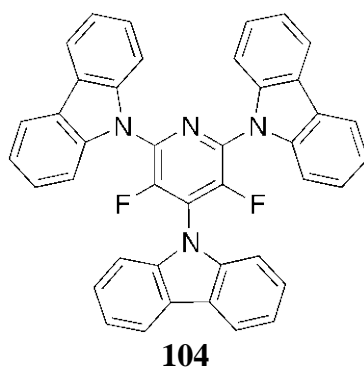
In a one-off procedure following the same method as above to synthesise monocarbazole derivative **103** the tricarbazole derivative **104** was isolated as creamy crystals (0.303 g, 5 %). m.p. 217-222 °C; δ_H (400 MHz, CDCl$_3$) 8.19-8.09 (m), 7.63-7.56 (m), 7.48-7.38 (m), 7.36-7.30 (m); δ_F (376 MHz, CDCl$_3$) 39.65 (2F, s); GC-MS and HRMS could not observe the expected mass of the compound; v_{max} / cm^{-1} (film) 1599, 1577, 1453, 1312, 1227, 747; Analysis (%) calculated for C$_{41}$H$_{24}$F$_2$N$_4$ (610): C, 80.64; H, 3.96; N, 9.17. Found C, 80.35; H, 3.97; N, 8.85.

3.2.25. Reaction of pentafluorotoluene with carbazole
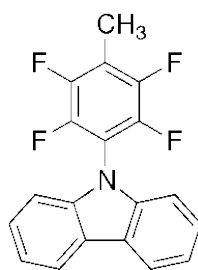
105

A solution of carbazole (2.672 g, 16 mmol) in THF (10 mL) and DMF (1 mL) was added dropwise to a stirred suspension of NaH (60 % dispersion in mineral oil) (1.6 g, 40 mmol) in THF (5 mL) under N_2 and left to stir at RT for 1 h. A solution of pentafluorotoluene (14.56 g, 80 mmol) in THF (1 mL) was added dropwise to the reaction mixture under reflux at 66 °C for 48 h. The solvent was evaporated and then water (20 mL) was added to the residue, yellow orange solid particles precipitated, and were filtered (5.029 g). Column chromatography purification using light petrol as eluting solvent gave **105** as white crystals (1.93 g, 37 %). m.p. 153-155 °C; δ_H (400 MHz, CDCl$_3$) 8.22 (2H, d, *J* 7.6 Hz), 7.52 (2H, td, *J* 7.2 and 1.2 Hz), 7.41 (2H, td, *J* 7.6 and 0.8 Hz), 7.23 (2H, d, *J* 7.6 Hz), 2.48 (3H, t, *J* 2.4 Hz); δ_F (376 MHz, CDCl$_3$) 19.80-19.72 (2F, m), 17.14-17.05 (2F, m); GC-MS (EI) *m/z* 329; v_{max} / cm^{-1} (film) 1620, 1512, 1311, 1226, 1181; Analysis (%) calculated for C$_{19}$H$_{11}$F$_4$N (329): C, 69.30; H, 3.34; N, 4.25. Found C, 69.47; H, 3.45; N, 4.49.

3.2.26. Reaction of pentafluorobenzoyl chloride with carbazole
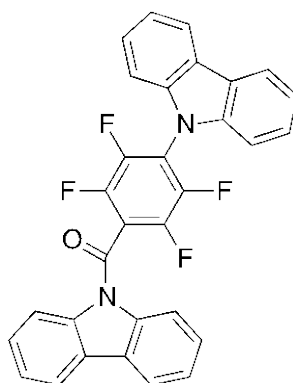
109

A solution of carbazole (0.668 g, 4 mmol) in THF (5 mL) and DMF (1 mL) was added dropwise to a stirred suspension of NaH (60 % dispersion in mineral oil) (0.2 g, 4 mmol) in THF (2 mL) under N_2 and left to stir at RT for 1 h. A solution of pentafluorobenzoyl chloride (0.94 g, 4 mmol) in THF (1mL) was added dropwise to the reaction mixture and stirred at RT for 24 h. The solvent was evaporated and then water (20 mL) was added to the residue. Orange yellow crystals precipitated and were filtered (1.32 g). Recrystallization from hot ethanol afforded **109** as creamy crystals (0.373 g, 36 %). m.p. 216-221 °C; δ_H (400 MHz, CDCl$_3$) 8.21 (1H, d, *J* 7.2 Hz), 8.11-8.06 (1H, m), 7.85-7.73 (4H, m), 7.56 (1H, td, *J* 7.6 and 1.2 Hz), 7.52-7.48 (2H, m), 7.43 (1H, td, *J* 8.0 and 0.8 Hz), 7.14-7.07 (6H, m); δ_F (376 MHz, CDCl$_3$) 22.95-22.86 (2F, m), 22.54-22.43 (2F, m); HRMS (ESI) *m/z* found 509.1269 (M+H)$^+$, C$_{31}$H$_{17}$F$_4$N$_2$O requires 509.1272; v_{max} /cm^{-1} (film) 1689 (C=O), 1492, 1477, 1443, 1332, 1310, 1225.

3.2.27. Reaction of pentafluorobenzamide with carbazole
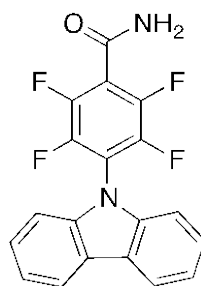
111

A solution of carbazole (2.672 g, 16 mmol) in THF (10 mL) and DMF (4 mL) was added dropwise to a stirred suspension of NaH (60 % dispersion in mineral oil) (1.44 g, 36 mmol) in THF (2 mL) under N_2 and left to stir at RT for 1 h. A solution of pentafluorobenzamide (3.376 g, 16 mmol) in THF (10 mL) and DMF (4 mL) was added dropwise to the reaction mixture and stirred at RT for 24 h. The solvent was evaporated and then water (20 mL) was added to the residue. The reaction mixture was extracted with DCM (25 mL × 3) and the combined organic layers dried over MgSO$_4$, filtered and evaporated to give **111** as yellow crystals (2.761 g, 48 %). m.p. 203-206 °C; δ_H (400 MHz, CDCl$_3$) 8.07 (2H, d, *J* 7.6 Hz), 7.42 (2H, t, *J* 8.0 Hz), 7.30 (2H, t, *J* 7.6 Hz), 7.08 (2H, d, *J* 8.0 Hz), 6.1-5.9 (2H, bs, NH$_2$); δ_F (376 MHz, CDCl$_3$) 23.18-23.09 (2F, m), 21.64-21.55 (2F, m); GC-MS (EI) *m/z* 358; v_{max} /cm^{-1} (film) 3321 (NH$_2$), 1680 (C=O),

1486, 1477, 1449, 1226, 1154; Analysis (%) calculated for $C_{19}H_{10}F_4N_2O$ (358): C, 63.68; H, 2.79; N, 7.82. Found C, 63.22; H, 2.72; N, 7.87.

3.2.28. Reaction of 3-(pentafluorophenyl)propionamide with carbazole

114
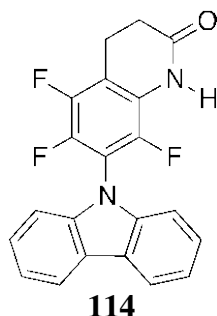
A solution of carbazole (0.167 g, 0.1 mmol) in THF (2mL) was added dropwise to a stirred suspension of NaH (60 % dispersion in mineral oil) (0.008 g, 0.2 mmol) in THF (1 mL) under N_2 and left to stir at RT for 1 h. A solution of 3-(pentafluorophenyl)propionamide (0.025 g, 0.1 mmol) in THF (2 mL) was added dropwise to the reaction mixture and stirred at RT for 24 h. The solvent was evaporated and then water (20 mL) was added to the residue. Orange crystals formed, and were filtered to give **114** (0.023 g, 63 %). m.p. 205-207 °C; δ_H (400 MHz, CDCl$_3$) 8.01 (2H, dd, *J* 7.6 and 0.8 Hz), 7.38-7.32 (m), 7.20-7.15 (m), 5.29-5.27 (1H, bs, NH), 2.98 (2H, t, *J* 8.0 Hz), 2.45 (2H, t, *J* 8.0 Hz) (integral values for the aromatic signals could not be determined accurately); δ_F (376 MHz, CDCl$_3$) 18.73-18.69 (1F, m), 5.36 (1F, t, *J* 21 Hz), -0.11 to -0.25 (1F, m); HRMS (ESI) *m/z* found 365.0912 (M−H)$^-$, $C_{21}H_{12}F_3N_2O$ requires 365.0907; v_{max}/cm^{-1}(film) 3418 (N-H), 1649 (C=O), 1501, 1450, 1335.

3.2.29. Reaction of methyl pentafluorobenzoate with carbazole
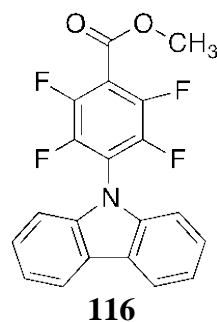
116

A solution of carbazole (0.668 g, 4 mmol) in THF (8mL) was added dropwise to a stirred suspension of NaH (60 % dispersion in mineral oil) (0.369 g, 9 mmol) in THF (4 mL) under N_2 and left to stir at RT for 1 h. A solution of methyl pentafluorobenzoate (1.808 g, 8 mmol) in THF (2 mL) was added dropwise to the reaction mixture and stirred at RT for 24 h. The solvent was evaporated and then water (20 mL) was added to the residue. The reaction mixture was extracted with diethyl ether (25 mL × 3) and the combined organic layers dried over $MgSO_4$, filtered and evaporated to give a yellow oil. Recrystallization from ethanol afforded **116** as white crystals (0.24 g, 16 %). m.p. 148-152 °C; δ_H (400 MHz, $CDCl_3$) 8.05 (2H, d, J 8.0 Hz), 7.40 (2H, td, J 7.6 and 1.2 Hz), 7.29 (2H, t, J 7.2 Hz), 7.08 (2H, d, J 8.0 Hz), 3.99 (3H, s); δ_F (376 MHz, $CDCl_3$) 24.46-24.37 (2F, m), 21.17-21.08 (2F, m); GC-MS (EI) m/z 373; ν_{max} /cm^{-1} (film) 1736 (C=O), 1296 (C-O), 1211, 1157, 1033.
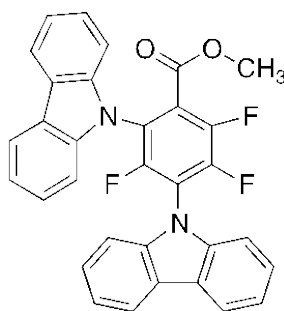
117

A solution of carbazole (0.668 g, 4 mmol) in THF (8mL) was added dropwise to a stirred suspension of NaH (60 % dispersion in mineral oil) (0.72 g, 18 mmol) in THF (4 mL) under N_2 and left to stir at RT for 1 h. A solution of methyl pentafluorobenzoate (1.808 g, 8 mmol) in THF (2 mL) was added dropwise to the reaction mixture under reflux at 66 °C for 24 h. The solvent was evaporated and then water (20 mL) was added to the residue. The reaction mixture was extracted with diethyl ether (25 mL × 3) and the combined organic layers dried over $MgSO_4$, filtered and evaporated to give a yellow oil. White crystals of **117** were afforded after recrystallization from hot ethanol (0.155 g, 15 %). m.p. 179-181 °C; δ_H (400 MHz, $CDCl_3$) 8.06 (4H, t, J 8.0 Hz), 7.45-7.39 (4H, m), 7.31-7.22 (4H, m), 7.18 (4H, d, J 8.0 Hz), 3.26 (3H, s); δ_F (376 MHz, $CDCl_3$) 40.64 (1F, d, J 13 Hz), 29.01 (1F, d, J 22 Hz), 24.57 (1F, dd, J 22 and 13 Hz); HRMS (ESI) m/z found 520.1387, $C_{32}H_{19}F_3N_2O_2$ requires 520.1393; ν_{max} /cm^{-1} (film) 1739 (C=O), 1621, 1475,

1444, 1331, 1227; Analysis (%) calculated for $C_{32}H_{19}F_3N_2O_2$ (520): C, 73.84; H, 3.68; N, 5.38. Found C, 73.00; H, 3.43; N, 5.27.

3.2.30. Reaction of decafluorobiphenyl with carbazole to synthesise the di-carbazole derivative
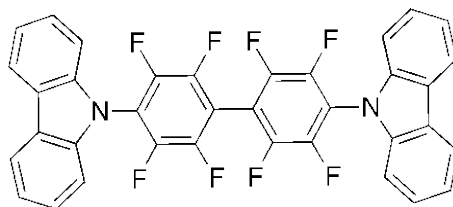
119

A solution of carbazole (1.336 g, 8 mmol) in THF (5mL) and DMF (1 mL) was added dropwise to a stirred suspension of NaH (60 % dispersion in mineral oil) (0.32 g, 8 mmol) in THF (3 mL) under N_2 and left to stir at RT for 1 h. A solution of decafluorobiphenyl (1.336 g, 4 mmol) in THF (2 mL) was added dropwise to the reaction mixture and stirred at RT for 24 h. The solvent was evaporated and then water (20 mL) was added to the residue, white crystals of **119** formed, and were filtered and washed with ethanol (1.913 g, 76 %). m.p. 296-298 °C; δ_H (400 MHz, CDCl$_3$) 8.18 (4H, d, J 7.6 Hz), 7.52 (4H, t, J 8.0 Hz), 7.39 (4H, t, J 7.6 Hz), 7.29 (4H, d, J 8.4 Hz); δ_F (376 MHz, CDCl$_3$) 25.69 (4F, s), 20.90 (4F, s); GC-MS and HRMS could not observed the expected mass of the compound; ν_{max} /cm^{-1} (film) 1625, 1507, 1474, 1257, 1225; Analysis (%) calculated for $C_{36}H_{16}F_8N_2$ (628): C, 68.78; H, 2.54; N, 4.45. Found C, 68.06; H, 2.43; N, 4.33.

3.2.31. Reaction of decafluorobiphenyl with carbazole to synthesise mono-carbazole derivative
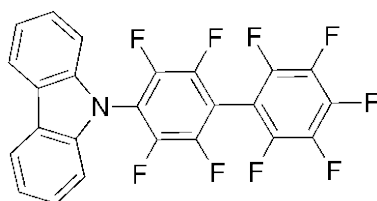
120

A solution of decafluorobiphenyl (2.672 g, 8 mmol) in THF (3mL) was added dropwise to a stirred suspension of NaH (60 % dispersion in mineral oil) (0.64 g, 16 mmol) in THF (2 mL) under N_2. A solution of carbazole (1.336 g, 8 mmol) in THF (4 mL) and DMF (1

mL) was added dropwise to the reaction mixture and left to stir at RT for 24 h. The solvent was evaporated and then water (20 mL) was added to the residue. White crystals formed, and were filtered (4.426 g). Column chromatography purification using light petrol as eluting solvent gave firstly di-carbazole compound **119** (22 %, data identical to the previous), secondly white crystals of **120** (1.114 g, 29 %). m.p. 258-260 °C; δ_H (400 MHz, CDCl$_3$) 8.19 (2H, d, *J* 7.6 Hz), 7.53 (2H, td, *J* 7.2 and 1.2 Hz), 7.41 (2H, td, *J* 7.6 and 1.2 Hz), 7.27 (2H, d, *J* 8.0 Hz); δ_F (376 MHz, CDCl$_3$) 25.36-25.27 (m), 25.05-24.61 (m), 20.81-20.73 (m), 12.55 (1F, t, *J* 23 Hz), 1.94-1.83 (m) (integral values could not be determined accurately); GC-MS and HRMS could not observe the expected mass of the compound; v_{max} / cm^{-1}(film) 1511, 1475, 1332, 1267, 1113, 1066; Analysis (%) calculated for C$_{24}$H$_8$F$_9$N (481): C, 59.89; H, 1.68; N, 2.91. Found C, 59.77; H, 1.61; N, 2.98.
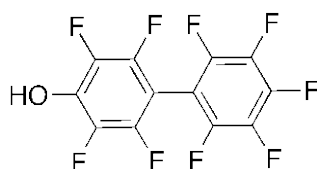
121

Further elution of the column using 9:1 light petrol:diethyl ether as eluting solvent afforded compound **121** as yellow crystals (0.173 g, 7 %). m.p. 218-221 °C; δ_H (400 MHz, DMSO-d$_6$) 9.0-8.6 (1H, bs, OH); δ_F (376 MHz, DMSO-d$_6$) 22.37-22.17 (2F, m), 13.61-13.58 (2F, m), 6.87 (1F, t, *J* 22 Hz), -0.69 to -0.90 (2F, m), -6.48 to -6.84 (2F, m); HRMS (ESI) *m/z* found 330.9813 (M–H)$^-$, C$_{12}$F$_9$O requires 330.9811; v_{max} /cm^{-1}(film) 3000-2450 (O-H), 1638, 1486, 1468, 1088.

3.2.32. Reaction of pentafluorobenzaldehyde with 2,2-(ethylenedioxy)bis(ethylamine)
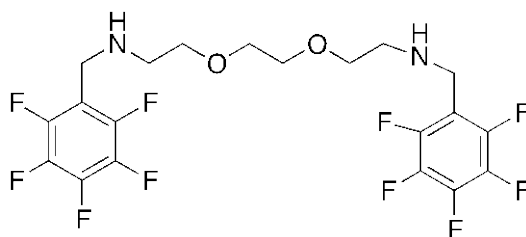
127

A solution of pentafluorobenzaldehyde (7.84 g, 40 mmol) in DCM (5 mL) was added dropwise to a solution of 2,2-(ethylenedioxy)bis(ethylamine) (2.96 g, 20 mmol) in DCM (5 mL) containing $MgSO_4$ (1 g) under N_2 and left to stir at RT for 5 h. $MgSO_4$ was filtered off and washed with DCM and the organic solvent evaporated to afford a yellow oil. A solution of sodium borohydride (1.512 g, 40 mmol) in H_2O (5 mL) and ethanol (10 mL) was added dropwise to the oil and the mixture left to stir at RT for 1 h. The ethanol was evaporated and the residue aqueous mixture was extracted with DCM (25 mL $\times$ 3) and the combined organic layers dried over $MgSO_4$, filtered and evaporated to give **127** as a yellow oil (7.799 g, 77 %). δ_H (400 MHz, $CDCl_3$) 3.89 (4H, s), 3.62-3.50 (8H, m), 2.73 (4H, t, J 5.2 Hz); δ_F (376 MHz, $CDCl_3$) 17.68-17.52 (4F, m), 5.80 (2F, t, J 20 Hz), -0.52 to -0.73 (4F, m), with very minor impurity; HRMS (ESI) m/z found 509.1272 (M+H)$^+$, $C_{20}H_{19}F_{10}N_2O_2$ requires 509.1281; v_{max} /cm^{-1} (film) 3329 (N-H), 2895, 1463, 1301; Analysis (%) calculated for $C_{20}H_{19}F_{10}N_2O_2$ (508): C, 47.25; H, 3.57; N, 5.51. Found C, 47.21; H, 3.77; N, 6.08.

3.2.33. Reaction of carbazole with bis-intercalator scaffold (127)

130
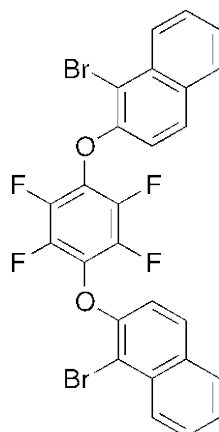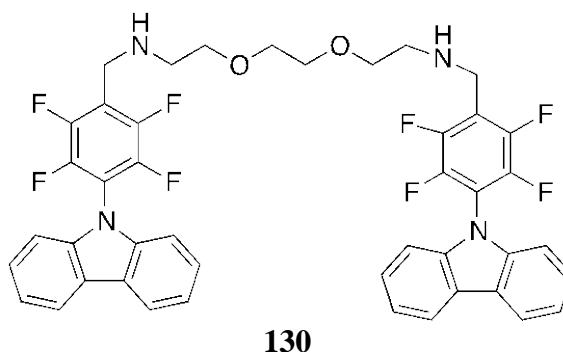
A solution of carbazole (0.334 g, 2 mmol) in THF (5mL) was added dropwise to a stirred suspension of NaH (60 % dispersion in mineral oil) (0.12 g, 3 mmol) in THF (2 mL) under N_2 and left to stir at RT for 1 h. A solution of compound **127** (0.508 g, 1 mmol) in THF (2 mL) was added dropwise to the reaction mixture and stirred at RT for 24 h. The solvent was evaporated and then water (20 mL) was added to the residue. The reaction mixture was extracted with DCM (25 mL $\times$ 3) and the combined organic layers dried over $MgSO_4$, filtered and evaporated to give **130** as a sticky yellow oil (0.776 g). Column chromatography purification using light petrol as eluting solvent afforded yellow crystals (0.018 g). m.p. 238-241 °C; HRMS (ESI) m/z found 803.2627 (M+H)$^+$, $C_{44}H_{35}F_8N_4O_2$

requires 803.2627; ^{1}H and ^{19}F NMR data were not fully consistent with the expected structure and further investigation is still required to characterize the product.

3.2.34. Reaction of mono carbazole derivative (103) with amine chain (125)
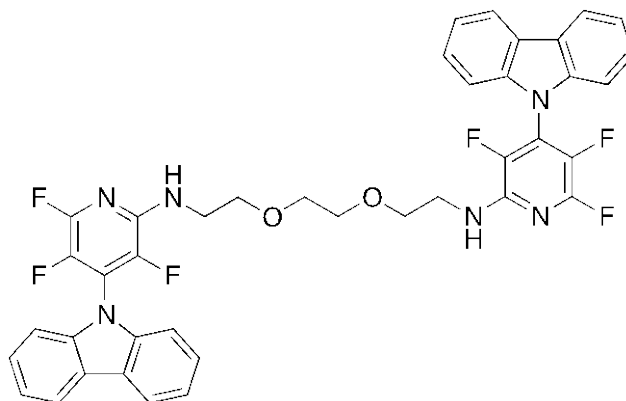
133

A solution of carbazole derivative **103** (0.474 g, 1.5 mmol) in THF (5mL) and DMF (1 mL) was added dropwise under N_2 to a solution of amine chain **125** (0.111 g, 0.7 mmol) and Et_3N (0.227 g, 2.2 mmol) in THF (2 mL) under reflux at 66 °C for 24 h. The solvent was evaporated and then water (20 mL) was added to the residue, creamy crystals were afforded (1.45 g). Column chromatography purification using 1:1 light petrol:diethyl ether as eluting solvent gave **133** as white crystals (0.332 g, 64 %). m.p. 66-73 °C; δ_H (400 MHz, CDCl$_3$) 8.13 (4H, d, *J* 7.6 Hz), 7.45 (4H, td, *J* 7.2 and 1.2 Hz), 7.35 (4H, td, *J* 7.6 and 0.8 Hz), 7.20 (4H, d, *J* 8.0 Hz), 5.22-5.13 (2H, bs, NH), 3.79-3.72 (8H, m), 3.75 (4H, s); δ_F (376 MHz, CDCl$_3$) 70.95-70.78 (m), 15.36-15.24 (m), 1.71-1.63 (m) (integration values would not be determined accurately); HRMS (ESI) *m/z* found 741.2407 (M+H)[+], $C_{40}H_{31}F_6N_6O_2$ requires 741.2407; ν_{max} / cm^{-1}(film) 3407 (N-H), 1509, 1249; elemental analysis was close to the calculated values although the value for the percentage of carbon was high, Analysis (%) calculated for $C_{40}H_{30}F_6N_6O_2$ (740): C, 64.86; H, 4.08; N, 11.35. Found C, 67.52; H, 3.73; N, 11.97.

3.2.35. Reaction of biphenyl carbazole derivative (120) with amine chain (125)
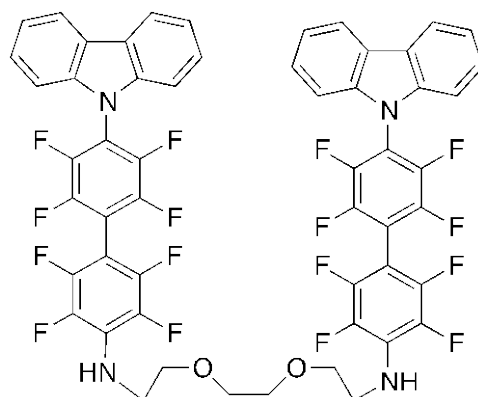
135

A solution of carbazole derivative **120** (0.481 g, 1 mmol) in dioxane (4 mL) was added dropwise under N_2 to a solution of amine chain **125** (0.074 g, 0.5 mmol) and Et_3N (0.151 g, 1.5 mmol) in dioxane (2 mL) under reflux at 101 °C for 24 h. The solvent was evaporated and then water (20 mL) was added to the residue, creamy crystals were afforded and recrystallized from hot ethanol to give **135** (0.500 g, 93 %). m.p. 106-111 °C; δ_H (400 MHz, CDCl$_3$) 8.18 (4H, d, *J* 7.6 Hz), 7.49 (4H, td, *J* 7.2 and 1.2 Hz), 7.38 (4H, td, *J* 8.0 and 0.8 Hz), 7.26 (4H, d, *J* 8.0 Hz), 4.73-4.65 (2H, bs, NH), 3.80-3.72 (8H, m), 3.76 (4H, s); δ_F (376 MHz, CDCl$_3$) 24.86-24.82 (4F, m), 21.13-21.09 (4F, m), 19.42-19.37 (4F, m), 2.06-1.91 (4F, m); The ^{1}H NMR and ^{19}F NMR spectra showed the presence of a minor by-product possibly the mono-arylated amine; HRMS (ESI) *m/z* found 1069.2052 (M–H)$^-$, $C_{54}H_{29}F_{16}N_4O_2$ requires 1069.2041; ν_{max} / cm^{-1}(film) 3428 (N-H), 1511, 1476, 1227, 1130; Analysis (%) calculated for $C_{54}H_{30}F_{16}N_4O_2$ (1070): C, 60.57; H, 2.82; N, 5.23. Found C, 59.10; H, 2.56; N, 4.66.

3.2.36. Reaction of bis-carbazole derivative with ethoxide

140   **141**   **142**
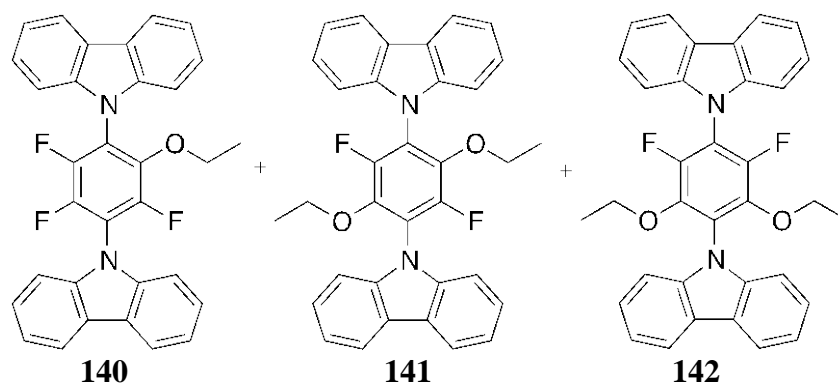
A solution of ethanol (0.092 g, 2 mmol) in THF (2mL) was added dropwise to a stirred suspension of NaH (60 % dispersion in mineral oil) (0.08 g, 2 mmol) in THF (2 mL) under N_2 and left to stir at RT for 1 h. A solution of carbazole derivative **100** (0.48 g, 1 mmol) in THF (5 mL) and DMF (1 mL) was added dropwise to the reaction mixture and stirred under reflux at 66 °C for 24 h. The solvent was evaporated and then water (20 mL) was added to the residue. The reaction mixture was extracted with diethyl ether (25 mL × 3) and the combined organic layers dried over $MgSO_4$, filtered and evaporated to give sticky creamy crystals. Recrystallization from ethanol afforded white crystals of a mixture of compounds **140**, **141** and **142** in ratio 8.3:1.25:1 with **140** being the major component (0.221 g). δ_H (400 MHz, CDCl$_3$) 8.12 (d, *J* 7.6 Hz), 7.49-7.42 (m), 7.36-7.28 (m), 7.25 (d, *J* 8.4 Hz), 3.69-3.65 (m), 0.77 (t, *J* 7.2 Hz), small multiplets were observed at 7.7 and 7.04 which could be due to the minor components **141** and **142** (integral values could not determined accurately).

Compound **140**, δ_F (376 MHz, CDCl$_3$) 26.59 (1F, d, *J* 10 Hz), 19.34 (1F, dd, *J* 23 and 10 Hz), 18.64 (1F, d, *J* 23 Hz); GC-MS (EI) *m/z* 506.

Compounds **141** and **142**, δ_F (376 MHz, CDCl$_3$) 25.24 (2F, s), 25.08 (2F, s); GC-MS (EI) *m/z* 532 and a signal at 21.0 suggested some starting **100** was present (*m/z* 480).

3.2.37. Reaction of isoquinoline with ethyl bromoacetate[94]

150
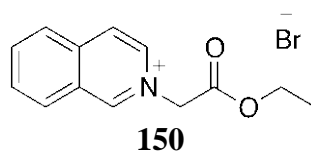
A solution of isoquinoline (0.97 g, 7.5 mmol) in ethyl acetate (2 mL) was added dropwise under N_2 to a solution of ethyl bromoacetate (0.835 g, 5 mmol) in ethyl acetate (2 mL) under reflux at 77 °C for 24 h. After 24 h refluxing **150** was afforded as yellow crystals and filtered (1.076 g, 73 %). m.p. 199-201 °C (lit., 199-201 °C);[101] δ_H (400 MHz, DMSO-d$_6$) 10.08 (1H, s), 8.78 (1H, dd, *J* 6.8 and 1.2 Hz), 8.68 (1H, d, *J* 6.8 Hz), 8.56 (1H, d, *J* 8.0 Hz), 8.42 (1H, d, *J* 8.0 Hz), 8.34 (1H, td, *J* 6.8 and 0.8 Hz), 8.13 (1H, td, *J* 8.0 and 0.8 Hz), 5.81 (2H, s), 4.28 (2H, q, *J* 7.2 Hz), 1.28 (3H, t, *J* 7.2 Hz); δ_C (100 MHz, DMSO-d$_6$) 165.60 (C=O), 150.81 (CH), 136.78 (CH), 136.33 (Cq), 135.22 (CH), 130.57 (CH), 129.74 (CH), 126.46 (CH), 125.77 (Cq), 124.53 (CH), 61.42 (CH$_2$), 59.25 (CH$_2$), 13.01

(CH$_3$). HRMS (ESI) m/z found 216.1015, C$_{13}$H$_{14}$NO$_2$ requires 216.1019; v_{max} / cm^{-1} (film) 2918, 1740 (C=O), 1470, 1225. Data in agreement with literature values.

3.3. Biological activity studies

3.3.1. DNA thermal denaturation assay

Trisma base buffer 2.5×10^{-3} M with pH 7.55 was prepared by dissolving 2-amino-2-(hydroxymethyl)-1,3-propanediol (0.30 g) in water (500 mL).

The stock solution of ACTD (1 mg/mL) was prepared by dissolving ACTD (5 mg) in DMSO (5 mL). The working solution of ACTD was prepared by dissolving ACTD stock solution (400 μL) in trisma base buffer (4 mL).

Ethylenediaminetetraacetic acid (EDTA) 10^{-2} M was prepared by dissolving solid EDTA (0.15 g) in distilled water (40 mL). EDTA solution 1.5×10^{-3} M was prepared by dissolving EDTA 10^{-2} M (1.5 mL) in distilled water (8.5 mL).

With the purpose of preparation 450 μg/mL DNA concentration of double strand calf thymus DNA a solution of DNA (0.01 g) in trisma base buffer (22.22 mL) was prepared and mixed thoroughly to allow DNA to dissolve in the solution. The solution transferred into small Eppendorf tubes and each tube contained (0.5 mL) and stored at -80 °C.

The stock solutions of the synthesised fluorinated compounds at a concentration of 10^{-2} M were prepared in DMSO.

The samples prepared according to table 3 were sealed in 3000 μL quartz cells and monitored at 260 nm on a UV- visible spectrophotometer. The thermal denaturation was followed between 50 °C and 90 °C.

Table 3. Preparation of DNA-compound complex samples for UV absorption to investigate *Tm* values

DNA without the synthesised fluorinated compound	DNA with the synthesised fluorinated compound
DMSO 70 μL	DMSO 70 μL
EDTA 100 μL	EDTA 100 μL
DNA 100 μL	DNA 100 μL
Buffer 2.7 mL	Buffer 2.7 mL
DMSO 30 μL	Fluorinated compound 30 μL

3.3.2. UV-visible absorption spectroscopy

Salmon sperm DNA (SS-DNA) (15 mg) was dissolved in distilled water (20 mL) pH 7.0 and stirred overnight and kept at 4 °C. Trisma base buffer 2.5×10^{-3} M with pH 7.55 was prepared by dissolving (0.30 g) in water (500 mL). A solution of SS-DNA in the buffer gave a ratio of UV absorbance at 260 and 280 nm (A_{260} / A_{280}) of 1.9, indicating that the DNA was sufficiently free of protein. The DNA concentration was determined via absorption spectroscopy using the molar absorption coefficient of 6600 $M^{-1}cm^{-1}$ (260 nm) for SS-DNA[102] and was found to be 1.5×10^{-4} M. The compounds were dissolved in DMSO at a concentration of 10^{-2} M and the UV absorption titration were performed by keeping the concentration of the test compound fixed while varying the SS-DNA concentration. Compound-DNA solutions were allowed to incubate for 30 min at room temperature before measurements were made. Absorption spectra were recorded using cuvettes of 1 cm path length at room temperature (25 ± 1°C).

3.3.3. Fluorescence spectroscopy

EB solution (0.3 mL) at a concentration of 1×10^{-6} in trisma base buffer was added to SS-DNA (0.3 mL) solution and then aliquots of each test compound solution (30, 60, 120, 180, 240, 300 μL of 10^{-6} M) was titrated into DNA/EB mixture. Each mixture was diluted up to 3 mL with trisma buffer, making the solution with varied concentrations of (1×10^{-6}, 2×10^{-6}, 4×10^{-6}, 6×10^{-6}, 8×10^{-6} and 1×10^{-5} M) each compound to SS-DNA. The mixtures was shaken and incubated at room temperature for 30 min. The fluorescence spectra of EB bound to SS-DNA were measured at an emission wavelength of 605 nm with excitation at 480 nm.

3.3.4. Hanging drop DNA crystallization method

Commercial cacodylate buffer, pH 6.5 was used; 50 mM isopropanol 15 % was used to prepare a stock buffer solution containing $MgCl_2$ (10 mM) by adding $MgCl_2$ (9 mg) to cacodylate buffer (10 mL). DNA solution (0.5 mM) was prepared by adding (600 μL) of buffer stock solution to the synthetic oligonucleotide CGCGAATTCGCG vial, which contained 314 nmol.

The synthesised fluorinated organic compounds were prepared in concentration (0.01 mol) in DMSO.

In hanging drop DNA crystallization method a 24-well multiwell plate, with low evaporation lid, were used. In order to set some drops on the lid of the plate for crystallization, DNA solution (20 µL) was added to the compound solution (2 µL). Dehydrating brine solution was placed in the wells under the drops; the plates left at RT or in the refrigerator until the drops dried or some crystals appeared and become ready for X-ray analysis.

3.3.5. Antimicrobial activity studies

The synthesised compounds at 10^{-2} M concentration were tested against two bacterial strains Gram-positive strain (*Escherichia coli*) and Gram-negative strain (*Staphylococcus aureus*) The disk diffusion method was used for the determination of antibacterial activity. The bacteria (100 µL) were added to *Muller-Hinton* agar media (25 mL), mixed well and poured into 90×14 mm petri plate (diameter and height respectively) and the media was allowed to solidify. Sterilized disks (6 mm in diameter) were saturated with the compound solution and placed gently on the inoculated agar plates. Each plate contained a blank disk, which was saturated with DMSO, the compound-containing disk and a control disk containing the known antibiotic ACTD. The petri plates were incubated at 37 °C for 48 h.

4. References

1. M. Cartwright, E. Parks, G. Pattison, R. Slater, G. Sandford, I. Wilson, D. Yufit, J. Howard, J. Christopher, and D. Miller, *Tetrahedron*, 2010, **66**, 3222–3227.

2. H. Jiang, W. Yue, X. Xuihong, and S. Zhu, *Tetrahedron*, 2007, **63**, 2315–2319.

3. W. Dolbier jr, *J. Fluorine Chem.*, 2005, **126**, 157–163.

4. K. Müller, C. Faeh, and F. Diederich, *Science*, 2007, **317**, 1881–1886.

5. L. Yagupolskii, *J. Fluorine Chem.*, 1995, **72**, 225–229.

6. M. Cartwright, L. Convery, T. Kraynck, G. Sandford, D. Yufit, J. Howard, J. Christopher, and D. Miller, *Tetrahedron*, 2010, **66**, 519–529.

7. E. Luzina and A. Popov, *Eur. J. Med. Chem.*, 2009, **44**, 4944–4953.

8. D. O'Hagan, *J. Fluorine Chem.*, 2010, **131**, 1071–1081.

9. R. Ko, J. Chu, and P. Chiu, *Tetrahedron*, 2011, **67**, 2542–2547.

10. J. Bégué and D. Bonnet-Delpon, *J. Fluorine Chem.*, 2006, **127**, 992–1012.

11. C. Isanbor and D. O'Hagan, *J. Fluorine Chem.*, 2006, **127**, 303–319.

12. A. Tressaud and G. Haufe, *Fluorine and Health Molecular Imaging, Biomedical Materials and Pharmaceuticals.*, Elsevier, Oxford, 2008.

13. A. Gakh and M. Burnett, *J. Fluorine Chem.*, 2011, **132**, 88–93.

14. K. Kirk, *J. Fluorine Chem.*, 2006, **127**, 1013–1029.

15. B. Smart, *J. Fluorine Chem.*, 2001, **109**, 3–11.

16. http://www.wiredchemist.com/chemistry/data/bond_energies_lengths.html (Date:8-8-2014)

17. http://www.webelements.com/periodicity/van_der_waals_radius (Date:8-8-2014)

18. P. Liu, A. Sharon, and C. Chu, *J. Fluorine Chem.*, 2008, **129**, 743–766.

19. K. Sakthivel and P. Cook, *Tetrahedron Lett.*, 2005, **46**, 3883–3887.

20. O. Fadeyi, S. Adamson, E. Myles, and C. Okoro, *Bioorg. Med. Chem. Lett.*, 2008, **18**, 4172–4176.

21. R. D. Chambers, *Fluorine in Organic Chemistry*, Blackwell, Durham, 2004.

22. G. Brooke, *J. Fluorine Chem.*, 1997, **87**, 1–76.

23. L. Markovskii, G. Furin, Y. Shermolovich, and G. Yakobson, *Izv. Akad. Nauk SSSR, Ser. Khim*, 1981, 867–869.

24. L. Wall, W. Pummer, J. Fearn, and J. Antonucci, *J. Res. Natl. Bur. Stand.,Sect. A*, 1963, **67**, 481–497.

25. M. Bellas, H. Price, and H. Suschitzky, *J. Chem. Soc. C*, 1967, 1249–1254.

26. P. Robson, M. Stacey, R. Stephens, and J. Tatlow, *J. Chem. Soc.*, 1960, 4754–4760.

27. J. Birchall and R. Haszeldine, *J. Chem. Soc.*, 1961, 3719–3727.

28. R. D. Chambers, M. Seabury, D. Williams, and N. Hughes, *J. Chem. Soc., Perkin Trans.1*, 1988, 255–257.

29. R. D. Chambers, M. Seabury, D. Williams, and N. Hughes, *J. Chem. Soc., Perkin Trans. 1*, 1988, 251–254.

30. L. Kobrina, G. Furin, and G. Yakobson, *Zh. Org. Khim*, 1970, **6**, 512-520.

31. J. Gonzalez, M. Edgar, M. Elsegood, and G. Weaver, *Org. Biomol. Chem.*, 2011, **9**, 2294–2305.

32. T. Gerasimova and N. Orlova, *J. Fluorine Chem.*, 1985, **28**, 361–380.

33. G. Sandford, R. Slater, D. Yufit, J. Howard, and A. Vong, *J. Org. Chem.*, 2005, **70**, 7208–7216.

34. A. Baron, G. Sandford, R. Slater, D. Yufit, J. Howard, and A. Vong, *Org. Chem.*, 2005, **70**, 9377–9381.

35. R. D. Chambers, J. Hutchinson, and W. Musgrave, *J. Chem. Soc. C*, 1964, 3736–3739.

36. R. Banks, J. Burgess, W. Cheng, and R. Haszeldine, *J. Chem. Soc.*, 1965, 575–581.

37. M. Cartwright, G. Sandford, J. Bousbaa, D. Yufit, J. Howard, J. Christopher, and D. Miller, *Tetrahedron*, 2007, **63**, 7027–7035.

38. X. Li, Y. Lin, Q. Wang, Y. Yuan, H. Zhang, and X. Qian, *Eur. J. Med. Chem.*, 2011, **46**, 1274–1279.

39. O. Kennard and W. Hunter, *Angew. Chemie Int. Ed. English*, 1991, **30**, 1254–1277.

40. O. Kennard, *Pure&Appl.Chem*, 1993, **65**, 1213–1222.

41. R. Wartell and A. Benight, *Phys. Rep.*, 1985, **126**, 67–107.

42. J. Watson and F. Crick, *Nature*, 1953, **171**, 737–738.

43. http://bio3400.nicerweb.com/Locked/media/ch01_08-DNA_double_helix.jpg (Date:1-2-2014).

44. G. Lenglet and M. David-Cordonnier, *J. Nucleic Acids*, 2010, **2010**, 1–17.

45. C. Qiao, S. Bi, Y. Sun, D. Song, H. Zhang, and W. Zhou, *Spectrochim. Acta. A. Mol. Biomol. Spectrosc.*, 2008, **70**, 136–143.

46. R. Martínez and L. Chacón-García, *Curr. Med. Chem.*, 2005, **12**, 127–151.

47. M. Sirajuddin, S. Ali, and A. Badshah, *J. phtochemistry Photobiol. B Biol.*, 2013, **124**, 1–19.

48. J. Zhao, W. Li, R. Ma, S. Chen, S. Ren, and T. Jiang, *Int. J. Mol. Sci.*, 2013, **14**, 16851–16865.

49. A. Rescifina, C. Zagni, M. Varrica, V. Pistarà, and A. Corsaro, *Eur. J. Med. Chem.*, 2014, **74**, 95–115.

50. A. Fabien, B. Tinant, E. Henon, D. Carrez, A. Croisy, and S. Bouquillon, *Dalt. Trans.*, 2010, **39**, 8982–8993.

51. A. Pizarro and P. Sadler, *Biochimie*, 2009, **91**, 1198–1211.

52. H. Setiyanto, V. Saraswaty, R. Hertadi, I. Noviandri, and B. Buchari, *Int. J. Electrochem. Sci.*, 2011, **6**, 2090–2100.

53. E. Pazos, J. Mosquera, M. Vázquez, and J. Mascareñas, *Chem. biochem.*, 2011, **12**, 1958–1973.

54. R. Palchaudhuri and P. Hergenrother, *Curr. Opin. Biotechnol.*, 2007, **18**, 497–503.

55. L. Marky and K. Breslauer, *Biochemistry-us.* 1987, **84**, 4359–4363.

56. C. Kelly, H. Hill, L. Bartolotti, and S. Varadarajan, *J. Mol. Struct. Theochem.*, 2009, **894**, 50–58.

57. M. Cory, D. Mckee, J. Kagan, D. Henry, and J. Milled, *J. Am. Chem. Soc.*, 1985, **107**, 2528–2536.

58. X. Li, Q. Wang, Y. Qing, Y. Lin, Y. Zhang, X. Qian, and J. Cui, *Bioorg. Med. Chem.*, 2010, **18**, 3279–3284.

59. D. Wolf, J. Rauch, M. Hausmann, and C. Cremer, *Biophys. Chem.*, 1999, **81**, 207–221.

60. H. Yang, Y. Zhuo, and X. Wu, *J. Phys. A: Math. Gen.*, 1994, **27**, 6147–6156.

61.   R. Wheelhouse and J. Chaires, *Methods. Mol. Biol.*, 2010, **613**, 55–70.

62.   A. Ducruix and R. Giege, *Crystallization of Nucleic Acids and Proteins a Pratical Approach*, Oxford, 1992.

63.   J. Jaumot and R. Gargallo, *Curr. Pharm. Des.*, 2012, **18**, 1900–1916.

64.   J. R. Lakowicz, *Principles of Fluorescence Spectroscopy*, Springer, Maryland, USA, third., 2006.

65.   W. Li, J. Xu, X. Guo, Q. Zhu, and Y. Zhao, *Spectrochim. Acta. Part A*, 1997, **1425**, 781–787.

66.   C. Kumart and R. Turner, *J. Photochem. photobiol.A:chem.*, 1993, **74**, 231–238.

67.   A. O'Neill and I. Chopra, *Expert Opin. Investig. Drugs*, 2004, **13**, 1045–1063.

68.   I. Galani, F. Kontopidou, M. Souli, P. Rekatsina, E. Koratzanis, J. Deliolanis, and H. Giamarellou, *Int. J. Antimicrob. Agents*, 2008, **31**, 434–439.

69.   EUCAST European committee on antimicrobial susceptibility testing European society of clinical microbiology and infectionus diseases, EUCAST diffusion method for antimicrobial susceptibility testing-version 3.0 (April 2013).

70.   M. Sirajuddin, S. Ali, N. Ali, M. Rashid, and M. Nawaz, *Spectrochem. Acta Part A Mol. Biomol. Spectrosc.*, 2012, **94**, 134–142.

71.   X. Guo and G. Liu, *Chinese Chem. Lett.*, 2013, **24**, 295–298.

72.   N. Ono, *The Nitro Group in Organic Synthesis*, Wiley-VCH, New York, 2001.

73.   K. Prakash and R. Nagarajan, *Tetrahedron Lett.*, 2013, **54**, 3635–3638.

74.   A. Núñez, A. Sánchez, C. Burgos, and J. Alvarez-Builla, *Tetrahedron*, 2007, **63**, 6774–6783.

75.   D. Ferraris, Y. Ko, T. Pahutski, R. Ficco, L. Serdyuk, C. Alemu, C. Bradford, T. Chiou, R. Hoover, S. Huang, S. Lautar, S. Liang, Q. Lin, M. Lu, M. Mooney, L. Morgan, Y. Qian, S. Tran, L. Williams, Q. Wu, J. Zhang, Y. Zou, and V. Kalish, *J. Med. Chem.*, 2003, **46**, 3138–3151.

76.   F. Bellezza, A. Cipiciani, R. Ruzziconi, and S. Spizzichino, *J. Fluorine Chem.*, 2008, **129**, 97–107.

77.   R. Smith and H. Suschitzky, *Tetrahedron*, 1961, **16**, 80–84.

78.   F. de Sa' Alves, E. Barreiro, and C. Fraga, *Mini Rev. Med. Chem*, 2009, **9**, 782–793.

79.   K. Dawood, T. Eldebss, H. El-Zahabi, M. Yousef, and P. Metz, *Eur. J. Med. Chem.*, 2013, **70**, 740–749.

80.   N. Desai, V. Joshi, K. Rajpara, H. Vaghani, and H. Satodiya, *J. Fluorine Chem.*, 2012, **142**, 67–78.

81.   B. Ashalatha, B. Narayana, K. Vijaya Raj, and N. Suchetha Kumari, *Eur. J. Med. Chem.*, 2007, **42**, 719–728.

82.   C. Comoy, E. Banaszak, and Y. Fort, *Tetrahedron*, 2006, **62**, 6036–6041.

83.   M. Bazin, L. Bodero, C. Tomasoni, B. Rousseau, C. Roussakis, and P. Marchand, *Eur. J. Med. Chem.*, 2013, **69**, 823–832.

84.   L. Mitchell and N. Barvian, *Tetrahedron Lett.*, 2004, **45**, 5669–5671.

85.   S. Dayan, F. Arslan, N. Kayacı, and N. Kalaycioglu, *Spectrochim. Acta. A. Mol. Biomol. Spectrosc.*, 2014, **120**, 167–175.

86.   S. Nakano, K. Takai, Y. Isaka, S. Takahashi, Y. Unno, N. Ogo, K. Matsuno, O. Takikawa, and A. Asai, *Biochem. Biophys. Res. Commun.*, 2012, **419**, 556–561.

87.   Z. Kaplancikli, *Marmara Pharm. J.*, 2011, **15**, 105–109.

88.   S. Tu, C. Ding, W. Hu, F. Li, Q. Yao, and A. Zhang, *Mol. Divers.*, 2011, **15**, 91–99.

89.   F. Zhang, L. Gan, and C. Zhou, *Bioorg. Med. Chem. Lett.*, 2010, **20**, 1881–1884.

90.   D. Zhu, M. Chen, M. Li, B. Luo, Y. Zhao, P. Huang, F. Xue, S. Rapposelli, R. Pi, and S. Wen, *Eur. J. Med. Chem.*, 2013, **68**, 81–88.

91.   W. Fröhner, K. Reddy, and H. Knölker, *Eur. J. Org. Chem.*, 2012, **2012**, 330–342.

92.   C. Frederick, L. Williams, G. Ughetto, I. Van Der Mare, J. Van Boom, A. Rich, and A. Wang, *Biochemistry-us*, 1990, **29**, 2538–2549.

93.   R. Szabó, Z. Bánóczi, G. Mezo, O. Láng, L. Kohidai, and F. Hudecz, *Biochim. Biophys. Acta*, 2010, **1798**, 2209–2216.

94.   F. Kröhnke, *Angew. Chem*, 1963, **75**, 317-329.

95.   F. Chen, F. Sha, K. Chin, and S. Chou, *Biophys. J.*, 2003, **84**, 432–439.

96.   H. Yoo and R. Rill, *J. Biochem. Mol. Biol.*, 2003, **36**, 305–311.

97.   M. Vives, R. Tauler, R. Eritja, and R. Gargallo, *Anal. Bioanal. Chem.*, 2007, **387**, 311–320.

98. M. Tariq, N. Muhammad, M. Sirajuddin, S. Ali, N. Shah, N. Khalid, M. Tahir, and M. Khan, *J. Organomet. Chem.*, 2013, **723**, 79–89.

99. H. Drew, R. Wing, T. Takano, C. Broka, S. Tanaka, K. Itakura, and R. Dickerson, *Biochemistry-us*, 1981, **78**, 2179–2183.

100. M. Sirajuddin, S. Ali, A. Haider, N. Shah, A. Shah, and M. Khan, *Polyhedron*, 2012, **40**, 19–31.

101. A. Katritzky, N. Grzeskowiak, and J. Alvarez-Builla, *J. Chem. soc.*, 1981, **1**, 1180–1185.

102. F. Shah, M. Sirajuddin, S. Ali, S. Abbas, M. Tahir, and C. Rizzoli, *Inorg. Chem. Acta*, 2013, **400**, 159–168.

Appendix

5. Appendix

5.1. X-ray crystallography data

5.1.1. Compound 57 X-ray crystal structure data
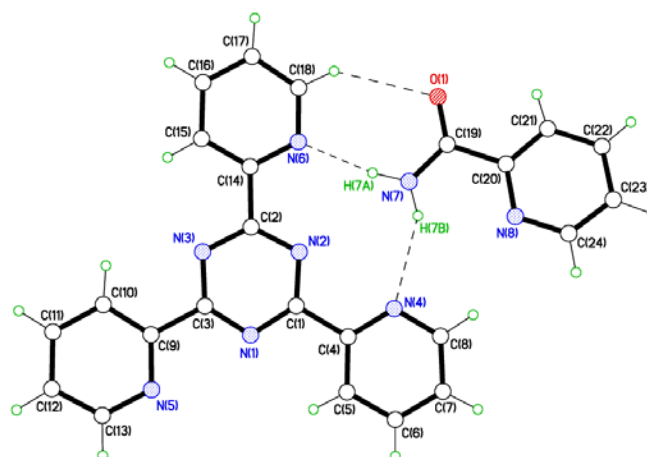
Table 1. Crystal data and structure refinement for gwals1.

Identification code	gwals1
Chemical formula	$C_{24}H_{18}N_8O$
Formula weight	434.46
Temperature	150(2) K
Radiation, wavelength	synchrotron, 0.7749 Å
Crystal system, space group	orthorhombic, Pbca
Unit cell parameters	a = 7.3663(10) Å $\langle$ = 90°
	b = 19.902(3) Å ® = 90°
	c = 27.418(4) Å © = 90°
Cell volume	4019.6(10) Å^3
Z	8
Calculated density	1.436 g/cm^3
Absorption coefficient $\lceil$	0.113 mm^1
F(000)	1808
Crystal colour and size	colourless, 0.25 0.02 0.02 mm^3
Reflections for cell refinement	5536 ($\lfloor$range 3.24 to 29.88°)
Data collection method	Bruker APEX 2 CCD diffractometer
	$\lceil$rotation with narrow frames
$\lfloor$range for data collection	3.24 to 30.23°
Index ranges	h 9 to 9, k 25 to 25, l 35 to 35
Completeness to $\lfloor$ = 30.23°	99.4 %
Intensity decay	0%

Reflections collected	45021		
Independent reflections	4596 (R_{int} = 0.0975)		
Reflections with $F^2 > 2\sigma$	3471		
Absorption correction	semi-empirical from equivalents		
Min. and max. transmission	0.972 and 0.998		
Structure solution	direct methods		
Refinement method	Full-matrix least-squares on F^2		
Weighting parameters a, b	0.0334, 1.1084		
Data / restraints / parameters	4596 / 0 / 370		
Final R indices [$F^2 > 2\sigma$]	R1 = 0.0472, wR2 = 0.1191		
R indices (all data)	R1 = 0.0649, wR2 = 0.1321		
Goodness-of-fit on F^2	1.031		
Largest and mean shift/su	0.001 and 0.000		
Largest diff. peak and hole	0.263 and 0.195 e $Å^3$		

Table 2. Atomic coordinates and equivalent isotropic displacement parameters ($Å^2$) for gwals1. U_{eq} is defined as one third of the trace of the orthogonalized U^{ij} tensor.

	x	y	z	U_{eq}
N(1)	0.73160(17)	0.43676(6)	0.74713(4)	0.0246(3)
C(1)	0.69099(19)	0.40316(7)	0.70633(5)	0.0231(3)
N(2)	0.62401(16)	0.34107(6)	0.70407(4)	0.0246(3)
C(2)	0.59711(19)	0.31225(7)	0.74751(5)	0.0227(3)
N(3)	0.62790(16)	0.34141(6)	0.79061(4)	0.0249(3)
C(3)	0.69554(19)	0.40361(7)	0.78827(5)	0.0231(3)
C(4)	0.72419(19)	0.43943(7)	0.65933(5)	0.0240(3)
C(5)	0.8081(2)	0.50186(7)	0.65956(5)	0.0268(3)
C(6)	0.8361(2)	0.53435(7)	0.61555(6)	0.0306(3)
C(7)	0.7807(2)	0.50312(7)	0.57323(6)	0.0317(3)
C(8)	0.6974(2)	0.44093(8)	0.57647(6)	0.0321(3)
N(4)	0.66935(17)	0.40856(6)	0.61850(4)	0.0279(3)
C(9)	0.72763(19)	0.43743(7)	0.83602(5)	0.0243(3)
C(10)	0.6975(2)	0.40240(7)	0.87889(5)	0.0292(3)
C(11)	0.7191(2)	0.43546(8)	0.92276(6)	0.0346(4)
C(12)	0.7693(2)	0.50211(8)	0.92246(6)	0.0330(3)
C(13)	0.8010(2)	0.53256(8)	0.87787(6)	0.0316(3)
N(5)	0.78175(17)	0.50183(6)	0.83484(4)	0.0287(3)
C(14)	0.52692(19)	0.24224(7)	0.74889(5)	0.0234(3)
C(15)	0.5004(2)	0.20940(8)	0.79265(5)	0.0318(3)
C(16)	0.4361(2)	0.14401(8)	0.79186(6)	0.0340(4)
C(17)	0.4006(2)	0.11371(7)	0.74802(5)	0.0285(3)
C(18)	0.4300(2)	0.15048(7)	0.70596(5)	0.0302(3)
N(6)	0.49213(18)	0.21340(6)	0.70581(4)	0.0270(3)
N(7)	0.4801(2)	0.26725(7)	0.60734(5)	0.0352(3)
C(19)	0.4457(2)	0.22246(7)	0.57309(6)	0.0297(3)
O(1)	0.41757(17)	0.16238(5)	0.58066(4)	0.0401(3)
C(20)	0.4403(2)	0.24883(7)	0.52151(5)	0.0279(3)
C(21)	0.4153(2)	0.20453(8)	0.48329(6)	0.0345(4)

C(22)	0.4048(2)	0.22959(9)	0.43644(6)	0.0400(4)
C(23)	0.4205(3)	0.29753(9)	0.42961(6)	0.0411(4)
C(24)	0.4487(3)	0.33805(8)	0.46970(6)	0.0378(4)
N(8)	0.45801(19)	0.31518(6)	0.51525(5)	0.0327(3)

Table 3.   Bond lengths [Å] and angles [°] for gwals1.

N(1)–C(3)	1.3336(17)	N(1)–C(1)	1.3373(17)
C(1)–N(2)	1.3320(17)	C(1)–C(4)	1.4970(19)
N(2)–C(2)	1.3365(17)	C(2)–N(3)	1.3359(17)
C(2)–C(14)	1.4867(19)	N(3)–C(3)	1.3360(17)
C(3)–C(9)	1.4911(19)	C(4)–N(4)	1.3394(18)
C(4)–C(5)	1.3878(19)	C(5)–C(6)	1.385(2)
C(6)–C(7)	1.378(2)	C(7)–C(8)	1.384(2)
C(8)–N(4)	1.3362(19)	C(9)–N(5)	1.3425(17)
C(9)–C(10)	1.384(2)	C(10)–C(11)	1.380(2)
C(11)–C(12)	1.377(2)	C(12)–C(13)	1.384(2)
C(13)–N(5)	1.3366(19)	C(14)–N(6)	1.3380(18)
C(14)–C(15)	1.380(2)	C(15)–C(16)	1.385(2)
C(16)–C(17)	1.370(2)	C(17)–C(18)	1.383(2)
C(18)–N(6)	1.3333(18)	N(7)–C(19)	1.319(2)
C(19)–O(1)	1.2313(17)	C(19)–C(20)	1.509(2)
C(20)–N(8)	1.3380(19)	C(20)–C(21)	1.382(2)
C(21)–C(22)	1.380(2)	C(22)–C(23)	1.370(2)
C(23)–C(24)	1.379(2)	C(24)–N(8)	1.331(2)

C(3)–N(1)–C(1)	114.56(12)	N(2)–C(1)–N(1)	125.85(12)
N(2)–C(1)–C(4)	117.90(12)	N(1)–C(1)–C(4)	116.25(12)
C(1)–N(2)–C(2)	114.31(12)	N(3)–C(2)–N(2)	125.22(13)
N(3)–C(2)–C(14)	116.34(12)	N(2)–C(2)–C(14)	118.45(12)
C(2)–N(3)–C(3)	115.04(12)	N(1)–C(3)–N(3)	124.99(12)
N(1)–C(3)–C(9)	119.20(12)	N(3)–C(3)–C(9)	115.80(12)
N(4)–C(4)–C(5)	123.29(13)	N(4)–C(4)–C(1)	116.68(12)
C(5)–C(4)–C(1)	120.03(12)	C(6)–C(5)–C(4)	118.72(14)
C(7)–C(6)–C(5)	118.62(14)	C(6)–C(7)–C(8)	118.72(14)
N(4)–C(8)–C(7)	123.70(14)	C(8)–N(4)–C(4)	116.94(13)
N(5)–C(9)–C(10)	123.29(13)	N(5)–C(9)–C(3)	117.18(12)
C(10)–C(9)–C(3)	119.52(12)	C(11)–C(10)–C(9)	118.77(14)
C(12)–C(11)–C(10)	119.01(14)	C(11)–C(12)–C(13)	118.18(14)
N(5)–C(13)–C(12)	124.15(14)	C(13)–N(5)–C(9)	116.55(13)
N(6)–C(14)–C(15)	122.49(13)	N(6)–C(14)–C(2)	116.50(12)
C(15)–C(14)–C(2)	121.01(12)	C(14)–C(15)–C(16)	118.67(14)
C(17)–C(16)–C(15)	119.50(14)	C(16)–C(17)–C(18)	117.96(14)
N(6)–C(18)–C(17)	123.60(13)	C(18)–N(6)–C(14)	117.77(12)
O(1)–C(19)–N(7)	124.65(15)	O(1)–C(19)–C(20)	119.42(13)
N(7)–C(19)–C(20)	115.93(13)	N(8)–C(20)–C(21)	123.04(14)
N(8)–C(20)–C(19)	117.44(12)	C(21)–C(20)–C(19)	119.51(13)
C(22)–C(21)–C(20)	118.87(15)	C(23)–C(22)–C(21)	118.63(15)
C(22)–C(23)–C(24)	118.75(15)	N(8)–C(24)–C(23)	123.76(15)
C(24)–N(8)–C(20)	116.93(13)		

Table 4.   Hydrogen coordinates and isotropic displacement parameters (Å^2) for gwals1.

	x	y	z	U
H(5)	0.846(2)	0.5207(9)	0.6896(7)	0.042(5)
H(6)	0.894(2)	0.5763(8)	0.6148(6)	0.030(4)
H(7)	0.796(2)	0.5244(9)	0.5416(7)	0.039(5)
H(8)	0.656(2)	0.4174(8)	0.5479(7)	0.038(5)
H(10)	0.665(2)	0.3558(9)	0.8774(6)	0.042(5)
H(11)	0.695(3)	0.4112(9)	0.9530(7)	0.049(5)
H(12)	0.783(3)	0.5274(9)	0.9525(7)	0.046(5)
H(13)	0.836(2)	0.5795(8)	0.8767(6)	0.030(4)
H(15)	0.524(3)	0.2317(9)	0.8228(8)	0.046(5)
H(16)	0.420(3)	0.1201(9)	0.8223(7)	0.046(5)
H(17)	0.356(2)	0.0690(9)	0.7458(5)	0.033(5)
H(18)	0.404(2)	0.1316(9)	0.6742(7)	0.036(5)
H(7B)	0.509(3)	0.3081(11)	0.5996(7)	0.047(5)
H(7A)	0.490(3)	0.2547(10)	0.6395(8)	0.047(5)
H(21)	0.410(2)	0.1584(9)	0.4911(6)	0.033(4)
H(22)	0.383(3)	0.1997(10)	0.4099(7)	0.048(5)
H(23)	0.406(3)	0.3178(10)	0.3970(8)	0.051(5)
H(24)	0.456(2)	0.3868(9)	0.4656(6)	0.040(5)

Table 5. Torsion angles [°] for gwals1.

C(3)–N(1)–C(1)–N(2)	1.6(2)	C(3)–N(1)–C(1)–C(4)	178.22(11)
N(1)–C(1)–N(2)–C(2)	0.2(2)	C(4)–C(1)–N(2)–C(2)	179.59(12)
C(1)–N(2)–C(2)–N(3)	1.7(2)	C(1)–N(2)–C(2)–C(14)	178.51(12)
N(2)–C(2)–N(3)–C(3)	1.9(2)	C(14)–C(2)–N(3)–C(3)	178.26(12)
C(1)–N(1)–C(3)–N(3)	1.3(2)	C(1)–N(1)–C(3)–C(9)	177.28(12)
C(2)–N(3)–C(3)–N(1)	0.3(2)	C(2)–N(3)–C(3)–C(9)	178.92(12)
N(2)–C(1)–C(4)–N(4)	5.47(19)	N(1)–C(1)–C(4)–N(4)	174.37(12)
N(2)–C(1)–C(4)–C(5)	174.51(13)	N(1)–C(1)–C(4)–C(5)	5.7(2)
N(4)–C(4)–C(5)–C(6)	0.4(2)	C(1)–C(4)–C(5)–C(6)	179.66(13)
C(4)–C(5)–C(6)–C(7)	0.5(2)	C(5)–C(6)–C(7)–C(8)	0.7(2)
C(6)–C(7)–C(8)–N(4)	1.0(2)	C(7)–C(8)–N(4)–C(4)	0.8(2)
C(5)–C(4)–N(4)–C(8)	0.5(2)	C(1)–C(4)–N(4)–C(8)	179.49(13)
N(1)–C(3)–C(9)–N(5)	3.9(2)	N(3)–C(3)–C(9)–N(5)	174.82(12)
N(1)–C(3)–C(9)–C(10)	177.38(13)	N(3)–C(3)–C(9)–C(10)	3.9(2)
N(5)–C(9)–C(10)–C(11)	1.9(2)	C(3)–C(9)–C(10)–C(11)	176.77(14)
C(9)–C(10)–C(11)–C(12)	0.1(2)	C(10)–C(11)–C(12)–C(13)	1.8(2)
C(11)–C(12)–C(13)–N(5)	1.7(3)	C(12)–C(13)–N(5)–C(9)	0.2(2)
C(10)–C(9)–N(5)–C(13)	2.0(2)	C(3)–C(9)–N(5)–C(13)	176.69(13)
N(3)–C(2)–C(14)–N(6)	178.58(12)	N(2)–C(2)–C(14)–N(6)	1.3(2)
N(3)–C(2)–C(14)–C(15)	1.6(2)	N(2)–C(2)–C(14)–C(15)	178.51(14)
N(6)–C(14)–C(15)–C(16)	0.3(3)	C(2)–C(14)–C(15)–C(16)	179.51(14)
C(14)–C(15)–C(16)–C(17)	0.0(3)	C(15)–C(16)–C(17)–C(18)	0.4(3)
C(16)–C(17)–C(18)–N(6)	0.5(3)	C(17)–C(18)–N(6)–C(14)	0.3(2)
C(15)–C(14)–N(6)–C(18)	0.1(2)	C(2)–C(14)–N(6)–C(18)	179.64(13)
O(1)–C(19)–C(20)–N(8)	175.10(15)	N(7)–C(19)–C(20)–N(8)	4.5(2)
O(1)–C(19)–C(20)–C(21)	4.1(2)	N(7)–C(19)–C(20)–C(21)	176.36(15)
N(8)–C(20)–C(21)–C(22)	1.2(3)	C(19)–C(20)–C(21)–C(22)	177.96(15)
C(20)–C(21)–C(22)–C(23)	0.3(3)	C(21)–C(22)–C(23)–C(24)	0.9(3)
C(22)–C(23)–C(24)–N(8)	1.4(3)	C(23)–C(24)–N(8)–C(20)	0.6(3)
C(21)–C(20)–N(8)–C(24)	0.7(2)	C(19)–C(20)–N(8)–C(24)	178.43(14)

Table 6. Hydrogen bonds for gwals1 [Å and °].

D–H...A	d(D–H)	d(H...A)	d(D...A)	<(DHA)
N(7)–H(7B)...N(4)	0.87(2)	2.38(2)	3.1538(18)	148.9(17)
N(7)–H(7A)...N(6)	0.92(2)	2.00(2)	2.9060(18)	170.4(18)
N(7)–H(7A)...N(2)	0.92(2)	2.66(2)	3.2119(18)	119.6(15)

5.1.2. Compound 71 X-ray crystal structure data
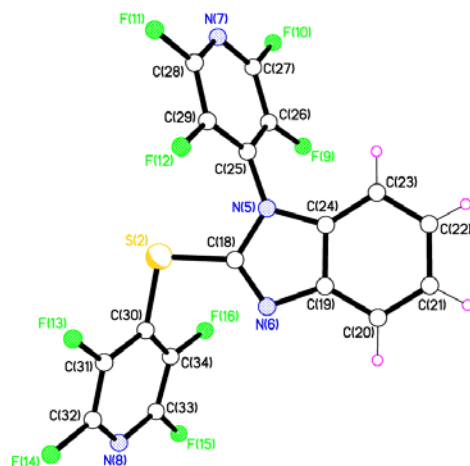
GW105 (M.M. 194.5)

Crystal data

$C_{17}H_4F_8N_4S$	$Z = 4$
$M_r = 448.30$	$F(000) = 888$
Triclinic, $P\bar{1}$	$D_x = 1.820$ Mg m^{-3}
$a = 9.4800$ (9) Å	Mo $K\alpha$ radiation, $\lambda = 0.71073$ Å
$b = 11.4612$ (11) Å	Cell parameters from 10303 reflections
$c = 15.7757$ (15) Å	$\theta = 2.5$–30.4°
$\alpha = 75.3725$ (14)°	$\mu = 0.30$ mm^{-1}
$\beta = 89.9135$ (15)°	$T = 150$ K
$\gamma = 80.8998$ (15)°	Block, colourless
$V = 1636.3$ (3) Å^3	$0.54 \times 0.43 \times 0.18$ mm

Data collection

Bruker APEX 2 CCD diffractometer	8270 reflections with $I > 2\sigma(I)$
Radiation source: fine-focus sealed tube	$R_{int} = 0.022$
ω rotation with narrow frames scans	$\theta_{max} = 30.6°$, $\theta_{min} = 1.9°$
Absorption correction: multi-scan *SADABS* v2 Sheldrick, G.M., (2012)	$h = -13 \square 13$
$T_{min} = 0.855$, $T_{max} = 0.948$	$k = -16 \square 16$
26360 measured reflections	$l = -22 \square 22$
9927 independent reflections	

Refinement

Refinement on F^2	Primary atom site location: structure-invariant di methods
Least-squares matrix: full	Hydrogen site location: difference Fourier map
$R[F^2 > 2\sigma(F^2)] = 0.037$	All H-atom parameters refined
$wR(F^2) = 0.098$	$w = 1/[\sigma^2(F_o^2) + (0.0461P)^2 + 0.6349P]$ $(F_o^2 + 2F_c^2)/3$
$S = 1.04$	$(\Delta/\sigma)_{max} < 0.001$
9927 reflections	$\Delta\rho_{max} = 0.46$ e Å^{-3}
573 parameters	$\Delta\rho_{min} = -0.45$ e Å^{-3}
0 restraints	

Fractional atomic coordinates and isotropic or equivalent isotropic displacement parameters (Å^2)

	x	y	z	$U_{iso}*/U_{eq}$
S1	0.49585 (3)	0.20478 (3)	0.19065 (2)	0.02209 (7)
C1	0.59489 (13)	0.08824 (11)	0.27336 (8)	0.0185 (2)
N1	0.71276 (11)	0.01179 (10)	0.25376 (7)	0.0177 (2)
N2	0.56785 (12)	0.06308 (10)	0.35642 (7)	0.0210 (2)
C2	0.67149 (13)	-0.03703 (11)	0.39583 (8)	0.0187 (2)
C3	0.69072 (15)	-0.10161 (13)	0.48402 (9)	0.0234 (3)
H3	0.628 (2)	-0.0785 (17)	0.5254 (12)	0.031 (5)*
C4	0.80493 (16)	-0.19653 (13)	0.50617 (9)	0.0254 (3)
H4	0.8253 (19)	-0.2415 (17)	0.5675 (12)	0.029 (4)*
C5	0.89784 (15)	-0.22724 (12)	0.44316 (9)	0.0240 (3)
H5	0.9789 (19)	-0.2934 (16)	0.4632 (11)	0.027 (4)*
C6	0.87936 (14)	-0.16516 (12)	0.35504 (8)	0.0210 (2)
H6	0.9438 (18)	-0.1872 (15)	0.3132 (11)	0.023 (4)*
C7	0.76373 (13)	-0.07041 (11)	0.33344 (8)	0.0174 (2)
C8	0.75508 (13)	0.00565 (11)	0.16956 (8)	0.0171 (2)
C9	0.75792 (13)	-0.10074 (11)	0.14197 (8)	0.0189 (2)
C10	0.79736 (15)	-0.10091 (12)	0.05775 (9)	0.0226 (2)
N3	0.83426 (13)	-0.00733 (11)	0.00126 (7)	0.0247 (2)
C11	0.83262 (14)	0.09306 (12)	0.02705 (9)	0.0226 (3)
C12	0.79386 (13)	0.10525 (11)	0.10904 (8)	0.0192 (2)
F1	0.71840 (9)	-0.19965 (7)	0.19479 (5)	0.02516 (17)
F2	0.79623 (11)	-0.20243 (8)	0.03027 (6)	0.0333 (2)
F3	0.87317 (10)	0.18791 (8)	-0.03013 (6)	0.0317 (2)
F4	0.79370 (9)	0.21141 (7)	0.12975 (5)	0.02467 (17)
C13	0.32903 (13)	0.15344 (12)	0.20599 (8)	0.0190 (2)
C14	0.30636 (14)	0.04332 (12)	0.19119 (8)	0.0217 (2)
C15	0.17270 (16)	0.01004 (12)	0.20405 (8)	0.0239 (3)

N4	0.06311 (13)	0.07775 (12)	0.22776 (7)	0.0258 (2)
C16	0.08399 (15)	0.18156 (13)	0.24219 (9)	0.0256 (3)
C17	0.21307 (15)	0.22374 (12)	0.23243 (8)	0.0224 (3)
F5	0.41278 (10)	-0.03037 (8)	0.16632 (6)	0.0327 (2)
F6	0.15093 (11)	-0.09700 (8)	0.19276 (6)	0.0350 (2)
F7	-0.02718 (10)	0.24836 (9)	0.26849 (6)	0.0382 (2)
F8	0.22586 (10)	0.32999 (8)	0.24943 (6)	0.0346 (2)
S2	0.60352 (4)	0.39585 (4)	0.34021 (2)	0.02995 (9)
C18	0.76539 (13)	0.45377 (12)	0.33019 (8)	0.0191 (2)
N5	0.80609 (11)	0.51147 (10)	0.24726 (6)	0.01684 (19)
N6	0.85779 (12)	0.44685 (10)	0.39289 (7)	0.0207 (2)
C19	0.96931 (13)	0.50245 (11)	0.35095 (8)	0.0172 (2)
C20	1.09716 (14)	0.51960 (12)	0.38672 (9)	0.0209 (2)
H20	1.1171 (19)	0.4913 (16)	0.4491 (12)	0.027 (4)*
C21	1.18910 (14)	0.57926 (12)	0.32937 (9)	0.0230 (3)
H21	1.278 (2)	0.5933 (17)	0.3502 (12)	0.033 (5)*
C22	1.15594 (14)	0.62184 (12)	0.23938 (9)	0.0218 (2)
H22	1.221 (2)	0.6642 (17)	0.2030 (12)	0.033 (5)*
C23	1.02935 (13)	0.60567 (12)	0.20275 (8)	0.0192 (2)
H23	1.0071 (18)	0.6336 (16)	0.1414 (11)	0.024 (4)*
C24	0.93948 (12)	0.54395 (11)	0.26057 (8)	0.0160 (2)
C25	0.73638 (13)	0.53086 (11)	0.16490 (8)	0.0168 (2)
C26	0.80634 (14)	0.49208 (12)	0.09673 (8)	0.0203 (2)
C27	0.73832 (16)	0.52315 (14)	0.01498 (9)	0.0258 (3)
N7	0.60959 (14)	0.58642 (13)	-0.00370 (8)	0.0296 (3)
C28	0.54228 (15)	0.62085 (14)	0.06052 (9)	0.0260 (3)
C29	0.59838 (14)	0.59610 (12)	0.14529 (8)	0.0198 (2)
F9	0.93779 (9)	0.42720 (8)	0.10919 (6)	0.02733 (17)
F10	0.80572 (11)	0.48686 (11)	-0.05041 (6)	0.0409 (2)
F11	0.41119 (10)	0.68572 (10)	0.04148 (6)	0.0403 (2)
F12	0.52337 (9)	0.63768 (8)	0.20600 (5)	0.02625 (17)
C30	0.62995 (16)	0.30251 (13)	0.44782 (8)	0.0250 (3)
C31	0.53099 (17)	0.32041 (15)	0.51020 (9)	0.0303 (3)
C32	0.5506 (2)	0.24321 (17)	0.59343 (10)	0.0377 (4)
N8	0.65730 (19)	0.15347 (14)	0.61787 (8)	0.0418 (4)
C33	0.7506 (2)	0.13563 (15)	0.55911 (10)	0.0366 (4)
C34	0.74250 (17)	0.20572 (14)	0.47336 (9)	0.0283 (3)
F13	0.41814 (11)	0.40941 (10)	0.49090 (7)	0.0405 (2)
F14	0.45641 (15)	0.26015 (13)	0.65348 (7)	0.0589 (4)
F15	0.85872 (14)	0.04282 (10)	0.58429 (8)	0.0531 (3)

F16	0.83880 (10)	0.17974 (9)	0.41726 (6)	0.0379 (2)

Geometric parameters (Å, º) for (gw105)

S1—C1	1.7592 (13)	S2—C30	1.7574 (13)
S1—C13	1.7683 (13)	S2—C18	1.7575 (13)
C1—N2	1.3028 (16)	C18—N6	1.3010 (16)
C1—N1	1.3922 (16)	C18—N5	1.3929 (15)
N1—C7	1.4004 (15)	N5—C24	1.4038 (15)
N1—C8	1.4024 (15)	N5—C25	1.4088 (15)
N2—C2	1.3976 (16)	N6—C19	1.3998 (16)
C2—C3	1.3981 (17)	C19—C24	1.3984 (16)
C2—C7	1.4005 (17)	C19—C20	1.3998 (17)
C3—C4	1.384 (2)	C20—C21	1.3855 (19)
C3—H3	0.942 (19)	C20—H20	0.964 (18)
C4—C5	1.401 (2)	C21—C22	1.3983 (19)
C4—H4	0.978 (18)	C21—H21	0.959 (19)
C5—C6	1.3897 (18)	C22—C23	1.3910 (18)
C5—H5	0.981 (18)	C22—H22	0.950 (19)
C6—C7	1.3910 (17)	C23—C24	1.3859 (17)
C6—H6	0.952 (17)	C23—H23	0.951 (17)
C8—C12	1.3896 (17)	C25—C26	1.3928 (17)
C8—C9	1.3910 (17)	C25—C29	1.3933 (17)
C9—F1	1.3326 (14)	C26—F9	1.3335 (15)
C9—C10	1.3801 (17)	C26—C27	1.3798 (18)
C10—N3	1.3045 (18)	C27—N7	1.310 (2)
C10—F2	1.3418 (16)	C27—F10	1.3326 (16)
N3—C11	1.3117 (19)	N7—C28	1.3074 (19)
C11—F3	1.3338 (15)	C28—F11	1.3354 (16)
C11—C12	1.3789 (18)	C28—C29	1.3837 (18)
C12—F4	1.3369 (15)	C29—F12	1.3309 (15)
C13—C17	1.3856 (18)	C30—C31	1.389 (2)
C13—C14	1.3887 (18)	C30—C34	1.390 (2)
C14—F5	1.3349 (15)	C31—F13	1.333 (2)
C14—C15	1.380 (2)	C31—C32	1.380 (2)
C15—N4	1.3084 (19)	C32—N8	1.304 (3)
C15—F6	1.3304 (16)	C32—F14	1.330 (2)

N4—C16	1.311 (2)	N8—C33	1.311 (3)
C16—F7	1.3314 (16)	C33—F15	1.335 (2)
C16—C17	1.380 (2)	C33—C34	1.383 (2)
C17—F8	1.3346 (16)	C34—F16	1.3229 (18)
C1—S1—C13	97.66 (6)	C30—S2—C18	99.24 (6)
N2—C1—N1	113.37 (11)	N6—C18—N5	113.81 (11)
N2—C1—S1	125.47 (10)	N6—C18—S2	127.09 (10)
N1—C1—S1	121.16 (9)	N5—C18—S2	119.08 (9)
C1—N1—C7	106.09 (10)	C18—N5—C24	105.55 (10)
C1—N1—C8	126.07 (10)	C18—N5—C25	129.43 (10)
C7—N1—C8	126.98 (10)	C24—N5—C25	124.96 (10)
C1—N2—C2	105.03 (10)	C18—N6—C19	104.93 (10)
N2—C2—C3	128.95 (12)	C24—C19—N6	110.56 (10)
N2—C2—C7	110.71 (11)	C24—C19—C20	119.95 (11)
C3—C2—C7	120.34 (12)	N6—C19—C20	129.49 (11)
C4—C3—C2	117.24 (12)	C21—C20—C19	117.32 (12)
C4—C3—H3	123.1 (11)	C21—C20—H20	122.9 (11)
C2—C3—H3	119.6 (11)	C19—C20—H20	119.7 (11)
C3—C4—C5	121.68 (12)	C20—C21—C22	121.75 (12)
C3—C4—H4	120.0 (11)	C20—C21—H21	120.9 (11)
C5—C4—H4	118.2 (11)	C22—C21—H21	117.4 (11)
C6—C5—C4	121.91 (13)	C23—C22—C21	121.69 (12)
C6—C5—H5	120.1 (10)	C23—C22—H22	119.8 (11)
C4—C5—H5	117.9 (10)	C21—C22—H22	118.5 (11)
C5—C6—C7	115.91 (12)	C24—C23—C22	116.00 (12)
C5—C6—H6	120.7 (10)	C24—C23—H23	122.1 (10)
C7—C6—H6	123.4 (10)	C22—C23—H23	121.8 (10)
C6—C7—N1	132.31 (12)	C23—C24—C19	123.26 (11)
C6—C7—C2	122.90 (11)	C23—C24—N5	131.57 (11)
N1—C7—C2	104.78 (10)	C19—C24—N5	105.15 (10)
C12—C8—C9	116.56 (11)	C26—C25—C29	116.42 (11)
C12—C8—N1	122.13 (11)	C26—C25—N5	121.16 (11)
C9—C8—N1	121.30 (11)	C29—C25—N5	122.29 (11)
F1—C9—C10	120.40 (11)	F9—C26—C27	119.95 (12)
F1—C9—C8	120.66 (11)	F9—C26—C25	121.05 (11)
C10—C9—C8	118.90 (11)	C27—C26—C25	119.00 (12)
N3—C10—F2	116.73 (12)	N7—C27—F10	116.56 (12)
N3—C10—C9	124.33 (12)	N7—C27—C26	124.45 (13)
F2—C10—C9	118.92 (12)	F10—C27—C26	118.99 (13)

C10—N3—C11	117.07 (12)	C28—N7—C27	116.79 (12)
N3—C11—F3	117.02 (12)	N7—C28—F11	116.83 (12)
N3—C11—C12	124.16 (12)	N7—C28—C29	124.53 (13)
F3—C11—C12	118.81 (12)	F11—C28—C29	118.63 (13)
F4—C12—C11	120.34 (11)	F12—C29—C28	120.37 (12)
F4—C12—C8	120.68 (11)	F12—C29—C25	120.81 (11)
C11—C12—C8	118.98 (12)	C28—C29—C25	118.78 (12)
C17—C13—C14	116.76 (12)	C31—C30—C34	117.33 (13)
C17—C13—S1	120.73 (10)	C31—C30—S2	119.53 (12)
C14—C13—S1	122.51 (10)	C34—C30—S2	123.04 (11)
F5—C14—C15	120.38 (12)	F13—C31—C32	119.94 (15)
F5—C14—C13	120.57 (12)	F13—C31—C30	121.37 (13)
C15—C14—C13	119.04 (12)	C32—C31—C30	118.69 (16)
N4—C15—F6	116.57 (13)	N8—C32—F14	117.00 (15)
N4—C15—C14	123.85 (13)	N8—C32—C31	124.06 (16)
F6—C15—C14	119.57 (13)	F14—C32—C31	118.94 (19)
C15—N4—C16	117.37 (12)	C32—N8—C33	117.53 (14)
N4—C16—F7	116.94 (13)	N8—C33—F15	117.24 (14)
N4—C16—C17	123.94 (13)	N8—C33—C34	124.11 (17)
F7—C16—C17	119.12 (13)	F15—C33—C34	118.65 (17)
F8—C17—C16	120.21 (12)	F16—C34—C33	120.48 (15)
F8—C17—C13	120.76 (12)	F16—C34—C30	121.25 (12)
C16—C17—C13	119.02 (13)	C33—C34—C30	118.26 (15)
C13—S1—C1—N2	-59.26 (12)	C30—S2—C18—N6	-12.89 (14)
C13—S1—C1—N1	120.13 (11)	C30—S2—C18—N5	165.31 (11)
N2—C1—N1—C7	0.48 (14)	N6—C18—N5—C24	-0.02 (15)
S1—C1—N1—C7	-178.98 (9)	S2—C18—N5—C24	-178.45 (9)
N2—C1—N1—C8	170.47 (11)	N6—C18—N5—C25	177.29 (12)
S1—C1—N1—C8	-8.98 (17)	S2—C18—N5—C25	-1.14 (19)
N1—C1—N2—C2	-0.82 (14)	N5—C18—N6—C19	-0.29 (15)
S1—C1—N2—C2	178.61 (9)	S2—C18—N6—C19	177.99 (10)
C1—N2—C2—C3	-179.25 (13)	C18—N6—C19—C24	0.50 (14)
C1—N2—C2—C7	0.86 (14)	C18—N6—C19—C20	-179.47 (13)
N2—C2—C3—C4	-178.61 (13)	C24—C19—C20—C21	0.58 (19)
C7—C2—C3—C4	1.26 (19)	N6—C19—C20—C21	-179.46 (13)
C2—C3—C4—C5	0.0 (2)	C19—C20—C21—C22	0.5 (2)
C3—C4—C5—C6	-0.8 (2)	C20—C21—C22—C23	-0.5 (2)
C4—C5—C6—C7	0.4 (2)	C21—C22—C23—C24	-0.66 (19)
C5—C6—C7—N1	179.22 (13)	C22—C23—C24—C19	1.81 (19)

C5—C6—C7—C2	0.86 (19)	C22—C23—C24—N5	-179.84 (12)
C1—N1—C7—C6	-178.48 (14)	N6—C19—C24—C23	178.21 (12)
C8—N1—C7—C6	11.6 (2)	C20—C19—C24—C23	-1.82 (19)
C1—N1—C7—C2	0.09 (13)	N6—C19—C24—N5	-0.51 (14)
C8—N1—C7—C2	-169.79 (12)	C20—C19—C24—N5	179.46 (11)
N2—C2—C7—C6	178.16 (12)	C18—N5—C24—C23	-178.25 (13)
C3—C2—C7—C6	-1.7 (2)	C25—N5—C24—C23	4.3 (2)
N2—C2—C7—N1	-0.58 (14)	C18—N5—C24—C19	0.32 (13)
C3—C2—C7—N1	179.52 (11)	C25—N5—C24—C19	-177.14 (11)
C1—N1—C8—C12	61.65 (17)	C18—N5—C25—C26	-125.19 (14)
C7—N1—C8—C12	-130.41 (13)	C24—N5—C25—C26	51.65 (17)
C1—N1—C8—C9	-117.25 (14)	C18—N5—C25—C29	59.05 (19)
C7—N1—C8—C9	50.69 (18)	C24—N5—C25—C29	-124.11 (13)
C12—C8—C9—F1	-178.04 (11)	C29—C25—C26—F9	-178.84 (11)
N1—C8—C9—F1	0.91 (18)	N5—C25—C26—F9	5.16 (18)
C12—C8—C9—C10	-0.40 (18)	C29—C25—C26—C27	2.01 (18)
N1—C8—C9—C10	178.56 (12)	N5—C25—C26—C27	-173.99 (12)
F1—C9—C10—N3	178.38 (13)	F9—C26—C27—N7	179.98 (13)
C8—C9—C10—N3	0.7 (2)	C25—C26—C27—N7	-0.9 (2)
F1—C9—C10—F2	-0.48 (19)	F9—C26—C27—F10	0.3 (2)
C8—C9—C10—F2	-178.14 (12)	C25—C26—C27—F10	179.47 (12)
F2—C10—N3—C11	178.57 (12)	F10—C27—N7—C28	179.12 (13)
C9—C10—N3—C11	-0.3 (2)	C26—C27—N7—C28	-0.5 (2)
C10—N3—C11—F3	178.67 (12)	C27—N7—C28—F11	179.78 (13)
C10—N3—C11—C12	-0.4 (2)	C27—N7—C28—C29	0.7 (2)
N3—C11—C12—F4	-179.29 (12)	N7—C28—C29—F12	178.20 (13)
F3—C11—C12—F4	1.65 (19)	F11—C28—C29—F12	-0.8 (2)
N3—C11—C12—C8	0.7 (2)	N7—C28—C29—C25	0.5 (2)
F3—C11—C12—C8	-178.37 (11)	F11—C28—C29—C25	-178.54 (12)
C9—C8—C12—F4	179.74 (11)	C26—C25—C29—F12	-179.55 (11)
N1—C8—C12—F4	0.80 (18)	N5—C25—C29—F12	-3.59 (19)
C9—C8—C12—C11	-0.25 (18)	C26—C25—C29—C28	-1.83 (18)
N1—C8—C12—C11	-179.19 (11)	N5—C25—C29—C28	174.12 (12)
C1—S1—C13—C17	116.39 (11)	C18—S2—C30—C31	123.43 (12)
C1—S1—C13—C14	-64.64 (11)	C18—S2—C30—C34	-60.14 (13)
C17—C13—C14—F5	-179.40 (11)	C34—C30—C31—F13	-178.59 (12)
S1—C13—C14—F5	1.58 (17)	S2—C30—C31—F13	-1.96 (19)
C17—C13—C14—C15	-0.53 (18)	C34—C30—C31—C32	0.9 (2)
S1—C13—C14—C15	-179.54 (10)	S2—C30—C31—C32	177.52 (11)
F5—C14—C15—N4	-179.49 (12)	F13—C31—C32—N8	179.59 (13)

C13—C14—C15—N4	1.6 (2)	C30—C31—C32—N8	0.1 (2)
F5—C14—C15—F6	1.00 (19)	F13—C31—C32—F14	-0.7 (2)
C13—C14—C15—F6	-177.88 (11)	C30—C31—C32—F14	179.82 (13)
F6—C15—N4—C16	177.64 (11)	F14—C32—N8—C33	179.76 (13)
C14—C15—N4—C16	-1.9 (2)	C31—C32—N8—C33	-0.5 (2)
C15—N4—C16—F7	-178.31 (12)	C32—N8—C33—F15	-179.31 (13)
C15—N4—C16—C17	1.1 (2)	C32—N8—C33—C34	-0.1 (2)
N4—C16—C17—F8	-179.25 (12)	N8—C33—C34—F16	-178.09 (14)
F7—C16—C17—F8	0.2 (2)	F15—C33—C34—F16	1.1 (2)
N4—C16—C17—C13	-0.1 (2)	N8—C33—C34—C30	1.1 (2)
F7—C16—C17—C13	179.30 (12)	F15—C33—C34—C30	-179.70 (13)
C14—C13—C17—F8	178.95 (11)	C31—C30—C34—F16	177.74 (12)
S1—C13—C17—F8	-2.02 (17)	S2—C30—C34—F16	1.2 (2)
C14—C13—C17—C16	-0.16 (18)	C31—C30—C34—C33	-1.4 (2)
S1—C13—C17—C16	178.87 (10)	S2—C30—C34—C33	-177.93 (11)

Computing details

Data collection: Bruker *APEX* 2; cell refinement: Bruker *SAINT*; data reduction: Bruker *SAINT*; program(s) used to solve structure: *SHELXS97* (Sheldrick, 2008); program(s) used to refine structure: *SHELXL2013* (Sheldrick, 2013); molecular graphics: Bruker *SHELXTL*; software used to prepare material for publication: Bruker *SHELXTL*.

Special details

Geometry. All esds (except the esd in the dihedral angle between two l.s. planes) are estimated usir full covariance matrix. The cell esds are taken into account individually in the estimation of esds i distances, angles and torsion angles; correlations between esds in cell parameters are only used wh are defined by crystal symmetry. An approximate (isotropic) treatment of cell esds is used for esti esds involving l.s. planes.

5.1.3. Compound 87 X-ray crystal structure data
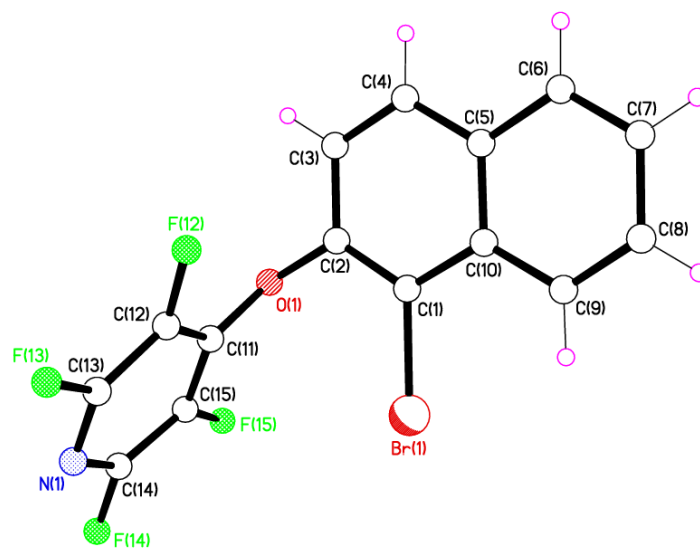
GW87

Crystal data

$C_{15}H_6BrF_4NO$	$F(000) = 364$
$M_r = 372.12$	$D_x = 1.884$ Mg m^{-3}
Monoclinic, $P2_1$	Mo $K\alpha$ radiation, $\lambda = 0.71073$ Å
$a = 4.6466\ (10)$ Å	Cell parameters from 3070 reflections
$b = 11.162\ (2)$ Å	$\theta = 2.4–27.9°$
$c = 12.646\ (3)$ Å	$\mu = 3.18$ mm^{-1}
$\beta = 90.888\ (3)°$	$T = 150$ K
$V = 655.8\ (2)$ Å^3	Plate, colourless
$Z = 2$	$0.82 \times 0.33 \times 0.05$ mm

Data collection

Bruker APEX 2 CCD diffractometer	3193 independent reflections
Radiation source: fine-focus sealed tube	2848 reflections with $I > 2\sigma(I)$
graphite	$R_{int} = 0.028$
ω rotation with narrow frames scans	$\theta_{max} = 28.3°$, $\theta_{min} = 1.6°$
Absorption correction: multi-scan $SADABS$ v2009/1, Sheldrick, G.M., (2009)	$h = -6 \rightarrow 6$
$T_{min} = 0.180$, $T_{max} = 0.857$	$k = -14 \rightarrow 14$
6477 measured reflections	$l = -16 \rightarrow 16$

Refinement

Refinement on F^2	Secondary atom site location: difference Fourier map
Least-squares matrix: full	Hydrogen site location: inferred from neighbouring sites
$R[F^2 > 2\sigma(F^2)] = 0.036$	H-atom parameters constrained
$wR(F^2) = 0.089$	$w = 1/[\sigma^2(F_o^2) + (0.0577P)^2]$ where $P = (F_o^2 + 2F_c^2)/3$
$S = 1.01$	$(\Delta/\sigma)_{max} = 0.001$
3193 reflections	$\Delta\rangle_{max} = 0.69$ e Å^{-3}
200 parameters	$\Delta\rangle_{min} = -0.48$ e Å^{-3}
1 restraint	Absolute structure: Refined as an inversion twin.
Primary atom site location: structure-invariant direct methods	Flack parameter: -0.013 (13)

Fractional atomic coordinates and isotropic or equivalent isotropic displacement parameters (Å^2)

	x	y	z	$U_{iso}*/U_{eq}$
Br1	0.18951 (10)	0.65833 (4)	0.74794 (3)	0.03178 (15)
C1	0.3059 (10)	0.5307 (4)	0.6596 (4)	0.0242 (9)
C2	0.4998 (10)	0.4480 (4)	0.6972 (4)	0.0272 (9)
C3	0.6131 (11)	0.3565 (5)	0.6315 (4)	0.0299 (10)
H3	0.7509	0.3011	0.6584	0.036*
C4	0.5196 (11)	0.3503 (5)	0.5292 (4)	0.0314 (11)
H4	0.5979	0.2910	0.4841	0.038*
C5	0.3075 (10)	0.4302 (4)	0.4883 (4)	0.0259 (9)
C6	0.2072 (11)	0.4204 (5)	0.3809 (4)	0.0322 (11)
H6	0.2838	0.3602	0.3362	0.039*
C7	0.0021 (12)	0.4971 (5)	0.3426 (4)	0.0344 (11)
H7	-0.0673	0.4890	0.2719	0.041*
C8	-0.1070 (11)	0.5882 (5)	0.4079 (4)	0.0314 (10)
H8	-0.2495	0.6414	0.3804	0.038*
C9	-0.0114 (10)	0.6016 (4)	0.5101 (4)	0.0278 (10)
H9	-0.0867	0.6640	0.5525	0.033*
C10	0.1977 (10)	0.5235 (4)	0.5527 (4)	0.0253 (9)
O1	0.6155 (7)	0.4558 (3)	0.7999 (3)	0.0296 (7)
C11	0.4411 (10)	0.4400 (4)	0.8856 (4)	0.0261 (9)
C12	0.2293 (11)	0.3532 (4)	0.8929 (4)	0.0280 (10)
F12	0.1667 (7)	0.2796 (3)	0.8116 (3)	0.0364 (7)
C13	0.0847 (11)	0.3432 (5)	0.9873 (4)	0.0309 (10)
F13	-0.1246 (7)	0.2613 (3)	0.9940 (3)	0.0403 (7)
N1	0.1368 (10)	0.4084 (4)	1.0713 (4)	0.0369 (10)
C14	0.3409 (12)	0.4893 (5)	1.0641 (4)	0.0365 (12)
F14	0.3959 (9)	0.5574 (4)	1.1492 (3)	0.0545 (10)
C15	0.4967 (11)	0.5098 (5)	0.9735 (4)	0.0292 (10)
F15	0.6983 (7)	0.5957 (3)	0.9708 (3)	0.0398 (7)

Geometric parameters (Å, °)

Br1—C1	1.895 (5)	C9—C10	1.406 (7)
C1—C2	1.370 (7)	O1—C11	1.374 (6)
C1—C10	1.438 (7)	C11—C15	1.379 (7)
C2—O1	1.400 (6)	C11—C12	1.386 (7)
C2—C3	1.422 (7)	C12—F12	1.344 (6)
C3—C4	1.360 (7)	C12—C13	1.383 (7)
C4—C5	1.421 (7)	C13—N1	1.308 (7)
C5—C10	1.421 (7)	C13—F13	1.339 (6)
C5—C6	1.433 (7)	N1—C14	1.314 (8)
C6—C7	1.364 (8)	C14—F14	1.339 (6)
C7—C8	1.410 (8)	C14—C15	1.383 (7)
C8—C9	1.368 (7)	C15—F15	1.341 (6)
C2—C1—C10	120.5 (4)	C11—O1—C2	120.0 (3)
C2—C1—Br1	119.6 (4)	O1—C11—C15	117.3 (4)
C10—C1—Br1	119.8 (3)	O1—C11—C12	124.8 (4)
C1—C2—O1	121.4 (4)	C15—C11—C12	117.7 (5)
C1—C2—C3	121.9 (4)	F12—C12—C13	120.6 (4)
O1—C2—C3	116.5 (4)	F12—C12—C11	121.5 (4)
C4—C3—C2	118.5 (5)	C13—C12—C11	118.0 (4)
C3—C4—C5	121.6 (5)	N1—C13—F13	117.0 (5)
C4—C5—C10	120.3 (4)	N1—C13—C12	124.8 (5)
C4—C5—C6	120.7 (5)	F13—C13—C12	118.2 (5)
C10—C5—C6	119.0 (5)	C13—N1—C14	116.8 (5)
C7—C6—C5	120.2 (5)	N1—C14—F14	117.6 (5)
C6—C7—C8	120.1 (5)	N1—C14—C15	124.0 (5)
C9—C8—C7	121.1 (5)	F14—C14—C15	118.4 (5)
C8—C9—C10	120.5 (5)	F15—C15—C11	120.3 (5)
C9—C10—C5	119.1 (4)	F15—C15—C14	120.9 (5)
C9—C10—C1	123.7 (4)	C11—C15—C14	118.7 (5)
C5—C10—C1	117.1 (4)		
C10—C1—C2—O1	177.7 (4)	C1—C2—O1—C11	66.6 (6)
Br1—C1—C2—O1	-0.2 (6)	C3—C2—O1—C11	-118.8 (5)
C10—C1—C2—C3	3.4 (7)	C2—O1—C11—C15	-143.5 (4)
Br1—C1—C2—C3	-174.5 (4)	C2—O1—C11—C12	41.8 (7)
C1—C2—C3—C4	-1.5 (7)	O1—C11—C12—F12	-3.7 (7)
O1—C2—C3—C4	-176.1 (4)	C15—C11—C12—F12	-178.4 (4)
C2—C3—C4—C5	-1.8 (8)	O1—C11—C12—C13	175.6 (4)
C3—C4—C5—C10	3.2 (8)	C15—C11—C12—C13	0.9 (7)
C3—C4—C5—C6	-178.6 (5)	F12—C12—C13—N1	177.9 (5)
C4—C5—C6—C7	179.5 (5)	C11—C12—C13—N1	-1.4 (8)
C10—C5—C6—C7	-2.2 (7)	F12—C12—C13—F13	-2.1 (7)
C5—C6—C7—C8	1.5 (8)	C11—C12—C13—F13	178.5 (4)
C6—C7—C8—C9	-0.2 (8)	F13—C13—N1—C14	-179.5 (4)

C7—C8—C9—C10	-0.5 (7)	C12—C13—N1—C14	0.4 (8)
C8—C9—C10—C5	-0.2 (7)	C13—N1—C14—F14	179.6 (5)
C8—C9—C10—C1	-179.1 (4)	C13—N1—C14—C15	1.1 (8)
C4—C5—C10—C9	179.8 (4)	O1—C11—C15—F15	5.2 (7)
C6—C5—C10—C9	1.6 (7)	C12—C11—C15—F15	-179.6 (4)
C4—C5—C10—C1	-1.3 (7)	O1—C11—C15—C14	-174.7 (4)
C6—C5—C10—C1	-179.5 (4)	C12—C11—C15—C14	0.4 (7)
C2—C1—C10—C9	176.9 (4)	N1—C14—C15—F15	178.6 (5)
Br1—C1—C10—C9	-5.2 (6)	F14—C14—C15—F15	0.1 (8)
C2—C1—C10—C5	-2.0 (6)	N1—C14—C15—C11	-1.5 (8)
Br1—C1—C10—C5	176.0 (3)	F14—C14—C15—C11	-180.0 (5)

Computing details

Data collection: Bruker *APEX* 2; cell refinement: Bruker *SAINT*; data reduction: Bruker *SAINT*; program(s) used to solve structure: *SHELXS97* (Sheldrick, 2008); program(s) used to refine structure: *SHELXL2012* (Sheldrick, 2012); molecular graphics: Bruker *SHELXTL*; software used to prepare material for publication: Bruker *SHELXTL*.

Special details

Geometry. All esds (except the esd in the dihedral angle between two l.s. planes) are estimated using the full covariance matrix. The cell esds are taken into account individually in the estimation of esds in distances, angles and torsion angles; correlations between esds in cell parameters are only used when they are defined by crystal symmetry. An approximate (isotropic) treatment of cell esds is used for estimating esds involving l.s. planes.

Refinement. Refined as a 2-component racemic twin.

5.1.4. Compound 95 X-ray crystal structure data
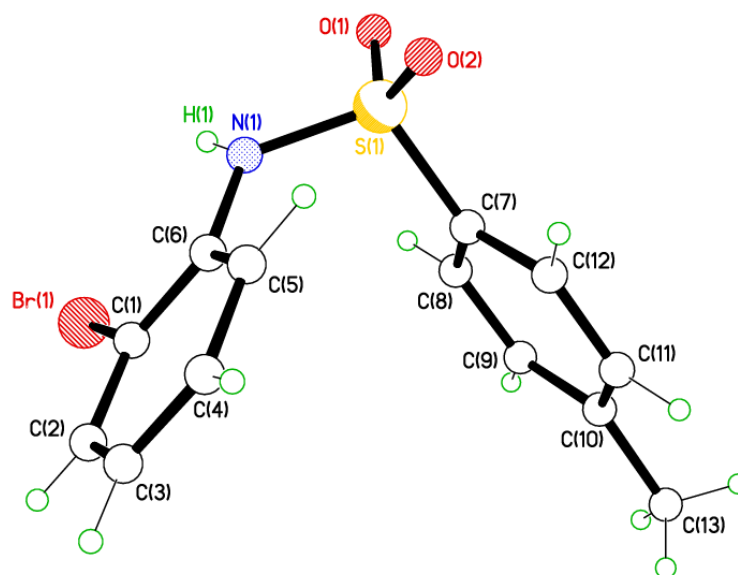
Crystal data

$C_{13}H_{12}BrNO_2S$	$D_x = 1.654$ Mg m^{-3}
$M_r = 326.21$	Synchrotron radiation, $\lambda = 0.7749$ Å
Orthorhombic, *Pbca*	Cell parameters from 9243 reflections
$a = 12.3969$ (4) Å	$\theta = 2.9$–$39.9°$
$b = 11.4900$ (4) Å	$\mu = 4.06$ mm^{-1}
$c = 18.3914$ (6) Å	$T = 100$ K
$V = 2619.68$ (15) Å^3	Plate, colourless
$Z = 8$	$0.15 \times 0.10 \times 0.02$ mm
$F(000) = 1312$	

Data collection

Bruker APEX 2 CCD diffractometer	5702 reflections with $I > 2\sigma(I)$
Radiation source: ALS Station 11.3.1	$R_{int} = 0.035$
ϕ rotation with narrow frames scans	$\theta_{max} = 40.2°$, $\theta_{min} = 2.9°$
Absorption correction: multi-scan *SADABS* v2 Sheldrick, G.M., (2009)	$h = -20\square20$
$T_{min} = 0.581$, $T_{max} = 0.923$	$k = -19\square19$
78378 measured reflections	$l = -30\square30$
6306 independent reflections	

Refinement

Refinement on F^2	Secondary atom site location: all non-H atoms fo direct methods
Least-squares matrix: full	Hydrogen site location: difference Fourier map
$R[F^2 > 2\sigma(F^2)] = 0.023$	All H-atom parameters refined
$wR(F^2) = 0.068$	$w = 1/[\sigma^2(F_o^2) + (0.0346P)^2 + 0.8758P]$ $(F_o^2 + 2F_c^2)/3$
$S = 1.05$	$(\Delta/\sigma)_{max} = 0.002$
6306 reflections	$\Delta\rangle_{max} = 0.68$ e Å^{-3}
212 parameters	$\Delta\rangle_{min} = -0.65$ e Å^{-3}
1 restraint	Extinction correction: *SHELXL*, Fc*=kFc[1+0.001xFc$^2\lambda^3$/sin(2θ)]$^{-1/4}$
Primary atom site location: structure-invariant di methods	Extinction coefficient: 0.0020 (3)

Fractional atomic coordinates and isotropic or equivalent isotropic displacement parameters (Å^2)

	x	y	z	U_{iso}*/U_{eq}
Br1	0.53732 (2)	0.70236 (2)	0.39424 (2)	0.02409 (4)
C1	0.43264 (7)	0.64932 (7)	0.46102 (5)	0.01728 (13)
C2	0.38746 (8)	0.54020 (8)	0.45004 (5)	0.02176 (15)
H2	0.4145 (14)	0.4934 (14)	0.4096 (8)	0.027 (4)*
C3	0.30889 (8)	0.50023 (8)	0.49756 (6)	0.02391 (17)
H3	0.2741 (15)	0.4253 (15)	0.4911 (10)	0.044 (5)*
C4	0.27627 (8)	0.56811 (9)	0.55402 (5)	0.02238 (16)
H4	0.2297 (15)	0.5477 (15)	0.5832 (11)	0.040 (5)*
C5	0.31984 (8)	0.67916 (9)	0.56504 (5)	0.02169 (15)
H5	0.2920 (14)	0.7285 (15)	0.6055 (8)	0.029 (4)*
C6	0.40019 (7)	0.72025 (7)	0.51837 (4)	0.01619 (13)
N1	0.44470 (7)	0.83216 (6)	0.52778 (4)	0.01859 (12)
H1	0.4751 (13)	0.8621 (15)	0.4939 (8)	0.035 (4)*
S1	0.48179 (2)	0.88400 (2)	0.60658 (2)	0.01705 (4)
O1	0.53878 (6)	0.98913 (6)	0.58867 (4)	0.02464 (14)
O2	0.39022 (6)	0.89095 (6)	0.65350 (4)	0.02307 (13)
C7	0.57070 (7)	0.78243 (7)	0.64511 (4)	0.01550 (12)
C8	0.67406 (8)	0.77075 (8)	0.61691 (5)	0.01988 (14)
H8	0.6988 (15)	0.8163 (15)	0.5781 (10)	0.036 (4)*
C9	0.74378 (8)	0.69108 (8)	0.64823 (5)	0.02000 (14)
H9	0.8137 (14)	0.6823 (14)	0.6292 (10)	0.031 (4)*
C10	0.71177 (7)	0.62181 (7)	0.70673 (4)	0.01657 (13)

C11	0.60753 (7)	0.63533 (8)	0.73389 (5)	0.02007 (14)
H11	0.5851 (13)	0.5862 (13)	0.7750 (9)	0.025 (4)*
C12	0.53683 (7)	0.71541 (8)	0.70365 (5)	0.01914 (14)
H12	0.4640 (12)	0.7324 (16)	0.7217 (10)	0.031 (4)*
C13	0.78728 (8)	0.53356 (9)	0.73867 (5)	0.02279 (16)
H13A	0.8541 (16)	0.5310 (17)	0.7125 (11)	0.047 (5)*
H13B	0.8022 (17)	0.5550 (18)	0.7851 (12)	0.053 (5)*
H13C	0.7568 (17)	0.4620 (17)	0.7419 (11)	0.052 (6)*

Geometric parameters (Å, º)

Br1—C1	1.8878 (9)	S1—C7	1.7547 (8)
C1—C2	1.3880 (12)	C7—C12	1.3887 (12)
C1—C6	1.3923 (12)	C7—C8	1.3889 (13)
C2—C3	1.3870 (14)	C8—C9	1.3845 (13)
C2—H2	0.977 (16)	C8—H8	0.937 (19)
C3—C4	1.3602 (15)	C9—C10	1.3958 (12)
C3—H3	0.969 (18)	C9—H9	0.940 (18)
C4—C5	1.4004 (13)	C10—C11	1.3942 (12)
C4—H4	0.822 (19)	C10—C13	1.4998 (13)
C5—C6	1.3971 (12)	C11—C12	1.3870 (13)
C5—H5	0.997 (16)	C11—H11	0.984 (16)
C6—N1	1.4100 (11)	C12—H12	0.982 (16)
N1—S1	1.6329 (8)	C13—H13A	0.96 (2)
N1—H1	0.806 (12)	C13—H13B	0.91 (2)
S1—O2	1.4281 (8)	C13—H13C	0.91 (2)
S1—O1	1.4377 (8)		
C2—C1—C6	121.49 (8)	N1—S1—C7	107.02 (4)
C2—C1—Br1	118.32 (7)	C12—C7—C8	120.99 (8)
C6—C1—Br1	120.17 (6)	C12—C7—S1	119.48 (7)
C3—C2—C1	119.40 (9)	C8—C7—S1	119.54 (6)
C3—C2—H2	122.5 (10)	C9—C8—C7	118.98 (8)
C1—C2—H2	118.0 (10)	C9—C8—H8	118.8 (11)
C4—C3—C2	120.00 (8)	C7—C8—H8	122.2 (11)
C4—C3—H3	118.0 (12)	C8—C9—C10	121.35 (8)
C2—C3—H3	121.9 (12)	C8—C9—H9	119.4 (11)

C3—C4—C5	121.22 (9)	C10—C9—H9	119.2 (11)
C3—C4—H4	122.9 (13)	C11—C10—C9	118.43 (8)
C5—C4—H4	115.9 (13)	C11—C10—C13	120.90 (8)
C6—C5—C4	119.60 (9)	C9—C10—C13	120.66 (8)
C6—C5—H5	120.9 (10)	C12—C11—C10	121.06 (8)
C4—C5—H5	119.5 (10)	C12—C11—H11	120.7 (9)
C1—C6—C5	118.28 (8)	C10—C11—H11	118.3 (9)
C1—C6—N1	120.91 (8)	C11—C12—C7	119.19 (8)
C5—C6—N1	120.78 (8)	C11—C12—H12	125.3 (11)
C6—N1—S1	123.49 (6)	C7—C12—H12	115.5 (11)
C6—N1—H1	118.5 (13)	C10—C13—H13A	111.3 (12)
S1—N1—H1	113.5 (13)	C10—C13—H13B	108.2 (13)
O2—S1—O1	118.82 (5)	H13A—C13—H13B	107.7 (18)
O2—S1—N1	109.45 (4)	C10—C13—H13C	112.2 (13)
O1—S1—N1	103.98 (4)	H13A—C13—H13C	111.4 (17)
O2—S1—C7	107.00 (4)	H13B—C13—H13C	105.7 (18)
O1—S1—C7	110.04 (4)		
C6—C1—C2—C3	-0.60 (13)	O2—S1—C7—C12	9.28 (8)
Br1—C1—C2—C3	-178.77 (7)	O1—S1—C7—C12	139.68 (7)
C1—C2—C3—C4	0.43 (14)	N1—S1—C7—C12	-107.96 (8)
C2—C3—C4—C5	0.66 (15)	O2—S1—C7—C8	-170.34 (7)
C3—C4—C5—C6	-1.57 (15)	O1—S1—C7—C8	-39.95 (8)
C2—C1—C6—C5	-0.31 (13)	N1—S1—C7—C8	72.42 (8)
Br1—C1—C6—C5	177.83 (7)	C12—C7—C8—C9	-0.22 (14)
C2—C1—C6—N1	-178.31 (8)	S1—C7—C8—C9	179.40 (7)
Br1—C1—C6—N1	-0.17 (11)	C7—C8—C9—C10	0.76 (14)
C4—C5—C6—C1	1.37 (13)	C8—C9—C10—C11	-0.71 (14)
C4—C5—C6—N1	179.37 (8)	C8—C9—C10—C13	178.27 (9)
C1—C6—N1—S1	-136.73 (8)	C9—C10—C11—C12	0.13 (14)
C5—C6—N1—S1	45.32 (12)	C13—C10—C11—C12	-178.85 (9)
C6—N1—S1—O2	-61.97 (9)	C10—C11—C12—C7	0.39 (14)
C6—N1—S1—O1	170.10 (8)	C8—C7—C12—C11	-0.34 (14)
C6—N1—S1—C7	53.65 (9)	S1—C7—C12—C11	-179.96 (7)

Hydrogen-bond geometry (Å, º)

D—H···A	D—H	H···A	D···A	D—H···A
N1—H1···Br1	0.81 (1)	2.71 (2)	3.0943 (8)	112 (2)
N1—H1···O1[i]	0.81 (1)	2.29 (2)	2.9740 (11)	143 (2)

Symmetry code: (i) -*x*+1, -*y*+2, -*z*+1.

Computing details

Data collection: Bruker *APEX* 2; cell refinement: Bruker *SAINT*; data reduction: Bruker *SAINT*; program(s) used to solve structure: *SHELXS97* (Sheldrick, 2008); program(s) used to refine structure: *SHELXL2012* (Sheldrick, 2012); molecular graphics: Bruker *SHELXTL*; software used to prepare material for publication: Bruker *SHELXTL*.

Special details

Geometry. All esds (except the esd in the dihedral angle between two l.s. planes) are estimated using the full covariance matrix. The cell esds are taken into account individually in the estimation of esds in distances, angles and torsion angles; correlations between esds in cell parameters are only used when they are defined by crystal symmetry. An approximate (isotropic) treatment of cell esds is used for estimating esds involving l.s. planes.

5.1.5. Compound 100 X-ray crystal structure data
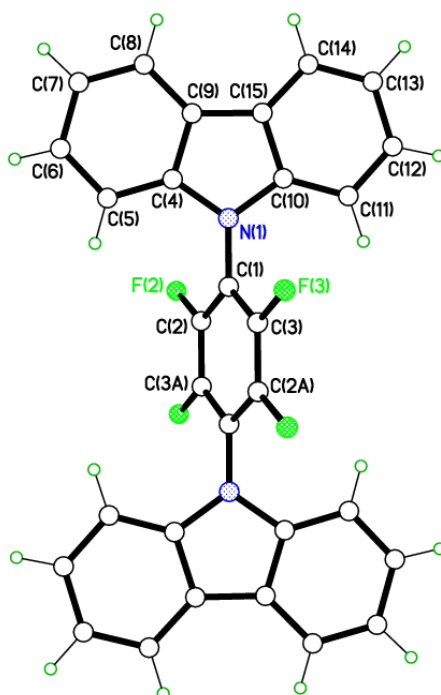
Table 1. Crystal data and structure refinement for gwals2.

Identification code	gwals2
Chemical formula	$C_{30}H_{16}F_4N_2$
Formula weight	480.45
Temperature	150(2) K
Radiation, wavelength	synchrotron, 0.7749 Å
Crystal system, space group	orthorhombic, Pbca
Unit cell parameters	a = 14.7832(5) Å $\alpha = 90°$
	b = 8.2739(3) Å $\beta = 90°$
	c = 17.6768(6) Å $\gamma = 90°$
Cell volume	2162.13(13) Å^3
Z	4
Calculated density	1.476 g/cm^3
Absorption coefficient μ	0.134 mm^1
F(000)	984
Crystal colour and size	colourless, 0.25 0.03 0.02 mm^3
Reflections for cell refinement	9941 (θ range 2.93 to 39.25°)
Data collection method	Bruker APEX 2 CCD diffractometer
	φ rotation with narrow frames

θ range for data collection	2.51 to 40.19°
Index ranges	h 24 to 24, k 13 to 13, l 29 to 28
Completeness to $\theta = 35.00°$	99.9 %
Intensity decay	0%
Reflections collected	30700
Independent reflections	5147 ($R_{int} = 0.0625$)
Reflections with $F^2 > 2\sigma$	4153
Absorption correction	semi-empirical from equivalents
Min. and max. transmission	0.967 and 0.997
Structure solution	direct methods
Refinement method	Full-matrix least-squares on F^2
Weighting parameters a, b	0.0839, 0.2174
Data / restraints / parameters	5147 / 0 / 195
Final R indices [$F^2 > 2\sigma$]	R1 = 0.0506, wR2 = 0.1448
R indices (all data)	R1 = 0.0608, wR2 = 0.1550
Goodness-of-fit on F^2	1.050
Largest and mean shift/su	0.001 and 0.000
Largest diff. peak and hole	0.502 and 0.427 e Å^3

Table 2. Atomic coordinates and equivalent isotropic displacement parameters ($\mathring{A}^2$) for gwals2. U_{eq} is defined as one third of the trace of the orthogonalized U^{ij} tensor.

	x	y	z	U_{eq}
C(1)	0.46278(6)	0.59709(10)	0.44209(4)	0.02303(15)
C(2)	0.41300(6)	0.55643(11)	0.50607(5)	0.02470(15)
F(2)	0.32779(4)	0.60636(8)	0.51282(4)	0.03373(15)
C(3)	0.55066(6)	0.53892(10)	0.43772(5)	0.02420(15)
F(3)	0.60254(4)	0.58138(8)	0.37924(3)	0.03276(15)
N(1)	0.42697(5)	0.69386(9)	0.38470(4)	0.02488(14)
C(4)	0.39698(5)	0.85197(10)	0.39373(5)	0.02277(15)
C(5)	0.40086(6)	0.94844(11)	0.45749(5)	0.02678(16)
C(6)	0.36719(7)	1.10398(12)	0.45100(6)	0.03168(19)
C(7)	0.33155(7)	1.16053(12)	0.38269(7)	0.0338(2)
C(8)	0.32852(6)	1.06317(12)	0.31937(6)	0.03023(18)
C(9)	0.36120(5)	0.90572(10)	0.32453(5)	0.02360(15)
C(10)	0.40922(6)	0.64446(11)	0.31067(5)	0.02467(15)
C(11)	0.42440(7)	0.49583(13)	0.27725(6)	0.03122(18)
C(12)	0.39521(8)	0.47640(15)	0.20313(6)	0.0372(2)
C(13)	0.35259(8)	0.60178(16)	0.16414(5)	0.0371(2)
C(14)	0.33904(7)	0.75016(13)	0.19771(5)	0.03111(19)
C(15)	0.36788(5)	0.77349(11)	0.27200(5)	0.02438(15)

Table 3. Bond lengths [Å] and angles [°] for gwals2.

C(1)–C(3)	1.3876(11)	C(1)–C(2)	1.3905(12)
C(1)–N(1)	1.3965(10)	C(2)–F(2)	1.3311(10)
C(2)–C(3')	1.3778(11)	C(3)–F(3)	1.3343(10)
C(3)–C(2')	1.3778(11)	N(1)–C(4)	1.3905(11)
N(1)–C(10)	1.3958(11)	C(4)–C(5)	1.3823(13)
C(4)–C(9)	1.4049(11)	C(5)–C(6)	1.3846(13)
C(6)–C(7)	1.3981(15)	C(7)–C(8)	1.3798(16)
C(8)–C(9)	1.3924(12)	C(9)–C(15)	1.4384(13)
C(10)–C(11)	1.3826(14)	C(10)–C(15)	1.4073(12)
C(11)–C(12)	1.3887(15)	C(12)–C(13)	1.3958(18)
C(13)–C(14)	1.3782(16)	C(14)–C(15)	1.3942(12)

C(3)–C(1)–C(2)	117.18(7)	C(3)–C(1)–N(1)	120.89(7)
C(2)–C(1)–N(1)	121.93(7)	F(2)–C(2)–C(3')	118.82(7)
F(2)–C(2)–C(1)	119.91(7)	C(3')–C(2)–C(1)	121.25(7)
F(3)–C(3)–C(2')	119.04(7)	F(3)–C(3)–C(1)	119.34(7)
C(2')–C(3)–C(1)	121.57(8)	C(4)–N(1)–C(10)	108.86(7)
C(4)–N(1)–C(1)	125.23(7)	C(10)–N(1)–C(1)	125.76(7)
C(5)–C(4)–N(1)	128.58(7)	C(5)–C(4)–C(9)	122.87(8)
N(1)–C(4)–C(9)	108.54(7)	C(4)–C(5)–C(6)	117.02(8)
C(5)–C(6)–C(7)	121.20(9)	C(8)–C(7)–C(6)	121.17(9)
C(7)–C(8)–C(9)	118.80(8)	C(8)–C(9)–C(4)	118.94(8)
C(8)–C(9)–C(15)	133.88(8)	C(4)–C(9)–C(15)	107.18(7)
C(11)–C(10)–N(1)	129.09(8)	C(11)–C(10)–C(15)	122.52(8)
N(1)–C(10)–C(15)	108.35(8)	C(10)–C(11)–C(12)	117.11(10)
C(11)–C(12)–C(13)	121.34(10)	C(14)–C(13)–C(12)	121.00(9)
C(13)–C(14)–C(15)	118.97(9)	C(14)–C(15)–C(10)	119.03(9)
C(14)–C(15)–C(9)	133.82(8)	C(10)–C(15)–C(9)	107.06(7)

Symmetry operations for equivalent atoms
' x+1,y+1,z+1

Table 4. Hydrogen coordinates and isotropic displacement parameters (Å^2) for gwals2.

	x	y	z	U
H(5)	0.4264(10)	0.9101(19)	0.5041(8)	0.034(4)
H(6)	0.3671(11)	1.174(2)	0.4937(9)	0.041(4)
H(7)	0.3073(10)	1.271(2)	0.3810(9)	0.039(4)
H(8)	0.3029(10)	1.100(2)	0.2730(9)	0.039(4)
H(11)	0.4548(11)	0.4058(19)	0.3037(8)	0.038(4)
H(12)	0.4056(13)	0.375(3)	0.1765(11)	0.059(5)
H(13)	0.3316(12)	0.587(2)	0.1111(9)	0.043(4)
H(14)	0.3066(11)	0.836(2)	0.1714(9)	0.041(4)

Table 5. Torsion angles [°] for gwals2.

C(3)–C(1)–C(2)–F(2)	178.83(8)	N(1)–C(1)–C(2)–F(2)	1.91(14)
C(3)–C(1)–C(2)–C(3')	0.62(15)	N(1)–C(1)–C(2)–C(3')	179.88(9)
C(2)–C(1)–C(3)–F(3)	176.68(8)	N(1)–C(1)–C(3)–F(3)	2.59(13)
C(2)–C(1)–C(3)–C(2')	0.62(15)	N(1)–C(1)–C(3)–C(2')	179.89(8)
C(3)–C(1)–N(1)–C(4)	118.55(10)	C(2)–C(1)–N(1)–C(4)	60.68(13)
C(3)–C(1)–N(1)–C(10)	66.49(12)	C(2)–C(1)–N(1)–C(10)	114.27(10)
C(10)–N(1)–C(4)–C(5)	179.99(9)	C(1)–N(1)–C(4)–C(5)	4.32(15)
C(10)–N(1)–C(4)–C(9)	1.10(10)	C(1)–N(1)–C(4)–C(9)	176.78(8)
N(1)–C(4)–C(5)–C(6)	178.96(9)	C(9)–C(4)–C(5)–C(6)	0.20(13)
C(4)–C(5)–C(6)–C(7)	0.44(14)	C(5)–C(6)–C(7)–C(8)	0.13(16)
C(6)–C(7)–C(8)–C(9)	0.43(15)	C(7)–C(8)–C(9)–C(4)	0.66(13)
C(7)–C(8)–C(9)–C(15)	179.33(9)	C(5)–C(4)–C(9)–C(8)	0.35(13)
N(1)–C(4)–C(9)–C(8)	178.63(8)	C(5)–C(4)–C(9)–C(15)	179.64(8)
N(1)–C(4)–C(9)–C(15)	1.38(9)	C(4)–N(1)–C(10)–C(11)	177.51(9)
C(1)–N(1)–C(10)–C(11)	1.86(15)	C(4)–N(1)–C(10)–C(15)	0.37(10)
C(1)–N(1)–C(10)–C(15)	176.02(8)	N(1)–C(10)–C(11)–C(12)	176.30(9)
C(15)–C(10)–C(11)–C(12)	1.31(14)	C(10)–C(11)–C(12)–C(13)	0.13(15)
C(11)–C(12)–C(13)–C(14)	0.83(17)	C(12)–C(13)–C(14)–C(15)	0.60(15)
C(13)–C(14)–C(15)–C(10)	0.54(13)	C(13)–C(14)–C(15)–C(9)	176.54(9)
C(11)–C(10)–C(15)–C(14)	1.55(13)	N(1)–C(10)–C(15)–C(14)	176.50(8)
C(11)–C(10)–C(15)–C(9)	178.53(8)	N(1)–C(10)–C(15)–C(9)	0.48(10)
C(8)–C(9)–C(15)–C(14)	4.79(17)	C(4)–C(9)–C(15)–C(14)	175.20(9)
C(8)–C(9)–C(15)–C(10)	178.87(9)	C(4)–C(9)–C(15)–C(10)	1.14(9)

Symmetry operations for equivalent atoms
' x+1,y+1,z+1

5.1.6. Compound 101 X-ray crystal structure data
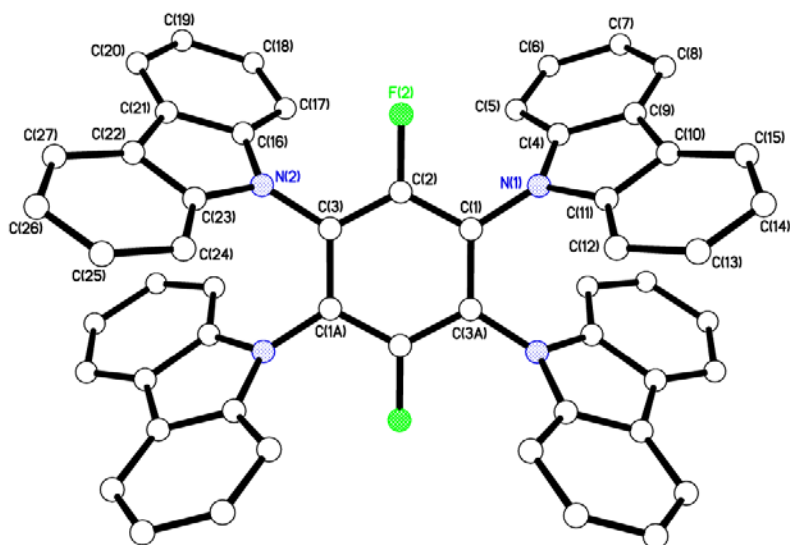
Table 1. Crystal data and structure refinement for gwals2a.

Identification code	gwals2a
Chemical formula	$C_{55}H_{34}Cl_2F_2N_4$
Formula weight	859.76
Temperature	150(2) K
Radiation, wavelength	synchrotron, 0.7749 Å
Crystal system, space group	monoclinic, $P2_1/c$
Unit cell parameters	a = 17.2455(14) Å $\quad$ $\langle$ = 90°
	b = 13.8799(12) Å $\quad$ $\circledR$ = 106.2291(11)°
	c = 18.1458(15) Å $\quad$ $\copyright$ = 90°
Cell volume	4170.4(6) Å^3
Z	4
Calculated density	1.369 g/cm^3
Absorption coefficient ⌈	0.260 mm^1
F(000)	1776
Crystal colour and size	colourless, 0.14 0.04 0.03 mm^3
Reflections for cell refinement	9809 (⌊ range 3.01 to 33.55°)
Data collection method	Bruker APEX 2 CCD diffractometer
	⌉ rotation with narrow frames
⌊ range for data collection	2.99 to 33.62°
Index ranges	h 24 to 24, k 19 to 19, l 25 to 25
Completeness to ⌊ = 33.62°	99.7 %

Intensity decay	0%
Reflections collected	119736
Independent reflections	12707 (R_{int} = 0.0735)
Reflections with $F^2 > 2\sigma$	10332
Absorption correction	semi-empirical from equivalents
Min. and max. transmission	0.965 and 0.992
Structure solution	direct methods
Refinement method	Full-matrix least-squares on F^2
Weighting parameters a, b	0.0705, 1.1150
Data / restraints / parameters	12707 / 132 / 750
Final R indices [$F^2 > 2\sigma$]	R1 = 0.0507, wR2 = 0.1351
R indices (all data)	R1 = 0.0623, wR2 = 0.1460
Goodness-of-fit on F^2	1.029
Largest and mean shift/su	0.001 and 0.000
Largest diff. peak and hole	0.475 and 0.484 e $Å^3$

Table 2. Atomic coordinates and equivalent isotropic displacement parameters (Å^2) for gwals2a. U_{eq} is defined as one third of the trace of the orthogonalized U^{ij} tensor.

	x	y	z	U_{eq}
C(1)	0.00026(7)	0.42833(8)	0.44472(6)	0.0255(2)
C(2)	0.00717(7)	0.52561(8)	0.43042(6)	0.0258(2)
F(2)	0.01985(5)	0.55015(5)	0.36296(4)	0.03078(16)
C(3)	0.00759(7)	0.59844(7)	0.48289(6)	0.0256(2)
N(1)	0.00271(6)	0.36120(7)	0.38757(6)	0.02704(19)
C(4)	0.05476(7)	0.35402(8)	0.31588(6)	0.0265(2)
C(5)	0.11803(8)	0.41555(9)	0.28169(7)	0.0310(2)
C(6)	0.16829(8)	0.38931(10)	0.21069(8)	0.0344(3)
C(7)	0.15570(9)	0.30449(11)	0.17452(8)	0.0384(3)
C(8)	0.09265(8)	0.24355(10)	0.20916(8)	0.0358(3)
C(9)	0.04166(7)	0.26789(8)	0.28069(7)	0.0280(2)
C(10)	0.02641(7)	0.22051(8)	0.33292(7)	0.0273(2)
C(11)	0.05261(7)	0.27965(8)	0.39796(7)	0.0260(2)
C(12)	0.11954(8)	0.25726(9)	0.45835(7)	0.0301(2)
N(2)	0.01735(6)	0.69439(7)	0.46298(6)	0.0271(2)
C(13)	0.15871(8)	0.17136(10)	0.45376(8)	0.0337(3)
C(14)	0.13222(8)	0.11033(9)	0.39045(8)	0.0343(3)
C(15)	0.06680(8)	0.13432(9)	0.32969(8)	0.0319(2)
C(16)	0.03724(8)	0.74544(8)	0.40410(7)	0.0285(2)
C(17)	0.10416(9)	0.71257(10)	0.34820(8)	0.0347(3)
C(18)	0.14865(10)	0.77974(11)	0.29717(9)	0.0429(3)
C(19)	0.12643(11)	0.87679(12)	0.30218(10)	0.0486(4)
C(20)	0.06023(10)	0.90902(10)	0.35800(9)	0.0415(3)
C(21)	0.01502(8)	0.84323(8)	0.41063(7)	0.0313(2)
C(22)	0.05443(8)	0.85239(8)	0.47637(7)	0.0304(2)
C(23)	0.07351(7)	0.75955(8)	0.50719(7)	0.0279(2)
C(24)	0.13980(8)	0.74214(9)	0.56935(8)	0.0325(2)
C(25)	0.18535(9)	0.82080(11)	0.60346(9)	0.0395(3)
C(26)	0.16560(9)	0.91385(10)	0.57527(10)	0.0429(3)
C(27)	0.10094(9)	0.93024(9)	0.51183(9)	0.0391(3)
C(28)	0.49970(7)	0.40149(8)	0.52054(6)	0.0250(2)
C(29)	0.50195(7)	0.47565(8)	0.57250(6)	0.0255(2)
F(29)	0.50932(5)	0.45172(5)	0.64594(4)	0.03052(16)
C(30)	0.50212(7)	0.57306(8)	0.55510(6)	0.0246(2)
N(3)	0.50121(6)	0.30563(7)	0.54496(6)	0.0279(2)
C(31)	0.44312(8)	0.26213(9)	0.57475(7)	0.0303(2)
C(32)	0.37564(9)	0.30244(11)	0.58978(8)	0.0375(3)
C(33)	0.32787(11)	0.24234(13)	0.62022(9)	0.0477(4)
C(34)	0.34688(12)	0.14558(13)	0.63447(10)	0.0547(5)
C(35)	0.41273(12)	0.10560(12)	0.61739(9)	0.0494(4)
C(36)	0.46183(9)	0.16388(9)	0.58651(7)	0.0362(3)
C(37)	0.53325(9)	0.14651(9)	0.56204(7)	0.0361(3)
C(38)	0.55652(8)	0.23501(9)	0.53713(7)	0.0303(2)
C(39)	0.62500(8)	0.24470(11)	0.51223(8)	0.0364(3)
C(40)	0.66933(10)	0.16151(13)	0.51026(9)	0.0473(4)
C(41)	0.64622(11)	0.07282(12)	0.53325(10)	0.0547(5)
C(42)	0.57905(11)	0.06450(10)	0.55961(10)	0.0492(4)
N(4)	0.50482(6)	0.64143(7)	0.61257(6)	0.02599(19)
C(43)	0.44710(7)	0.65066(8)	0.65324(6)	0.0256(2)
C(44)	0.38074(8)	0.59266(9)	0.65106(7)	0.0307(2)

C(45)	0.33270(8)	0.61884(10)	0.69754(8)	0.0338(3)
C(46)	0.34957(8)	0.69983(10)	0.74450(8)	0.0355(3)
C(47)	0.41457(8)	0.75843(10)	0.74490(7)	0.0329(2)
C(48)	0.46387(7)	0.73402(8)	0.69856(6)	0.0264(2)
C(49)	0.53479(7)	0.77766(8)	0.68510(6)	0.0270(2)
C(50)	0.55885(7)	0.71859(8)	0.63254(6)	0.0255(2)
C(51)	0.62788(8)	0.73705(9)	0.61000(7)	0.0310(2)
C(52)	0.67175(8)	0.81857(10)	0.63964(8)	0.0358(3)
C(53)	0.64789(9)	0.87943(10)	0.69045(8)	0.0385(3)
C(54)	0.57963(9)	0.85960(9)	0.71364(7)	0.0343(3)
C(55)	0.2110(6)	0.4710(8)	0.3941(5)	0.077(2)
Cl(1)	0.2164(2)	0.5292(3)	0.48154(15)	0.1015(12)
Cl(2)	0.28814(15)	0.5144(2)	0.35603(14)	0.0751(5)
C(55X)	0.2132(11)	0.4733(16)	0.4095(9)	0.136(4)
Cl(1X)	0.2085(2)	0.5000(3)	0.5042(3)	0.133(2)
Cl(2X)	0.2835(4)	0.5294(4)	0.3771(5)	0.188(3)
C(55Y)	0.2307(6)	0.5624(9)	0.3760(6)	0.145(3)
Cl(1Y)	0.2419(4)	0.4996(6)	0.4608(5)	0.174(2)
Cl(2Y)	0.3010(3)	0.5347(5)	0.3244(4)	0.188(3)

Table 3.   Bond lengths [Å] and angles [°] for gwals2a.

C(1)–C(2)	1.3864(15)	C(1)–N(1)	1.4036(14)
C(1)–C(3')	1.4074(15)	C(2)–F(2)	1.3461(12)
C(2)–C(3)	1.3873(15)	C(3)–N(2)	1.4023(14)
C(3)–C(1')	1.4074(15)	N(1)–C(4)	1.4014(15)
N(1)–C(11)	1.4023(14)	C(4)–C(5)	1.3879(17)
C(4)–C(9)	1.4030(15)	C(5)–C(6)	1.3855(19)
C(6)–C(7)	1.394(2)	C(7)–C(8)	1.382(2)
C(8)–C(9)	1.3907(18)	C(9)–C(10)	1.4446(17)
C(10)–C(15)	1.3938(16)	C(10)–C(11)	1.4045(16)
C(11)–C(12)	1.3866(17)	C(12)–C(13)	1.3843(17)
N(2)–C(23)	1.4019(15)	N(2)–C(16)	1.4027(15)
C(13)–C(14)	1.3974(19)	C(14)–C(15)	1.380(2)
C(16)–C(17)	1.3837(19)	C(16)–C(21)	1.4064(16)
C(17)–C(18)	1.385(2)	C(18)–C(19)	1.396(2)
C(19)–C(20)	1.372(2)	C(20)–C(21)	1.3919(18)
C(21)–C(22)	1.4406(19)	C(22)–C(27)	1.3915(18)
C(22)–C(23)	1.4067(16)	C(23)–C(24)	1.3845(18)
C(24)–C(25)	1.3858(19)	C(25)–C(26)	1.396(2)
C(26)–C(27)	1.379(2)	C(28)–C(29)	1.3892(15)
C(28)–N(3)	1.4003(14)	C(28)–C(30")	1.4092(15)
C(29)–F(29)	1.3444(12)	C(29)–C(30)	1.3885(15)
C(30)–N(4)	1.4011(14)	C(30)–C(28")	1.4092(15)
N(3)–C(31)	1.4011(15)	N(3)–C(38)	1.4025(15)
C(31)–C(32)	1.3853(19)	C(31)–C(36)	1.4039(18)
C(32)–C(33)	1.391(2)	C(33)–C(34)	1.390(3)
C(34)–C(35)	1.375(3)	C(35)–C(36)	1.397(2)
C(36)–C(37)	1.442(2)	C(37)–C(42)	1.393(2)
C(37)–C(38)	1.4056(18)	C(38)–C(39)	1.384(2)
C(39)–C(40)	1.391(2)	C(40)–C(41)	1.393(3)
C(41)–C(42)	1.376(3)	N(4)–C(50)	1.3993(14)
N(4)–C(43)	1.4009(14)	C(43)–C(44)	1.3908(17)
C(43)–C(48)	1.4019(16)	C(44)–C(45)	1.3858(17)
C(45)–C(46)	1.3914(19)	C(46)–C(47)	1.3833(19)
C(47)–C(48)	1.3944(16)	C(48)–C(49)	1.4454(17)
C(49)–C(54)	1.3914(17)	C(49)–C(50)	1.4054(16)
C(50)–C(51)	1.3864(17)	C(51)–C(52)	1.3837(18)
C(52)–C(53)	1.395(2)	C(53)–C(54)	1.384(2)
C(55)–Cl(1)	1.760(6)	C(55)–Cl(2)	1.767(6)
C(55X)–Cl(2X)	1.679(11)	C(55X)–Cl(1X)	1.781(10)
C(55Y)–Cl(1Y)	1.731(10)	C(55Y)–Cl(2Y)	1.768(10)
C(2)–C(1)–N(1)	119.10(10)	C(2)–C(1)–C(3')	117.88(10)
N(1)–C(1)–C(3')	123.01(10)	F(2)–C(2)–C(1)	117.45(9)
F(2)–C(2)–C(3)	117.96(9)	C(1)–C(2)–C(3)	124.43(10)
C(2)–C(3)–N(2)	119.54(10)	C(2)–C(3)–C(1')	117.69(10)
N(2)–C(3)–C(1')	122.75(10)	C(4)–N(1)–C(11)	108.40(9)
C(4)–N(1)–C(1)	125.00(10)	C(11)–N(1)–C(1)	125.50(10)
C(5)–C(4)–N(1)	129.41(11)	C(5)–C(4)–C(9)	121.82(11)
N(1)–C(4)–C(9)	108.72(10)	C(6)–C(5)–C(4)	117.60(12)
C(5)–C(6)–C(7)	121.36(13)	C(8)–C(7)–C(6)	120.58(13)
C(7)–C(8)–C(9)	119.19(12)	C(8)–C(9)–C(4)	119.44(12)
C(8)–C(9)–C(10)	133.44(11)	C(4)–C(9)–C(10)	107.10(10)
C(15)–C(10)–C(11)	119.33(12)	C(15)–C(10)–C(9)	133.40(11)

C(11)–C(10)–C(9)	107.27(10)	C(12)–C(11)–N(1)	129.13(11)
C(12)–C(11)–C(10)	122.30(11)	N(1)–C(11)–C(10)	108.52(10)
C(13)–C(12)–C(11)	117.25(11)	C(23)–N(2)–C(3)	125.36(10)
C(23)–N(2)–C(16)	108.62(9)	C(3)–N(2)–C(16)	124.94(10)
C(12)–C(13)–C(14)	121.24(12)	C(15)–C(14)–C(13)	121.13(12)
C(14)–C(15)–C(10)	118.69(12)	C(17)–C(16)–N(2)	129.53(11)
C(17)–C(16)–C(21)	122.12(12)	N(2)–C(16)–C(21)	108.32(11)
C(16)–C(17)–C(18)	117.44(13)	C(17)–C(18)–C(19)	121.01(15)
C(20)–C(19)–C(18)	121.26(14)	C(19)–C(20)–C(21)	118.91(13)
C(20)–C(21)–C(16)	119.22(13)	C(20)–C(21)–C(22)	133.38(12)
C(16)–C(21)–C(22)	107.39(11)	C(27)–C(22)–C(23)	119.14(13)
C(27)–C(22)–C(21)	133.62(12)	C(23)–C(22)–C(21)	107.23(10)
C(24)–C(23)–N(2)	129.40(11)	C(24)–C(23)–C(22)	122.13(11)
N(2)–C(23)–C(22)	108.43(11)	C(23)–C(24)–C(25)	117.54(12)
C(24)–C(25)–C(26)	121.03(14)	C(27)–C(26)–C(25)	121.06(13)
C(26)–C(27)–C(22)	119.01(13)	C(29)–C(28)–N(3)	119.65(10)
C(29)–C(28)–C(30")	117.66(10)	N(3)–C(28)–C(30")	122.67(10)
F(29)–C(29)–C(30)	117.40(10)	F(29)–C(29)–C(28)	117.82(10)
C(30)–C(29)–C(28)	124.65(10)	C(29)–C(30)–N(4)	119.47(10)
C(29)–C(30)–C(28")	117.69(10)	N(4)–C(30)–C(28")	122.83(10)
C(28)–N(3)–C(31)	125.42(10)	C(28)–N(3)–C(38)	125.81(10)
C(31)–N(3)–C(38)	108.53(10)	C(32)–C(31)–N(3)	129.23(12)
C(32)–C(31)–C(36)	122.17(12)	N(3)–C(31)–C(36)	108.57(12)
C(31)–C(32)–C(33)	117.35(15)	C(34)–C(33)–C(32)	121.23(17)
C(35)–C(34)–C(33)	121.00(14)	C(34)–C(35)–C(36)	119.22(15)
C(35)–C(36)–C(31)	118.96(15)	C(35)–C(36)–C(37)	133.85(14)
C(31)–C(36)–C(37)	107.19(11)	C(42)–C(37)–C(38)	119.24(15)
C(42)–C(37)–C(36)	133.40(14)	C(38)–C(37)–C(36)	107.36(11)
C(39)–C(38)–N(3)	129.19(12)	C(39)–C(38)–C(37)	122.44(12)
N(3)–C(38)–C(37)	108.35(12)	C(38)–C(39)–C(40)	116.94(15)
C(39)–C(40)–C(41)	121.38(16)	C(42)–C(41)–C(40)	121.14(14)
C(41)–C(42)–C(37)	118.83(15)	C(50)–N(4)–C(43)	108.26(9)
C(50)–N(4)–C(30)	126.33(10)	C(43)–N(4)–C(30)	124.98(10)
C(44)–C(43)–N(4)	129.21(10)	C(44)–C(43)–C(48)	121.85(11)
N(4)–C(43)–C(48)	108.91(10)	C(45)–C(44)–C(43)	117.26(11)
C(44)–C(45)–C(46)	121.76(12)	C(47)–C(46)–C(45)	120.58(12)
C(46)–C(47)–C(48)	118.93(12)	C(47)–C(48)–C(43)	119.58(11)
C(47)–C(48)–C(49)	133.42(11)	C(43)–C(48)–C(49)	107.00(10)
C(54)–C(49)–C(50)	119.38(11)	C(54)–C(49)–C(48)	133.48(11)
C(50)–C(49)–C(48)	107.13(10)	C(51)–C(50)–N(4)	129.02(11)
C(51)–C(50)–C(49)	122.22(11)	N(4)–C(50)–C(49)	108.70(10)
C(52)–C(51)–C(50)	117.24(12)	C(51)–C(52)–C(53)	121.46(13)
C(54)–C(53)–C(52)	120.92(12)	C(53)–C(54)–C(49)	118.74(12)
Cl(1)–C(55)–Cl(2)	109.9(4)	Cl(2X)–C(55X)–Cl(1X)	118.2(8)
Cl(1Y)–C(55Y)–Cl(2Y)	116.0(7)		

Symmetry operations for equivalent atoms
' x,y+1,z+1   " x+1,y+1,z+1

Table 4.   Hydrogen coordinates and isotropic displacement parameters (Å^2) for gwals2a.

	x	y	z	U
H(5)	0.1277(10)	0.4752(12)	0.3079(10)	0.039(4)
H(6)	0.2142(10)	0.4318(12)	0.1856(10)	0.039(4)
H(7)	0.1939(11)	0.2890(13)	0.1230(11)	0.044(5)
H(8)	0.0833(11)	0.1829(13)	0.1853(11)	0.046(5)
H(12)	0.1369(10)	0.3005(12)	0.5033(10)	0.037(4)
H(13)	0.2061(11)	0.1543(13)	0.4961(10)	0.041(4)
H(14)	0.1599(11)	0.0476(13)	0.3903(10)	0.043(4)
H(15)	0.0485(10)	0.0939(12)	0.2853(9)	0.037(4)
H(17)	0.1187(10)	0.6446(13)	0.3441(10)	0.041(4)
H(18)	0.1974(12)	0.7581(14)	0.2590(12)	0.053(5)
H(19)	0.1595(14)	0.9240(17)	0.2651(13)	0.069(6)
H(20)	0.0426(12)	0.9776(14)	0.3634(11)	0.053(5)
H(24)	0.1550(11)	0.6765(13)	0.5884(10)	0.042(4)
H(25)	0.2322(12)	0.8136(14)	0.6489(11)	0.051(5)
H(26)	0.1974(12)	0.9685(15)	0.5991(12)	0.056(5)
H(27)	0.0860(11)	0.9954(14)	0.4893(11)	0.047(5)
H(32)	0.3631(11)	0.3720(14)	0.5813(11)	0.048(5)
H(33)	0.2800(12)	0.2696(15)	0.6323(12)	0.057(5)
H(34)	0.3123(13)	0.1058(16)	0.6573(12)	0.067(6)
H(35)	0.4245(12)	0.0403(15)	0.6273(12)	0.055(5)
H(39)	0.6414(11)	0.3092(13)	0.4952(10)	0.045(5)
H(40)	0.7180(12)	0.1671(14)	0.4920(11)	0.053(5)
H(41)	0.6773(13)	0.0165(16)	0.5293(12)	0.063(6)
H(42)	0.5632(12)	0.0005(15)	0.5770(11)	0.057(5)
H(44)	0.3682(10)	0.5345(12)	0.6160(10)	0.041(4)
H(45)	0.2849(11)	0.5795(14)	0.6970(11)	0.048(5)
H(46)	0.3144(11)	0.7148(13)	0.7770(11)	0.048(5)
H(47)	0.4240(11)	0.8146(13)	0.7780(10)	0.044(5)
H(51)	0.6438(10)	0.6956(12)	0.5738(10)	0.038(4)
H(52)	0.7212(11)	0.8334(13)	0.6251(10)	0.046(5)
H(53)	0.6821(11)	0.9380(13)	0.7112(10)	0.046(5)
H(54)	0.5625(11)	0.9026(14)	0.7489(10)	0.047(5)
H(55A)	0.1576	0.4831	0.3572	0.093
H(55B)	0.2172	0.4006	0.4025	0.093
H(55C)	0.2217	0.4030	0.4065	0.163
H(55D)	0.1597	0.4881	0.3737	0.163
H(55E)	0.2346	0.6321	0.3879	0.174
H(55F)	0.1757	0.5501	0.3422	0.174

Table 5. Torsion angles [°] for gwals2a.

N(1)–C(1)–C(2)–F(2)	3.12(17)	C(3')–C(1)–C(2)–F(2)	175.83(10)
N(1)–C(1)–C(2)–C(3)	178.35(11)	C(3')–C(1)–C(2)–C(3)	0.6(2)
F(2)–C(2)–C(3)–N(2)	2.88(17)	C(1)–C(2)–C(3)–N(2)	178.10(11)
F(2)–C(2)–C(3)–C(1')	175.80(10)	C(1)–C(2)–C(3)–C(1')	0.6(2)
C(2)–C(1)–N(1)–C(4)	64.52(16)	C(3')–C(1)–N(1)–C(4)	116.59(13)
C(2)–C(1)–N(1)–C(11)	128.95(12)	C(3')–C(1)–N(1)–C(11)	49.94(17)
C(11)–N(1)–C(4)–C(5)	177.77(12)	C(1)–N(1)–C(4)–C(5)	9.30(19)
C(11)–N(1)–C(4)–C(9)	0.15(13)	C(1)–N(1)–C(4)–C(9)	168.32(10)
N(1)–C(4)–C(5)–C(6)	177.65(12)	C(9)–C(4)–C(5)–C(6)	0.30(18)
C(4)–C(5)–C(6)–C(7)	0.35(19)	C(5)–C(6)–C(7)–C(8)	0.6(2)
C(6)–C(7)–C(8)–C(9)	0.1(2)	C(7)–C(8)–C(9)–C(4)	0.55(19)
C(7)–C(8)–C(9)–C(10)	177.50(13)	C(5)–C(4)–C(9)–C(8)	0.76(18)
N(1)–C(4)–C(9)–C(8)	178.59(11)	C(5)–C(4)–C(9)–C(10)	177.76(11)
N(1)–C(4)–C(9)–C(10)	0.07(13)	C(8)–C(9)–C(10)–C(15)	1.8(2)
C(4)–C(9)–C(10)–C(15)	179.93(13)	C(8)–C(9)–C(10)–C(11)	178.49(14)
C(4)–C(9)–C(10)–C(11)	0.27(13)	C(4)–N(1)–C(11)–C(12)	177.04(12)
C(1)–N(1)–C(11)–C(12)	14.56(19)	C(4)–N(1)–C(11)–C(10)	0.32(13)
C(1)–N(1)–C(11)–C(10)	168.08(11)	C(15)–C(10)–C(11)–C(12)	2.50(18)
C(9)–C(10)–C(11)–C(12)	177.22(11)	C(15)–C(10)–C(11)–N(1)	179.92(10)
C(9)–C(10)–C(11)–N(1)	0.36(13)	N(1)–C(11)–C(12)–C(13)	179.42(12)
C(10)–C(11)–C(12)–C(13)	2.38(18)	C(2)–C(3)–N(2)–C(23)	129.13(13)
C(1')–C(3)–N(2)–C(23)	49.48(17)	C(2)–C(3)–N(2)–C(16)	64.18(16)
C(1')–C(3)–N(2)–C(16)	117.21(13)	C(11)–C(12)–C(13)–C(14)	0.62(19)
C(12)–C(13)–C(14)–C(15)	1.0(2)	C(13)–C(14)–C(15)–C(10)	0.94(19)
C(11)–C(10)–C(15)–C(14)	0.77(18)	C(9)–C(10)–C(15)–C(14)	178.86(13)
C(23)–N(2)–C(16)–C(17)	177.69(12)	C(3)–N(2)–C(16)–C(17)	9.1(2)
C(23)–N(2)–C(16)–C(21)	0.59(13)	C(3)–N(2)–C(16)–C(21)	169.17(10)
N(2)–C(16)–C(17)–C(18)	179.12(13)	C(21)–C(16)–C(17)–C(18)	1.05(19)
C(16)–C(17)–C(18)–C(19)	0.1(2)	C(17)–C(18)–C(19)–C(20)	0.5(3)
C(18)–C(19)–C(20)–C(21)	0.4(2)	C(19)–C(20)–C(21)–C(16)	1.5(2)
C(19)–C(20)–C(21)–C(22)	177.55(15)	C(17)–C(16)–C(21)–C(20)	1.85(19)
N(2)–C(16)–C(21)–C(20)	179.72(12)	C(17)–C(16)–C(21)–C(22)	177.39(11)
N(2)–C(16)–C(21)–C(22)	1.04(13)	C(20)–C(21)–C(22)–C(27)	1.0(3)
C(16)–C(21)–C(22)–C(27)	178.05(14)	C(20)–C(21)–C(22)–C(23)	179.81(14)
C(16)–C(21)–C(22)–C(23)	1.10(13)	C(3)–N(2)–C(23)–C(24)	13.89(19)
C(16)–N(2)–C(23)–C(24)	177.59(12)	C(3)–N(2)–C(23)–C(22)	168.41(11)
C(16)–N(2)–C(23)–C(22)	0.11(13)	C(27)–C(22)–C(23)–C(24)	3.55(19)
C(21)–C(22)–C(23)–C(24)	177.16(11)	C(27)–C(22)–C(23)–N(2)	178.55(11)
C(21)–C(22)–C(23)–N(2)	0.75(13)	N(2)–C(23)–C(24)–C(25)	179.33(12)
C(22)–C(23)–C(24)–C(25)	3.24(19)	C(23)–C(24)–C(25)–C(26)	0.9(2)
C(24)–C(25)–C(26)–C(27)	1.1(2)	C(25)–C(26)–C(27)–C(22)	0.8(2)
C(23)–C(22)–C(27)–C(26)	1.4(2)	C(21)–C(22)–C(27)–C(26)	179.50(14)
N(3)–C(28)–C(29)–F(29)	3.02(16)	C(30")–C(28)–C(29)–F(29)	175.49(10)
N(3)–C(28)–C(29)–C(30)	178.87(11)	C(30")–C(28)–C(29)–C(30)	0.4(2)
F(29)–C(29)–C(30)–N(4)	3.89(16)	C(28)–C(29)–C(30)–N(4)	179.75(11)
F(29)–C(29)–C(30)–C(28")	175.52(10)	C(28)–C(29)–C(30)–C(28")	0.3(2)
C(29)–C(28)–N(3)–C(31)	61.14(16)	C(30")–C(28)–N(3)–C(31)	120.42(13)
C(29)–C(28)–N(3)–C(38)	125.23(13)	C(30")–C(28)–N(3)–C(38)	53.22(17)
C(28)–N(3)–C(31)–C(32)	3.2(2)	C(38)–N(3)–C(31)–C(32)	177.72(13)
C(28)–N(3)–C(31)–C(36)	175.05(11)	C(38)–N(3)–C(31)–C(36)	0.49(13)
N(3)–C(31)–C(32)–C(33)	179.53(13)	C(36)–C(31)–C(32)–C(33)	2.5(2)
C(31)–C(32)–C(33)–C(34)	0.4(2)	C(32)–C(33)–C(34)–C(35)	1.4(2)
C(33)–C(34)–C(35)–C(36)	1.1(2)	C(34)–C(35)–C(36)–C(31)	0.9(2)

C(34)–C(35)–C(36)–C(37)	179.54(15)	C(32)–C(31)–C(36)–C(35)	2.74(19)
N(3)–C(31)–C(36)–C(35)	178.89(12)	C(32)–C(31)–C(36)–C(37)	177.57(12)
N(3)–C(31)–C(36)–C(37)	0.80(14)	C(35)–C(36)–C(37)–C(42)	0.8(3)
C(31)–C(36)–C(37)–C(42)	179.60(15)	C(35)–C(36)–C(37)–C(38)	178.82(15)
C(31)–C(36)–C(37)–C(38)	0.81(14)	C(28)–N(3)–C(38)–C(39)	7.5(2)
C(31)–N(3)–C(38)–C(39)	177.98(12)	C(28)–N(3)–C(38)–C(37)	174.51(11)
C(31)–N(3)–C(38)–C(37)	0.03(13)	C(42)–C(37)–C(38)–C(39)	2.01(19)
C(36)–C(37)–C(38)–C(39)	177.65(12)	C(42)–C(37)–C(38)–N(3)	179.83(12)
C(36)–C(37)–C(38)–N(3)	0.51(14)	N(3)–C(38)–C(39)–C(40)	179.90(12)
C(37)–C(38)–C(39)–C(40)	2.14(19)	C(38)–C(39)–C(40)–C(41)	0.8(2)
C(39)–C(40)–C(41)–C(42)	0.7(2)	C(40)–C(41)–C(42)–C(37)	0.9(2)
C(38)–C(37)–C(42)–C(41)	0.4(2)	C(36)–C(37)–C(42)–C(41)	179.14(15)
C(29)–C(30)–N(4)–C(50)	128.70(12)	C(28")–C(30)–N(4)–C(50)	50.67(17)
C(29)–C(30)–N(4)–C(43)	59.72(16)	C(28")–C(30)–N(4)–C(43)	120.91(13)
C(50)–N(4)–C(43)–C(44)	178.50(12)	C(30)–N(4)–C(43)–C(44)	5.63(19)
C(50)–N(4)–C(43)–C(48)	0.51(13)	C(30)–N(4)–C(43)–C(48)	172.36(10)
N(4)–C(43)–C(44)–C(45)	179.72(12)	C(48)–C(43)–C(44)–C(45)	1.95(18)
C(43)–C(44)–C(45)–C(46)	0.2(2)	C(44)–C(45)–C(46)–C(47)	1.4(2)
C(45)–C(46)–C(47)–C(48)	1.2(2)	C(46)–C(47)–C(48)–C(43)	0.53(18)
C(46)–C(47)–C(48)–C(49)	179.91(13)	C(44)–C(43)–C(48)–C(47)	2.17(18)
N(4)–C(43)–C(48)–C(47)	179.66(11)	C(44)–C(43)–C(48)–C(49)	178.17(11)
N(4)–C(43)–C(48)–C(49)	0.00(13)	C(47)–C(48)–C(49)–C(54)	0.2(2)
C(43)–C(48)–C(49)–C(54)	179.39(13)	C(47)–C(48)–C(49)–C(50)	179.10(13)
C(43)–C(48)–C(49)–C(50)	0.50(13)	C(43)–N(4)–C(50)–C(51)	176.37(12)
C(30)–N(4)–C(50)–C(51)	10.89(19)	C(43)–N(4)–C(50)–C(49)	0.83(13)
C(30)–N(4)–C(50)–C(49)	171.92(11)	C(54)–C(49)–C(50)–C(51)	2.47(18)
C(48)–C(49)–C(50)–C(51)	176.61(11)	C(54)–C(49)–C(50)–N(4)	179.89(11)
C(48)–C(49)–C(50)–N(4)	0.82(13)	N(4)–C(50)–C(51)–C(52)	178.81(12)
C(49)–C(50)–C(51)–C(52)	1.95(18)	C(50)–C(51)–C(52)–C(53)	0.4(2)
C(51)–C(52)–C(53)–C(54)	0.7(2)	C(52)–C(53)–C(54)–C(49)	0.2(2)
C(50)–C(49)–C(54)–C(53)	1.33(19)	C(48)–C(49)–C(54)–C(53)	177.45(13)

Symmetry operations for equivalent atoms
' x,y+1,z+1 " x+1,y+1,z+1

5.1.7. Compound 105 X-ray crystal structure data
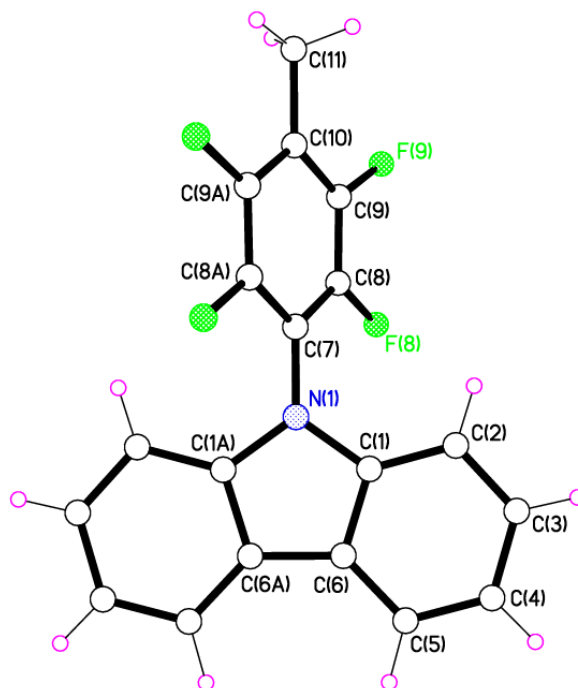
Crystal data

$C_{19}H_{11}F_4N$	$D_x = 1.491$ Mg m^{-3}
$M_r = 329.29$	Mo $K\alpha$ radiation, $\lambda = 0.71073$ Å
Orthorhombic, *Pbcn*	Cell parameters from 6104 reflections
$a = 7.6086$ (6) Å	$\theta = 2.6$–31.3°
$b = 12.4954$ (9) Å	$\mu = 0.12$ mm^{-1}
$c = 15.4335$ (11) Å	$T = 150$ K
$V = 1467.30$ (19) Å^3	Block, yellow
$Z = 4$	$0.77 \times 0.40 \times 0.20$ mm
$F(000) = 672$	

Data collection

Bruker APEX 2 CCD diffractometer	2365 independent reflections
Radiation source: fine-focus sealed tube	2014 reflections with $I > 2\sigma(I)$
graphite	$R_{int} = 0.023$
ω rotation with narrow frames scans	$\theta_{max} = 31.5°$, $\theta_{min} = 2.6°$
Absorption correction: multi-scan *SADABS* v2 Sheldrick, G.M., (2009)	$h = -10 \square 11$
$T_{min} = 0.911$, $T_{max} = 0.976$	$k = -17 \square 18$
16055 measured reflections	$l = -22 \square 22$

Refinement

Refinement on F^2	Primary atom site location: structure-invariant di methods
Least-squares matrix: full	Secondary atom site location: all non-H atoms fr direct methods
$R[F^2 > 2\sigma(F^2)] = 0.046$	Hydrogen site location: mixed
$wR(F^2) = 0.139$	H atoms treated by a mixture of independent and constrained refinement
$S = 1.04$	$w = 1/[\sigma^2(F_o^2) + (0.0907P)^2 + 0.222P]$ $(F_o^2 + 2F_c^2)/3$
2365 reflections	$(\Delta/\sigma)_{max} < 0.001$
127 parameters	$\Delta\rangle_{max} = 0.44$ e Å^{-3}
0 restraints	$\Delta\rangle_{min} = -0.19$ e Å^{-3}

Fractional atomic coordinates and isotropic or equivalent isotropic displacement parameters (Å^2)

	x	y	z	$U_{iso}*/U_{eq}$	Occ. (<1)
N1	0.0000	0.30863 (8)	0.2500	0.0239 (2)	
C1	0.05896 (12)	0.24315 (7)	0.18205 (5)	0.0230 (2)	
C2	0.13210 (15)	0.27195 (8)	0.10282 (6)	0.0290 (2)	
H2	0.1476 (19)	0.3461 (12)	0.0855 (9)	0.037 (4)*	
C3	0.18233 (16)	0.18998 (8)	0.04738 (7)	0.0334 (2)	
H3	0.2374 (19)	0.2069 (10)	-0.0071 (9)	0.037 (4)*	
C4	0.15930 (15)	0.08220 (9)	0.07009 (7)	0.0336 (3)	
H4	0.192 (2)	0.0274 (12)	0.0299 (10)	0.043 (4)*	
C5	0.08732 (14)	0.05423 (8)	0.14951 (7)	0.0290 (2)	
H5	0.0751 (19)	-0.0222 (11)	0.1654 (9)	0.031 (3)*	
C6	0.03737 (12)	0.13535 (7)	0.20680 (6)	0.0231 (2)	
C7	0.0000	0.42095 (10)	0.2500	0.0230 (3)	
C8	-0.08293 (13)	0.47953 (8)	0.18501 (6)	0.0272 (2)	
F8	-0.16961 (10)	0.42791 (6)	0.12201 (4)	0.0388 (2)	
C9	-0.07794 (14)	0.59024 (9)	0.18442 (8)	0.0345 (3)	
F9	-0.15644 (11)	0.64085 (7)	0.11771 (6)	0.0531 (3)	
C10	0.0000	0.64836 (11)	0.2500	0.0381 (4)	
C11	0.0000	0.76857 (13)	0.2500	0.0609 (7)	
H11A	0.0613	0.7947	0.3017	0.091*	0.5
H11B	-0.1214	0.7947	0.2504	0.091*	0.5
H11C	0.0601	0.7947	0.1980	0.091*	0.5

Geometric parameters (Å, º)

N1—C7	1.4035 (15)	C6—C6^i	1.4497 (18)
N1—C1^i	1.4037 (10)	C7—C8^i	1.3928 (11)
N1—C1	1.4037 (10)	C7—C8	1.3929 (11)
C1—C2	1.3909 (13)	C8—F8	1.3403 (12)
C1—C6	1.4097 (12)	C8—C9	1.3839 (14)
C2—C3	1.3882 (14)	C9—F9	1.3478 (13)
C2—H2	0.971 (15)	C9—C10	1.3796 (14)
C3—C4	1.4026 (15)	C10—C9^i	1.3796 (15)
C3—H3	0.963 (14)	C10—C11	1.502 (2)
C4—C5	1.3872 (14)	C11—H11A	0.9800
C4—H4	0.957 (16)	C11—H11B	0.9800
C5—C6	1.3977 (13)	C11—H11C	0.9800
C5—H5	0.990 (14)		
C7—N1—C1^i	125.65 (5)	C1—C6—C6^i	107.15 (5)
C7—N1—C1	125.65 (5)	C8^i—C7—C8	116.59 (12)
C1^i—N1—C1	108.69 (10)	C8^i—C7—N1	121.71 (6)
C2—C1—N1	129.34 (8)	C8—C7—N1	121.70 (6)
C2—C1—C6	122.14 (8)	F8—C8—C9	119.33 (9)
N1—C1—C6	108.50 (8)	F8—C8—C7	119.49 (9)
C3—C2—C1	117.47 (9)	C9—C8—C7	121.17 (10)
C3—C2—H2	120.0 (8)	F9—C9—C10	120.26 (10)
C1—C2—H2	122.5 (8)	F9—C9—C8	117.50 (11)
C2—C3—C4	121.33 (9)	C10—C9—C8	122.22 (10)
C2—C3—H3	119.7 (8)	C9—C10—C9^i	116.48 (13)
C4—C3—H3	118.9 (8)	C9—C10—C11	121.76 (6)
C5—C4—C3	120.80 (9)	C9^i—C10—C11	121.76 (6)
C5—C4—H4	119.7 (10)	C10—C11—H11A	109.5
C3—C4—H4	119.5 (9)	C10—C11—H11B	109.5
C4—C5—C6	118.92 (9)	H11A—C11—H11B	109.5
C4—C5—H5	119.9 (8)	C10—C11—H11C	109.5
C6—C5—H5	121.2 (8)	H11A—C11—H11C	109.5
C5—C6—C1	119.33 (8)	H11B—C11—H11C	109.5
C5—C6—C6^i	133.51 (6)		
C7—N1—C1—C2	1.64 (12)	C1—N1—C7—C8^i	-124.67 (7)
C1^i—N1—C1—C2	-178.36 (12)	C1^i—N1—C7—C8	-124.67 (7)
C7—N1—C1—C6	-179.96 (5)	C1—N1—C7—C8	55.33 (7)

C1^i—N1—C1—C6	0.04 (5)	C8^i—C7—C8—F8	-178.01 (10)
N1—C1—C2—C3	178.93 (9)	N1—C7—C8—F8	1.99 (10)
C6—C1—C2—C3	0.72 (15)	C8^i—C7—C8—C9	1.79 (7)
C1—C2—C3—C4	0.38 (17)	N1—C7—C8—C9	-178.21 (7)
C2—C3—C4—C5	-0.83 (18)	F8—C8—C9—F9	-2.38 (14)
C3—C4—C5—C6	0.17 (17)	C7—C8—C9—F9	177.83 (8)
C4—C5—C6—C1	0.90 (15)	F8—C8—C9—C10	176.09 (8)
C4—C5—C6—C6^i	-178.87 (13)	C7—C8—C9—C10	-3.71 (14)
C2—C1—C6—C5	-1.38 (15)	F9—C9—C10—C9^i	-179.75 (11)
N1—C1—C6—C5	-179.91 (8)	C8—C9—C10—C9^i	1.83 (7)
C2—C1—C6—C6^i	178.45 (10)	F9—C9—C10—C11	0.25 (11)
N1—C1—C6—C6^i	-0.09 (12)	C8—C9—C10—C11	-178.17 (7)
C1^i—N1—C7—C8^i	55.33 (7)		

Symmetry code: (i) -x, y, -z+1/2.

Computing details

Data collection: Bruker *APEX* 2; cell refinement: Bruker *SAINT*; data reduction: Bruker *SAINT*; program(s) used to solve structure: *SHELXS97* (Sheldrick, 2008); program(s) used to refine structure: *SHELXL2012* (Sheldrick, 2012); molecular graphics: Bruker *SHELXTL*; software used to prepare material for publication: Bruker *SHELXTL*.

Special details

Geometry. All esds (except the esd in the dihedral angle between two l.s. planes) are estimated using the full covariance matrix. The cell esds are taken into account individually in the estimation of esds in distances, angles and torsion angles; correlations between esds in cell parameters are only used when they are defined by crystal symmetry. An approximate (isotropic) treatment of cell esds is used for estimating esds involving l.s. planes.

5.1.8. Compound 111 X-ray crystal structure data
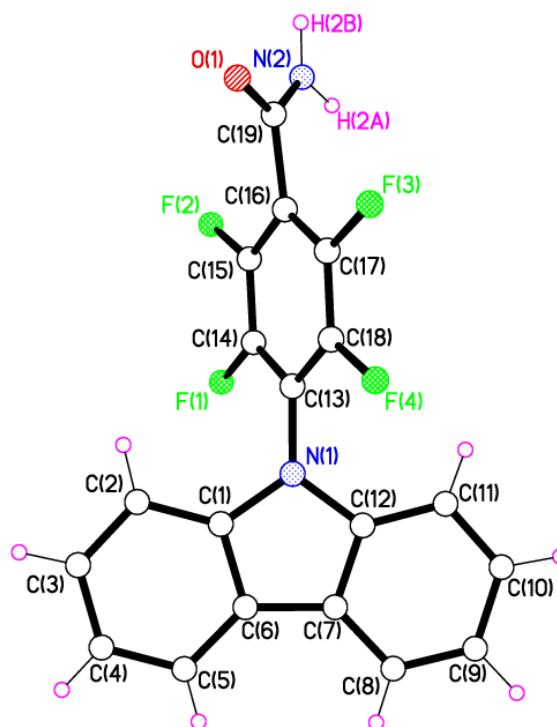
GW92

Crystal data

C$_{19}$H$_{10}$F$_4$N$_2$O	D_x = 1.542 Mg m^{-3}
M_r = 358.29	Mo $K\alpha$ radiation, λ = 0.71073 Å
Orthorhombic, *Pbca*	Cell parameters from 1594 reflections
a = 13.571 (4) Å	θ = 2.9–20.0°
b = 7.963 (2) Å	μ = 0.13 mm^{-1}
c = 28.555 (9) Å	T = 150 K
V = 3085.8 (15) Å^3	Plate, colourless
Z = 8	0.54 × 0.17 × 0.04 mm
F(000) = 1456	

Data collection

Bruker APEX 2 CCD diffractometer	1736 reflections with $I > 2\sigma(I)$
Radiation source: fine-focus sealed tube	R_{int} = 0.132
ω rotation with narrow frames scans	θ_{max} = 26.5°, θ_{min} = 2.1°
Absorption correction: multi-scan *SADABS* v2	h = -16→16

Sheldrick, G.M., (2012)	
$T_{min} = 0.933$, $T_{max} = 0.995$	$k = -9 \square 9$
25328 measured reflections	$l = -35 \square 35$
3161 independent reflections	

Refinement

Refinement on F^2	Secondary atom site location: all non-H atoms fo direct methods
Least-squares matrix: full	Hydrogen site location: difference Fourier map
$R[F^2 > 2\sigma(F^2)] = 0.049$	All H-atom parameters refined
$wR(F^2) = 0.132$	$w = 1/[\sigma^2(F_o^2) + (0.0571P)^2]$ where $P = (F_o^2 + 2F_c^2)/3$
$S = 0.99$	$(\Delta/\sigma)_{max} < 0.001$
3161 reflections	$\Delta\rho_{max} = 0.25$ e Å^{-3}
276 parameters	$\Delta\rho_{min} = -0.23$ e Å^{-3}
0 restraints	Extinction correction: *SHELXL*, $Fc^* = kFc[1+0.001xFc^2\lambda^3/\sin(2\theta)]^{-1/4}$
Primary atom site location: structure-invariant di methods	Extinction coefficient: 0.0049 (8)

Fractional atomic coordinates and isotropic or equivalent isotropic displacement parameters (Å^2)

	x	y	z	$U_{iso}*/U_{eq}$
N1	0.04871 (17)	0.1369 (3)	0.35349 (8)	0.0378 (6)
C1	0.0740 (2)	0.1025 (4)	0.30676 (10)	0.0373 (7)
C2	0.0590 (2)	-0.0423 (4)	0.28075 (11)	0.0426 (8)
H2	0.026 (2)	-0.134 (4)	0.2948 (10)	0.049 (9)*
C3	0.0935 (2)	-0.0441 (5)	0.23534 (12)	0.0483 (8)
H3	0.083 (2)	-0.140 (4)	0.2159 (10)	0.048 (9)*
C4	0.1424 (2)	0.0930 (4)	0.21631 (13)	0.0487 (8)
H4	0.166 (2)	0.091 (3)	0.1859 (11)	0.042 (8)*
C5	0.1591 (2)	0.2355 (4)	0.24234 (11)	0.0449 (8)
H5	0.193 (2)	0.320 (4)	0.2305 (10)	0.043 (9)*
C6	0.12468 (19)	0.2421 (3)	0.28843 (10)	0.0383 (7)
C7	0.1301 (2)	0.3663 (4)	0.32544 (10)	0.0377 (7)
C8	0.1703 (2)	0.5272 (4)	0.32842 (13)	0.0474 (8)
H8	0.200 (2)	0.575 (4)	0.3024 (11)	0.046 (9)*
C9	0.1663 (3)	0.6117 (4)	0.37006 (13)	0.0547 (9)
H9	0.199 (2)	0.724 (4)	0.3729 (10)	0.060 (9)*
C10	0.1202 (2)	0.5411 (4)	0.40912 (13)	0.0497 (9)

H10	0.122 (2)	0.602 (4)	0.4381 (10)	0.052 (9)*
C11	0.0771 (2)	0.3840 (4)	0.40700 (12)	0.0440 (8)
H11	0.0468 (19)	0.341 (3)	0.4337 (10)	0.040 (8)*
C12	0.0840 (2)	0.2982 (3)	0.36497 (10)	0.0371 (7)
C13	-0.0088 (2)	0.0320 (3)	0.38198 (10)	0.0334 (7)
C14	-0.1036 (2)	-0.0119 (3)	0.36898 (9)	0.0346 (7)
F1	-0.14277 (12)	0.05460 (19)	0.32971 (5)	0.0432 (5)
C15	-0.1600 (2)	-0.1206 (3)	0.39521 (10)	0.0351 (7)
F2	-0.25108 (12)	-0.1617 (2)	0.37997 (6)	0.0463 (5)
C16	-0.1248 (2)	-0.1897 (3)	0.43664 (9)	0.0332 (7)
C17	-0.0316 (2)	-0.1421 (3)	0.44970 (10)	0.0363 (7)
F3	0.00820 (12)	-0.2019 (2)	0.49005 (5)	0.0446 (5)
C18	0.0255 (2)	-0.0352 (3)	0.42344 (10)	0.0367 (7)
F4	0.11782 (11)	0.00170 (19)	0.43845 (6)	0.0468 (5)
C19	-0.1803 (2)	-0.3235 (3)	0.46370 (10)	0.0389 (7)
O1	-0.14247 (15)	-0.4619 (2)	0.46851 (8)	0.0496 (6)
N2	-0.2671 (2)	-0.2802 (3)	0.48027 (10)	0.0487 (8)
H2A	-0.287 (3)	-0.171 (5)	0.4789 (13)	0.088 (13)*
H2B	-0.301 (3)	-0.351 (4)	0.4983 (12)	0.067 (11)*

Geometric parameters (Å, º)

N1—C13	1.403 (3)	C10—C11	1.382 (4)
N1—C1	1.405 (4)	C10—H10	0.96 (3)
N1—C12	1.410 (3)	C11—C12	1.384 (4)
C1—C2	1.387 (4)	C11—H11	0.93 (3)
C1—C6	1.408 (4)	C13—C18	1.380 (4)
C2—C3	1.379 (4)	C13—C14	1.384 (4)
C2—H2	0.94 (3)	C14—F1	1.349 (3)
C3—C4	1.388 (5)	C14—C15	1.378 (4)
C3—H3	0.95 (3)	C15—F2	1.350 (3)
C4—C5	1.375 (5)	C15—C16	1.389 (4)
C4—H4	0.93 (3)	C16—C17	1.373 (4)
C5—C6	1.397 (4)	C16—C19	1.516 (4)
C5—H5	0.89 (3)	C17—F3	1.358 (3)
C6—C7	1.449 (4)	C17—C18	1.373 (4)
C7—C8	1.395 (4)	C18—F4	1.357 (3)
C7—C12	1.400 (4)	C19—O1	1.224 (3)
C8—C9	1.367 (5)	C19—N2	1.316 (4)
C8—H8	0.93 (3)	N2—H2A	0.92 (4)

C9—C10	1.397 (5)	N2—H2B	0.89 (4)
C9—H9	1.00 (3)		
C13—N1—C1	124.8 (2)	C9—C10—H10	118.0 (18)
C13—N1—C12	126.6 (2)	C10—C11—C12	117.1 (3)
C1—N1—C12	108.4 (2)	C10—C11—H11	118.8 (17)
C2—C1—N1	129.4 (3)	C12—C11—H11	124.0 (17)
C2—C1—C6	122.0 (3)	C11—C12—C7	122.6 (3)
N1—C1—C6	108.6 (2)	C11—C12—N1	128.9 (3)
C3—C2—C1	117.5 (3)	C7—C12—N1	108.5 (2)
C3—C2—H2	123.6 (17)	C18—C13—C14	116.4 (2)
C1—C2—H2	118.9 (17)	C18—C13—N1	122.8 (2)
C2—C3—C4	121.5 (4)	C14—C13—N1	120.8 (2)
C2—C3—H3	120.1 (17)	F1—C14—C15	118.6 (3)
C4—C3—H3	118.3 (17)	F1—C14—C13	119.4 (2)
C5—C4—C3	121.1 (3)	C15—C14—C13	122.0 (3)
C5—C4—H4	117.6 (17)	F2—C15—C14	119.1 (2)
C3—C4—H4	121.3 (17)	F2—C15—C16	119.5 (2)
C4—C5—C6	119.0 (3)	C14—C15—C16	121.4 (3)
C4—C5—H5	120.6 (18)	C17—C16—C15	116.0 (2)
C6—C5—H5	120.3 (19)	C17—C16—C19	120.9 (2)
C5—C6—C1	118.9 (3)	C15—C16—C19	122.8 (3)
C5—C6—C7	134.1 (3)	F3—C17—C16	120.0 (2)
C1—C6—C7	107.0 (2)	F3—C17—C18	117.2 (2)
C8—C7—C12	118.8 (3)	C16—C17—C18	122.8 (3)
C8—C7—C6	133.7 (3)	F4—C18—C17	118.8 (2)
C12—C7—C6	107.5 (2)	F4—C18—C13	119.9 (2)
C9—C8—C7	119.3 (3)	C17—C18—C13	121.3 (3)
C9—C8—H8	120.6 (18)	O1—C19—N2	124.8 (3)
C7—C8—H8	120.1 (18)	O1—C19—C16	118.8 (3)
C8—C9—C10	120.9 (3)	N2—C19—C16	116.4 (3)
C8—C9—H9	119.5 (18)	C19—N2—H2A	120 (2)
C10—C9—H9	119.6 (18)	C19—N2—H2B	120 (2)
C11—C10—C9	121.2 (3)	H2A—N2—H2B	118 (3)
C11—C10—H10	120.6 (18)		
C13—N1—C1—C2	-7.7 (5)	C1—N1—C12—C7	0.9 (3)
C12—N1—C1—C2	176.9 (3)	C1—N1—C13—C18	120.3 (3)
C13—N1—C1—C6	175.0 (2)	C12—N1—C13—C18	-65.1 (4)
C12—N1—C1—C6	-0.4 (3)	C1—N1—C13—C14	-58.5 (4)

N1—C1—C2—C3	-178.5 (3)	C12—N1—C13—C14	116.1 (3)
C6—C1—C2—C3	-1.5 (4)	C18—C13—C14—F1	177.5 (2)
C1—C2—C3—C4	0.6 (5)	N1—C13—C14—F1	-3.6 (4)
C2—C3—C4—C5	0.6 (5)	C18—C13—C14—C15	-1.8 (4)
C3—C4—C5—C6	-0.9 (5)	N1—C13—C14—C15	177.0 (2)
C4—C5—C6—C1	0.0 (4)	F1—C14—C15—F2	2.4 (4)
C4—C5—C6—C7	178.6 (3)	C13—C14—C15—F2	-178.3 (2)
C2—C1—C6—C5	1.3 (4)	F1—C14—C15—C16	-178.3 (2)
N1—C1—C6—C5	178.8 (2)	C13—C14—C15—C16	1.1 (4)
C2—C1—C6—C7	-177.7 (3)	F2—C15—C16—C17	179.8 (2)
N1—C1—C6—C7	-0.1 (3)	C14—C15—C16—C17	0.4 (4)
C5—C6—C7—C8	1.5 (6)	F2—C15—C16—C19	6.0 (4)
C1—C6—C7—C8	-179.8 (3)	C14—C15—C16—C19	-173.4 (3)
C5—C6—C7—C12	-178.1 (3)	C15—C16—C17—F3	179.1 (2)
C1—C6—C7—C12	0.7 (3)	C19—C16—C17—F3	-6.9 (4)
C12—C7—C8—C9	2.0 (4)	C15—C16—C17—C18	-1.2 (4)
C6—C7—C8—C9	-177.5 (3)	C19—C16—C17—C18	172.8 (3)
C7—C8—C9—C10	-1.8 (5)	F3—C17—C18—F4	1.4 (4)
C8—C9—C10—C11	-0.1 (5)	C16—C17—C18—F4	-178.3 (2)
C9—C10—C11—C12	1.8 (5)	F3—C17—C18—C13	-179.9 (2)
C10—C11—C12—C7	-1.6 (4)	C16—C17—C18—C13	0.4 (4)
C10—C11—C12—N1	178.8 (3)	C14—C13—C18—F4	179.8 (2)
C8—C7—C12—C11	-0.3 (4)	N1—C13—C18—F4	1.0 (4)
C6—C7—C12—C11	179.3 (3)	C14—C13—C18—C17	1.1 (4)
C8—C7—C12—N1	179.4 (3)	N1—C13—C18—C17	-177.7 (3)
C6—C7—C12—N1	-1.0 (3)	C17—C16—C19—O1	-56.4 (4)
C13—N1—C12—C11	5.3 (5)	C15—C16—C19—O1	117.1 (3)
C1—N1—C12—C11	-179.4 (3)	C17—C16—C19—N2	123.8 (3)
C13—N1—C12—C7	-174.4 (3)	C15—C16—C19—N2	-62.7 (4)

Hydrogen-bond geometry (Å, º)

D—H$\cdots A$	D—H	H$\cdots A$	$D\cdots A$	D—H$\cdots A$
N2—H2$A$$\cdots$O1[i]	0.92 (4)	1.94 (4)	2.835 (3)	166 (3)
N2—H2$B$$\cdots$F3[ii]	0.89 (4)	2.65 (3)	3.168 (3)	118 (3)
N2—H2$B$$\cdots$F4[ii]	0.89 (4)	2.43 (4)	3.307 (3)	167 (3)

Symmetry codes: (i) -x-1/2, y+1/2, z; (ii) x-1/2, -y-1/2, -z+1.

Computing details

Data collection: Bruker *APEX* 2; cell refinement: Bruker *SAINT*; data reduction: Bruker *SAINT*; program(s) used to solve structure: *SHELXS97* (Sheldrick, 2008); program(s) used to refine structure: *SHELXL2013* (Sheldrick, 2013); molecular graphics: Bruker *SHELXTL*; software used to prepare material for publication: Bruker *SHELXTL*.

Special details

Geometry. All esds (except the esd in the dihedral angle between two l.s. planes) are estimated using the full covariance matrix. The cell esds are taken into account individually in the estimation of esds in distances, angles and torsion angles; correlations between esds in cell parameters are only used when they are defined by crystal symmetry. An approximate (isotropic) treatment of cell esds is used for estimating esds involving l.s. planes.

5.1.9. Compound 116 X-ray crystal structure data
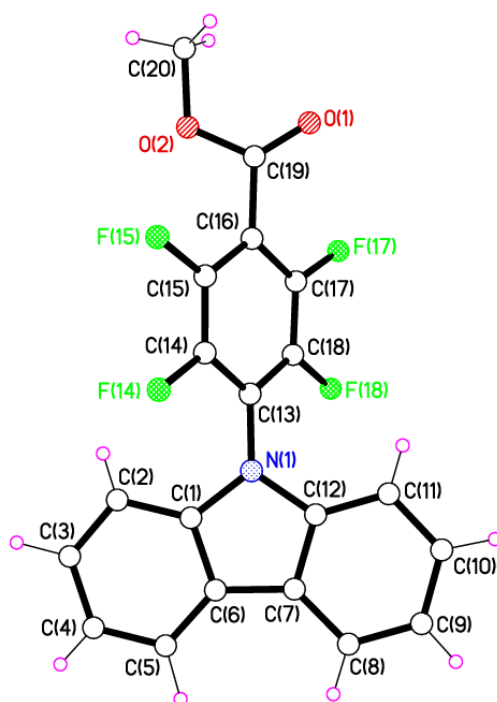
GW89

Crystal data

$C_{20}H_{11}F_4NO_2$	$F(000) = 760$
$M_r = 373.30$	$D_x = 1.529$ Mg m^{-3}
Monoclinic, $P2_1/n$	Mo $K\alpha$ radiation, $\lambda = 0.71073$ Å
$a = 10.738$ (5) Å	Cell parameters from 1630 reflections
$b = 8.060$ (4) Å	$\theta = 2.8–20.9°$
$c = 18.743$ (9) Å	$\mu = 0.13$ mm^{-1}
$\beta = 91.914$ (9)°	$T = 150$ K
$V = 1621.3$ (14) Å^3	Tablet, colourless
$Z = 4$	$0.38 \times 0.18 \times 0.06$ mm

Data collection

Bruker APEX 2 CCD diffractometer	3171 independent reflections
Radiation source: fine-focus sealed X-ray tube	2156 reflections with $I > 2\sigma(I)$
graphite	$R_{int} = 0.075$

204

⌐rotation with narrow frames scans	$\theta_{max} = 26.0°$, $\theta_{min} = 2.2°$
Absorption correction: multi-scan *SADABS* v2 Sheldrick, G.M., (2009)	$h = -13\Box13$
$T_{min} = 0.952$, $T_{max} = 0.992$	$k = 0\Box9$
24001 measured reflections	$l = 0\Box22$

Refinement

Refinement on F^2	Primary atom site location: structure-invariant di methods
Least-squares matrix: full	Secondary atom site location: all non-H atoms fo direct methods
$R[F^2 > 2\sigma(F^2)] = 0.041$	Hydrogen site location: difference Fourier map
$wR(F^2) = 0.094$	Only H-atom coordinates refined
$S = 1.01$	$w = 1/[\sigma^2(F_o^2) + (0.0382P)^2 + 0.1557P]$ $(F_o^2 + 2F_c^2)/3$
3171 reflections	$(\Delta/\sigma)_{max} < 0.001$
278 parameters	$\Delta\rho_{max} = 0.18$ e Å^{-3}
0 restraints	$\Delta\rho_{min} = -0.19$ e Å^{-3}

Fractional atomic coordinates and isotropic or equivalent isotropic displacement parameters (Å^2)

	x	y	z	U_{iso}*/U_{eq}
N1	0.85756 (17)	0.5249 (2)	0.26300 (11)	0.0318 (5)
C1	0.7748 (2)	0.4961 (3)	0.31861 (14)	0.0334 (6)
C2	0.6555 (2)	0.4269 (3)	0.31502 (16)	0.0402 (7)
H2	0.621 (2)	0.396 (3)	0.2730 (14)	0.048*
C3	0.5963 (3)	0.4034 (3)	0.37881 (17)	0.0486 (7)
H3	0.509 (3)	0.352 (4)	0.3755 (15)	0.058*
C4	0.6536 (3)	0.4453 (4)	0.44403 (17)	0.0503 (8)
H4	0.612 (3)	0.428 (4)	0.4864 (15)	0.060*
C5	0.7709 (3)	0.5158 (3)	0.44726 (16)	0.0437 (7)
H5	0.808 (2)	0.550 (4)	0.4956 (14)	0.052*
C6	0.8324 (2)	0.5426 (3)	0.38356 (14)	0.0349 (6)
C7	0.9543 (2)	0.6072 (3)	0.36804 (13)	0.0344 (6)
C8	1.0512 (3)	0.6758 (4)	0.41013 (16)	0.0455 (7)
H8	1.042 (3)	0.681 (4)	0.4610 (16)	0.055*
C9	1.1583 (3)	0.7246 (4)	0.37752 (18)	0.0493 (8)

H9	1.219 (3)	0.771 (3)	0.4068 (18)	0.059*
C10	1.1705 (3)	0.7101 (4)	0.30427 (17)	0.0453 (7)
H10	1.250 (3)	0.746 (3)	0.2848 (16)	0.054*
C11	1.0754 (2)	0.6437 (3)	0.26069 (15)	0.0374 (7)
H11	1.084 (2)	0.636 (3)	0.2125 (15)	0.045*
C12	0.9689 (2)	0.5919 (3)	0.29373 (13)	0.0313 (6)
C13	0.8371 (2)	0.4866 (3)	0.19060 (13)	0.0303 (6)
C14	0.7317 (2)	0.5410 (3)	0.15204 (13)	0.0301 (6)
F14	0.64686 (12)	0.63473 (16)	0.18547 (7)	0.0366 (4)
C15	0.7140 (2)	0.5072 (3)	0.08089 (14)	0.0310 (6)
F15	0.60909 (12)	0.56754 (18)	0.04800 (7)	0.0406 (4)
C16	0.8010 (2)	0.4220 (3)	0.04221 (13)	0.0320 (6)
C17	0.9075 (2)	0.3701 (3)	0.08051 (14)	0.0340 (6)
F17	0.99628 (13)	0.28389 (19)	0.04747 (9)	0.0450 (4)
C18	0.9227 (2)	0.3951 (3)	0.15271 (14)	0.0333 (6)
F18	1.02318 (12)	0.32964 (18)	0.18693 (8)	0.0426 (4)
C19	0.7856 (2)	0.3830 (3)	-0.03600 (14)	0.0350 (6)
O1	0.86958 (17)	0.3861 (2)	-0.07698 (10)	0.0486 (5)
O2	0.66870 (15)	0.3407 (2)	-0.05347 (9)	0.0398 (5)
C20	0.6456 (3)	0.2960 (4)	-0.12776 (17)	0.0476 (7)
H20A	0.559 (3)	0.266 (4)	-0.1294 (18)	0.071*
H20B	0.662 (3)	0.387 (4)	-0.1567 (17)	0.071*
H20C	0.703 (3)	0.204 (4)	-0.1400 (16)	0.071*

Geometric parameters (Å, °)

N1—C13	1.402 (3)	C10—H10	0.98 (3)
N1—C1	1.411 (3)	C11—C12	1.384 (4)
N1—C12	1.416 (3)	C11—H11	0.91 (3)
C1—C2	1.397 (3)	C13—C18	1.392 (3)
C1—C6	1.398 (3)	C13—C14	1.393 (3)
C2—C3	1.385 (4)	C14—F14	1.354 (3)
C2—H2	0.89 (3)	C14—C15	1.368 (3)
C3—C4	1.392 (4)	C15—F15	1.356 (3)
C3—H3	1.02 (3)	C15—C16	1.384 (3)
C4—C5	1.381 (4)	C16—C17	1.394 (3)
C4—H4	0.94 (3)	C16—C19	1.503 (4)
C5—C6	1.400 (4)	C17—F17	1.347 (3)
C5—H5	1.02 (3)	C17—C18	1.372 (4)
C6—C7	1.447 (3)	C18—F18	1.344 (3)
C7—C8	1.398 (4)	C19—O1	1.204 (3)

C7—C12	1.412 (3)	C19—O2	1.330 (3)
C8—C9	1.378 (4)	O2—C20	1.452 (3)
C8—H8	0.96 (3)	C20—H20A	0.96 (4)
C9—C10	1.388 (5)	C20—H20B	0.94 (3)
C9—H9	0.92 (3)	C20—H20C	1.00 (3)
C10—C11	1.393 (4)		
C13—N1—C1	126.62 (19)	C12—C11—H11	122.5 (16)
C13—N1—C12	125.5 (2)	C10—C11—H11	120.4 (17)
C1—N1—C12	107.81 (19)	C11—C12—C7	122.4 (2)
C2—C1—C6	121.8 (2)	C11—C12—N1	129.2 (2)
C2—C1—N1	129.0 (2)	C7—C12—N1	108.4 (2)
C6—C1—N1	109.1 (2)	C18—C13—C14	116.2 (2)
C3—C2—C1	117.3 (3)	C18—C13—N1	121.7 (2)
C3—C2—H2	122.3 (18)	C14—C13—N1	122.1 (2)
C1—C2—H2	120.4 (18)	F14—C14—C15	119.2 (2)
C2—C3—C4	121.5 (3)	F14—C14—C13	118.9 (2)
C2—C3—H3	116.6 (16)	C15—C14—C13	121.8 (2)
C4—C3—H3	121.9 (16)	F15—C15—C14	117.3 (2)
C5—C4—C3	120.9 (3)	F15—C15—C16	120.3 (2)
C5—C4—H4	119.2 (18)	C14—C15—C16	122.3 (2)
C3—C4—H4	119.8 (17)	C15—C16—C17	115.8 (2)
C4—C5—C6	118.8 (3)	C15—C16—C19	124.1 (2)
C4—C5—H5	118.8 (15)	C17—C16—C19	120.1 (2)
C6—C5—H5	122.4 (15)	F17—C17—C18	117.8 (2)
C1—C6—C5	119.6 (2)	F17—C17—C16	119.9 (2)
C1—C6—C7	107.4 (2)	C18—C17—C16	122.2 (2)
C5—C6—C7	133.0 (2)	F18—C18—C17	118.7 (2)
C8—C7—C12	119.1 (2)	F18—C18—C13	119.8 (2)
C8—C7—C6	133.6 (3)	C17—C18—C13	121.4 (2)
C12—C7—C6	107.3 (2)	O1—C19—O2	124.7 (2)
C9—C8—C7	118.6 (3)	O1—C19—C16	123.8 (2)
C9—C8—H8	123.0 (17)	O2—C19—C16	111.5 (2)
C7—C8—H8	118.3 (18)	C19—O2—C20	115.4 (2)
C8—C9—C10	121.5 (3)	O2—C20—H20A	103 (2)
C8—C9—H9	116 (2)	O2—C20—H20B	109.3 (19)
C10—C9—H9	123 (2)	H20A—C20—H20B	112 (3)
C9—C10—C11	121.4 (3)	O2—C20—H20C	108.6 (18)
C9—C10—H10	117.0 (18)	H20A—C20—H20C	114 (3)
C11—C10—H10	121.6 (18)	H20B—C20—H20C	109 (3)

C12—C11—C10	117.0 (3)		
C13—N1—C1—C2	-1.0 (4)	C1—N1—C13—C18	-127.8 (3)
C12—N1—C1—C2	-177.9 (2)	C12—N1—C13—C18	48.5 (3)
C13—N1—C1—C6	176.5 (2)	C1—N1—C13—C14	53.7 (3)
C12—N1—C1—C6	-0.4 (3)	C12—N1—C13—C14	-129.9 (3)
C6—C1—C2—C3	-0.9 (4)	C18—C13—C14—F14	-178.1 (2)
N1—C1—C2—C3	176.3 (2)	N1—C13—C14—F14	0.4 (3)
C1—C2—C3—C4	-0.7 (4)	C18—C13—C14—C15	-0.4 (3)
C2—C3—C4—C5	1.6 (4)	N1—C13—C14—C15	178.1 (2)
C3—C4—C5—C6	-0.9 (4)	F14—C14—C15—F15	-1.5 (3)
C2—C1—C6—C5	1.6 (4)	C13—C14—C15—F15	-179.2 (2)
N1—C1—C6—C5	-176.1 (2)	F14—C14—C15—C16	175.5 (2)
C2—C1—C6—C7	179.3 (2)	C13—C14—C15—C16	-2.2 (4)
N1—C1—C6—C7	1.6 (3)	F15—C15—C16—C17	177.9 (2)
C4—C5—C6—C1	-0.6 (4)	C14—C15—C16—C17	1.0 (4)
C4—C5—C6—C7	-177.7 (3)	F15—C15—C16—C19	-2.8 (4)
C1—C6—C7—C8	177.8 (3)	C14—C15—C16—C19	-179.7 (2)
C5—C6—C7—C8	-4.9 (5)	C15—C16—C17—F17	178.9 (2)
C1—C6—C7—C12	-2.2 (3)	C19—C16—C17—F17	-0.4 (4)
C5—C6—C7—C12	175.1 (3)	C15—C16—C17—C18	2.9 (4)
C12—C7—C8—C9	-0.7 (4)	C19—C16—C17—C18	-176.5 (2)
C6—C7—C8—C9	179.3 (3)	F17—C17—C18—F18	-1.5 (3)
C7—C8—C9—C10	1.3 (4)	C16—C17—C18—F18	174.6 (2)
C8—C9—C10—C11	-0.8 (5)	F17—C17—C18—C13	178.2 (2)
C9—C10—C11—C12	-0.4 (4)	C16—C17—C18—C13	-5.6 (4)
C10—C11—C12—C7	1.1 (4)	C14—C13—C18—F18	-176.0 (2)
C10—C11—C12—N1	178.0 (2)	N1—C13—C18—F18	5.4 (3)
C8—C7—C12—C11	-0.6 (4)	C14—C13—C18—C17	4.2 (3)
C6—C7—C12—C11	179.5 (2)	N1—C13—C18—C17	-174.3 (2)
C8—C7—C12—N1	-178.0 (2)	C15—C16—C19—O1	142.3 (3)
C6—C7—C12—N1	2.0 (3)	C17—C16—C19—O1	-38.4 (4)
C13—N1—C12—C11	4.8 (4)	C15—C16—C19—O2	-39.3 (3)
C1—N1—C12—C11	-178.3 (2)	C17—C16—C19—O2	140.0 (2)
C13—N1—C12—C7	-177.9 (2)	O1—C19—O2—C20	0.1 (4)
C1—N1—C12—C7	-1.0 (3)	C16—C19—O2—C20	-178.2 (2)

Hydrogen-bond geometry (Å, º)

D—H⋯A	D—H	H⋯A	D⋯A	D—H⋯A

| C20—H20A···F14[i] | 0.96 (4) | 2.54 (3) | 3.335 (4) | 140 (2) |

Symmetry code: (i) -*x*+1, -*y*+1, -*z*.

Computing details

Data collection: Bruker *APEX* 2; cell refinement: Bruker *SAINT*; data reduction: Bruker *SAINT*; program(s) used to solve structure: *SHELXS97* (Sheldrick, 2008); program(s) used to refine structure: *SHELXL2012* (Sheldrick, 2012); molecular graphics: Bruker *SHELXTL*; software used to prepare material for publication: Bruker *SHELXTL*.

Special details

Geometry. All esds (except the esd in the dihedral angle between two l.s. planes) are estimated using the full covariance matrix. The cell esds are taken into account individually in the estimation of esds in distances, angles and torsion angles; correlations between esds in cell parameters are only used when they are defined by crystal symmetry. An approximate (isotropic) treatment of cell esds is used for estimating esds involving l.s. planes.

Refinement. Refined as a 2-component twin with 180 degree rotation about reciprocal axis 1 0 1.

5.2. DNA thermal denaturation assay data
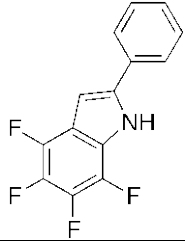
5.2.1. DNA thermal denaturation study of compound 41-DNA complex

Compound 14-DNA complex			Mean value	DNA	ACTD-DNA	Δ Tm	Compound 41
Tm °C (1)	Tm °C (2)	Tm °C (3)	Tm °C	Tm °C	Tm °C	Tm °C	
69	70	70	70	67	84	3	
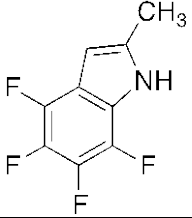
5.2.2. DNA thermal denaturation study of compound 42-DNA complex

Compound 15-DNA complex			Mean value	DNA	ACTD-DNA	Δ Tm	Compound 42
Tm °C (1)	Tm °C (2)	Tm °C (3)	Tm °C	Tm °C	Tm °C	Tm °C	
69	72	71	71	67	84	4	
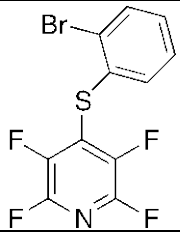
5.2.3. DNA thermal denaturation study of compound 46-DNA complex

Compound 19-DNA complex			Mean value	DNA	ACTD-DNA	Δ Tm	Compound 46
Tm °C (1)	Tm °C (2)	Tm °C (3)	Tm °C	Tm °C	Tm °C	Tm °C	
70	72	69	70	67	84	3	
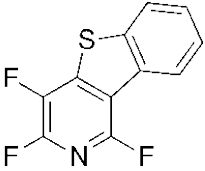
5.2.4. DNA thermal denaturation study of compound 48-DNA complex

Compound 21-DNA complex			Mean value	DNA	ACTD-DNA	Δ Tm	Compound 48
Tm °C (1)	Tm °C (2)	Tm °C (3)	Tm °C	Tm °C	Tm °C	Tm °C	
71	72	70	71	67	84	4	
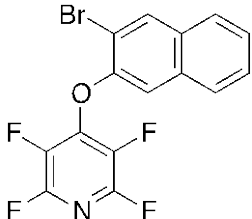
5.2.5. DNA thermal denaturation study of compound 82-DNA complex

Compound 53-DNA complex			Mean value	DNA	ACTD-DNA	Δ Tm	Compound 82
Tm °C (1)	Tm °C (2)	Tm °C (3)	Tm °C	Tm °C	Tm °C	Tm °C	
69	71	64	69	67	84	2	
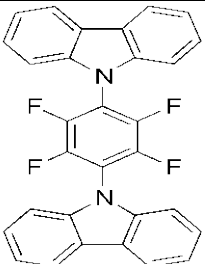
5.2.6. DNA thermal denaturation study of compound 83-DNA complex

Compound 54-DNA complex			Mean value	DNA	ACTD-DNA	Δ Tm	Compound 83
Tm °C (1)	Tm °C (2)	Tm °C (3)	Tm °C	Tm °C	Tm °C	Tm °C	
68	79	73	73	67	84	6	
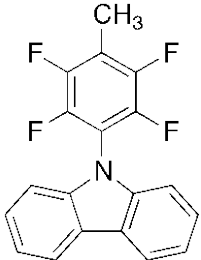
5.2.7. DNA thermal denaturation study of compound 87-DNA complex

Compound 58-DNA complex			Mean value	DNA	ACTD-DNA	Δ Tm	Compound 87
Tm °C (1)	Tm °C (2)	Tm °C (3)	Tm °C	Tm °C	Tm °C	Tm °C	
83	62	78	78	67	84	11	

5.2.8. DNA thermal denaturation study of compound 100-DNA complex

Compound 71-DNA complex			Mean value	DNA	ACTD-DNA	Δ Tm	Compound 100
Tm °C (1)	Tm °C (2)	Tm °C (3)	Tm °C	Tm °C	Tm °C	Tm °C	
77	72	78	77	67	84	10	

5.2.9. DNA thermal denaturation study of compound 105-DNA complex

Compound 76-DNA complex			Mean value	DNA	ACTD-DNA	△ Tm	Compound 105
Tm °C (1)	Tm °C (2)	Tm °C (3)	Tm °C	Tm °C	Tm °C	Tm °C	
83	80	69	80	67	84	13	

5.3. UV-visible spectroscopy data

5.3.1. UV-visible spectra of compound 42

The a spectra showed the absorbance of the compound in absence (a), and in the presence of 5.6 μM (b), 10 μM (c), 15 μM (d), 20 μM (e), 24 μM (f), and 28 μM (g) DNA. The arrow shows increasing DNA concentration. Inside graph is the plot of $A_0 / (A-A_0)$ vs. 1/ [DNA] for determination of K and ΔG values.
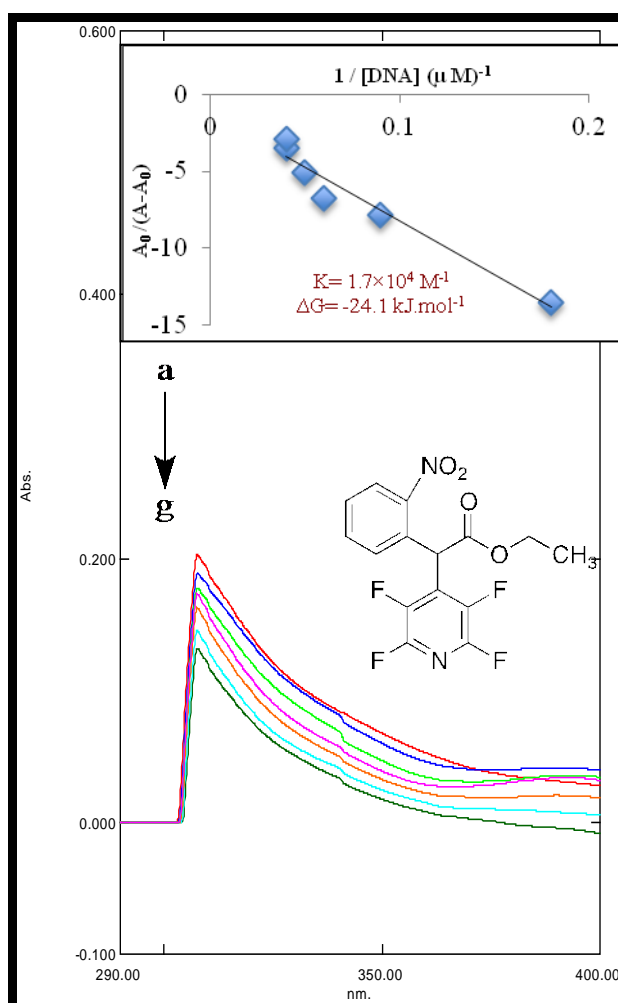
Absorption spectra of 1×10^{-3} M of compound **42**, $R^2 = 0.95048$ for six points.

5.3.2. UV-visible spectra of compound 46
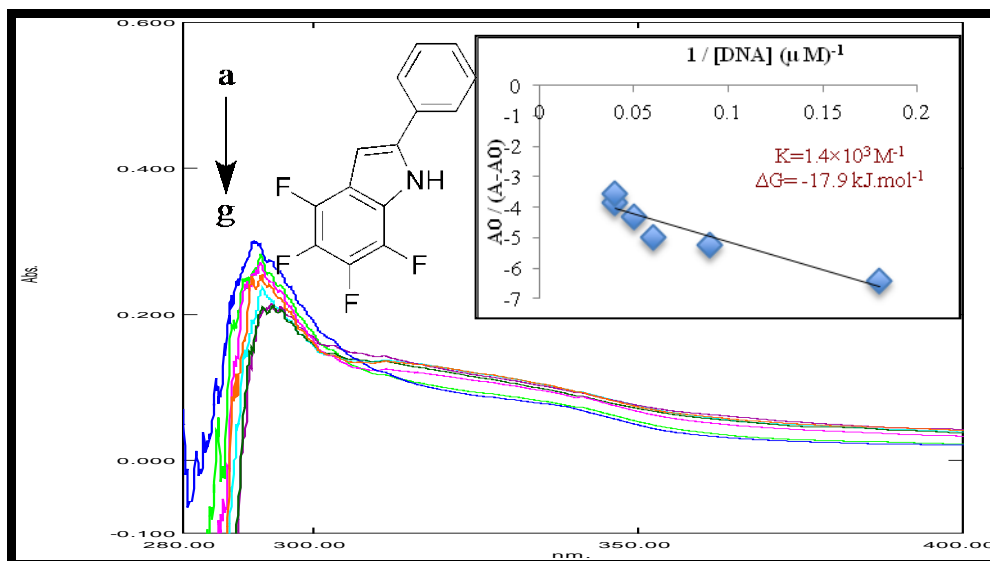
Absorption spectra of 1×10^{-2} M of compound **46**, $R^2 = 0.97533$ for six points.
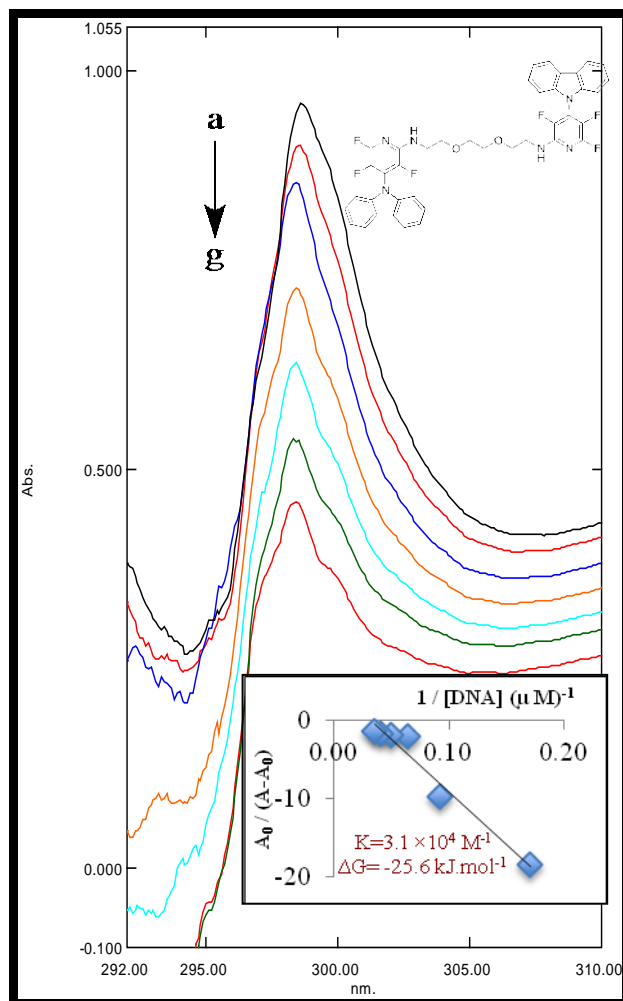
5.3.3. UV-visible spectra of compound 48
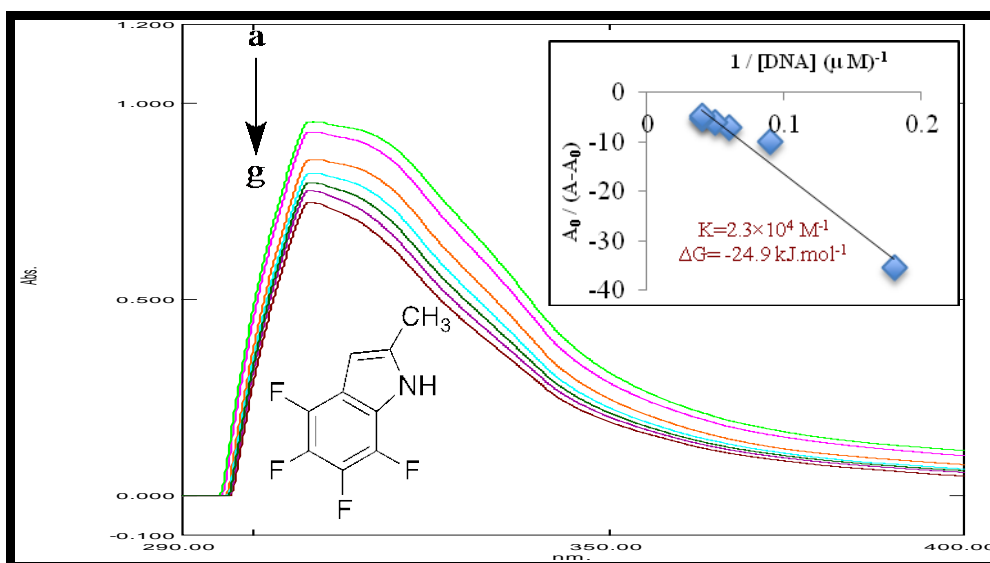
Absorption spectra of 1×10^{-2} M of compound **48**, $R^2 = 0.96026$ for six points.
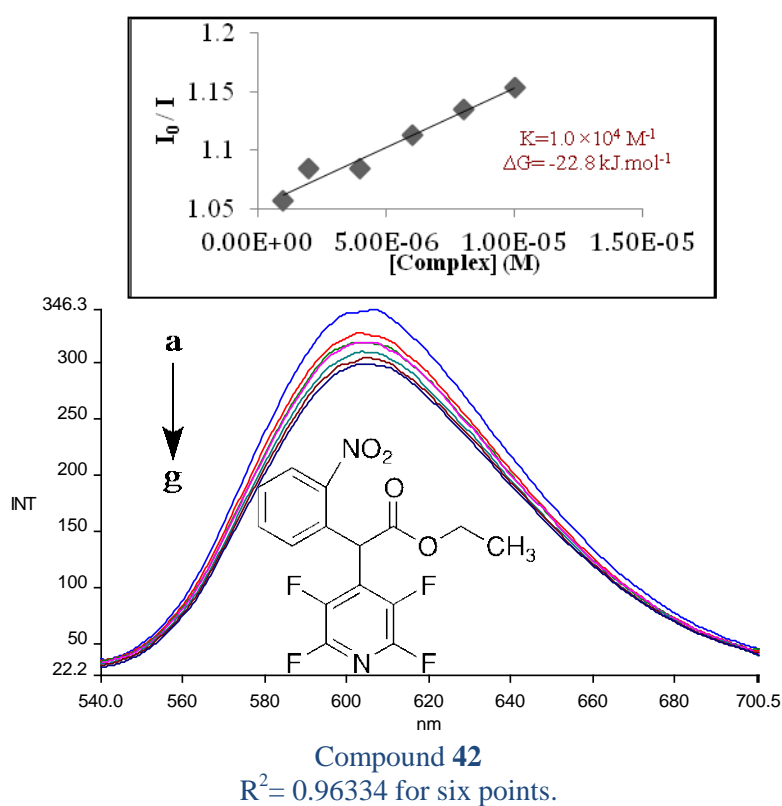
5.3.4. UV-visible spectra of compound 59
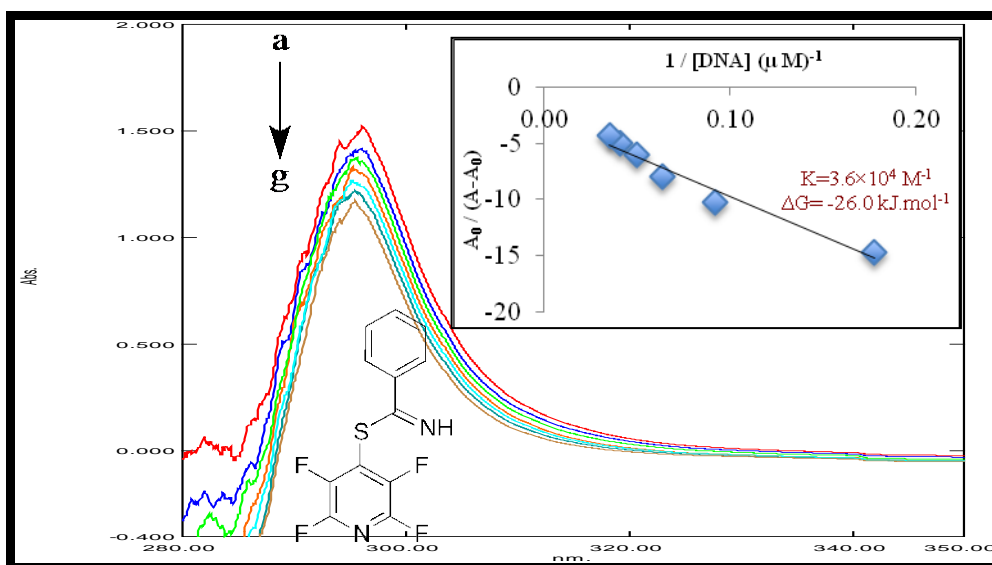
Absorption spectra of 1×10^{-3} M of compound **59**, $R^2 = 0.96103$ for six points.

5.3.5. UV-visible spectra of compound 68
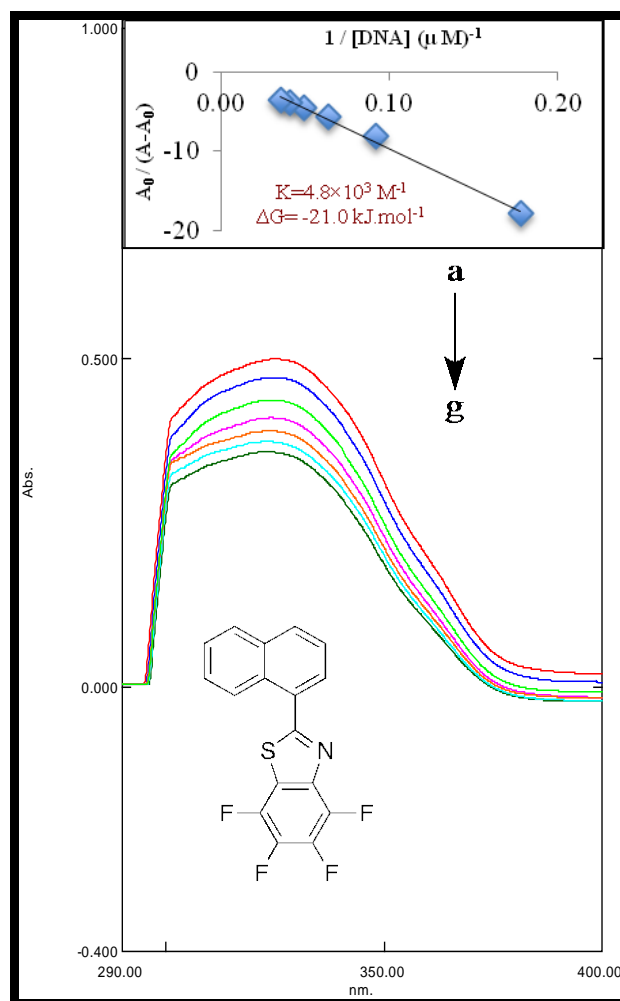
Absorption spectra of 1×10^{-3} M of compound **68**, $R^2 = 0.99238$ for six points.

5.3.6. UV-visible spectra of compound 71
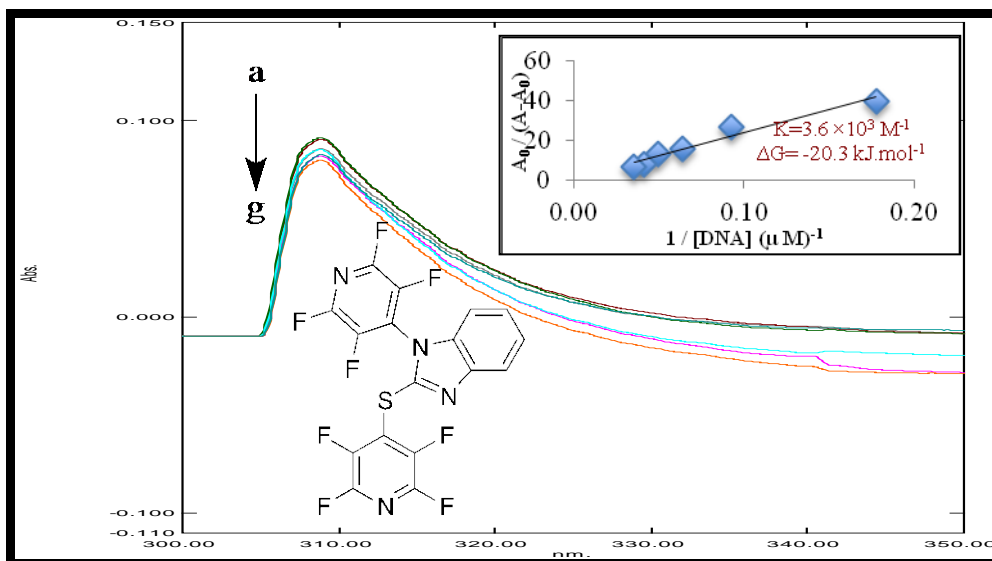
Absorption spectra of 1×10^{-3} M of compound **71**, $R^2 = 0.95796$ for six points.

5.3.7. UV-visible spectra of compound 76
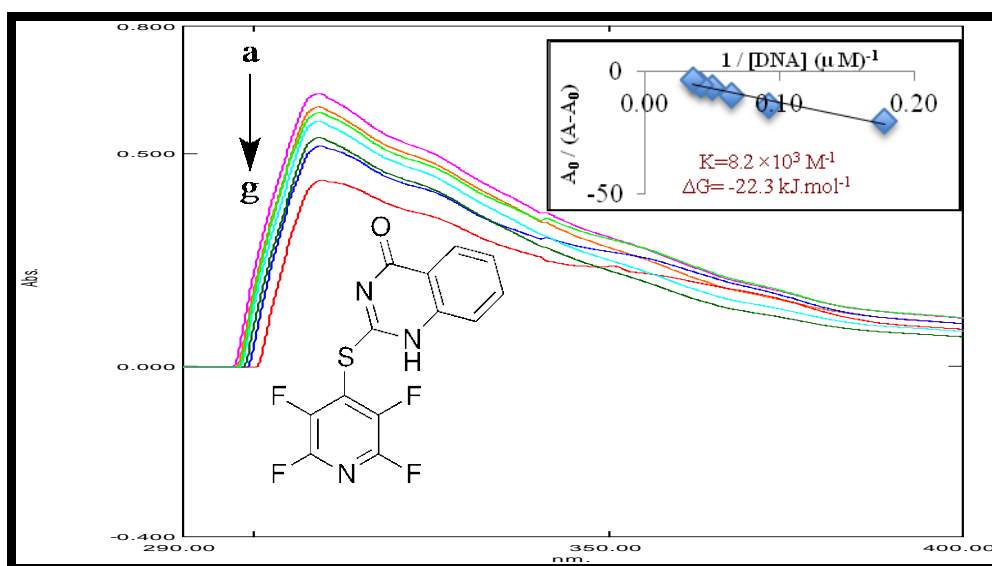
Absorption spectra of 1×10^{-3} M of compound **76**, $R^2 = 0.93289$ for six points.

5.3.8. UV-visible spectra of compound 83
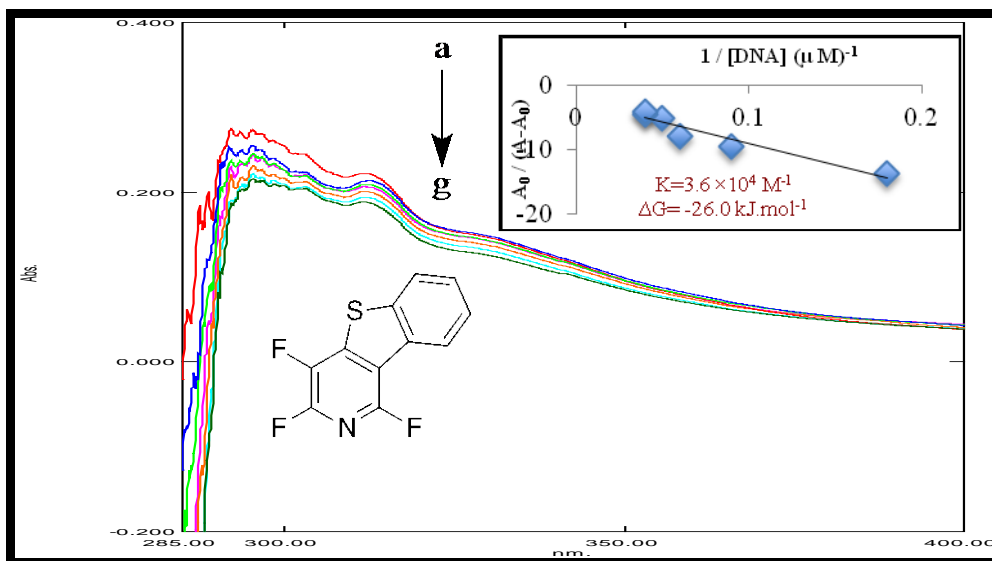
Absorption spectra of 1×10^{-3} M of compound **83**, R^2= 0.92403 for six points.

5.3.9. UV- visible spectra of compound 84
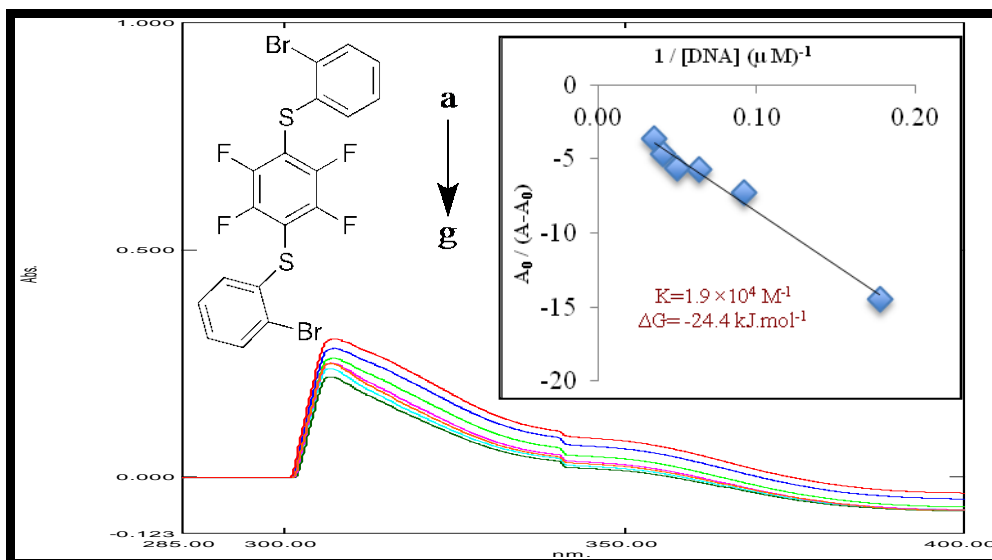
Absorption spectra of 1×10^{-2} M of compound **84**, R^2= 0.98136 for six points.

5.3.10. UV-visible spectra of compound 87
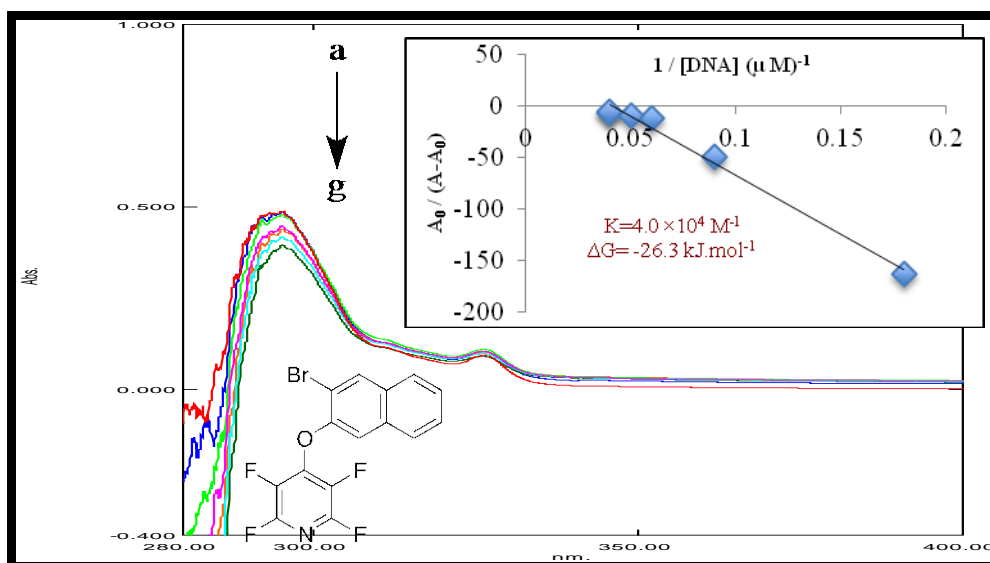
Absorption spectra of 1✕ 10^{-3} M of compound **87**, R^2= 0.98613for six points.

5.3.11. UV-visible spectra of compound 90
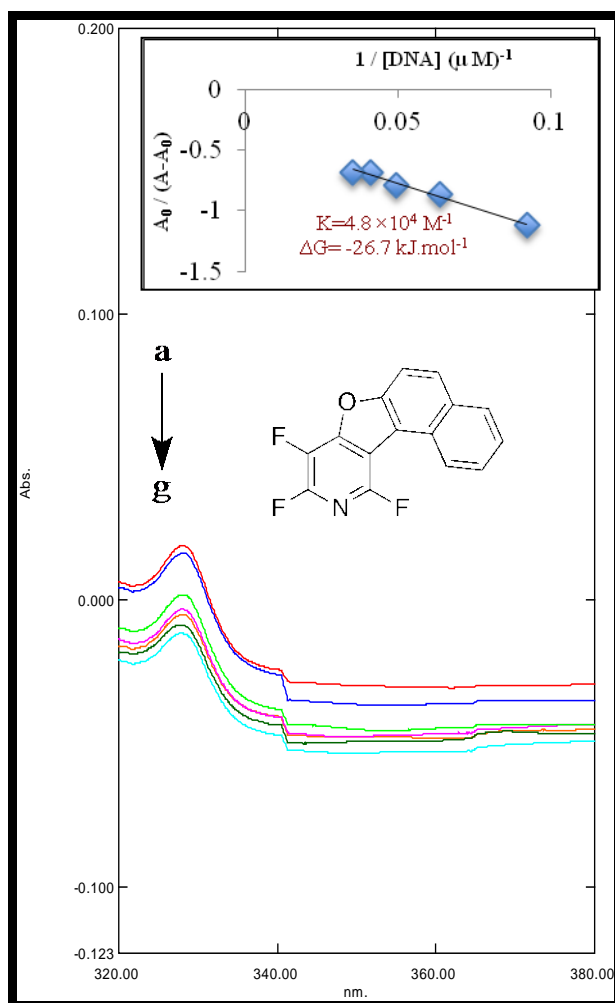
Absorption spectra of 1×10^{-3} M of compound **90**, $R^2 = 0.98438$ for six points.

5.3.12. UV-visible spectra of compound 96
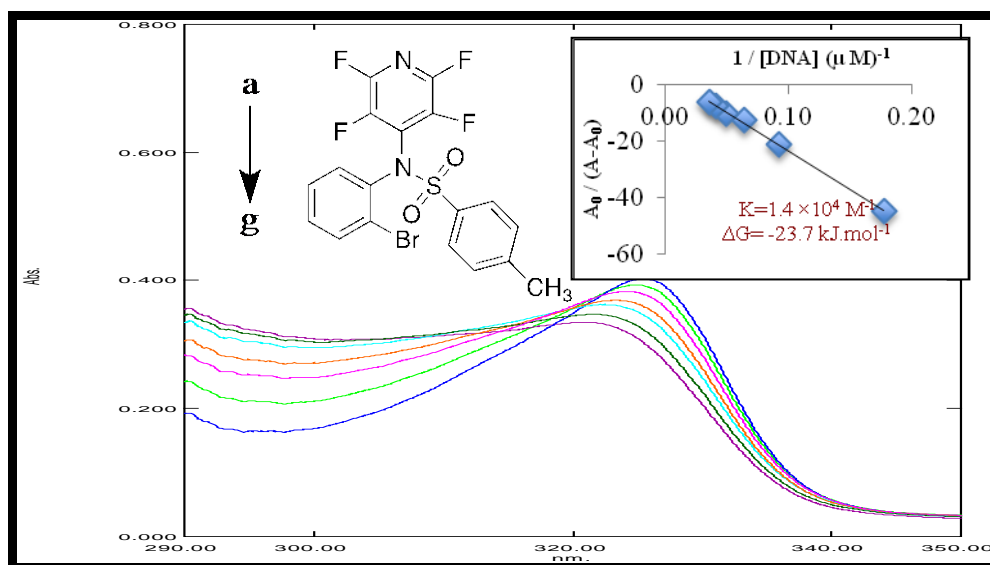
Absorption spectra of 1×10^{-2} M of compound **96**, $R^2 = 0.99816$ for six points.

5.3.13. UV-visible spectra of compound 100
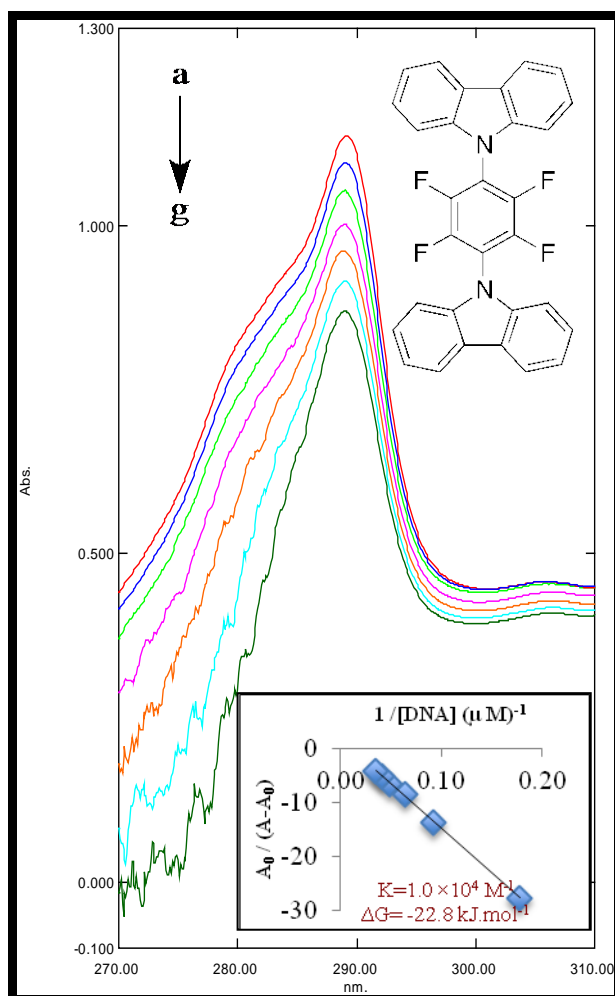
Absorption spectra of 1×10^{-3} M of compound **100**, $R^2 = 0.99967$ for six points.

5.3.14. UV-visible spectra of compound 102
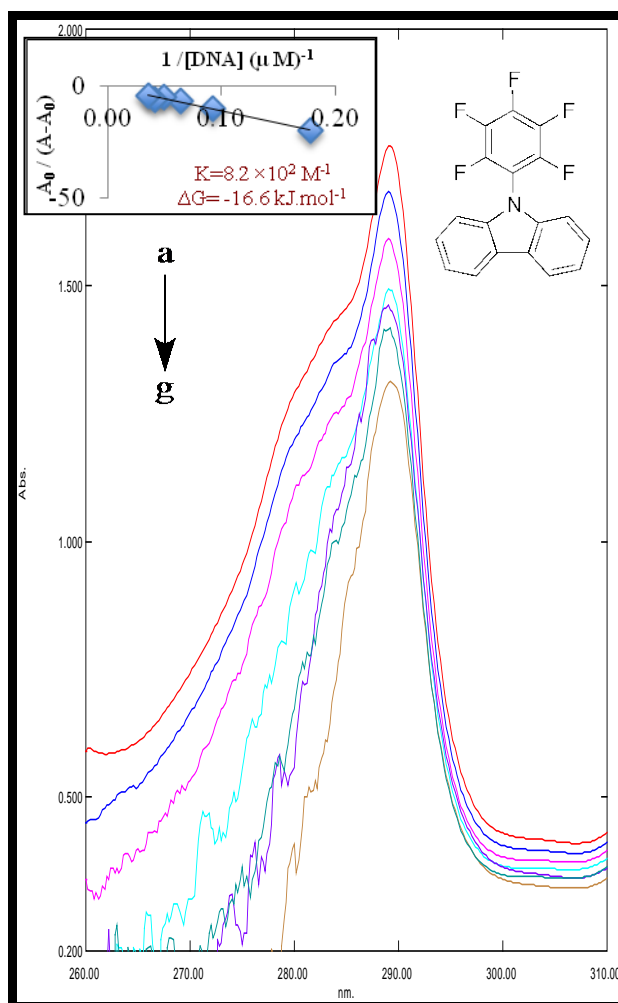
Absorption spectra of 1×10^{-3} M of compound **102**, $R^2 = 0.98702$ for six points.

5.3.15. UV-visible spectra of compound 103
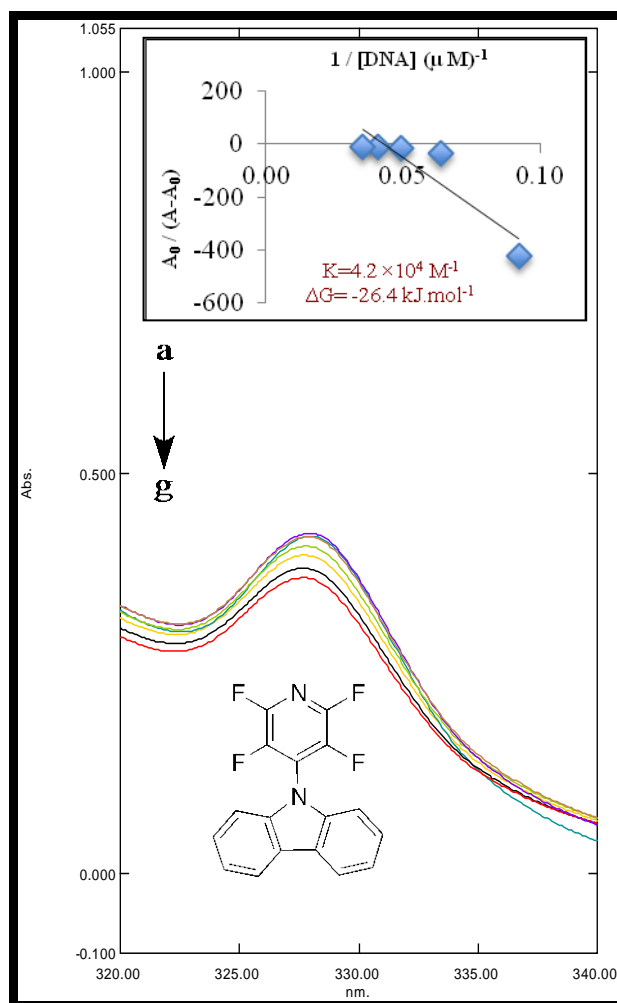
Absorption spectra of 1×10^{-3} M of compound **103**, $R^2 = 0.81914$ for six points.

5.3.16. UV-visible spectra of compound 105
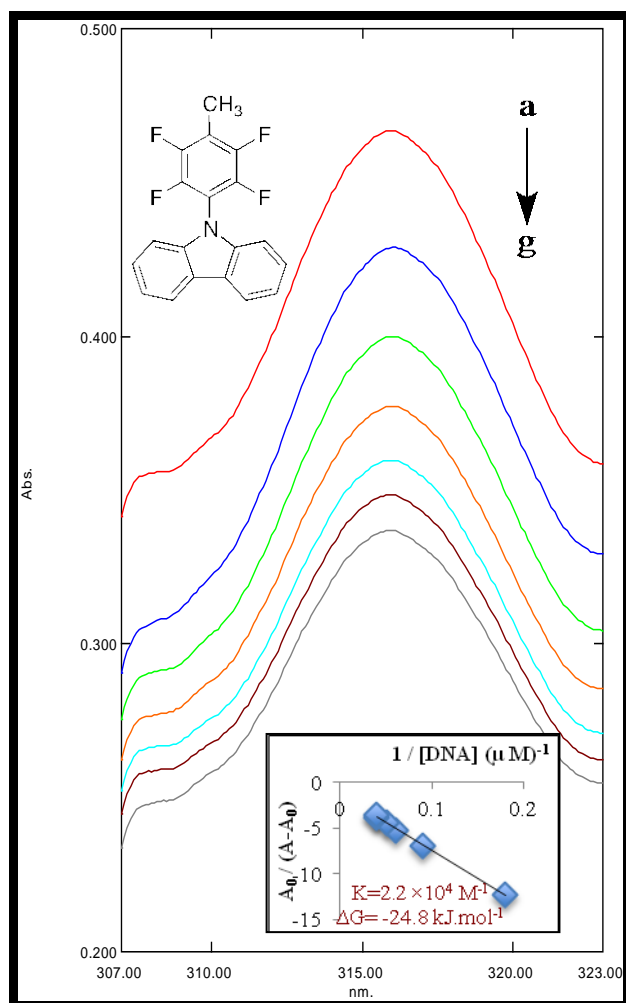
Absorption spectra of 1×10^{-3} M of compound **105**, $R^2 = 0.99806$ for six points.

5.3.17. UV-visible spectra of compound 109
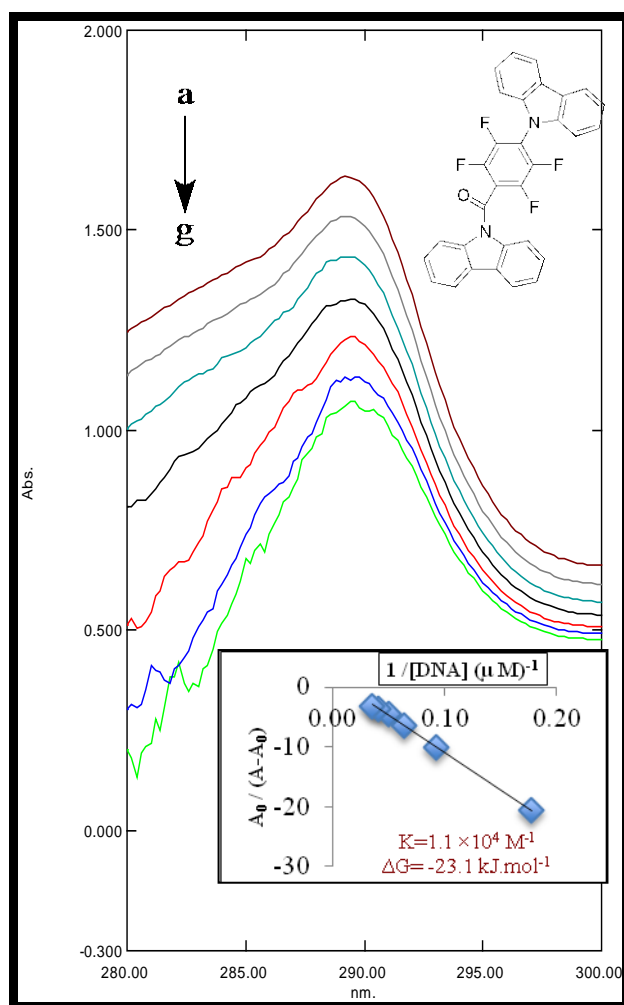
Absorption spectra of 1×10^{-3} M of compound **109**, $R^2 = 0.99961$ for six points.

5.3.18. UV-visible spectra of compound 111
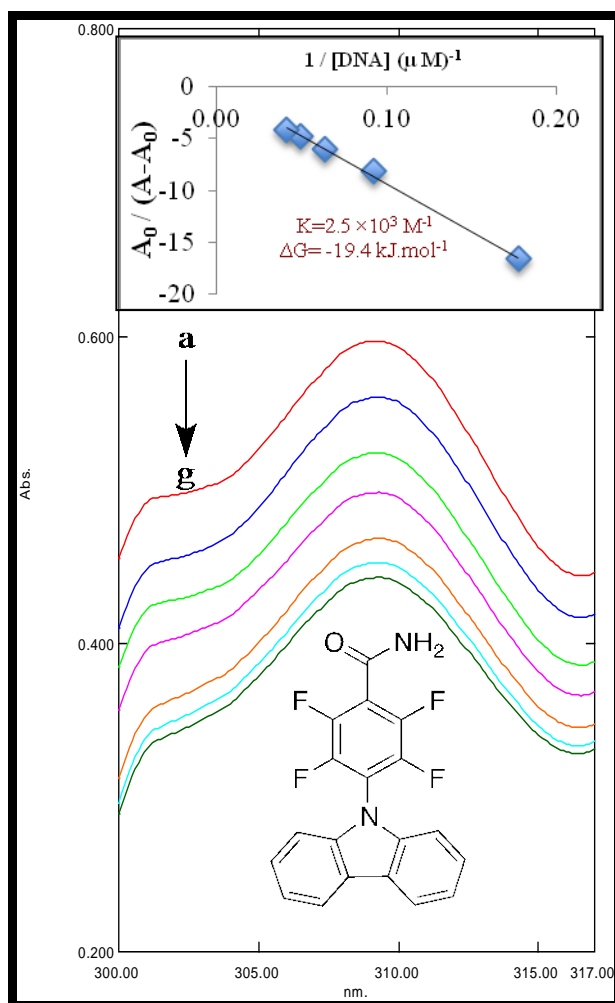
Absorption spectra of 1×10^{-3} M of compound **111**, $R^2 = 0.99732$ for six points).

5.3.19. UV-visible spectra of compound 114
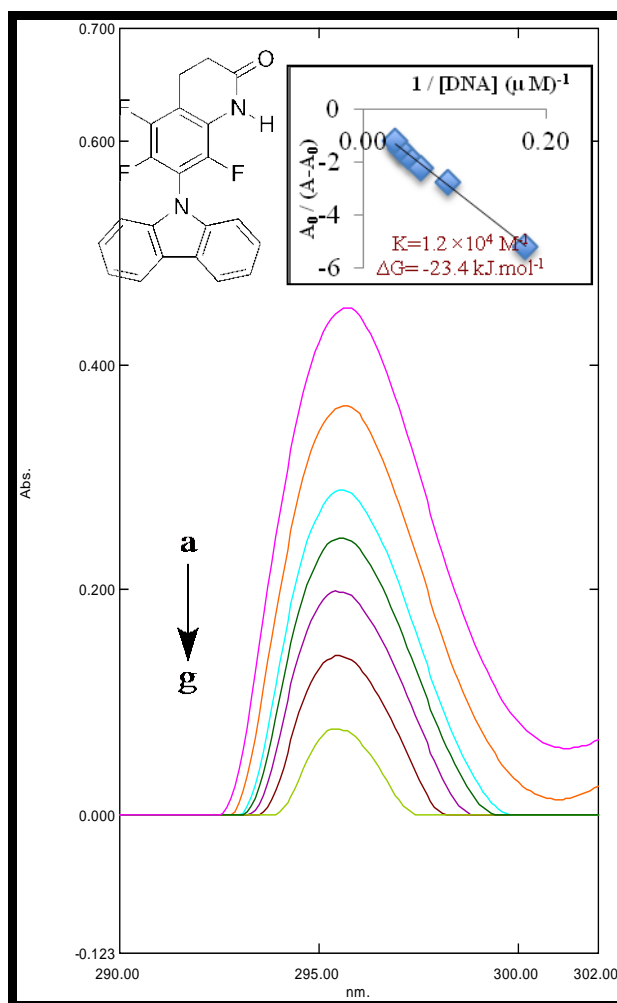
Absorption spectra of 1×10^{-3} M of compound **114**, $R^2 = 0.99603$ for six points.

5.3.20. UV-visible spectra of compound 116
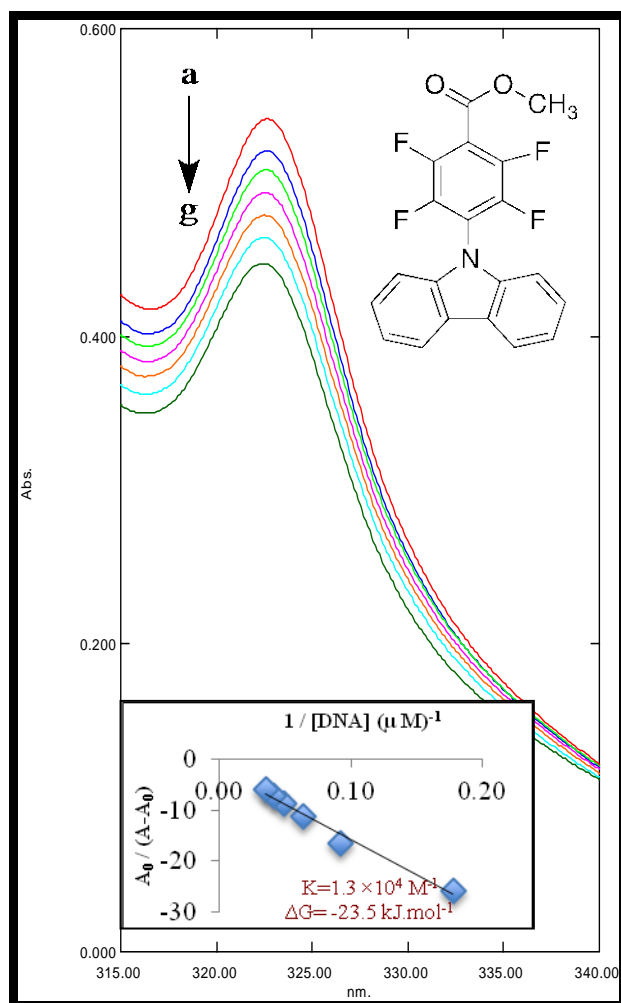
Absorption spectra of 1×10^{-3} M of compound **116**, $R^2 = 0.98178$ for six points.

5.3.21. UV-visible spectra of compound 117
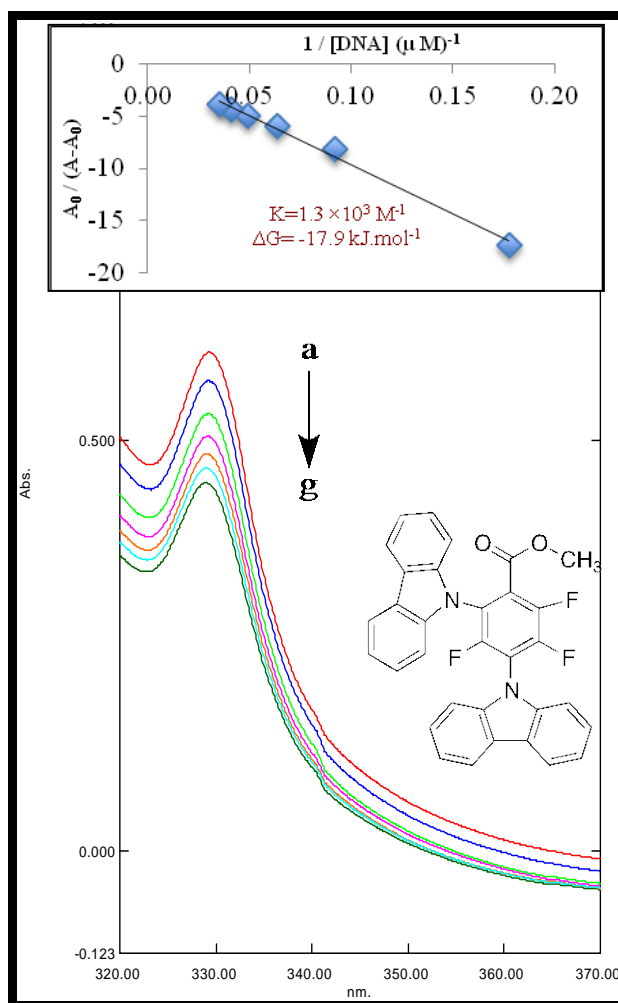
Absorption spectra of 1×10^{-3} M of compound **117**, $R^2 = 0.99227$ for six points.

5.3.22. UV-visible spectra of compound 120

Absorption spectra of 1✖ 10⁻³ M of compound **120**, R²= 0.98451 for six points.
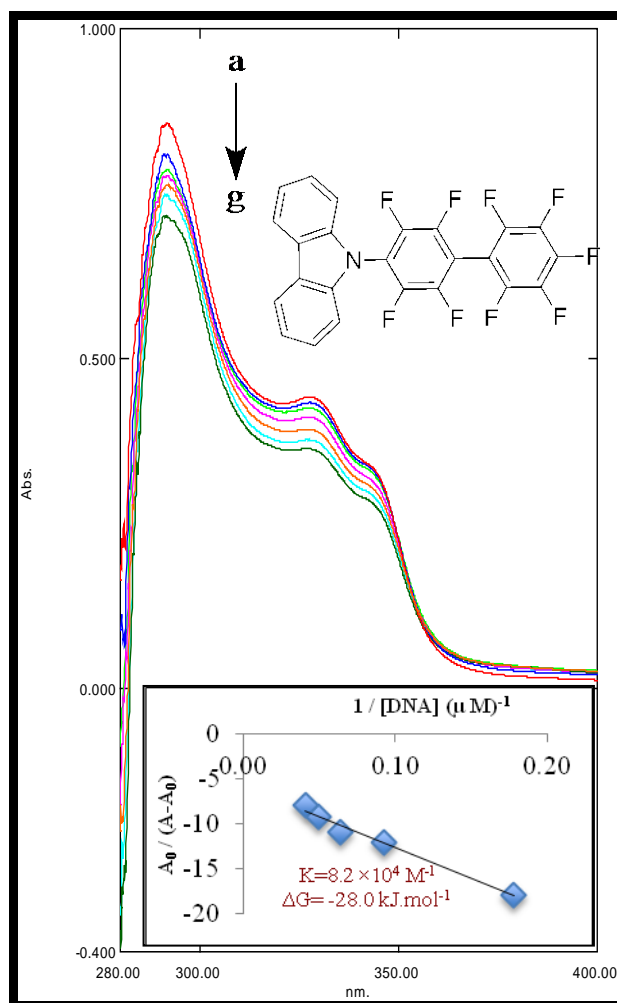
Absorption spectra of 1×10^{-3} M of compound **120**, $R^2 = 0.98451$ for six points.

5.3.23. UV-visible spectra of compound 133

Absorption spectra of 1✖ 10⁻³ M of compound **133**, R²= 0.9629 for six points.

5.3.24. UV-visible spectra of compound 135
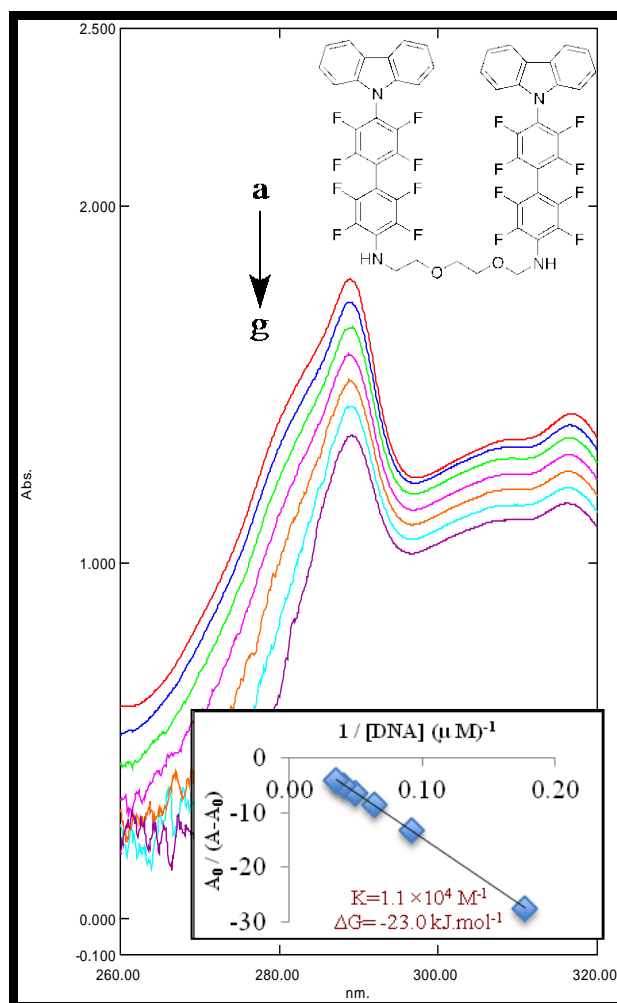
Absorption spectra of 1×10^{-3} M of compound **135**, $R^2 = 0.99983$ for six points.

5.4. Fluorescence spectroscopy data for the ethidium bromide displacement assay

Emission spectra of SS-DNA-EB in trisma base buffer on titration of the synthesised compounds. K_{ex} = 480 nm; [EB] = 1 $\times$ 10^{-6} M; [DNA] = 1.5 $\times$ 10^{-4} M. The arrow shows the increase of the complex concentration (a) 0.0, (b) 1 $\times$ 10^{-6}, (c) 2 $\times$ 10^{-6}, (d) 4 $\times$ 10^{-6}, (e) 6 $\times$ 10^{-6}, (f) 8 $\times$ 10^{-6}, (g) 1 $\times$ 10^{-5} M. Inside graph is the plot of I_0 / I vs. complex concentration for determination of K and ΔG values.

5.4.1. Fluorescence spectra of compound 42
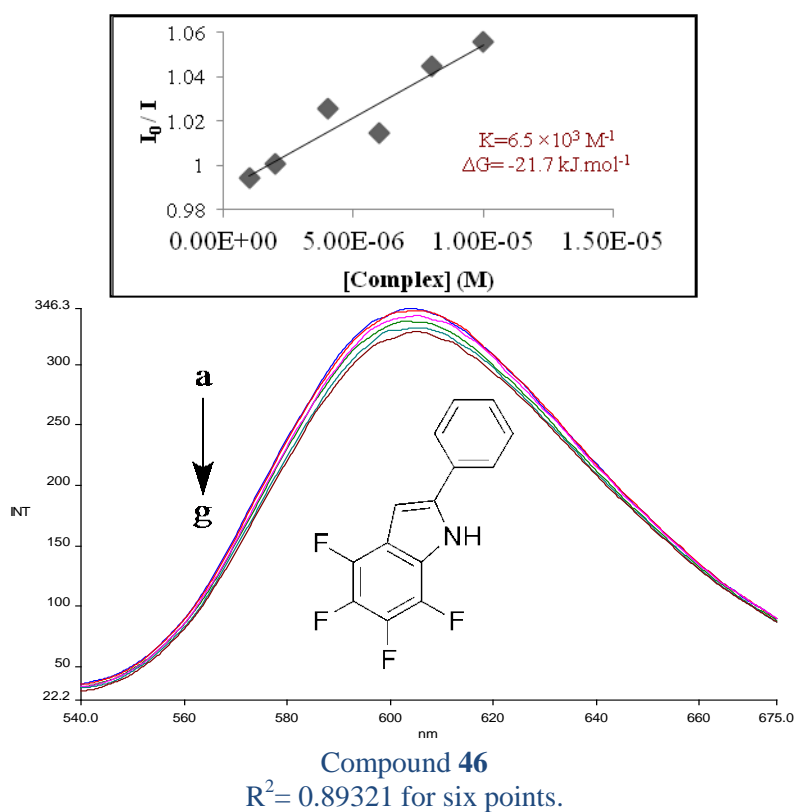
Compound **42**
R^2= 0.96334 for six points.

234

5.4.2. Fluorescence spectra of compound 46

Compound **46**

$R^2 = 0.89321$ for six points.

5.4.3. Fluorescence spectra of compound 48

Compound **48**

$R^2 = 0.99657$ for six points.
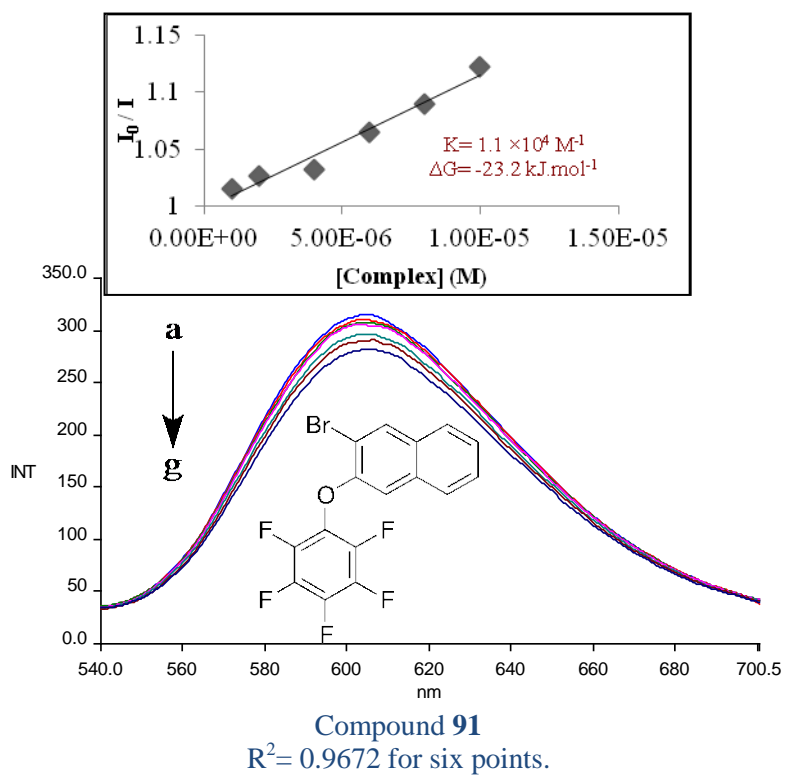
5.4.4. Fluorescence spectra of Compound 59

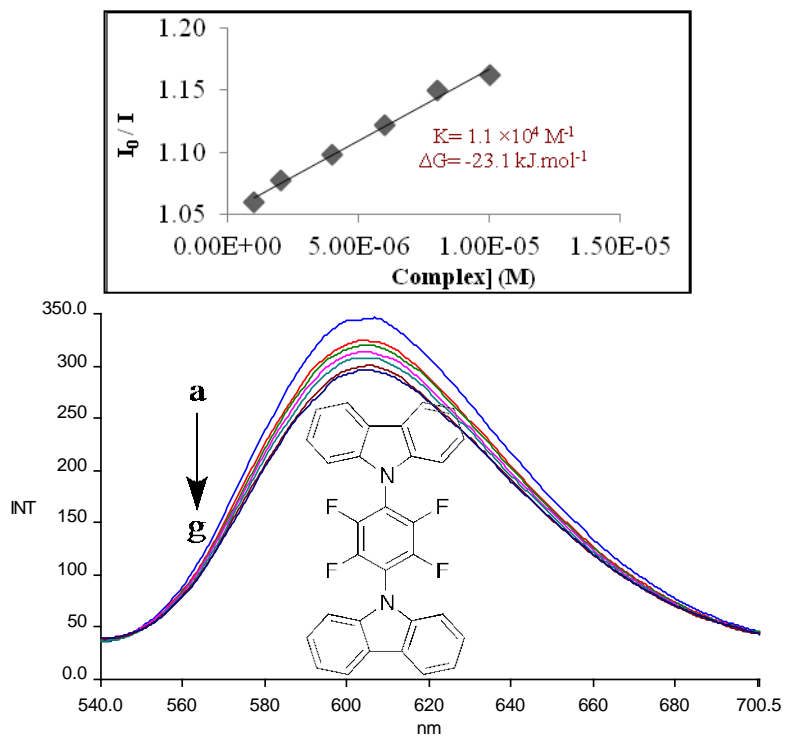

Compound **59**
$R^2 = 0.94588$ for six points.

5.4.5. Fluorescence spectra of Compound 68

Compound **68**
$R^2 = 0.96175$ for six points.
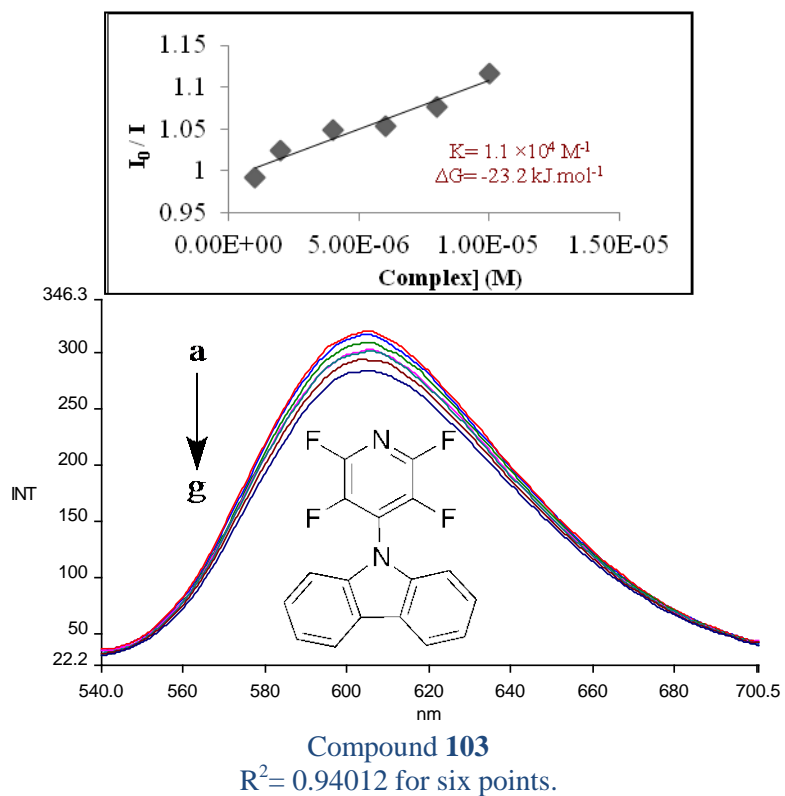
5.4.6. Fluorescence spectra of Compound 71

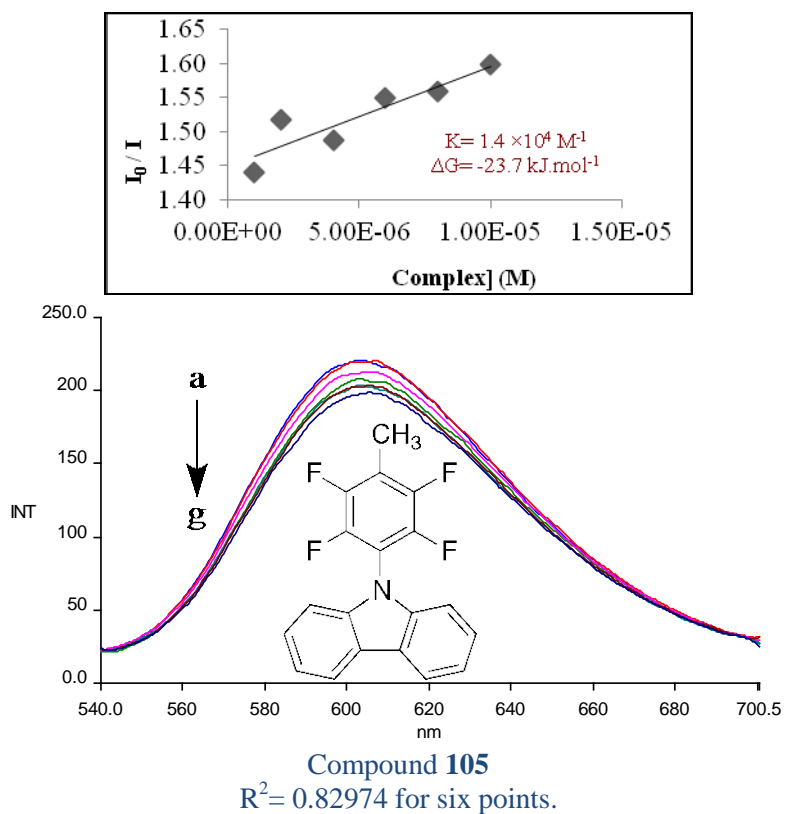Compound **71**
$R^2 = 0.9718$ for six points.

5.4.7. Fluorescence spectra of Compound 76

Compound **76**
$R^2 = 0.98563$ for six points.

237
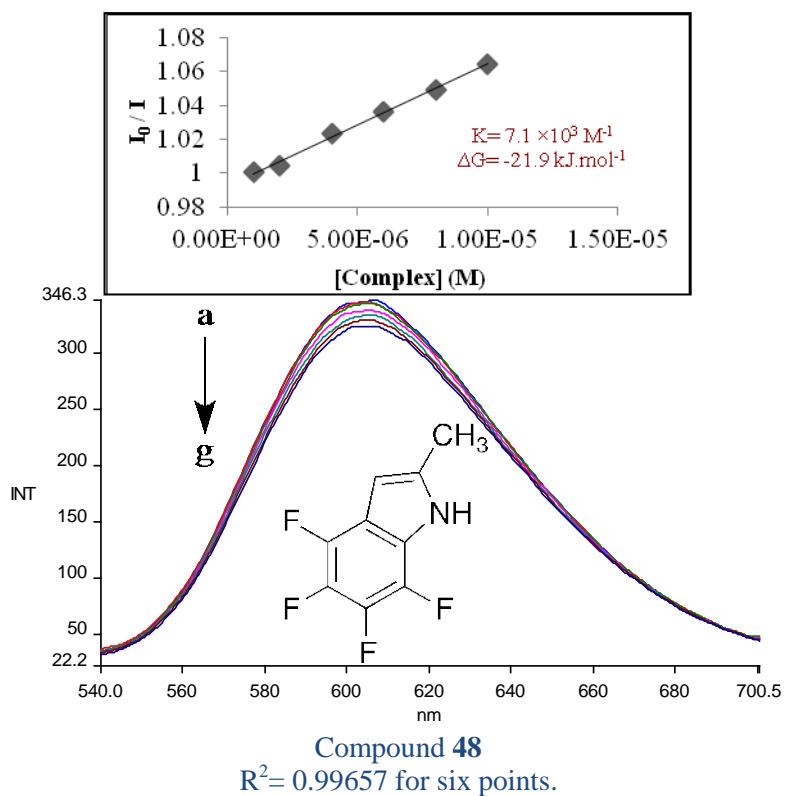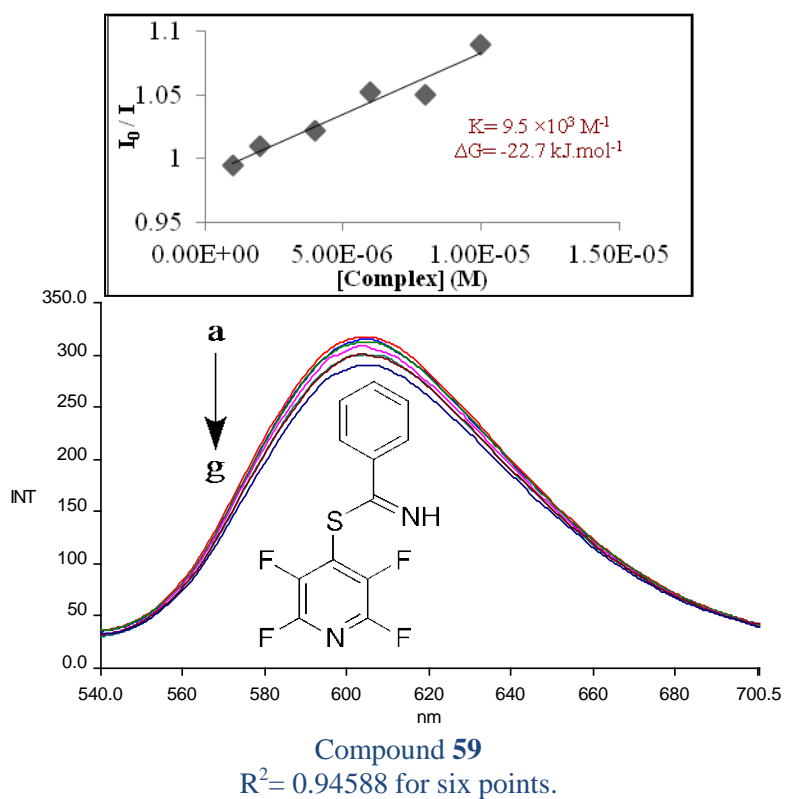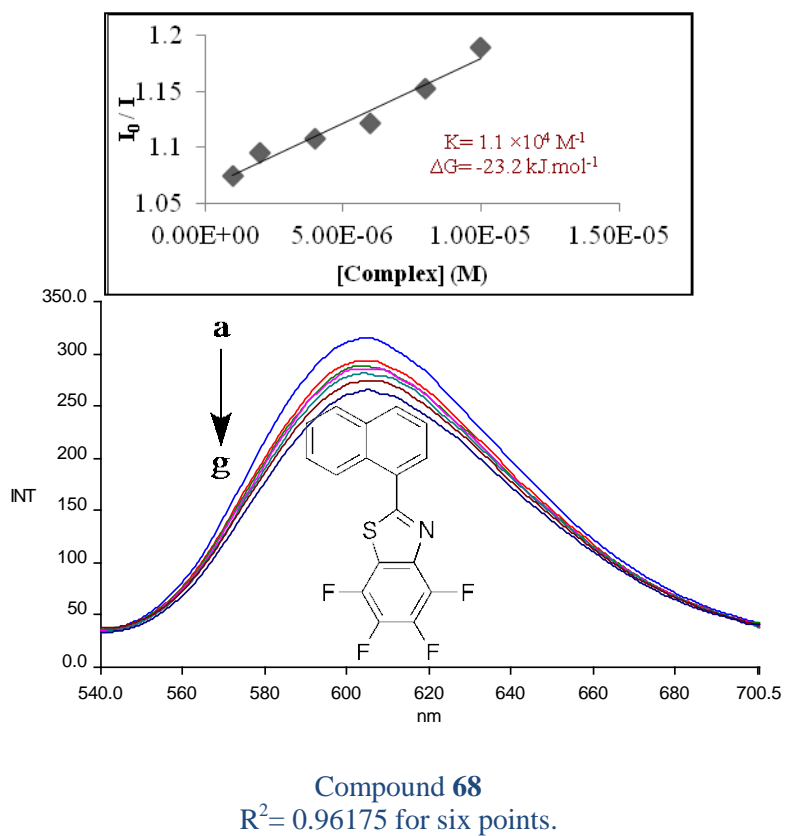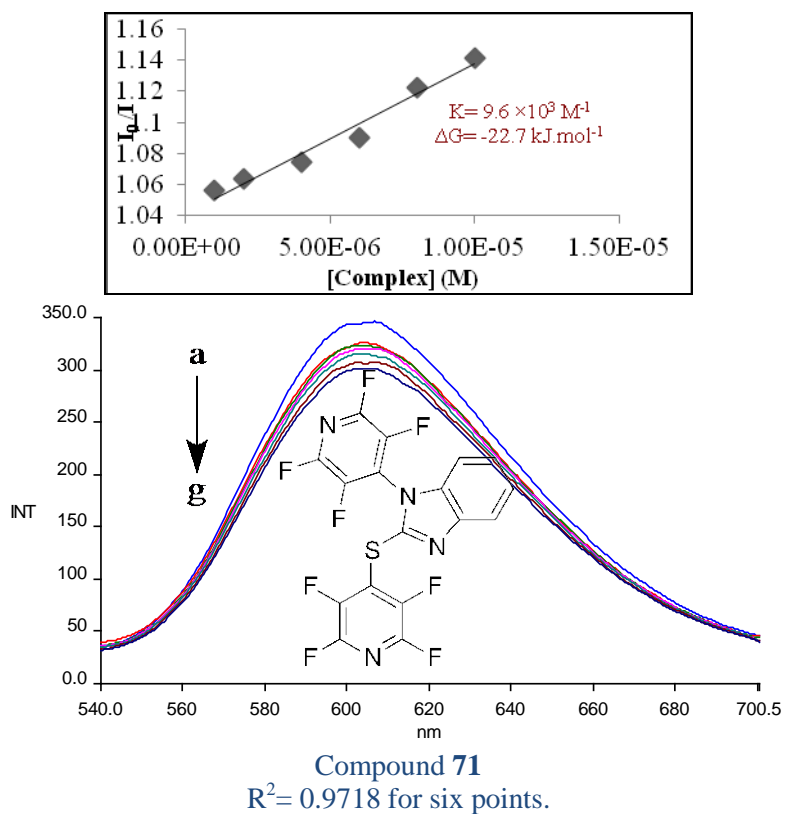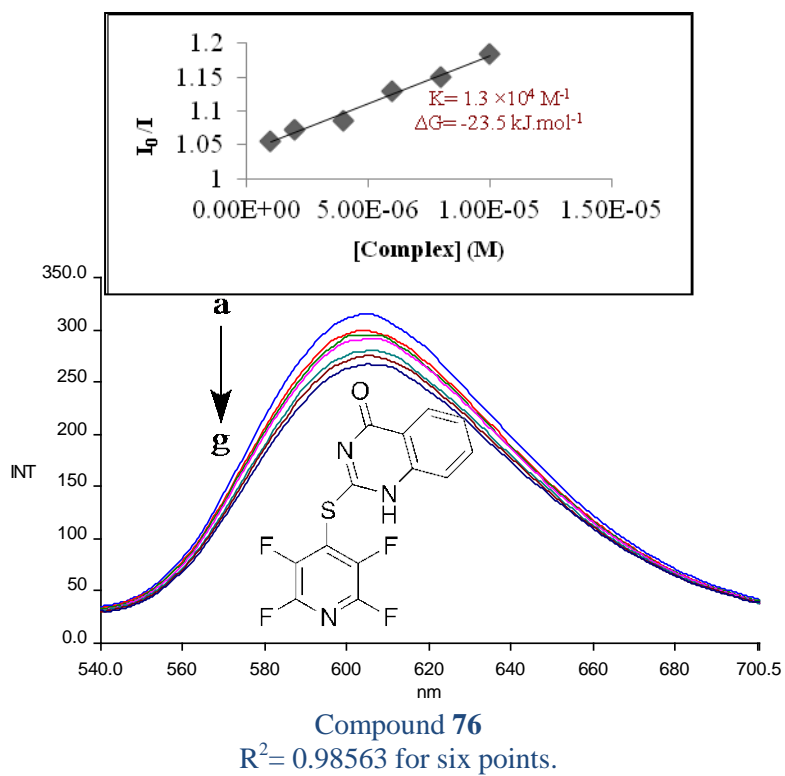
5.4.8. *Fluorescence spectra of compound 82*
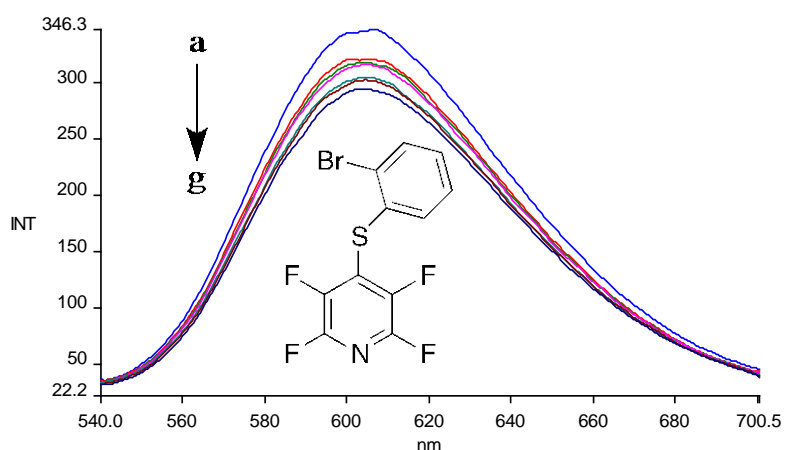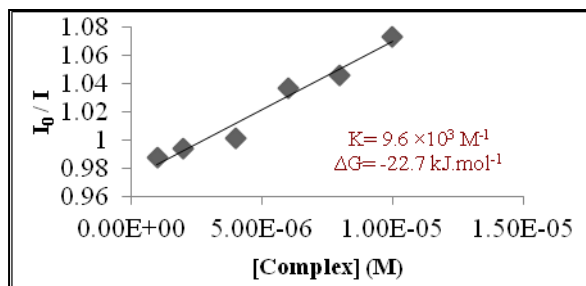
Compound **82**
$R^2 = 0.96344$ for six points.

5.4.9. *Fluorescence spectra of compound 83*
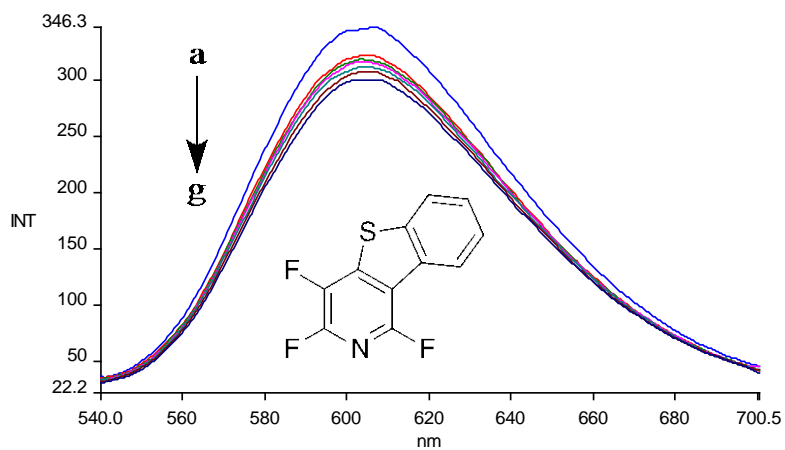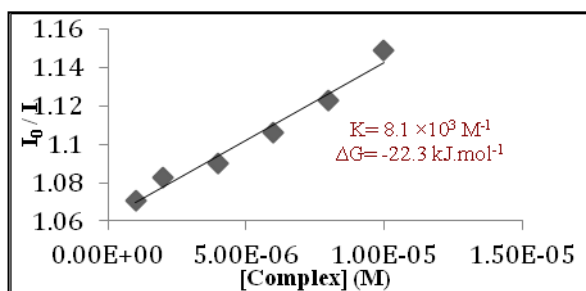
Compound **83**
$R^2 = 0.97382$ for six points.

5.4.10. Fluorescence spectra of compound 84
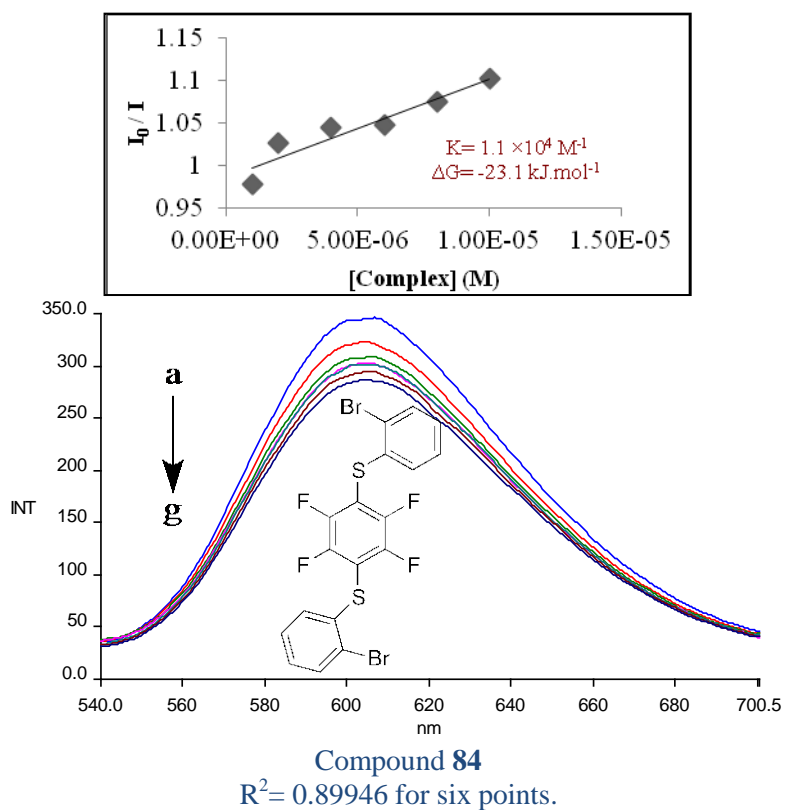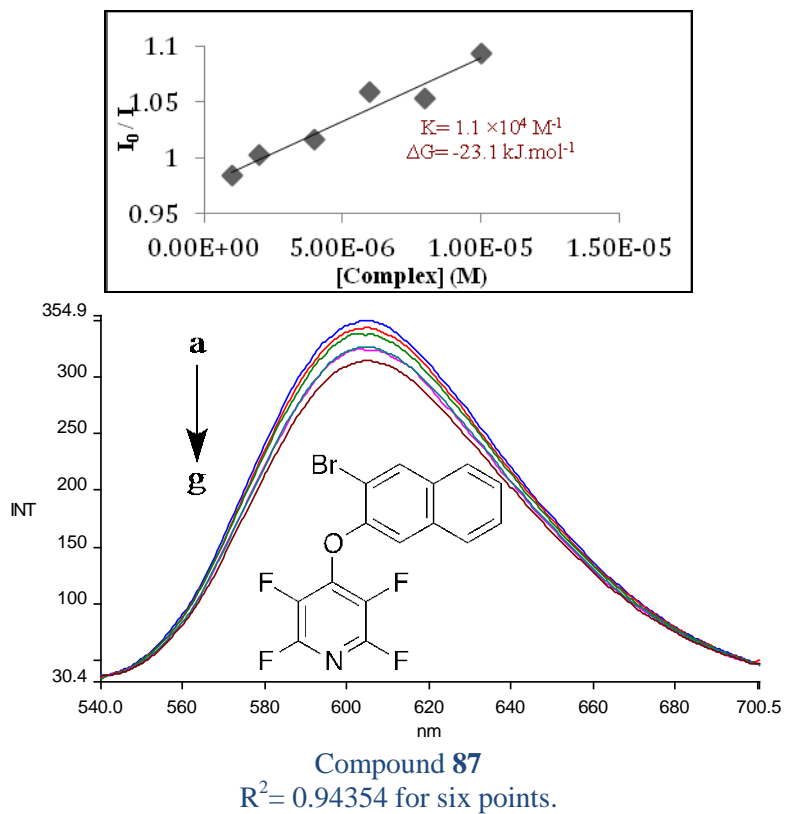
Compound **84**
$R^2 = 0.89946$ for six points.
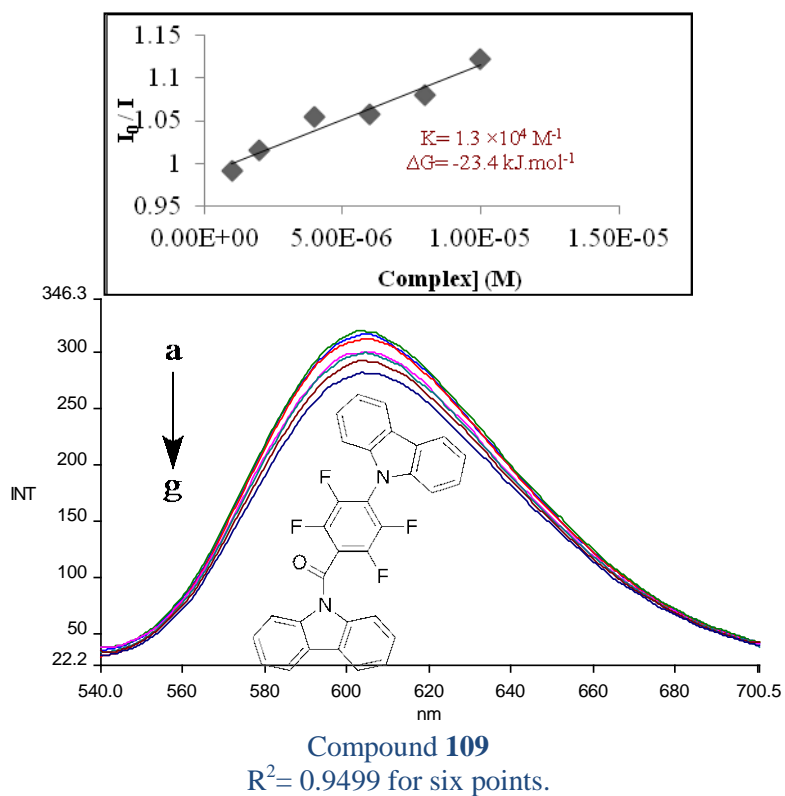
5.4.11. Fluorescence spectra of compound 87

Compound **87**
$R^2 = 0.94354$ for six points.

5.4.12. Fluorescence spectra of compound 90

Compound **90**
R^2= 0.90266 for six points.

5.4.13. Fluorescence spectra of compound 91
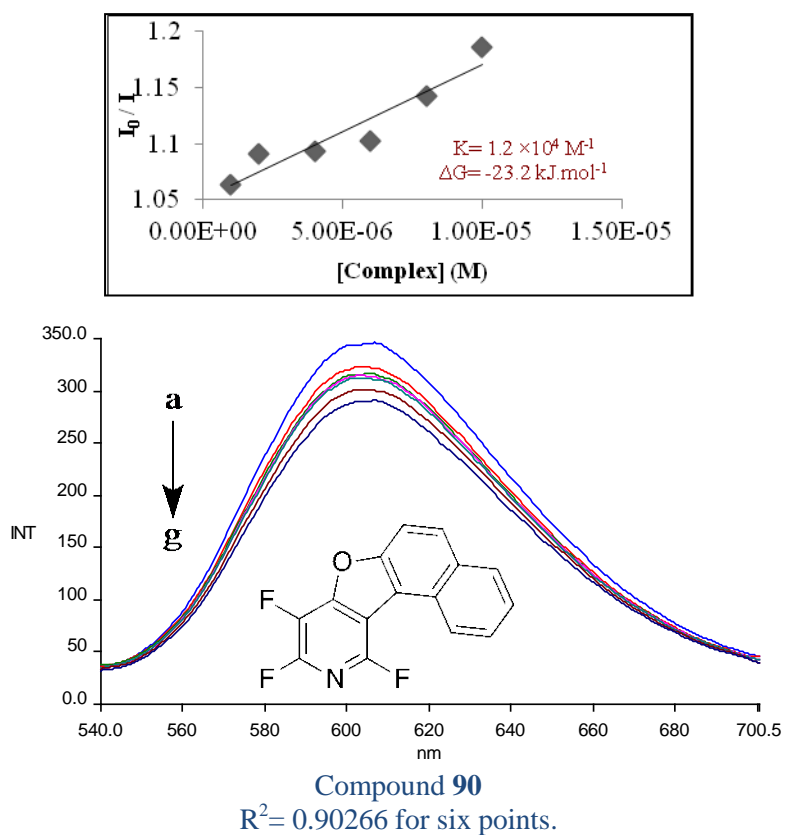
Compound **91**
R^2= 0.9672 for six points.

5.4.14. Fluorescence spectra of compound 96
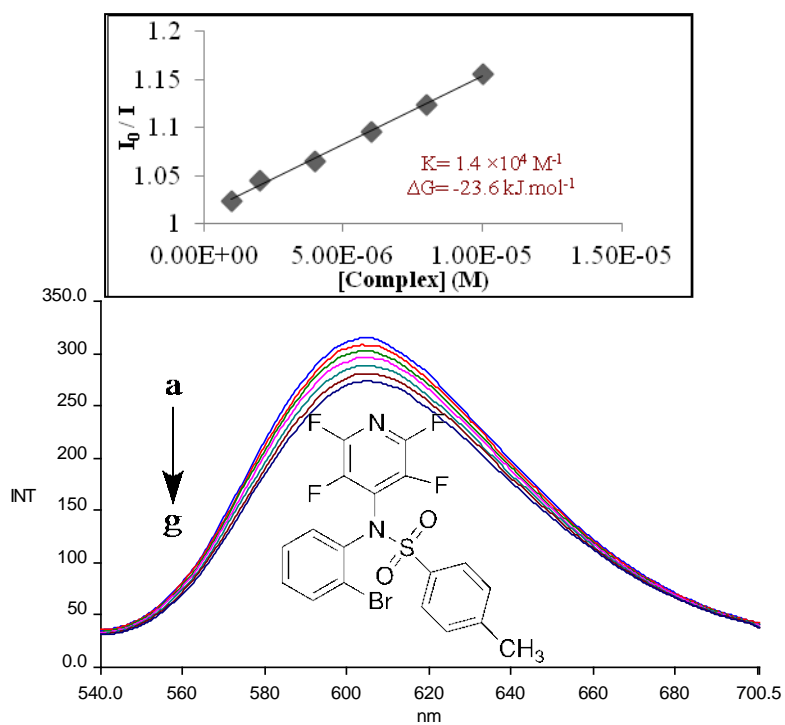
Compound **96**
R^2= 0.99667 for six points.

5.4.15. Fluorescence spectra of compound 100

Compound **100**
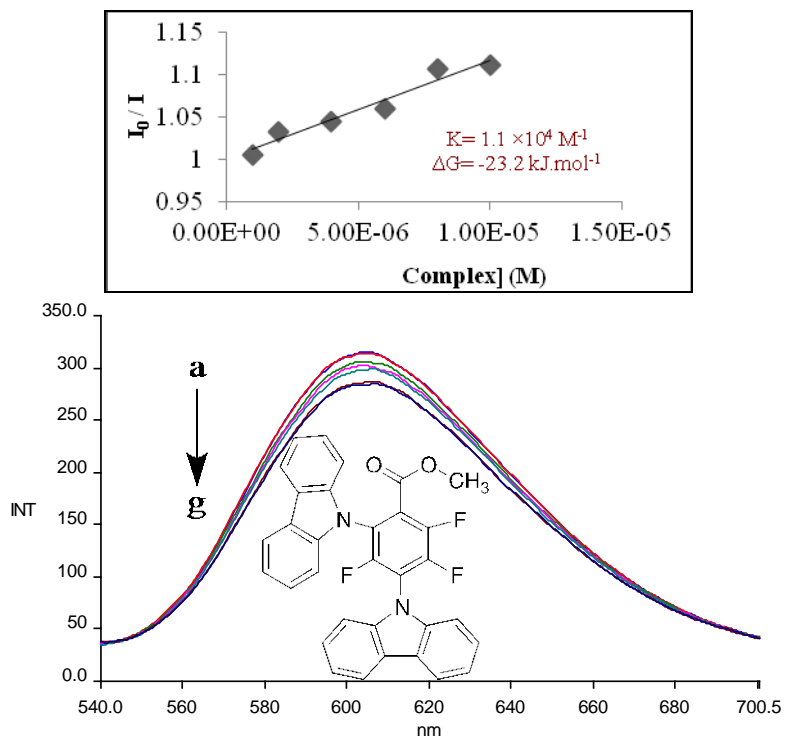R^2= 0.99024 for six points.

5.4.16. Fluorescence spectra of compound 102
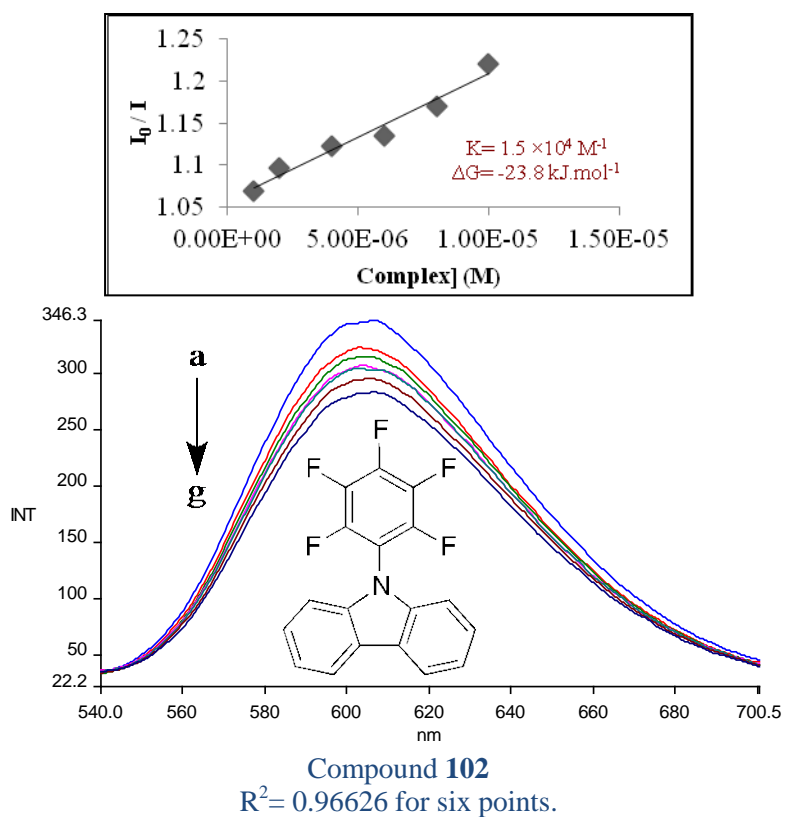
Compound **102**
$R^2 = 0.96626$ for six points.

5.4.17. Fluorescence spectra of compound 103

Compound **103**
$R^2 = 0.94012$ for six points.

5.4.18. Fluorescence spectra of compound 105

Compound **105**

R^2= 0.82974 for six points.

5.4.19. Fluorescence spectra of compound 109

Compound **109**

R^2= 0.9499 for six points.

5.4.20. Fluorescence spectra of compound 111

Compound **111**
$R^2 = 0.90178$ for six points.

5.4.21. Fluorescence spectra of compound 114
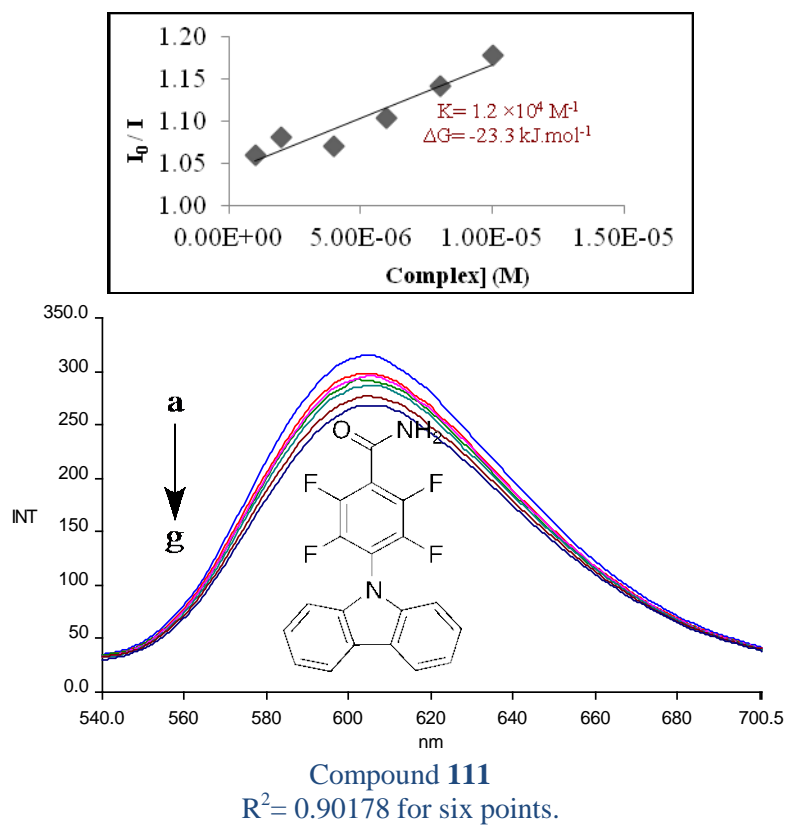
Compound **114**
$R^2 = 0.91145$ for six points.
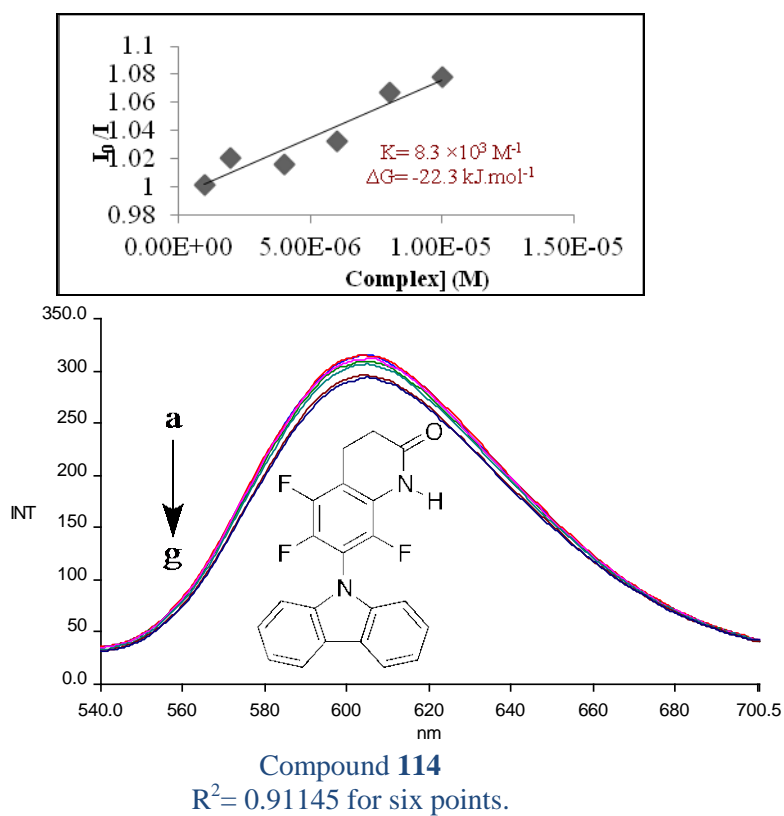
5.4.22. *Fluorescence spectra of compound 116*
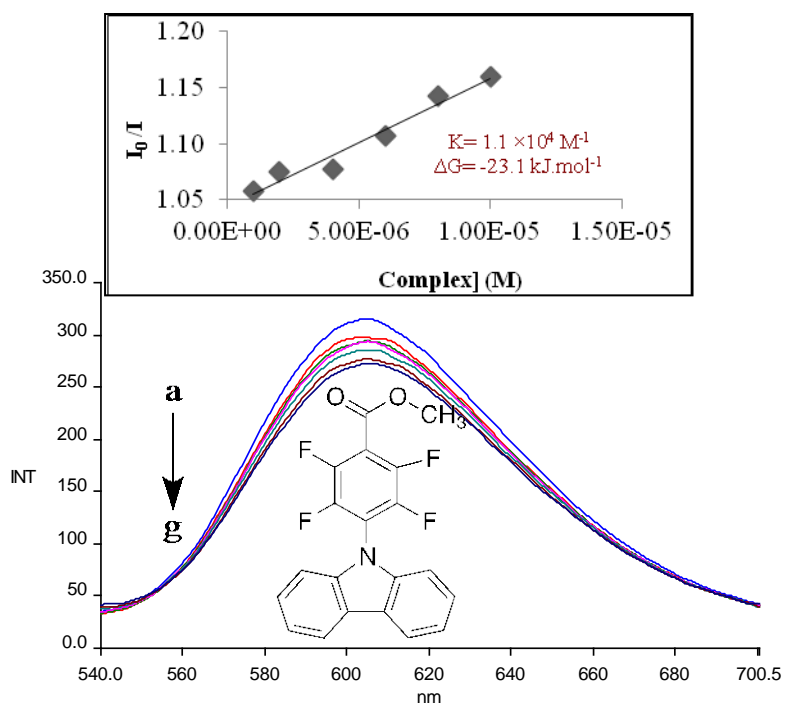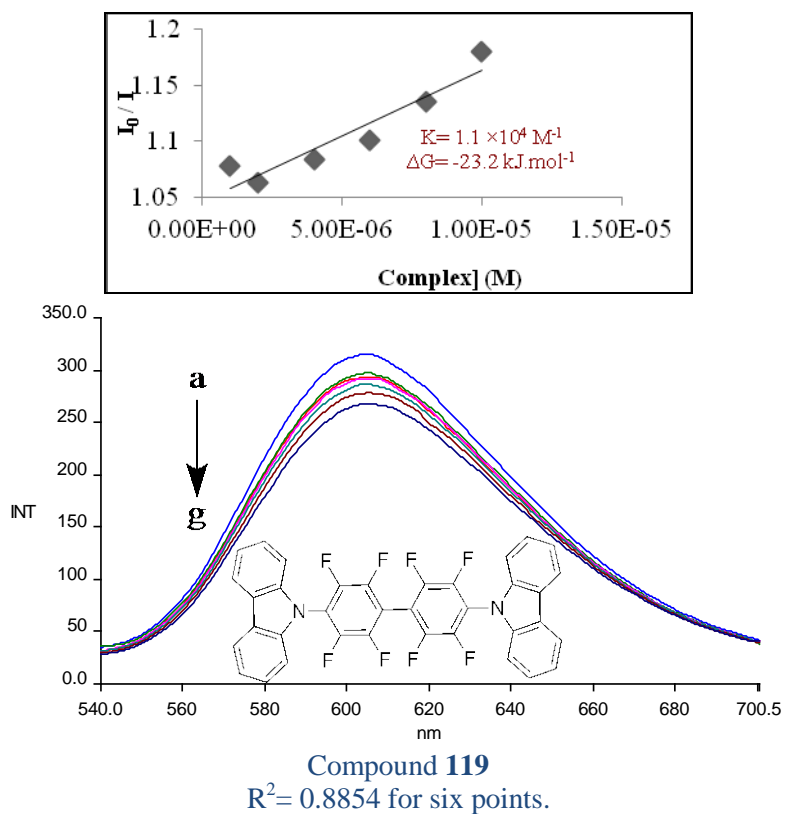

Compound **116**
$R^2 = 0.96138$ for six points.
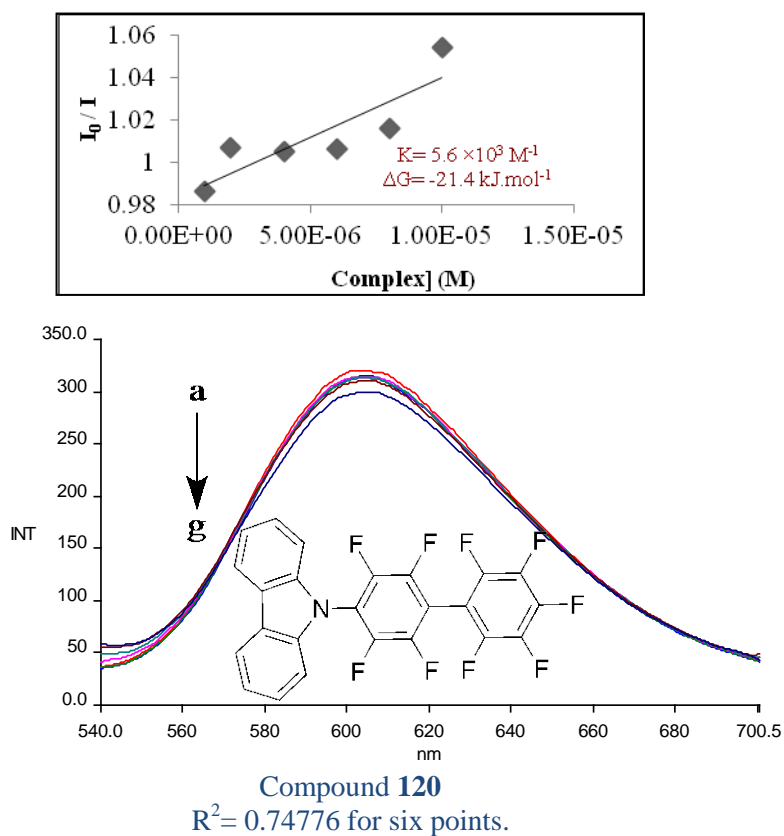
5.4.23. *Fluorescence spectra of compound 117*
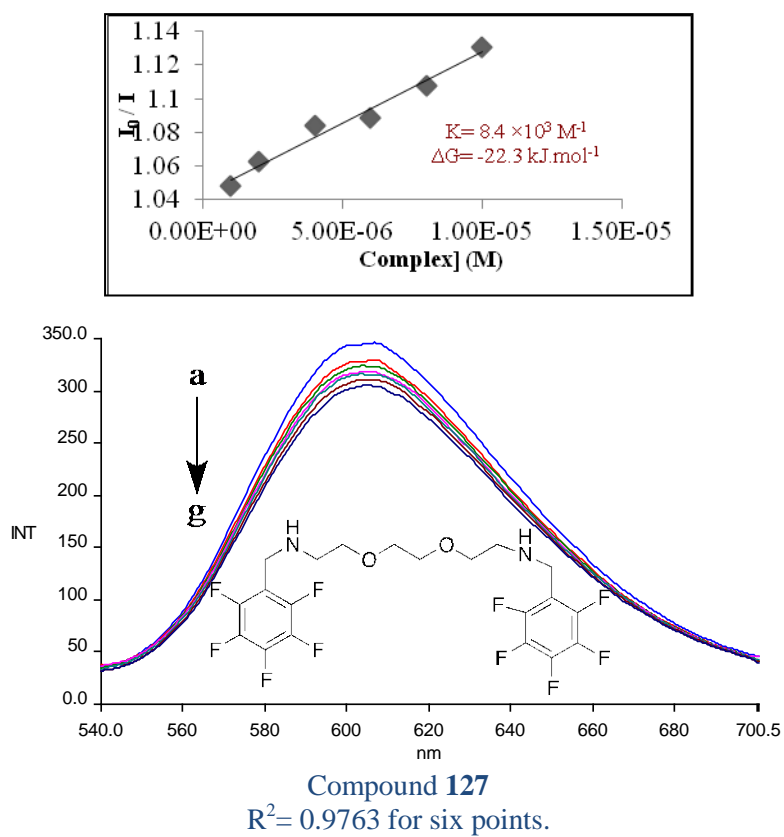

Compound **117**
$R^2 = 0.95205$ for six points.
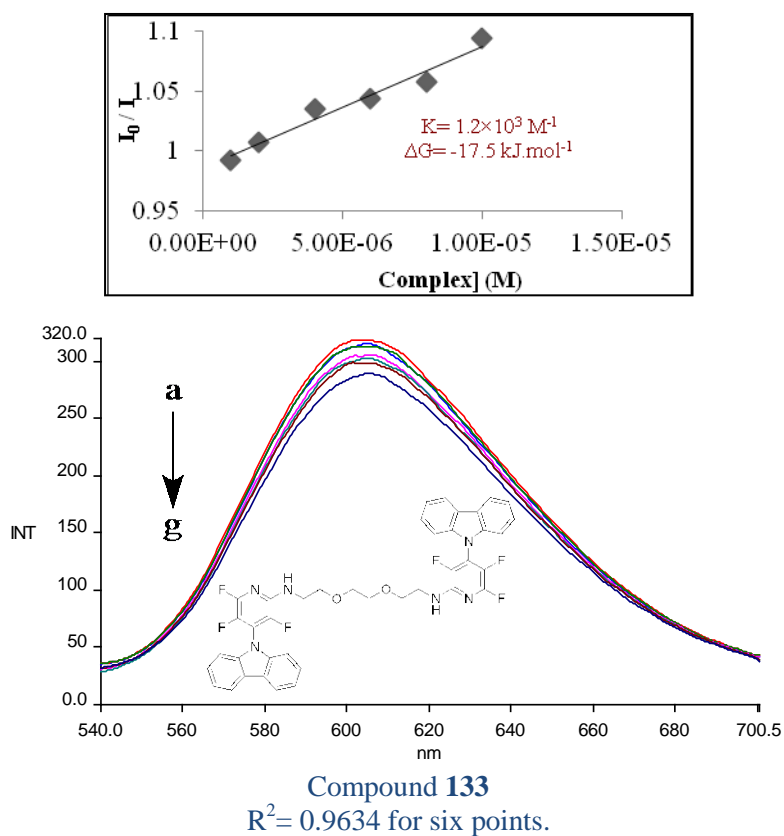
5.4.24. Fluorescence spectra of compound 119

Compound **119**
R^2= 0.8854 for six points.

5.4.25. Fluorescence spectra of compound 120

Compound **120**
R^2= 0.74776 for six points.

5.4.26. Fluorescence spectra of compound 127

Compound **127**
$R^2 = 0.9763$ for six points.

5.4.27. Fluorescence spectra of compound 133

Compound **133**
$R^2 = 0.9634$ for six points.

5.4.28. Fluorescence spectra of compound 135

Compound **135**
R^2= 0.96518 for six points.